THE UNIVERSITY *of* EDINBURGH

WATER TREATMENT IN RURAL INDIA USING SUNLIGHT AND LOW-COST MATERIALS

Victoria Porley

A Thesis submitted for the degree of Doctor of Philosophy

The University of Edinburgh

December 2022

Declaration

I declare that this Thesis has been composed solely by myself and that it has not been submitted, in whole or in part, in any previous application for a degree. Except where stated otherwise by reference or acknowledgement, the work presented is entirely my own.

Victoria Porley

December 2022

Acknowledgements

The work presented within this Thesis is the result of the support and guidance of many key individuals. First of all, I must thank my supervisors, Professor Neil Robertson and Dr Efthalia Chatzisymeon, for all of their support (academic and otherwise!) throughout the duration of my studies. Their expert knowledge has helped me become a better scientist, and their guidance has helped boost my confidence. I am extremely grateful for the encouragement and support they have both given.

As well as my supervisors at the University of Edinburgh, I must also thank those who guided me during field work in India at the Indian Institute of Technology Kharagpur, specifically Professor B. C. Meikap, Dr Somnath Ghosal and Professor Pulak Mishra. Their support in not only the academic aspects of my work, but ensuring my safety, comfort and overall well-being during my research visits is greatly appreciated. In addition to the academic members of staff at IIT Kharagpur, I must highlight the help that was given to me by then-PhD student Dr Debashri Paul. The assistance Debashri gave in training me in various new microbiological techniques, as well as being a good friend during and since my visit, made the overall experience much more enjoyable and successful.

Many more past and present PhD students have been an incredible support to me throughout my research journey. Firstly, all members of the Robertson and Environmental Engineering research groups that I had the pleasure of working with; I am forever grateful to the support we have given each other (academic and moral!), from Friday pizza lunches, to working late in the lab helping each other through projects, I will always value the time we worked together. In addition to those students I worked with directly, I also want to thank the PhD students from outside my group who have been incredible friends and the most valuable support network I could have asked for as we went through our PhD journeys. From demonstrating in the undergraduate teaching labs together, to enjoying completely non-science related catch-ups, the friends I have made and the community we have built has been one of the largest factors to helping me make it through the difficulties of the past four years. Ella Rice, Hannah Logan,

Lisette Warren and Imogen Christopher (and of course Georgia Dodsworth, one of my oldest friends and the honorary member of the chemistry clan): thank you for everything!

It would be impossible to describe the enjoyment of my PhD journey without acknowledging those who run the teaching labs, where I was able to develop my own teaching skills and confidence as a scientist: something that became a very significant part of my time at the University of Edinburgh. My most sincere gratitude goes to Dr Murray Low, Jennifer Anderson, Craig Ross and Dr Michael Cowley for making being a demonstrator such a great experience, and one that helped my time as a PhD student be so much more enjoyable.

There have been many people who have helped with the data collected required for this Thesis who I must also extend my gratitude to. For this, I would like to thank Dr Lorna Eades for helping run ICP-OES measurements, Dr Nicola Cayzer and Dr Fraser Laidlaw for help with SEM, and Dr Stephen Francis and Dr Gwilherm Kerherve for help with XPS.

I am also very grateful to the James Hutton Institute for hosting the research placement that allowed me to acquire much of the microbiology data required for this Thesis. The expertise and guidance I received there was extremely helpful. I learned so much in just three weeks and massively appreciate all those who helped, including Dr Lisa Avery, Dr Eulyn Pagaling, Claire Newman, Dr Duncan White and Charlotte Winspear.

Of course, none of this work would have been possible without the funding, training and support of the Scottish Government's Hydro Nation Scholarship Program. I am forever grateful to the HNSP for giving me this incredible opportunity, and for the amazing network it has provided me with in all things water-related. The training courses and field trips provided significantly helped me to appreciate the wider water industry and made me a better water scientist and steward. To all those who run the course and my fellow scholars; it has been an absolute pleasure to be part of the Hydro Nation Family. Particular thanks go to Professor Bob Ferrier, Dr Rowan Ellis, Dr Rachel Helliwell, Barry Greig, Jon Rathjen, Linda Wood, Nikki Dodd and Laura Logie for their help and support, from ensuring I got back from India safely during the first Covid-19 lock-down,

helping me with contacts for advancing my career, and generally being an approachable and encouraging support network!

And last but certainly not least, I must thank my family for all their support and motivation. My parents, grandparents, and siblings - thank you for believing in me every step of the way, all through school projects, exam stress and listening to my endless talk about chemistry and physics. Included alongside my family is also my best and oldest friend Becky Miller, who has been my biggest champion and a source of inspiration all the way up from primary school to now. And finally, to my partner, Dr Daniel Clark, for being there for me through the highs and lows, and helping me believe I could do this. The past four years have been extremely difficult at points, but you've somehow helped make them some of the best years of my life.

Thank you.

Lay Summary

A lack of safe drinking water leads to over half a million entirely preventable deaths per year, clearly highlighting that it is of great importance that a low-cost, safe and simple method for water purification be found, in order to widen access for rural communities who are most vulnerable. This is essential for meeting the United Nation's Sustainable Development Goals (SDGs), specifically Goal 6: "clean water and sanitation – ensure availability and sustainable management of water and sanitation for all", to be achieved by 2030. India in particular has been identified as having the highest number of people without safe water close to home, demonstrating the importance of implementing a reliable and accessible method of point-of-source water treatment.

One of the best candidates for such an aim is to use a light-activated catalyst, known as a photocatalyst, which can be used to react with organic contaminants, including microbes and toxic chemicals, to clean water. These materials are not used up during the treatment process, removing the need for high chemical dosing like traditional water treatment methods may use, and can be designed to be activated by sunlight, thus removing the need for high energy lamps.

The most commonly used photocatalyst is titanium dioxide, TiO_2, which performs very well under UV light, but poorly under visible light. Since the spectrum of light from solar irradiation is only made up of $<5\%$ UV, changing the chemical properties of TiO_2 such that is can also be activated by visible light could improve solar activity and make the treatment method more suitable for use in rural settings.

In order for the photocatalyst to be suitable, it must be efficient under a wide range of the solar spectrum. In an attempt to achieve this goal, materials have been developed here which showed an improved visible light performance relative to TiO_2, specifically composites with zinc-iron oxides and bismuth, whereby the bismuth-titania materials were found to be the best performers studied as part of this Thesis.

As well as the synthetic work performed here, work has also been conducted to improve

the practicality of photocatalytic water treatment by immobilisation of the catalyst onto a convenient support, such that recapture and reuse is simple, and there are no risks of the catalyst leaching into the water supply. Hence, one of the important parts of this Thesis has been the testing of different supports, with focus given to the use of glass chips produced by grinding down used glass bottles. These were proven to improve catalyst adhesion relative to the more expensive and commonly used alternative, smooth glass beads.

Thorough testing has been conducted to ensure the catalyst is effective against a wide range of pollutants, including chemical and pathogenic contaminants that are typically resistant to low-cost alternatives such as solar disinfection, chlorination or boiling. Laboratory tests revealed that the catalysts could remove chemical contaminants, as well as microbial ones which could pose serious health concerns should they remain in the water course.

Hence, consideration of all key criteria, including the material properties, the safety and stability, cost, implementation ease, and the suitability in various communities, are of paramount importance for meeting the aims of this project.

Abstract

Access to safe drinking water is essential yet threatened for many, with the United Nations highlighting the importance of providing clean water for all as one of their Sustainable Development Goals to be met by 2030. Provision of drinking water in India is of particular importance, as the majority of the population live in rural areas without sufficient access to water, leading to illnesses which could be easily prevented. The large population and land coverage of the country makes installing widespread centralised water treatment facilities to service all inhabitants extremely difficult, and many households rely on their own means of treating water. Traditional methods of point-of-use water treatment, such as filtration, chlorination and boiling all have limitations, meaning there is a need for finding an improved method.

One of the best candidates for such an aim is to use solar driven heterogeneous photocatalysis, whereby a semiconductor material is used to facilitate the generation of reactive oxidising species (ROS), which destroy organic pollutants and pathogens contaminating the water, leading it to be disinfected and safe for human consumption.

However, photocatalysis is often limited in its applications due to the reliance on titania (TiO_2) as the catalyst, which requires UV irradiation for efficient generation of the ROS species. Thus, if the material properties of titania can be enhanced through chemical and structural modifications, such that the system is activated by visible light, it will be a highly useful tool for use in rural settings. This is of particular importance as TiO_2 is inexpensive relative to many novel high functioning photocatalysts, such as those based on silver nanoparticles and other materials which are less abundant than Ti or O. It is also biologically and chemically inert, and is frequently produced on an industrial scale for many varied uses. Thus, building on the high efficiency of TiO_2 under UV irradiation with chemical modifications can help to create high functioning visible light-activated photocatalysts that are affordable and non-toxic, making them ideal for such an application.

In this Thesis, work has been conducted to address the practical limitations of photo-

catalytic water treatment, with the goal of making it suitable for implementing in rural areas on a local, decentralised scale. Field studies were conducted in India, hosted by the Indian Institute of Technology in Kharagpur, during which time catalyst materials were tested with real water samples under solar irradiation, to more closely replicate the conditions in which the treatment method would be used. This helped to build upon lab-scale testing, and highlight areas required for further optimisation. It was found that the catalysts studied (commercial P25 TiO_2 and a bismuth titanate material prepared by previous member of the Robertson research group, Dr Gylen Odling, referred to as BTO-TiO_2) were more successful at removing bacteria from the water samples than solar disinfection alone. However, it was also noticed that there was a significant loss of catalyst over the course of the investigations, and not all could be recaptured. In this study, the catalyst was immobilised on small glass beads, but the adhesion was not as robust as required for the level of use, and the coating would become damaged.

Following these field investigations, the main limitations to practical photocatalytic water treatment were highlighted and motived the remaining work for this Thesis. One of the main concerns preventing implementation of such a technique is the difficulty in recapturing the nanopowder catalyst from the water once treatment has been completed. Typically, the catalyst is added as a slurry, which is beneficial for utilising the high surface area of the catalyst, but makes it very difficult to recapture and therefore reuse, as expensive microfilters or centrifuges would be required, adding costs and complexity to the process. The use of glass beads in the field studies improved this and simplified the set-up required, but improvements were still needed. In this work, focus has been given to improving immobilisation of the catalyst powder, primarily focusing on the use of glass as a substrate, whilst adjusting the structure to find a practical balance between costs, surface area, ease of use and robustness of the applied film. Studies were conducted which showed that mixing a suspension of the catalyst with a solution of tetraethyl orthosilicate helped to improve adhesion by forming SiO_2 during sintering, which acted as a glue to hold the catalyst to the surface more effectively. Further, glass chips were used which were formed from ground down used glass bottles, which were successful in replacing glass beads as a high surface area support with lower costs and without the need for intensive chemical pre-treatment to prepare the surface for coating.

As well as improving practical aspects, studies were also conducted to explore methods for enhancing the photochemical properties of TiO_2, in order to increase the photocatalytic activity under the whole solar spectrum, not just the UV portion. Firstly, studies focused on attempts to make composites of zinc-iron oxide ($ZnFe_2O_4$) semiconductors with commercial P25 TiO_2. The synthesis involved adding zinc and iron precursor salts in a solution of ethylene glycol and water in the presence of P25 TiO_2 and either oxalic acid or ammonia to initiate the reaction. It was found that both acid and base methods led to a significant increase in visible light performance, with the base synthesis being the most simple to perform. However, the same high activity was not observed for tests performed under UV or simulated solar irradiation, where the performance was worsened relative to P25 TiO_2.

Following this, a different approach was taken, whereby TiO_2 was synthesised *in-situ* in the presence of bismuth in a reverse-micelle sol-gel approach, in an attempt to build on the success of the BTO-TiO_2 material studied during field testing. This led to much better performance than the ZnFeO/TiO_2 composites, with excellent visible light activity, and UV activity similar to that of P25 TiO_2. The materials were also shown to be stable with repeated use. The materials did not however outperform BTO-TiO_2, which was prepared *via* a sequential ionic layer adsorption reaction (SILAR) route. SILAR methods have practical limitations that this work attempted to address, and therefore finding the right balance between simplicity of preparation, long-term stability, costs and performance is very important for finding materials suitable for the specific application of solar driven water treatment in rural areas.

Contents

Chapter 1

Introduction

1.1 The Global Water Problem

It is widely understood that the quality of ones life, and indeed existence at all, is intimately tied to the quality of the water that is available for consumption. Given the dependence of human health on having a safe water supply, it is unacceptable that anyone should have to resort to drinking water that has the potential to cause serious illness. However, this is the unfortunate reality for many, with the World Health Organisation (WHO) claiming that almost 30% of the global population rely on a source of water for drinking which has been contaminated with faecal bacteria,[1] which in turn leads to approximately 829,000 entirely preventable deaths every year; 300,000 of which are children.[1] According to the UN, by 2050 at least one in four people is likely to live in a country affected by chronic or recurring shortages of fresh water.[2]

Further, as anthropological behaviours increase the demand for larger scale industrial chemical and pharmaceutical processes, many communities, particularly those in less developed parts of the world, are more at risk of having their water source contaminated with a plethora of chemical complexes, particulates and microorganisms which have the potential to have serious health consequences. For example, the extent of bacterial contamination can be exacerbated by the increased quantity of pharmaceuticals leading to antibiotic resistance, and thus more difficulty in removing such bacteria.[3] Further, it has been suggested that microplastics, a rapidly emerging contaminant, can also act as sites for increased bacterial growth,[4] as well as being a vector for persistent organic

pollutants (POPs) adsorbed onto the surface.[5] Not only does this have severe health consequences, but also seriously impacts social aspects, such as education. In 2016, one third of all primary schools lacked basic drinking water, sanitation and hygiene means; limiting children's access to education, particularly girls.[6] Thus, widening access to sufficient quantities of adequately treated water not only has the potential to reduce global health crises caused by preventable illness, but also to make many aspects of life more comfortable in general, and perhaps help to close the gender gap in education.

This dire situation is being addressed by the United Nation's Sustainable Development Goals (SDGs), aimed to be met by 2030. Specifically, Goal 6 of 17 is to ensure clean water and sanitation for all, and is also recognised as being necessary for many of the other goals, thus arguably one of particular importance to strive for.[6] In order to meet this goal, it is important to ensure that a means of water treatment is available to everyone, be that a connection to a centralised municipal water treatment plant, or a point-of-source treatment method for individual use.

However, it is often the case that commonly used methods of water treatment are energy intensive and require large quantities of chemical reagents, which in turn leads to them being too expensive for use in less affluent areas, where people typically rely on some of the most severely contaminated water sources.[7] In India, where a significant portion of the population live in rural areas (66% in 2018[8]), often without access to treated water, this is particularly apparent. Further, WaterAid reported in 2018 that India is the country with the highest number of people without access to clean water close to home.[9] As a result, introducing a novel method of water treatment for India's rural villages would make a significant contribution to addressing SDG 6 and significantly reducing the extent of the global water problem.

1.2 Solar-based Treatments as a Possible Solution

There is a clear need to develop a robust, safe, easily-maintained and affordable method of point-of-source water treatment, in order for it to be easily implemented in India's rural villages, some of which are without electricity and far from urbanised areas, making

implementation of large-scale treatment facilities infeasible. Frequently employed water treatment processes often involve multiple steps to first remove larger contaminants and then ultimately disinfect the water to remove any remaining pathogens that can lead to disease.[7] Conventional technologies typically use chlorination as the means of disinfection, though UV and ozone treatments are also becoming more widespread.[7]

Chlorination is not always suitable due to the requirement of highly trained operators for plants which use chlorine gas rather than diluted chlorine, the possibility of toxic by-products, the potential for poor taste, and its ineffectiveness against eggs of certain parasites which contaminate the water. Although more effective against a range of biological contaminants, UV technologies are very energy intensive and require that the lamps be replaced every 6-12 months, which also contain toxic mercury.[10] Thus, these typically used methods do not lend themselves to use in rural areas.

Key criteria for household water treatment and safe storage (HWTS) methods include:[11]

- High effectiveness against the full range of pathogens, and possibly chemical contaminants, under a wide range of conditions,
- Low labour inputs for operation and maintenance,
- High productivity i.e. can produce several litres a day to meet all needs,
- Positive effects of water aesthetics and taste,
- High robustness and user safety,
- Attractive design - some communities may be put off if the treatment technology is an eye-sore,
- Automatic shut-down mechanism if treatment effectiveness is compromised,
- Integrated safe storage,
- Local availability of product and replacement parts.

One attractive solution to meet many of these criteria is to utilise freely available resources, such that extensive installation and the need for hard-to-procure components are not necessary. One such source of freely available power is solar irradiation, which has the potential to directly treat water, or to power electrical systems that treat water in different ways, such as by ozonation. By using the Sun's light directly, very simple

treatment systems can be set up, such that the availability of clean water can be widened to include many rural communities that would not otherwise be able to install a complex water treatment system. Solar disinfection of water by direct exposure to sunlight is known as SODIS, and opens many doors for water treatment in rural communities, such as in India.

1.2.1 Solar disinfection - SODIS

An example of such a water treatment method already being employed globally[12] is solar disinfection (SODIS) of water, which involves placing contaminated water in a bottle, typically plastic, and exposing it to sunlight for several hours. SODIS, introduced by Acra in 1984,[13] is also a technique which does not depend on an electrical energy supply or chemical addition, making it cheap and simple to employ. According to a 2009 study by Meierhofer and Landolt,[12] SODIS was used daily in India, and thus shows that it is practically feasible and accessible.

A study conducted by Rose et al. demonstrated that SODIS was a practical method for increasing water safety in Tamil Nadu, India, and led to a significant reduction in the incidence, duration and severity of diarrhoea in children, with most women in the study feeling as though SODIS was feasible and sustainable.[14] Many studies have been conducted demonstrating the positive results of SODIS achieved in practice.[15–19] Typically, countries with the highest numbers of vulnerable people who require a means of treating water, such as refugees and displaced people, tend to have more favourable conditions for SODIS.[11,20]

Exposure to sunlight inactivates susceptible pathogens by three possible mechanisms; UV inactivation, thermal inactivation, or the synergistic combination of the two former mechanisms. The effect of UV and high temperature on reducing the numbers of viable bacteria in water has been well documented, with the accepted threshold for achieving disinfection from UV being a constant irradiation of 500 W/m^2 for at least 3 hours, and the temperature requirement being at least 45°C or higher, with typical exposure requirements being for 5-6 hours.[20] For many pathogens, it is the synergistic combination of both factors that is required for inactivation. For example, a study using cysts of the

protozoa *Acanthamoeba polyphaga* under simulated sunlight showed a direct correlation between inactivation and temperature. At 40°C, no appreciable reduction was observed during irradiation, but 3.6 log reduction in viable cysts was observed after 60 hours at 50 °C, and a 3.3 log reduction at 55 °C after only 4 hours.[21]

The mechanism of bacterial inactivation is thought to be due to a combination of damage to DNA and proteins of the microorganisms present, caused by the formation of reactive oxygen species (ROS), such as singlet oxygen, superoxide, hydrogen peroxide and hydroxyl radicals.[11] ROS generation can be mediated by photosensitisers present in the water (such as organic molecules or iron), or by molecules within the pathogen itself. These are known as exogenous and endogenic mechanisms, respectively. UV A light (315 - 400 nm) can induce protein oxidation and aggregation within exposed bacteria, leading to disruptions of metabolic function and accelerated cell ageing.[22]

It has been shown that the enzyme components of the respiratory chain including NADPH and succinate oxidases are affected, resulting in the inhibition of ATP generation.[23] There is a small germicidal effect also induced by the visible region, though this is caused by sensitisers such as porphyrins[24] and carotenoids,[25] and is not through direct irradiation. In terms of the effect of temperature, thermal inactivation, or pasteurisation, operates in a similar way by causing damage to proteins such as enzymes which are important for the respiratory chain. Different bacteria will have slightly different temperatures at which this process begins to take place, starting from 40 °C. However, the mechanism of disinfection is less understood for viruses and protozoa due to their different structures (see Section 1.3.3 on pathogens of concern in water).

The placement of the water-containing vessel itself (e.g. a plastic bottle) is also important, in order to increase the penetration of UV-light into the water. The inclination of the bottle can have an effect, though adjusting the bottle throughout the day can become tedious and impractical. Rather, it is important to ensure that the bottle is in a location which receives unbroken sunlight exposure over the course of the day, such that no shadows will pass over the bottle, which would reduce the temperature and incident light.[11] It has been shown that receiving an uninterrupted dose of UV A irradiation is a

critical parameter for ensuring effective microbial inactivation.[26]

One of the biggest concerns for the suitability and uptake of SODIS is the limitation of functionality and implementation over the whole year. A study in Haiti using 1.5 L polyethylene terephthalate (PET) bottles investigated this by conducting SODIS in January, where the weather is cooler with less intensive solar irradiation. It was found that, rather than the standard 5-6 hours, an exposure of 2 days was required to ensure 100% success in microbial inactivation, with no inactivation achieved on days with solar intensity lower than 500 W/m^2.[27] This raises major feasibility issues since cloudy, unfavourable weather is out of the users control and often unpredictable. It is also not recommended that SODIS be conducted during periods of heavy rainfall.[11]

A further limitation is the risk of regrowth of bacteria that can occur if the SODIS process could not completely inactivate the bacteria present, depending on storage conditions. Several studies found regrowth after various time periods ranging from 18 hours and one week,[28–30] though these studies used different practical conditions. This demonstrators that SODIS can vary in reliability depending on the conditions it is conducted under. As such, the shelf life of the water cleaned *via* SODIS is limited to a recommended time frame of up to 24 hours after treatment has concluded,[11] in order to prevent any remaining bacteria from reactivating and multiplying.

Another concern for SODIS is the choice of material and size for the vessel. In terms of size, it is recommended that bottles no larger than 2 L with a maximum penetration depth of 10 cm be used, since the penetration of light through water significantly decreases with the depth of water, even when it is clear and free of turbidity.[11,18] Glass bottles and jars have been suggested for use in SODIS, since borosilicate glass can transmit up to 90% of UV A (315 - 400 nm) and 45% of UV B (280 - 320 nm), which is known to be germicidal[31] so could enhance the rate and extent of disinfection significantly. However, glass has practical limitations, due to it being heavy, especially when filled, which is not ideal for large batch reactors.

They are also susceptible to breakage, which could lead to high cost of replacements,

as well as injuries. As such, it is recommended that polyethylene terephthalate (PET) containers be used over glass, as PET bottles are also widely available in low- and middle-income countries.[11] However, PET does not transmit UV B, which limits the efficiency of SODIS, but much UV A can still be transmitted (85-90%). Further, a study by Asiimwe et al. found that the performance of SODIS in glass and PET containers was comparable under sub-Saharan weather conditions,[32] suggesting that users should choose which ever container is more readily available, and that the effect of reduced UV B penetration with PET is not a significant enough concern to prevent implementation. The PET bottles are also much lighter and less likely to break.

However, concerns have been raised over the stability of certain plastics, particularly under prolonged exposure to heat, UV and moisture; and the potential for leaching of plasticisers and monomers to occur under such conditions. The process of making thermoplastics involves polymerising a chosen monomer into a high molecular weight polymer (often in the presence of a catalyst), which is then mixed with various additives. It is then melted, mixed, extruded and pelletised to form a resin.[33] Studies have been conducted to explore the leaching of antimony from PET bottles, which is of concern due to the use of Sb_2O_3 as a catalyst during manufacturing. Antimony can have very severe consequences on health, with a guideline concentration in water of 6 ppb,[34] though this can be exceeded if the bottle is exposed to temperatures above 65 °C.[35,36] This is an important concern to keep in mind when using plastic bottles, particularly since photocatalysis can not remove such inorganic contaminants. However, antimony does not bioaccumulate,[34] which reduces risks if leaching were to occur.

Many plastic resins also contain monomers or additives that may act as endocrine disruptors (ED), which are molecules that interact with biological processes that rely on hormones. More explicitly, The Endocrine Society defines these substances as *"products that interfere with hormone biosynthesis, metabolism, or action resulting in a deviation from normal homeostatic control or preproduction"*.[37]

Some of the most common EDs are those which antagonise or mimic actions of the body's naturally occurring estrogen, which are said to display estrogenic activity (EA) through

the presence of an insufficiently hindered phenol group, which enables them to bind to estrogen receptors. Unfortunately, leaching of these molecules at very low (nanomolar or picomolar) concentrations is often possible, since the polymerisation is rarely complete and additives are not chemically part of the polymeric structure.[33] The leaching process of monomers and additives can be accelerated by exposure to UV radiation, moisture, heat and microwave radiation. This posses clear issues for using it as a container for water to be purified as a result of exposure to sunlight.

Bisphenol-A (BPA) is one of the most commonly known chemicals used in plastics resins that can have adverse health effects as a result of acting like an ED, and has subsequently been removed from many manufacturing processes. However, a study by Yang et al. in 2011 showed that plastics free of BPA still exhibit leaching of EDs when exposed to the aforementioned stressers.[33] It was found that for some samples, including low density polyethylene (LDPE) and glycol-modified polyethylene terephthalate (PETG) resins, there was no detectable EA before adding any stress, but subsequently showed EA after being stressed, particularly by UV. Samples studied of products made of PETG resins, advertised as BPA-free, all showed detectable quantities of EDs, again with this being particularly increased by exposure to UV light.

Polycarbonate (PC) bottles have been used for SODIS, arising concerns due to the BPA content. A study conducted by Brede et al. found that thermal stresses can cause the release of BPA from PC containers such as baby bottles which undergo exposure to boiling water and may be cleaned in a dish washing machine.[38] This suggests that BPA leaching could also occur during SODIS in PC bottles, though the temperatures and time frames used are likely to be lower than those in the study, with temperatures achieved during SODIS rarely increasing above 55 °C, as found through field studies in India, Bahrain and Spain.[39]

Further, the tolerable daily intake (TDI) according to the European Food Safety Authority (EFSA) of BPA is 4 μg/kg,[40] which is higher than the levels detected in the study by Brede et al., suggesting that the benefit of obtaining pathogen-free water by conducting SODIS in plastic bottles outweighs the risk of leaching, though other plastic materials

that do not contain BPA, such as PET, are preferred if available.

One study by Wegelin et al.[41] investigated the stability of PET bottles in SODIS over extended use by exposing filled and emptied water bottles to natural sunlight for periods of 15, 30, 63 and 126 days. It was found that photo-products were only formed on the outer surface of the PET bottles, though the quantity of the products formed did increase with exposure time. The content of the water within the bottles did not appear to change during the extended exposure times with respect to aldehydes, organic photo-products, additives or phthalate concentrations, which were all detected, if at all, well below the limits for safe drinking water, which suggests that PET bottles are suitable for SODIS.

This finding was corroborated by Schmid et al.,[42] who conducted a study on the stability of PET by monitoring the release of plasticisers i(2-ethylhexyl)adipate (DEHA) and i(2-ethylhexyl)phthalate (DEHP). It was found that, after 17 hours of exposure to sunlight, the levels of DEHA and DEHP did not exceed the recommended levels for safe drinking water, and also did not reach levels notably higher than those measured from commercial bottles water. Further, Ubomba-Jaswa et al.[43] also found that genotoxic chemicals were detected in water following continuous exposure to sunlight without refilling for 1 to 6 months, though the levels detected were similar to control samples that were stored in the dark, indicating that conducting SODIS is not the primary cause, and should not worry or deter people from up-taking SODIS.

Hence, despite leaching from PET having been detected to be possible, and possibly more probable after prolonged exposure to conditions necessary for SODIS, a conclusion often reached amongst SODIS researches is that the risk of exposure to toxic levels of leached chemicals is low, and does not outweigh the potential benefit of microbial removal,[42] which poses a more immediate health risk. It is advised that, in order to mitigate any risk of exposure to leached chemicals which may build up within the bottle if used over extended periods of time without correct cleaning in between uses, that PET bottles should be used for up to 6 months and then replaced.[43]

In addition to the choice of container, other factors can effect the implementation or

efficiency of SODIS. Turbidity is one such factor that can decrease the effectiveness of SODIS by preventing sufficient light penetration from occurring.[20,44] It is recommended that SODIS only be conducted on water with a minimum turbidity of 30 NTU (nephelometric turbidity units),[11] despite water collected from hot, arid climates often having higher turbidities, such as in Kenya, where a study by Joyce et al. found samples with turbidity of higher than 200 NTU, where it was found only 1% of the incident UV radiation could penetrate the water samples,[45] though inactivation of *E. coli* was still possible due to thermal action alone. This is promising, though it is unlikely to be sufficient for more resistant pathogens. However, it should also be noted that, despite the reduction in light penetration, turbidity can help to increase the temperature of the water and cause convection currents, which also help with mixing of water, aiding the bactericidal action.[46]

Methods to reduce the turbidity in order to ensure the dual action of both UV and thermal inactivation are possible include simple filtration and the use of minerals such as potassium sulphate and the seeds of plants like *Moringa oleifera*.[20] However, one drawback of adding such steps to the treatment of water is the need for training, and the possible reduction in community acceptance if complex systems or extensive manpower is required.

Irrespective of the feasibility and effective implementation protocols followed, the actual uptake and continued, committed use of SODIS largely depends on societal attitudes and community acceptance of the proposed water treatment method. Despite proven results, compliance often declines after monitoring and promotion from researchers or other invested parties concludes.[47] Many factors may play into the societal acceptance of SODIS, particularly the costs incurred. Although this is a low-cost method in comparison to other treatment types, it is important to bear in mind that many rural communities depend on water sources such as wells and rivers, collection and direct consumption from which does not incur any cost other than of the container itself.

Further, having to collect water can often be an extremely laborious task, with long journeys often required. For example, in Sub-Saharan Africa, over 25% of the population

takes 30 minutes for a single round trip of water collection, often with the responsibility falling on women and children.[20] As a result, many communities may wish to reduce any further effort in treating water, or skip the step altogether, due to the efforts already required, which can limit time available for education or self-care. Thus, a benefit of SODIS is that it is a passive treatment technique which is less expensive and labour intensive than boiling or chlorination, though the cost of fresh bottles and containers may limit uptake. Indeed, it was commented on by participants in a 2020 study conducted in Ethiopia by Bitew et al. that treating water *via* SODIS was easier than through boiling, as it saved money which would otherwise go towards fuel for fire, and also eradicated the risk of burns.[48] Further, the study highlighted the willingness of users to consistently use SODIS if their neighbours were happy with results and could recommend it to them, as well as the desire to protect vulnerable members of their community from sickness, such as pregnant women and children, who they would like to be able to support through school, which clean water helps to facilitate.

However, another 2020 study conducted by Martinez et al. in rural Bolivia largely found community disapproval unwillingness to use SODIS,[49] implying that the same social patterns and attitudes towards SODIS cannot be assumed for all rural communities, and careful consideration must be made when evaluating which water treatment types are most appropriate. The issues that arose from this study were a concern of incomplete disinfection if the water was only heated, not irradiated with UV (referred to by the participants as 'half-boiling'), as well as poor taste. It may be the case that enhancing SODIS could help to mitigate some of these concerns and increase uptake. It has been suggested that ceramic filtration may provide a suitable means of point-of-source water treatment, as continued use is common due to the simple operation and convenience. Good microbial inactivation is shown in field studies,[50] though filters can become blocked and require replacement, and small pathogens such as some viruses are often not removed during filtration.

One drawback that may limit uptake and community acceptance is the availability of suitable containers, such as enough plastic bottles to meet the volume requirements of the users. A study conducted by Altherr et al. in Nicaragua showed that, on average,

families own only 1.25 bottles per person, with bottles used for SODIS typically holding between 1.5 to 2 L. This would result in the preparation of 1.88 to 2.5 L of clean water per day, weather permitting, despite the daily use per person estimated by the families as being 3 L.[51] However, it has been recommended that the daily provision of water for a family should be between 50 and 100 L per person, per day.[52] It is clear that ensuring sufficient availability of suitable containers is crucial for feasible uptake of this method. Further, many families will be more likely to use SODIS if they know others that use the method and find it improves the taste or appearance of the water, as well as health of the users. Understanding the need for, and function of, SODIS also increases the willingness to use it, though often there are lapses in continued use. For example, some users may not commit to continued use of SODIS, particularly if significant improvements in taste are not noticeable. It has been suggested that social support and schemes aimed at habit development would be beneficial, as well as simply explaining the function.[53]

In addition to the uptake of SODIS depending on social attitudes, so does its effectiveness. One major set-back for the implementation of water treatment at the personal or household scale in general is the issue of re-contamination to the stored water supply. Studies have shown that even for water which has been treated, such as by SODIS, boiling or with at-home chlorination systems, the faecal contamination can be detected where it was originally free from detectable bacteria immediately following treatment.[20] One study showed that this was due to *E. coli* on hands of users and that the cups used to collect water from the storage vessel also showed high levels of bacterial contamination.[54] Frequently, water is scooped from containers with hands which may have bacterial contamination, and bacteria can also build up on the container itself if not cleaned correctly.

The importance of hand washing and good sanitation is paramount to ensure treated water remains safe to drink, though this is challenging for many communities where obtaining large enough quantities of clean water for drinking, cooking, sanitation and hygiene is very difficult using methods such as boiling and chlorination, as these can be expensive and time-consuming. SODIS can be much cheaper if suitable containers are owned, which can help to mitigate this problem by allowing larger volumes of water to be treated easily, though there are size limitations for the containers that should be used.

In order to help meet volume demands and help to improve sanitation facilities as well as the availability of water from drinking and cooking, improvements should be made on the simplistic SODIS technique.

Many methods have been suggested and tested in an attempt to enhance the efficiency of SODIS, such that it is more effective and thus safer. One practical aspect to try to improve is the temperature reached during SODIS, since warm temperatures between 25-40°C are ideal for many bacterial species to grow. Thus, if the temperature of the water does not exceed this range, the extent of disinfection could be limited, or even cause more bacteria to grow if UV intensity is insufficient. Such methods to increase the temperature include blackening the bottom of the bottle or laying the bottles on a dark surface, as well as using a solar collector or reflector in order to increase both the temperature and UV intensity simultaneously. However, the use of dark backgrounds or placing on metal sheets has been found to offer an accelerating effect of less than 30%,[11,55] which experts feel does not constitute a reduced exposure time.[11] Rather, solar collectors are preferred as these can significantly increase the treatment efficiency and reduce the time required,[11] though such systems are more technical and sophisticated, which may reduce accessibility.

The use of mirrors to produce solar collectors is a way to increase the effectiveness of SODIS by allowing a more efficient use of solar photon flux, and can mitigate the effect of reduced solar intensity as the position of the Sun changes, such as when compound parabolic concentrators (CPCs) are in use.[25,46,56] Such systems can also allow for larger volumes of water to be treated more effectively, reducing the need for many small bottles. For example, a CPC was employed to allow for the disinfection of 25 L of water in 6 hours or more of sunlight, where all *E. coli* was observed to be inactivated, though more slowly than in smaller containers.[46] The reactor employed in this study is shown in Figure 1.1.

Figure 1.1: Image from study by Ubomba[46] on the implementation of a CPC with a 25 L methacrylate tube for enhanced SODIS, presented with permission from John Wiley and Sons Publishing.

Research has also been conducted on the use of chemical additives, though this may not be possible in certain regions due to limitations with procuring some chemicals. Simple additives such as lime juice have been shown to enhance SODIS and be effective against *E. coli*.[57,58] The combination of the increased acidity caused by the addition of citric acid from the lime juice with the UV irradiation is believed to be the cause for the accelerated disinfection observed through this technique. Harding et al.[57] found that adding lime juice at a concentration of 1.5% to 2 L PET bottles of tap water water spiked with *E. coli* caused a significant increase in the extent of deactivation achieved within the 30 minute test period under UV irradiation.

It was also observed that lime slurries prepared by finely chopping whole citrus fruits and adding to the test solution offered slight improvements relative to the lime juice, with the SODIS-lime slurry combination inactivating *E. coli* beyond the levels of detection. It was also found that adding lime improved the efficacy against MS2 bacteriophage (a virus that only targets bacteria, not humans), though not as significantly as for *E. coli*. SODIS with and without lime did not prove effective against murine norovirus, highlighting that more intensive enhancements or a combination of techniques is required when more resistant pathogens are present. It is also important to note that, whilst the addition of citric acid obtained from limes or lemons does not pose any health risks, it will impact the flavour of the water, which in term will affect uptake depending on personal taste

preferences.

A combination of copper sulphate and ascorbate has also been observed to accelerate the inactivation of MS2 coliphage, *E. coli* and *Enterococcus* spp. during SODIS,[58] with the increase in rate having an approximately linear dependence on the concentration of each reagent. Due to the impracticality of obtaining copper sulphate in some rural communities, copper wire was tested, which also substantially increase the inactivation rates observed. Copper is known to be toxic to aquatic organisms, and the combination of copper and ascorbate has also been shown to present disinfection in the dark,[58,59] which could extend the useful period of SODIS to include months of the year with less intense solar irradiation and more cloud cover. However, the effectiveness is limited by the fact that ascorbate can be used up rapidly in the presence of copper, as well as the potential complexation of copper in the presence of dissolved organic matter (DOM) which may reduce its reactivity.

Riboflavin has also been used in multiple studies to enhance SODIS, with Heaselgrave et al. finding it to significantly enhance the inactivation of *E. coli*, *F. solani, C. albicans* and *A. polyphaga* trophozoites, though inactivation was not achieved after 6 hours for *C.parvum* oocysts and *Ascaris suum* which have very resistant walls.[22] The enhancement observed due to the addition of riboflavin is thought to be caused by either direct transfer of protons or electrons from the riboflavin to or from the target substrate, generating free radicals, or by the facilitated formation of singlet oxygen.

Shaking the bottles prior to being filled to increase the amount of dissolved oxygen has also been suggested as a simple but effective way to improve the efficacy of SODIS.[17,60] This is due to the critical role of oxygen in SODIS, which cannot operate effectively under anaerobic conditions[60] as a result of the mechanism depending on the production of ROS species.

1.2.2 Photocatalysis for Water Treatment

The ease of implementing SODIS makes it an attractive option for rural areas, despite the associated drawbacks. However, being able to enhance the process and make it more

efficient and dependable, whilst still being powered solely by the Sun, would make the method much more viable. There are many ways of enhancing SODIS, as discussed above in Section 1.2.1, though one of the more promising methods is photocatalysis. Practically, this would utilise the same SODIS system that would typically be adopted, such as filling plastic bottles with water and exposing to sunlight, but with the simple addition of a photocatalyst material to the bottle or container, in order to increase the rate and extent of decontamination.

Due to the use of a catalyst rather than a chemical additive, fewer resources would be consumed, which has the potential to be more time and cost effective (though this would be dependent on the choice of catalyst and its lifetime, as discussed in Section 1.2.2.2). There would be an additional cost of installation compared to SODIS alone, due to the use of the photocatalyst, but the improvement to water quality and safety may lead to a societal shift towards willingness to utilise such a treatment method when results are felt in terms of improvement to health. Fewer cases of illnesses will reduce medical costs and prevent individuals from needing to take time out of work and prevent loss of income, which may offset any initial resistance towards implementation.

A significant aspect which makes photocatalysis such a great candidate for addressing the need for improved decentralised water treatment is the fact that there has been an increased demand for energy in the water sector, and *vice versa*, with the two sectors being innately interlinked.[7,61–63] Hence, as well as providing the vital resource of clean, drinkable water to communities where it is currently scarce, this technology also has potential for reducing the energy requirements of water purification systems where SODIS alone is insufficient, and subsequently having a significant environmental impact. This is a crucial aspect to bear in mind when attempting to advance water purification technologies, due to current energy usage being widely accepted to be unsustainable.

A further benefit of photocatalysis over SODIS alone is the enhanced ability to remove chemical contaminants. As discussed above, one concern for many promoters or potential users of SODIS is the possible leaching of molecules such as endocrine disruptors into the water. However, by performing photocatalysis, there is the possibility that any

leached chemical contaminants will be broken down during disinfection, and not be detectable, though more research is needed in this area. As discussed in the following Section (1.2.2.1), the photocatalysis mechanism is based on the production of reactive oxygen species (ROS), such as highly oxidising hydroxyl radicals, which would be produced in higher quantities than if just using SODIS alone, which would help to further attack pathogenic species present, increasing the extent of inactivation of susceptible species, as well as being able to inactivate other pathogens that are commonly found to be resistant to un-modified SODIS. In addition, photocatalysis is a particularly attractive method to remove bacterial pollutants from water since it would not use or produce any carcinogenic, malodorous or mutagenic compounds during the process.[64]

1.2.2.1 The Photocatalysis Process

Since the introduction of colloidal semiconductors in 1977,[65] the field of photocatalysis has grown rapidly,[66] with titania leading the way as the most promising semiconductor for this application. Its high photoreactivity, affordability, photostability, non-toxicity and chemical and biological inertness make it the natural choice for both fundamental research and practical applications.[67]

The mechanism of photocatalysis can be summarised by Figure 1.2, where (1) indicates the photoexcitation of an electron from the valence band (VB) to the conduction band (CB), *via* the absorption of a photon ($h\nu$) of sufficient energy; and (2) is the recombination of charge, which is one of the leading causes of reduced efficiency in such reactions. Once the charge carriers are separated after photoexcitation takes place, provided they do not recombine, they are free to take part in redox reactions. It is these redox reactions that provide the mode of action for water purification, and indeed other chemical reactions for which photocatalysis may be applied. The direct reduction of an electron acceptor (A) and oxidation of a hole acceptor/electron donor (D) can also be seen.

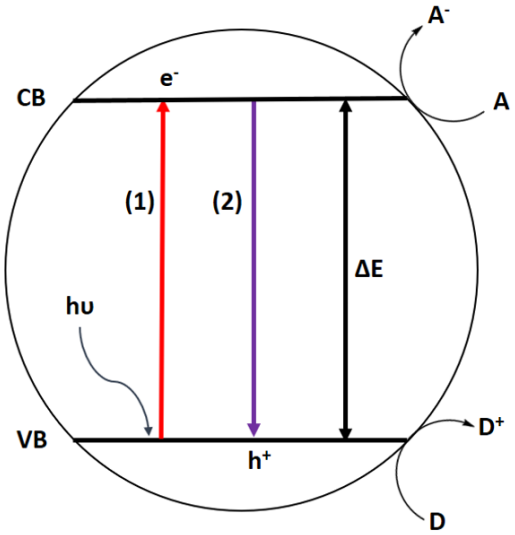

Figure 1.2: Schematic demonstrating the photophysical processes that occur during excitation of a semiconductor photocatalysis, which can be utilised for water purification

More explicitly, the photoelectrons and photoholes can each go on to take part in reduction and oxidation reactions, respectively, based upon the following pathways:

$$TiO_2 + h\nu \longrightarrow TiO_2(e^- + h^+)$$

Photoelectrons:

$$e^- + M^{n+} \longrightarrow M^{(n-1)+}$$

$$e^- + O_2 \longrightarrow O_2^-$$

$$2\,e^- + O_2 + H_2O \longrightarrow H_2O_2$$

$$e^- + H_2O_2 + H^+ \longrightarrow {}^{\bullet}OH + H_2O$$

Photoholes:

$$h^+ + H_2O_{(ads)} \longrightarrow {}^{\bullet}OH + H^+$$

$$h^+ + OH^- \longrightarrow {}^{\bullet}OH$$

$${}^{\bullet}OH + R_{(ads)} \longrightarrow R^{\bullet}_{(ads)} + H_2O$$

From the above equations, it is clear that photocatalysis possesses the dual functionality of being able to both reduce heavy metals present in the water to safer oxidation states (e.g. Cr(VI) to Cr(III)), as well as oxidise harmful organic complexes, which are eventually degraded to form only carbon dioxide and water.[66] The degradation of these pollutants depends on the presence of the highly oxidising hydroxyl radical, making photocatalysis an example of an advanced oxidation process (AOP). There are a wide range

of processes which fall under the umbrella of advanced oxidation, with some being more studied, established or suitable for water purification than others. An AOP is defined as a reaction which follows the two step process of (i) *in-situ* formation of reactive oxidative species, and (ii) the reaction of oxidants with target contaminants.[68] Which radicals form preferentially, the reaction mechanisms and efficiency of contaminant destruction varies between each individual AOP and how it is implemented. Some other examples of AOPs include ozonation, electrochemical processes, catalysis, physical (e.g. plasma), ultrasound, microwave and electron beam, as summarised in Figure 1.3.

Catalytic processes can operate with or without the irradiation of light as a way to initiate the reaction. An example of a catalytic process that works without light is a Fenton process. This combines ferrous iron and hydrogen peroxide under acidic conditions to obtain the hydroxyl radical. The maximum catalytic reactivity for iron is at pH 3. This can also be used under irradiation of light in a photo-Fenton process, whereby the absorption of a photon leads to iron being reduced to the Fe(II) state, along with the formation of a hydroxyl radical. This is a homogeneous catalysis mechanism, but heterogeneous photo-catalytic processes are also very useful AOPs, specifically the use of a semi-conductor material such as titania.[68] This semiconductor-based photocatalysis forms the basis of this work on account of its high potential to be a suitable candidate for the specific goal of developing a water purification system that can operate successfully in rural India.

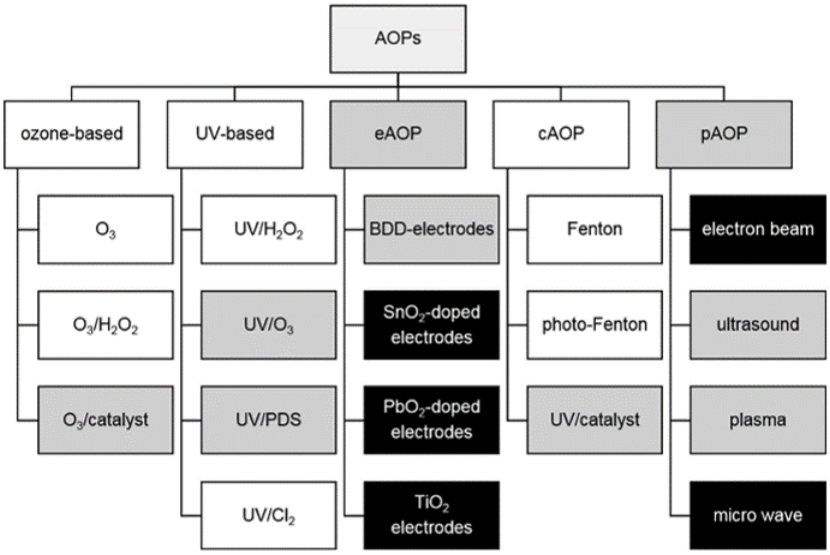

Figure 1.3: Summary of AOPs currently studied or implemented for water purification purposes,[68] presented with permission from Elsevier Publishing. Established at full scale in white, investigated at lab or pilot-plant level in grey and tested at lab-scale in black.

Often, a combination of the various AOP techniques summarised in Figure 1.3 can be used for increased reaction efficiency, such as a titania-based photocatalysis process coupled with a photo-Fenton one.[69] However, this type of system is not always transferable to a rural setting, as is the aim here, which would require low maintenance such that it can operate without the need for highly trained professionals. For example, a pilot-plant implemented by Margugan et al.[69] operated at highly acidic conditions in order to optimise the Fenton process, which makes it unfavourable for use in rural villages which may not have the infrastructure for a large-scale chemical plant. Thus, if a titania-based photocatalytic process can be optimised, it would hold a lot of potential for filling the gap and providing a simple, safe, low-cost and robust water purification system.

Although the oxidising power of the hydroxyl radicals formed during photocatalysis is very strong, the success of the process ultimately depends on whether the charge carriers are formed with sufficient energy to induce the relevant redox reactions, as well as have lifetimes long enough to go on to be involved in such reactions before recombining. This is dependent on the efficiency of the light absorption process required to initiate the photocatalytic process. Following the initial photon absorption, the separation of the electron-hole pair needs to be sufficient such that recombination does not occur and prevent the charge carriers being able to undergo charge transfer to the adsorbed species

on the semiconductor catalyst surface. Recombination is common since excited electrons and holes are thermodynamically unstable, and thus have a tendency to recombine, resulting in a lower energy system.[70]

The recombination of charge carriers can occur radiatively as light emitted, or non-radiatively, resulting in heat. Both of these are wasted forms of energy when conducting photocatalysis.[71] The heat released from charge recombination can be detected using methods such as time-resolved photoacoustic spectroscopy (TRPAS).[67] This method was used by Leytnar and Hupp to show that approximately 60% of trapped electron-hole pairs recombine on a timescale of roughly 25 ns, accompanied by the release of 154 $kJmol^{-1}$ of energy as heat.[72] Thus, increasing the separation of the electrons and holes can significantly improve the efficiency of photocatalysts.

Further, the energy required to drive the necessary redox reactions is dependent on the locations of the conduction and valence bands of the semiconductor employed, effectively setting an appropriate range for them to fall between, as shown in Figure 1.4. If the corresponding band gap is too small, the relevant chemistry cannot take place. This is a limitation of band gap engineering for improving visible light absorption.

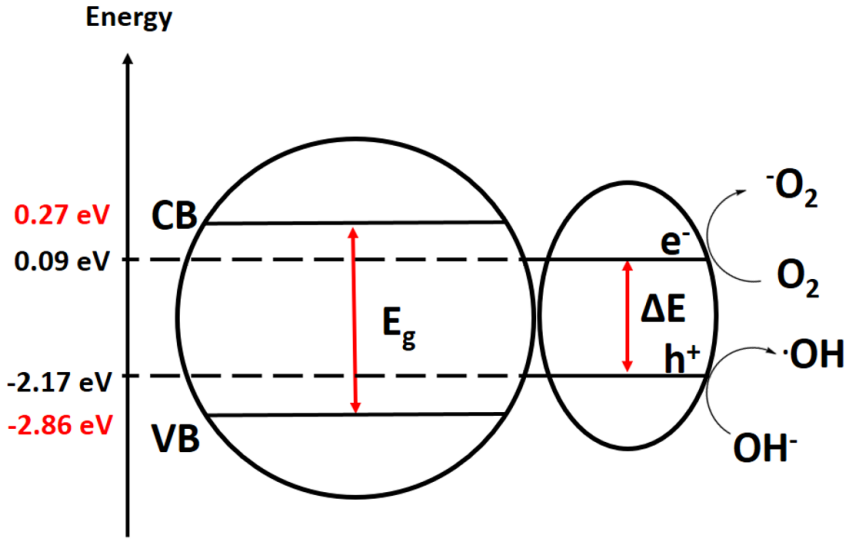

Figure 1.4: Schematic to indicate the relationship between the band gap of the semiconductor and the energy required for the necessary redox reactions to take place. The energy values in red indicate the band level energies for titania, where the values in black are the redox potentials for the necessary reactions

As well as the ability of photocatalysis to remove chemical pollutants and reduce heavy

metals, it is also well known for its success in removing bacteria from contaminated water. It has been proposed that the mechanism for this consists of oxidative damage to the cell wall, followed by the underlying cell membrane, eventually leading to increased permeability and eventually the free efflux of intracellular contents, as well as disruption to genetic material; causing cell death.[73–75] Also important to note, is that the use of photocatalysis for water remediation is most relevant to waters with bacteria or complex organic molecules as the main contaminants of concern, as the mechanism of photocatalysis does not allow for the removal of inorganic contaminants such as arsenic. For this purpose, an additional step in the treatment system would be necessary to remove this separately.

1.2.2.2 Practical Photocatalysis - Making the Process Applicable to Rural Areas

The simple operation of photocatalysis makes it appealing for use in regions where there does not exist sufficient infrastructure to install a centralised water-treatment plant, and instead robust and simple point-of-source methods are required. However, ongoing barriers exist which have thus far prevented this technology moving from its current status as being largely in its research and development phase to being widely implemented in practice. One significant barrier includes the poor visible light absorption of many commonly used semiconductor photocatalysts, such as titania. Due to the solar emission spectrum only containing 5% UV light, photocatalysts which operate under UV irradiation are severely limited in their maximum efficiencies, and as such are limited in how much of an enhancement relative to SODIS alone they can provide. As such, developing novel high functioning photocatalysts which can operate under visible light has become an active area of research.

One such way to enhance the performance of photocatalyst is to combine two semiconductor materials with different band gaps, in order to form a heterojunction band gap architecture. In the case of enhancing titania, a semiconductor with a narrower band gap may be used such that more visible light may be absorbed, and the interface between the two band gaps can allow for the excited charges to be separated and thus recombination is hindered.[76] This can increase the lifetime of the photoelectrons and photoholes pro-

duced, meaning they are more likely to be involved in the advanced oxidation processes that are utilised for water treatment.

Heterojunction band gaps can take three forms, type-I, type-II and type-III, as shown in Figure 1.5. Type-II is most effective in improving catalyst performance since the position of the valence and conduction bands in semiconductor 2 are higher than those in semiconductor 1. The difference in chemical potential leads to band bending at the interface of the junction, which in turn drives the photogenerated holes and electrons to move in opposite directions across the built-in field.[76] This causes the charge separation which is desired for increasing the lifetime of charged particles, giving the material the potential for improved efficacy for water treatment.

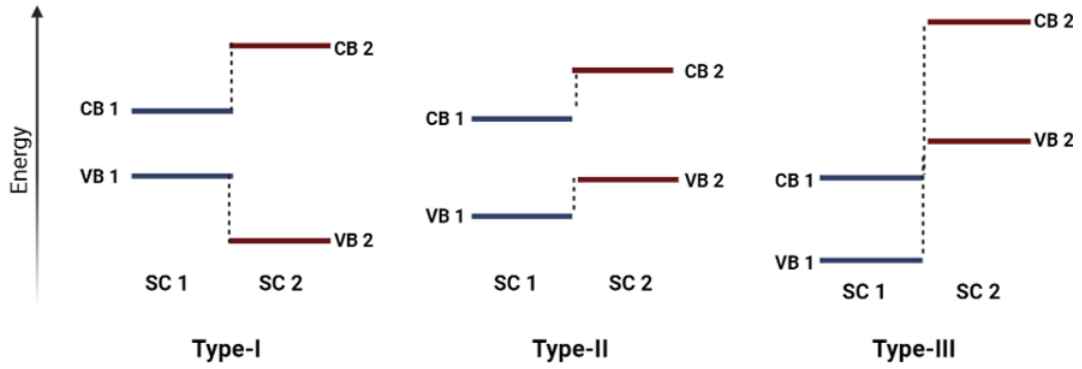

Figure 1.5: Schematic to indicate the different types of heterojunction band gap structure, where "SC" is semiconductor, "VB" is valence band and "CB" is conduction band.

As well as changing the chemical properties, the practicalities of the system in which the photocatalyst is deployed in are also important. One barrier which limits the practicality and usability of solar photocatalysis is the need to recapture the catalyst material once the treatment has finished. Most photocatalysts exist as nanoparticles, and as such are extremely difficult to extract from water, especially without access to expensive instruments such as centrifuges and fine porosity microfilters. This significantly limits the re-usability of the photocatalyst and hence the appeal, simplicity and cost-effectiveness. As a result, immobilising the photocatalyst onto a support which can be easily extracted from the water has become the focus of many research endeavours. Indeed, this is one of the most important practical issues to address in order to make such a treatment

method feasible and safe. Without sufficient immobilisation, photocatalyst material can lead into the water, resulting in loss of material and thus a drop in activity with repeated use, as well as the more serious issue of any possible health impacts caused by repeated consumption of suspended photocatalyst particles.

The morphology of the photocatalyst is also extremely important to consider. Despite the advantage of having a photocatalyst with a small particle size, and thus high surface area, meaning the rate of photocatalytic degradation is high relative to larger particles, this has also led to health concerns. Much research has been conducted to suggest that nanoparticles could be detrimental to health, so a catalyst with particle size as small as P25 TiO_2 should arguably be avoided for low-cost water treatment methods. For large-scale industrial processes with sufficient capacity to completely remove any catalyst particles that enter the water supply, this would not be of major concern, but for the specific application of rural areas which will not necessarily have access to ultra-centrifuges or micro-filters, larger particles may be more appropriate in the event of particle leaching off the support it is immobilised on.

Environmental science research suggests there are toxicological effects of ultra-fine particles (those less than 100 nm in diameter[77]). Several studies have been conducted on animals to investigate the toxicology of TiO_2. One study was conducted whereby mice were injected with solutions of 150 mg/kg lab-synthesised TiO_2 with an average grain size of 5 nm, and their organs analysed for titanium content via ICP-MS analysis.[78] It was found that this TiO_2 (5 nm) entered organs of mice more easily than a control sample of bulk TiO_2 (15-20 μm in size). The order of titanium accumulation in the organs was liver > kidneys > spleen > lung > brain > heart. Parameters for assessing organ damage all increased significantly after the study (these include enzymes and hormones typically released when organs are damaged). It was therefore concluded that nano-anatase TiO_2 of doses higher than 10 mg/kg had toxic effects and an inflammatory response for the liver, kidney and myocardium of mice, as well as metabolism imbalance of blood sugar and lipid.

Another study found that TiO_2 can induce DNA damage and genetic instability in

mice.[79] This study is particularly useful when considering the potentially harmful effects of using P25 TiO_2 for water treatment in rural areas, as the mice used in the study were exposed to TiO_2 *via* addition of the nanoparticles to their drinking water. Thus it gives insight into the effects of ingestion, as opposed to inhalation or injection. It was found that TiO_2 induced DNA deletions, breaks in the double-strand structure and inflammation.

TiO_2 was classified as a group 2B carcinogen by the IARC (International Agency for Research on Cancer – part of the WHO) in 2010 – a substance that is "possibly carcinogenic to humans" via inhalation. According to the assessment report in which TiO_2 is so classified, it states that studies that used ultra-fine or nano-sized TiO_2 particles ($\sim$ 20 nm) showed enhances toxicity relative to the fine particles ($\sim$ 250 nm) studied previously in the 1989 report by IARC on TiO_2. This could suggest that moving towards larger particle size would alleviate some of the health concerns with prolonged exposure to titania, and outweigh the negative effect of a reduction in photocatalytic activity. In this sense, the larger particle sizes, which are traditionally seen as a disadvantage, may help to improve safety, and therefore user acceptance.

Much research into development of photocatalysts is focused on application to industrial settings, either for water treatment or chemical synthesis, where economic concerns are less of a limitation. For implementation in rural India, it is crucial that any proposed water treatment system be affordable. As a result, the use of low-cost materials is a basic criterion for developing photocatalysts intended for such an application, rather than scientific advancement and interest alone. Further detail on material development of novel photocatalysts is given in Chapters 5 and 6.

1.2.2.3 The Importance of Field Testing for the Advancement and Implication of Photocatalysis

Despite work being conducted to address the barriers to implementation outlined in Sections 1.2.2.2 and 1.2.1, a gap in academic research is the correlation between laboratory findings and practical implementation. There have been many exciting advancements

made in this field, with many promising new materials being proposed (as discussed in more detail in Chapters 5 and 6), but the testing of new materials and reactor systems is typically limited to being conducted under idealised or simulated conditions, which may over-represent the success of technology, and under-represent the practical limitations. In order to fully evaluate the suitability of any newly developed photocatalytic system designed with the intention of applying to treating water under solar illumination, field testing must be conducted.[80]

Examples of field tests that have been conducted under solar illumination exist in the literature and show promising results, but are often conducted with a stirred system of nanoparticles, rather than immobilised catalysts. For example, a ZnO suspension was employed by Vela et al.[81] to remove various endocrine disruptors under solar irradiation with water flowing through tubes lined with reflective solar concentrators and a large tank (250 L) for mechanical stirring. Although the pilot plant was successful for removing the studied contaminants, such systems are not practical for the specific context of rural Indian villages, which may lack electrification and the resources necessary for maintenance.

Much field testing of TiO_2 was conducted to establish the material as a potential option for water treatment in the late 1990's and early 2000's. For example, a study conducted by Herrmann et al.[82] in 1999 showed that the use of a suspension of titania added to water allowed for an enhanced rate of degradation of 4-chlorophenol relative to that achieved with SODIS. However, this study used compound parabolic concentrators (CPCs) and a pump to allow for the flow of water through a series of tubes, as shown in Figure 1.6. Although this set up significantly helps to increase efficiency, unfortunately the use of a suspension rather than immobilised photocatalayst, as well as the use of a pump which would require a source of electricity and added installation costs, this set-up is not applicable for many rural villages.

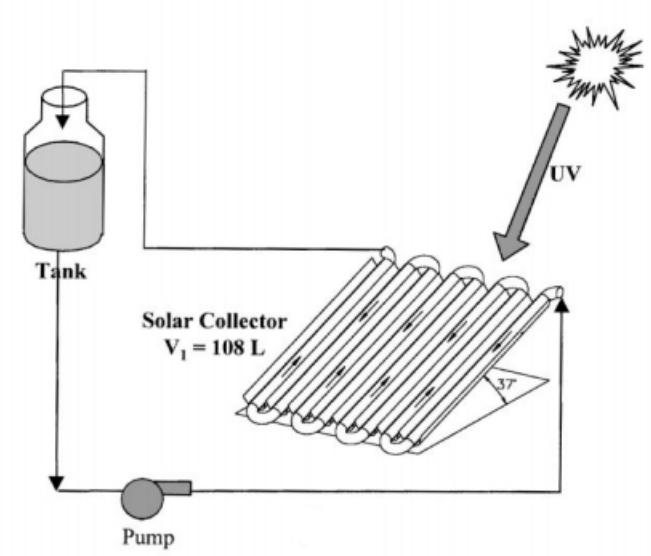

Figure 1.6: Schematic presented by Herrmann et al.[82] to indicate the operation of the pilot water treatment system used in their 1999 study, presented with permission from Elsevier Publishing.

This is a typical example of how field testing is often conducted and reported in the literature, with many other studies existing that included similar set-ups for pilot-scale titania-based photocatalytic systems, using free suspensions, pumps and CPCs.[25,83–85] These studies confirmed the potential for photocatalysis to practically enhance SODIS for a range of both chemical and biological contaminants, though the implementation is questionable, particularly considering the resources available to many communities such treatment types are targeted for (as discussed in Section 1.2.1).

Building on such foundational studies, some field testing has been reported whereby the photocatalyst employed is immobilised, helping to increase the practicality of the treatment process. One such example is the study by Gelover et al,[86] which used TiO_2 immobilised on glass cylinders (4 mm internal diameter, 6 mm external diameter, 6 mm long) *via* a sol-gel method. These cylinders were inserted into 2 L PET bottles which were 3/4 filled, leading to an estimated 87.5 mg of TiO_2 per litre of water. This study also presents a possible means of improving accessibility by employing a home-made solar collector, referred to as a solar box throughout the study, which was produced from five wooden squares all coated in aluminium foil: one as the base for the bottle to be placed on, and the rest placed around the sides at 30° to the vertical axis. The study found that the presence of TiO_2 significantly increased the efficiency of the system. Further, bacte-

rial regrowth was observed after 1 day for the water treated through SODIS alone, but no detectable regrowth was observed for the water treated with photocatalysis. This is an extremely promising study that has laid good groundwork for the practical implementation and feasibility of photocatalysis for water treatment. However, the glass cylinders used are likely to be fragile, and the custom design will increase the costs of the system, as well as limit the availability of necessary parts. The same applies for the solar collector, though it is more convenient that the specially designed CPCs employed in many other studies. The study also did not explore the long term stability of the photocatalyst coating, damage to which would lead to flaking of the catalyst and thus contamination of the water supply. It is important to understand the lifetime of a photocatalyst coating before the possible implementation of the treatment, in order to avoid health repercussions.

A 2004 study by Duffy et al.[87] highlighted the benefit of titania photocatalysis over SODIS for removing both chemical and biological pollutants, as SODIS is less effective for chemical decontamination. They also explored the important concept of immobilisation of the photocatalyst to mitigate the difficult recapture logistics. However, the testing in this study consisted of using natural solar irradiation for bacterial studies, but simulated light sources in a laboratory with a test volume of only 30 mL for the chemical tests, which does not closely match real-world conditions.

Using ZnO rather than TiO_2, Danwittayakul et al. conducted a study which included both preliminary laboratory testing as well as field testing of a prototype photocatalytic reactor for enhanced SODIS, performed under natural sunlight in Thailand.[88] The water treatment was performed inside an LDPE bag, with ZnO immobilised onto polyester and cellulose supports. The bag was placed on a black surface to encourage heating.

Their laboratory studies determined that the polyester support allowed for slightly higher degradation efficiencies, which were then used for the field tests, for which a sample of 10^7 colony forming units per mL (CFU/mL) of *E. coli* in water was used. It was observed that a 98% inactivation of *E. coli* could be achieved within 15 minutes of exposure to sunlight. The experiments were repeated for 5 consecutive days, using the same set of photocatalysts each time, with no visible degradation of the photocatalysts occurring and

bacterial inactivation still occurring consistently. Zinc was detected through ICP-OES to leach into the water, though the extent of this leaching decreased each day over the course of the study. The UV intensity and temperature of the water were also tracked over the course of the experiment, which is very useful to quantify the rates of photocatalytic disinfection, such that any fluctuations in observed activity can be more easily explained for an accurate evaluation of the efficacy of the treatment system.

Though this study extended testing to 5 days of repeated use in order to evaluate stability, there was no quantification of how long the photocatalyst films may last with long term use, and how their stability is affected by any physical or chemical factors they may be exposed to during continued use by non-researchers, as intended. Indeed, this highlights some of the gaps which are present in the literature with regards to field testing.

Despite the numerous studies across the literature that focus on filed trials of photocatalysis, particularly framed in the context of enhanced SODIS, there still remains a significant gap between academic interest and industrial- or household-scale application. Though these studies have allowed for significant progress in the field of photocatalysis, helping researchers to understand the differences between laboratory and practical conditions, there is still crucial information missing.

Firstly, most studies conduced in the field refer to studies under natural sunlight, not necessarily under the exact conditions they are intended for. For example, many studies, including those discussed above, use specially prepared solutions of water spiked with a specific pathogen or chemical and track its loss over the course of treatment. However, studies have shown that the efficiency of photocatalysis depends on the composition of the water itself,[85,89] and as such it is important to understand what the main contaminants of concern are for different regions where the technology may be deployed, and how this can effect the short- and long-term function of the photocatalysts. For example, some areas may be more prone to chemical contamination, such as industrial run-off, including from pharmaceuticals and chemical industries, which will alter the composition of the water that needs to be treated. The chemical composition of water is very significant, as not only can it affect the activity of the catalyst, but it can also contribute to which

microbes are able to grow, and how resistant they may be to treatment. A particularly dangerous example of this is antibiotic resistance.[3]

Further, as discussed in Section 1.2.1, turbidity is an important factor that will affect the treatment, which is tied to the content of the water. The hardness of the water will also be important for catalyst function and lifetime, as the deposition of minerals on the catalyst surface can reduce the number of active sites available for the remove of organic contaminants, as well as lead to fowling and a reduction in the lifetime of the catalyst. Thus, without considering the content of, or using water directly collected from communities identified as being good candidates for such a water treatment type, important information is missed.

This also plays into the reusability and lifetime of the photocatalyst, as water with a higher concentration of contaminants will likely lead to a more rapid decline in activity. This will require either more frequent replacement of the catalyst, or the use of techniques to regenerate the catalyst, such as washing or calcination, which may not be possible in many of the rural communities the treatment is intended for. Ideally, studies should be conducted over long-term periods of investigation, in order to track closely how the treatment systems fare with the daily use that they would be require for.

Another extremely important factor that is rarely considered in practice is the possibility of any health implications from photocatalytic water treatment systems, such as catalyst leaching or the formation of side products if degradation is not complete. Although TiO_2 is considered chemically and biologically inert and non-toxic, studies suggest that the presence of nanoparticles in water can be hazardous to human health.[90] This further confirms the importance of long-term testing of the quality of photocatalyst coatings, as leaching of the catalyst into the water intended for consumption may be problematic after prolonged periods of ingestion.

Further, many studies are conducted at a batch or pilot scale, which would require the use of specially designed vessels, where many people can only access commercial PET bottles of 0.5 - 2 L. Again, in this sense, the practicality of installation and ease of use

should be carefully considered. Is the higher cost of installation that may be associated with these types of system off-set by an more efficient process and ease of treating larger volumes, or is it too high and difficult to operate that use is not able to be realised? These are important questions which must be answered before systems are installed.

Finally, there is a clear need to consider social science and the likelihood of rural communities adopting a new treatment system, as well as simply if it can work in practice, rather than simply the chemistry, physics and biology that's in play. Although such research can prove that photocatalysis allows for a more significant bacterial inactivation and chemical degradation than SODIS, as well as other methods such as boiling or chlorination, it rarely provides insight into societal perceptions and how easy, safe and practical continued use is. For example, studies considering the financial situations of target communities would help to access whether or not a novel photocatalyst or reactor system is actually affordable by those it is designed for. Further, cultural and social practices will play into how much water is consumed daily, and thus how much is required to be treated, with the comparison of efficiency in different volumes of vessel rarely compared or commented on. The way water is stored and used will also effect how long it can remain uncontaminated for, with transfer to other vessels being a mode for recontamination. Thus, understanding social practices, attitudes and education levels is an extremely important factor to keep in mind and explore in order to take this technology from a largely research phase to being used by vulnerable communities to provide a real benefit.

For long-term, safe and reliable use, it is crucial that the water treatment system remains affordable, simple to operate, and favourable to rural communities, so performing studies that confirm this in practice are crucial for bridging the gap between academic interest and real-world application.

1.3 Water Quality Parameters and Standards

In order to fully appreciate the efficacy of photocatalysis as a method for water purification, it is critical to first appreciate the types of contaminants most prevalent in drinking

water sources and the concentrations of such pollutants relative to the guidelines for what should be expected for safe, potable water.

1.3.1 Ionic and Particulate Contaminants

Useful parameters used to measure the extent of particulate pollution are the total dissolved solids (TDS), salt levels and conductivity of a given water sample. According to the WHO, TDS levels should not exceed 1000 ppm for potable water,[91] and is optimum for palatability between 300 and 600 ppm,[92] and significantly below this range the content of essential minerals may be too low (e.g. below around 100 ppm). However, it is also noted by WHO that the exact correlation between health consequences and TDS levels cannot be explicitly defined without knowing the components of the dissolved content in the water.

For the case of India in particular where it is more common to use decentralised water sources such as wells, the extent of such contamination strongly correlates to the means of its collection. For example, groundwater sourced from wells is likely to be rich in mineral contaminants and result in hard water, where as surface water sources from rivers and ponds is often softer, but also more exposed to bacterial contaminants. With this example in mind, it is clear that characterisation of a water source intended for purification is performed in order to reveal the identity of the target pollutants to be removed, such that the most effective method for that given pollutant is employed.

1.3.2 Chemical Contaminants

Due to rapid development in many industries to improve the quality and convenience of modern-day life, chemical contamination of water sources is becoming much more frequent and severe. For example, an unfortunate consequence of improved medical access is the pollution of water sources with pharmaceutical materials, particularly antibiotics. According to the European Medicines Agency (EMA),[93] the potential environmental risk is defined as a risk quotient (RQ) given by:

$$\mathrm{RQ} = \frac{\mathrm{PEC}}{\mathrm{PNEC}} \tag{1.1}$$

where PEC is the predicted environmental concentration (the calculated concentration of a given contaminant is the environment based on exposure models), and PNEC is the predicted no-effect concentration (the maximum concentration of a contaminant that can be present for no adverse effects of exposure in an ecosystem to be measured). In the guidelines presented by EMA, it is stated that: *"If the PEC value is below 0.01 µg/L, and no other environmental concerns are apparent, it is assumed that the medicinal product is unlikely to represent a risk for the environment following its prescribed usage in patients"*. However, according to a study conducted by Espindolda et al. in 2020, many contaminants of emerging concern (CEC)were detected in water supplies above this limit,[94] including those listed in Table 1.1.

Table 1.1: Pharmaceutical CECs in water supplies, compiled by[94]

CEC	Use	Molecular formula	Where Detected	Concentration (µg/L)
Azythromycin	Antibiotic used to treat chest infections, skin infections, Lyme disease, and some sexually transmitted infections	$C_{38}H_{72}N_2O_{12}$	Surface water	0.06 - 0.1
			Wastewater	0.66-1.68
Oxytetracycline	Broad spectrum antibiotic against a range of bacterial infections	$C_{22}H_{24}N_2O_9$	Surface water	0.34
			Wastewater	0.35
Ibuprofen	Nonsteroidal anti-inflammatory painkiller	$C_{13}H_{18}O_2$	Groundwater	0.05
			Surface water	1.0
			Wastewater	4.1
Amoxicillin	Penicillin-type antibiotic used to fight infections such as in the nose, ear, throat, skin or urinary tract	$C_{16}H_{19}N_3O_5S$	Surface water	0.2
			Wastewater	6.9
Diclofenac	Nonsteroidal anti-inflammatory painkiller.	$C_{14}H_{11}Cl_2NO_2$	Groundwater	0.04
			Surface water	0.14-0.31
			Wastewater	0.61-2.43

If the ratio of PEC to PNEC gives a RQ of below 1, further testing of the water is not necessary and it can be concluded that the substance and/or its metabolites are present in safe quantities. For a quotient above 1, further evaluation of the effects of the drug on the aquatic environment and human health are required.[93] These parameters define the risk of particular chemical contaminants for causing environmental damage, such as to aquatic life, but do not specifically outline the dangers to human health alone. However, they are still useful guidelines for understanding which pollutants are important to try reducing such that toxicity levels are not reached and aquatic as well as human life is

protected. With regards to human health specifically, the following toxicity calculation can be applied:

$$\mathrm{GV} = \frac{\mathrm{TDI} \times bw \times P}{\mathrm{C}} \tag{1.2}$$

where GV is the guideline value, TDI is the tolerable daily intake, bw is body weight, P is the fraction of the TDI allocated to drinking water (as opposed to other sources of ingestion) and C is the daily drinking-water consumption. TDI is estimated for a given person based on their weight and the amount of a substance that can be ingested over a lifetime without appreciable health risk. Thus, if the detected level of a given chemical contaminant exceeds the GV, more enhanced purification methods must be employed in order to reduce the risk to human health. Given that the quantities of pollutants can often exceed the safe guideline PEC level, and that full toxicity information over prolonged periods is not always well understood, particularly for CECs which have not always been found in water supplies and are thus not well monitored, the potential for many chemical contaminants to exceed the guideline GV is high. This implies robust water treatment methods are required, both in rural and urban settings, to control the composition of water to be within safe, recommended guidelines.

As well as the direct health impacts caused by human consumption of water contaminated with pharmaceutical substances, there is also the general risk of antibiotic resistance caused by this, increasing the extent and robustness of potentially harmful bacterial contamination. A study by Helwig et al.[95] identified many commonly used medical substances in Scottish hospitals that have RQ's higher than 1, meaning further work needs to be done to reduce the levels of such contaminants entering the water supply leaving the hospital in order to prevent environmental damage and the rise of antibiotic resistance.

However, pharmaceuticals are not the only class of chemical contaminants which pose a threat to human health. Additional emerging contaminants include dyes from the clothing industry, surfactants and detergents from hygiene products, endocrine disruptors and pesticides. The European Union Water Framework Directive (EUWFD) sets

guidelines for the presence of such contaminants.[96] For example, it has designated the removal of commonly used pesticide pentachlorophenol (PCP) as a priority on account of its renal, carcinogenic and neurological effects. PCP and other examples of molecules from these hazardous materials classes were used in a study by Odling et al.,[97] demonstrating the ability of photocatalysis to effectively remove such contaminants. Further non-pharmaceutical CECs are listed in Table 1.2, though this list is not exhaustive.

Table 1.2: Examples of common non-Pharmaceutical CECs in water supplies, compiled by[94]

CEC	Use	Molecular formula	Where Detected	Concentration (μg/L)
Galaxolide	Synthetic compound with sweet floral odour, used in perfumes and detergents	$C_{18}H_{26}O$	Groundwater	0.043
			Surface water	0.2-4.8
			Wastewater	25
Tonalid	Synthetic fragrant oil used in cosmetics	$C_{18}H_{26}O$	Groundwater	7.5×10^{-3}
			Surface water	0.95
			Wastewater	1.9
Progesterone	Female sex hormone, often prescribed in birth control medications and to treat various medical conditions	$C_{21}H_{30}O_2$	Groumdwater	$2.8\text{-}4.1 \times 10^{-3}$
			Surface water	0.2
Estradiol	Female sex hormone (main estrogen), often prescribed in birth control medications and to treat various medical conditions	$C_{18}H_{24}O_2$	Groundwater	0.1×10^{-3}
			Surface water	0.01-0.2
Estrone	Female sex hormone(estrogen), also used to treat various medical conditions	$C_{18}H_{22}O_2$	Groundwater	1.1×10^{-3}
			Surface water	4.6×10^{-3}
			Wastewater	0.01-0.18
Estriol	Female sex hormone (estrogen), also used to treat various medical conditions	$C_{18}H_{24}O_3$	Groundwater	0.16×10^{-3}
			Surface water	1.9×10^{-3}
			Wastewater	4.9×10^{-3}
Testosterone	Male sex hormone, also prescribed to treat various medical conditions	$C_{19}H_{28}O_2$	Groundwater	$4.3\text{-}6 \times 10^{-3}$
			Surface water	0.21
Clomazone	Agricultural herbicide	$C_{12}H_{14}ClNO_2$	Groundwater	2.7 - 10.8
			Surface water	3.2 - 15.7
Carbendazim	Agricultural fungicide, not approved for use in the EU	$C_9H_9N_3O_2$	Groundwater	1.6
			Surface water	0.2 - 4.5
			Wastewater	0.014 - 0.078
Nicotine	Central nervous system and parasympathetic nervous system stimulant, often used in cigarettes	$C_{10}H_{14}N_2$	Groundwater	8.07
			Wastewater	1.1 - 14.6
Caffeine	Central nervous system stimulant, often used in beverages	$C_8H_{10}N_4O_2$	Groundwater	0.045
			Surface water	6.0
			Wastewater	66

As introduced in Section 1.2.1, the presence of endocrine disruptors in water sources used for drinking can lead to serious health consequences, with several of the CECs listed in Table 1.2 being identified as EDs. Further, several of the CECs in Tables 1.1 and 1.2 are harmful to aquatic life, so should not be allowed to build up in water. In order to help

gain a clear understanding of health impacts of certain chemicals that enter water systems, and thus be able to define a TDI, study and monitoring is required. In an attempt to regulate particularly potent or recurring contaminants with potentially serious ability to harm either human health or the environment, in 2015 the European Union launched a watch list of primary substances or groups of concern which were to be monitored. This list includes hormones such as estrogens (of natural and synthetic origin); pharmaceuticals such as the antibiotic clarithromycin, amoxicillin, and erythromycin; pesticides such as acetamiprid, metaflumizone, and triallate; as well as others from industries such as personal care and chemical synthesis.[98,99] There is still much classification and monitoring that is required in order to fully understand what the safe guideline quantities for the full extent of possible chemical contamination, but it remains clear that a water treatment system that is effective against a broad range of chemical contaminants is crucial for maintaining both a healthy environment, as well as healthy consumers.

According to a 2009 statement from The Endocrine Society,[37] assessing a particular substances potential to be an ED is not a straight forward task, as the mechanisms through which they can act are much broader than originally recognised. There are many biologically pathways that can be interacted with, making the potential for disruption from a foreign chemical very high. Molecules identified as EDs include both naturally occurring and synthetic chemicals. Synthetic EDs include industrial solvents and lubricants (e.g. polychlorinated biphenyls (PCBs), polybrominated biphenyls (PBBs), dioxins), pesticides (e.g. methoxychlor, chloropyrifos, dichlorodipenyltrichloroethane (DDT)) fungicides (e.g. vinclozin), pharmaceutical agents (e.g.diethylstilbestrol (DES)), and plastics (e.g. bisphenol A (BPA)). Natural EDs include phytoestrogens, which are found in food, including genistein and coumestrol. Difficulty in categorising materials as EDs arises due to the range in structure and lack of general structural similarity, though typically they tend to be less than 1000 Daltons in molecular weight and contain halogen substituted groups, as well as a phenolic moiety, which is thought to mimic natural steroid hormone receptors as analogues or antagonists. It has also been suggested that heavy metals and metalloids can even behave as EDs. This emphasises the importance of exercising caution with regards to defining the standards for safety of drinking water, and that a treatment method that can remove as many chemical contaminants as possible would be extremely

valuable for ensuring no adverse health effects over short- and long-term time frames.

Chemical contaminants can also cause harm to humans outside of endocrine disrupting effects, being toxic or harmful through other routes. It is generally considered that aromatic hydrocarbons are more hazardous than aliphatic hydrocarbons with respect to narcotic effect, irritation and fatality.[100] However, it must also be considered that the size and complexity of molecules within the subclasses of aromatic and aliphatic will vary, with consequences on their relative health impacts. For example, it has been observed that branched aliphatic hydrocarbons are less potent that the straight side chain hydrocarbons of the same molecular mass in terms of their ability to affect the nervous system. Additionally, it is generally found that the longer the chain, the higher the extent of skin irritation and narcotic action that can be caused.[100]

Though variation is observed, it is generally found that aliphatic hydrocarbons become more detrimental to health from paraffins, olefins, cycloparaffins and unsaturated cycloparaffins, respectively. Typically, aromatic hydrocarbons have a lower minimum dose to reach narcotic or fatal effects relative to the former aliphatic groups.[100] An example can be given for hexane, cyclohexane, and benzene, where hexane and cyclohexane are comparable in terms of safety, and benzene is significantly more hazardous. Hexane is known to have negative consequences for the nervous system and is classified as a neurotoxin.[101] Cyclohexane can cause depression of the central nervous system and, at high concentrations, has narcotic effects.

However, it does not have adverse effects on the blood, through which it is transported around the body following inhalation. Benzene, on the other hand, does have toxic effects on the blood and is also a well known carcinogen. It can also cause convulsions, paralysis and fatalities from severe exposure. Milder exposure can still lead to significant issues such as breathlessness, dizziness, nausea, headaches and intoxication.[101] In a review of the toxicity of commonly used solvents,[102] on a three point scale of *preferred, usable* and *undesirable*, hexane and cyclohexane were both classified as *usable*, whereas benzene was in the *undesirable* category. Thus, the use of benzene as a solvent is uncommon due to its high toxicity and carcinogenic nature, highlighting the increased risk to health of

aromatics relative to aliphatic and saturated cyclic analogues.

Additionally, phenols, hydroxylated benzene products are known to be toxic, and can also form during metabolism of ingested benzene,[100] further increasing the health risk. Preferential removal of more complex structures with properties such as aromatic moieties, halogen substituents, and high molecular mass would be beneficial to ensuring the safety of drinking water.

1.3.3 Microbes and Pathogens

As well as chemical contaminants and any other physical debris present in water, microbes must also be removed before human consumption. However, just as with chemical contaminants, not all microbes present in water pose any clinical threat to humans, and so water treatment methods only need to focus on removing those microbes that may cause illness i.e. the pathogens. In order to appreciate which pathogens are more susceptible to certain treatment methods than others, and thus understand which treatments may be more appropriate for certain locations, and which may need developing further, it is crucial to have an understanding of the different structures and various adaptations of certain pathogens that give rise to these behaviours. There are five classes of microbes:

1. Bacteria (prokaryote)
2. Archaea (prokaryote)
3. Viruses (non-living)
4. Unicellular fungi (eukaryote)
5. Unicellular protists (eukaryote)

The archaea are non-pathogenic, and as such are not considered as a contaminant which is necessary to remove from water intended for drinking. The other classes of microbes listed above contain species that are either harmless, good, or pathogenic to humans. Key differences between the microbe groups are presented in Table 1.3 (note: Mb and Kb refer to megabases and kilobases of nuceotides respectively):

Table 1.3: Classes of Microbes

Feature	Bacteria	Archaea	Unicellular Protists	Unicellular Fungi	Viruses
Size	0.2 - 5 μm	0.2 - 5 μm	10 - 100 nm	10 - 100 nm	20 - 200 nm (giant up to 1 μm)
Genome size	0.13 - 14 Mb	0.5 - 5.7 Mb	8 - 140 Mb	8 - 15 Mb	3 Kb - 1.2 Mb
Genome	Single circular dsDNA	Single circular dsDNA	Linear dsDNA	Linear dsDNA	Linear or circular, ss or ds RNA, or ss or ds DNA
Nucleus	no	no	yes	yes	no
Membrane-bound organelles	no	no	yes	yes	no
Contain peptidoglycan	contain peptidoglycan	lack peptidoglycan	some contain cellulose	chitin	no cell walls
Cell membranes	Ester-linked lipids	Ester-linked lipids	Ester-linked lipids	Ester-linked lipids	May have envelope derived from host membrane

The different structures and various adaptations of species within these groups influences their ability to survive in certain environments, and even resist traditional methods of inactivation, such as commonly used chlorination. For certain pathogens, this is becoming increasingly concerning as phenomena such as antibiotic resistance and vaccine hesitancy are rising, both of which are listed in the World Health Organisation's top 10 biggest threats to global health,[103] which can increase the potential impact and degree of harm caused by certain pathogens if humans should become exposed to them. In this section, focus will be given specifically to water-borne pathogens that are necessary to remove to ensure water is safe to drink, rather than hazardous pathogens in general that aren't primarily found in water supplies (such as those transmitted through alternate routes e.g. those that primarily grow in food or are airborne).

Due to the possibility for certain microbes to cause disease when ingested, guidelines for the presence of such contaminants in water are quite strict. For example, guidelines published by the WHO for safe drinking water state: *"Ideally, drinking-water should not contain any microorganisms known to be pathogenic — capable of causing disease — or any bacteria indicative of faecal pollution. To ensure that a drinking-water supply satisfies these guidelines, samples should be examined regularly. The detection of Escherichia coli provides definite evidence of faecal pollution; in practice, the detection of thermotolerant (faecal) coliform bacteria is an acceptable alternative".*[104]

It is clear from this statement that, for water to be classed as suitable for human consumption, there must be no pathogens present, such that the risk of becoming ill is

mitigated. Unfortunately, there is often a shortfall in meeting this criterion in many parts of the world, highlighting the need for increased understanding of which pathogens may be causing illness and how they behave in certain conditions, specifically those relevant to where the water was sourced from, how it was cleaned (if at all), and how it was stored, all of which will contribute to the microorganisms present upon ingestion.

1.3.3.1 Bacteria

When considering pathogens in water, bacteria are probably the most widely studied group, particularly with regards to treatment using photocatalysis, which is likely due to the relative ease in culturing and studying them compared to other pathogenic groups. Their variety and adaptability also pose a significant threat to human health, confirming the importance of their inclusion in such studies. Bacteria are able to replicate very rapidly in favourable conditions, and as such it is important that they are removed from water to a point where they are no longer detectable, or it could be possible that any remaining after treatment could replicate and reach content levels that would be able to pose serious health risks.

Bacteria are roughly categorised into two sub-groups: Gram negative (e.g. *E. coli*, *Legionella*) and Gram positive (e.g. *Enterococci*). This grouping system is determined by structural differences and how this affects stability, whereby Gram positive bacteria have a thick cell wall consisting of many layers of peptidoglycan;[105] a polymer made up of linear glycan strands (specifically containing residues of N-acetylglucosamine and N-acetylmuramic acid) cross-linked by short peptides, which forms a mesh-like structure.[106]

Gram negative bacteria, on the other hand, have a much thinner cell wall made up of a single layer of peptidoglycan, but this layer is sandwiched between two layers of cell membranes:[105] the inner layer is a standard phospholipid bilayer, where as the outer bacterial membrane has a slightly different structure, containing lipopolysaccharide (an endotoxin that can cause an aggressive response from the immune system of an infected individual and can lead to toxic shock) as well as other proteins such as porins. The structure of the peptidoglycan found in *E. coli* cell walls in shown in Figure 1.7.

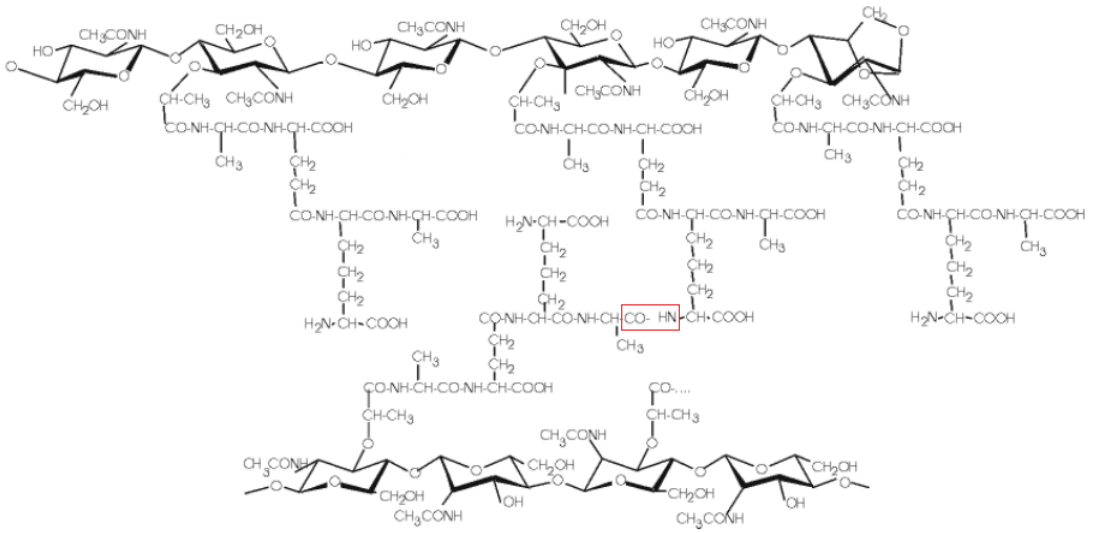

Figure 1.7: Structure of peptidoglycan found in *E. coli*, as adapted from Mengin et al.[107] Note the peptide linking bond shown in the red box.

The two types of bacteria can be differentiated by performing the Gram staining test, which is essentially used to detect peptidogylcan, where the final result of the test results in Gram positive bacteria staining purple, and Gram negative staining pink. Both can be pathogenic, and have adaptations that can make each category more resistant to certain pressures than the other. The structure of the cell walls plays a significant role in the resistance of a given bacterium, but the response to stresses can be complex, so it is not the only factor to consider. For example, it has been found that some Gram negative bacteria are more resistant to certain antibiotics, such as penicillin, detergents that could normally break down peptidoglycan, and the antimicrobial enzyme lysozyme which is produced by animals as an immune response, as a result of their cell wall being harder to penetrate due to the presence of the outer membrane.

In contrast, Gram positive bacteria such as *Enterococci* have been observed to be more resistant to chlorination[108] and UV than Gram negative bacterium *E. coli* as a result of the thicker layer of peptidoglycan. Bacteria can also produce proteins to repair cell damage as well as other survival mechanisms such as aggregation, and attachment to surfaces.[108] Further the composition of water is important, with one study finding Gram positive bacteria to be more resistant chlorine, but once organic matter was added to the water, the Gram negative bacteria became more resistant,[109] due to stabilisation against permeabilisation of the membrane (an effect present for both groups but more

significant for Gram negative). Indeed, the study by[109] suggests that extensive membrane damage is not the primary cause of cell inactivation as a result of chlorination, but rather the occurrence of more subtle events, such as uncoupling of the electron chain or enzyme inactivation, though the envelopes (outer membrane) present in Gram negative bacteria play an important role in resistance to chlorine in the presence of organic matter, which is postulated to be due to the accessibility of chlorine to targets within the cell.

Structural differences are presented in Figure 1.8.

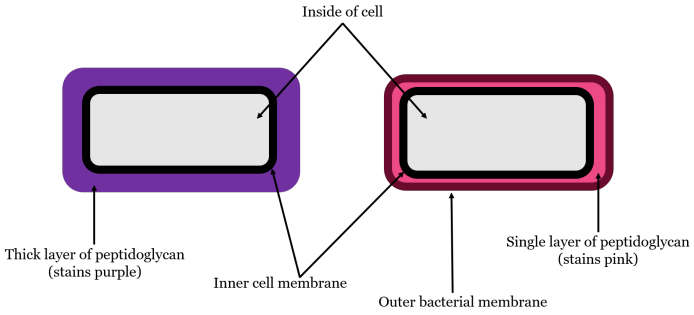

Figure 1.8: Difference in cell wall structures for Gram positive (left) and Gram negative (right)

There have been many studies throughout the literature that indicate photocatalysis is promising for the removal of both gram positive and gram negative bacteria.[64,110–112] This is key to the importance of applying photocatalysis to this context, as bacterial content can often be the leading cause of ill health caused by drinking poor quality water. Bacteria of concern to human health are shown in Table 1.4

Table 1.4: Waterborne bacteria of concern, as listed by the WHO[91]

Bacterial Pathogen	Health Significance	Persistence in Water Supplies	Resistance to Chlorine	Relative Infectivity	Important Animal Source
Burkholderia pseudomallei	High	May multiply	Low	Low	No
Campylobacter jejuni, C. coli	High	Moderate	Low	Moderate	Yes
Escherichia coli – Pathogenic	High	Moderate	Low	Low	Yes
E. coli – Enterohaemorrhagic	High	Moderate	Low	High	Yes
Legionella spp.	High	May multiply	Low	Moderate	No
Non-tuberculous mycobacteria	Low	May multiply	High	Low	No
Pseudomonas aeruginosa	Moderate	May multiply	Moderate	Low	No
Salmonella typhi	High	Moderate	Low	Low	No
Other salmonellae	High	May multiply	Low	Low	Yes
Shigella spp.	High	Short	Low	High	No
Vibrio cholerae	High	Short to long	Low	Low	No
Yersinia enterocolitica	High	Long	Low	Low	Yes

There are multiple strains of *Escherichia coli* (*E. coli*); some are harmless to humans, others are pathogenic. The detection of *E. coli* in water is used as a marker of faecal contamination due to its presence in the intestines of humans and other animals. For this reason, *E. coli* is one of the most widely studied bacteria, particularly with respect to public health, which is reflected in it being highlighted in guidelines for microbial content published by the WHO, which states: *"there should be no E. coli detectable in any 100 mL sample of water intended for human consumption, and no more than 10 coliform organisms in 100 mL"*.[104,113] (Note here: coliform bacteria are defined as being rod-like, gram-negative, non-spore forming bacteria, which can ferment lactose to produce acid and gas when incubated at 35-37 °C. *E. coli* is an example of a coliform bacterium).

Although it is understood that *E. coli* is susceptible to inactivation *via* SODIS, as well as photocatalysis, it is important to still include this species of bacteria in studies on the efficacy of photocatalytic water treatment systems. This is due to it acting as a marker for faecal contamination, which can often imply the presence of other, more potentially harmful pathogens which are harder to study but also are spread primarily through faeces. Further, being able to remove *E. coli* acts as a proof of concept and validates the treatment method as being worthy of continued study, as the removal of *E. coli* is often tested in the first instance when considering pathogenic inactivation.

The fact that *E. coli* does not form spores is important to understanding why it is readily inactivated by many traditional water treatment methods. Some bacteria, can form spores that have a thicker outer cortex made of peptidoglycan as well as being able to produce specialised proteins like small acid-soluble proteins (SASPs) which bind to the DNA and shield it from UV, high temperatures and the action of certain enzymes.[114] They can also have much more efficient DNA repair machinery to correct the mutations caused by radiation. Bacteria with such adaptations can survive the harsh conditions induced through water treatment and persist. For *E. coli*, as well as other species, not being able to form these resilient spore phases as a response to low nutrients or unfavourable conditions makes them much easier to inactivate.

Although more resistant than *E. coli*, *Salmonella typhi*, the Gram negative bacterium responsible for the disease typhoid fever, spread by the faecal-oral route, has also been observed to be responsive to SODIS treatment,[115] possibly because it is also non-spore forming so has less defence against the unfavourable heat and radiation conditions. Another strain of *Salmonella*, *Salmonella enterica*, was studied alongside *E.coli* and *Pseudomonsa aeruginosa* (another bacterial pathogen) to demonstrate the ability of TiO_2 under UVA light to effectively inactive these bacteria.[116] This is promising, as both of these classes of bacteria have the ability to make humans very ill, so the possibility of being able to safely remove them from drinking water using photocatalytically enhanced SODIS is very reassuring.

Shigella is also a class of non-spore forming, Gram negative bacteria which can cause shigellosis (diarrhoea, vomiting and fever) which have been found to be even more receptive to inactivation via SODIS than both *Salmonella* and *E. coli*.[115] In the same study, *Vibrio cholerea* (the Gram negative bacterium which causes cholera) was found to be even more susceptible to SODIS, which is an important finding with regards to public health in rural areas where there have been many reported outbreaks of cholera. In 2007 there was a cholera epidemic which started in Orissa, India, as well as more than 10 outbreaks across African nations between 2000 and 2019. In 2017, WHO described an outbreak in Yemen caused by exacerbation of poor sanitation and health care conditions

as a result of ongoing war, as "the worst cholera outbreak in the world". *Vibrio cholerea* is well known as a water-borne pathogen and disproportionately affects those communities without advanced water treatment systems, thus making SODIS and enhanced SODIS methods extremely attractive to mitigate further negative health consequences.

However, the study of these four pathogens does suggest that there are many factors in play which can affect the relative susceptibility of the bacteria to SODIS. For example, *Vibrio cholorea* is more stable in water with higher salt concentrations, which can mean that it is easier to inactivate via SODIS when the salt content is low. This is thought to be the reason behind differing results from another study which observed *Vibrio cholera* to be significantly more resistant to SODIS than *Salmonella typhi* (*Shigella* was the least resistant),[117] where a phosphate-buffered saline was used to dilute the bacteria during the SODIS treatment. This shows the complex adaptations of bacteria and just how many environmental factors can play into the observed inactivation behaviour.

Bacillus cereus is an example of a Gram positive spore-forming bacterium which is most commonly known for its ability to cause severe food poisoning, as the presence of the spores allows the bacterium to survive at high temperatures if the food it was originally present in was not cooked sufficiently to remove the bacterium before it could form the spores. Despite the spores making various species of *Bacillus* bacteria detectable in water, WHO states that no water-borne transmission of *Bacillus* has been recorded,[118] so it is not a pathogen of concern for this study due to no confirmed clinical significance. Though not many of the key pathogens of concern, as listed by WHO, are spore-forming, it is still useful to study their behaviour as a response to SODIS and/or photocatalysis, as they are a useful model for more hazardous species within the virus or protist families, which cannot be studied without rigorous safety regulations.[119]

1.3.3.2 Viruses

Viruses are extremely abundant, with experts believing there are of the order of 1×10^{31} viruses on Earth,[120] more than the known number of stars in the Universe. Many viruses, such as bacteriophages, only target bacteria and thus are harmless, possibly even beneficial to humans. However, there are also many virus, approximately 200 of the known

virus species,[121] which can infect human hosts; some of these can be transmitted through water and cause significant health impacts.

All viruses contain genetic information, either as single stranded (ss) or double stranded (ds) RNA or DNA (ssRNA, dsRNA, ssDNA, dsDNA), or a combination of these, which is kept inside a shell known as a capsid, with no other organelles inside. The capsid is made up of proteins, rather than a phospholipid bilayer which is typically seen in bacteria and animal cells. This capsid can help protect the viral DNA from UV damage, attack from certain enzymes which are typically released as an immune response, and to extremes in temperature and pH. Due to the lack of any other organelles, the virus can not replicate by itself and requires a host to reproduce its genetic information, meaning viruses are typically classified as being non-living. As a result, some viruses also have a phospholipid bilayer with virulence factors attached, which are protein structures that help the viruses bind to host cells, which surrounds the capsid, offering extra protection and allows the virus to merge with host cells and infect them more easily.

According to the WHO, *"Specific viruses may be less sensitive to disinfection than bacteria and parasites (e.g. adenovirus is less sensitive to UV light). Viruses can persist for long periods in water. Infective doses are typically low"*.[91] Unlike the main bacteria of concern outlined by the WHO and presented in Table 1.4, all major viruses of concern have both high health concerns and persistence in water sources, meaning they pose a much greater threat as a group, as shown in Table 1.5.

Table 1.5: Waterborne Viruses of concern, as listed by the WHO[91]

Viral Pathogen	Health Significance	Persistence in Water Supplies	Resistance to Chlorine	Relative Infectivity	Important Animal Source
Adenoviruses	High	Long	Moderate	High	No
Enteroviruses	High	Long	Moderate	High	No
Astroviruses	High	Long	Moderate	High	No
Hepatitis A viruses	High	Long	Moderate	High	No
Hepatitis E viruses	High	Long	Moderate	High	Potentially
Noroviruses	High	Long	Moderate	High	Potentially
Sapoviruses	High	Long	Moderate	High	Potentially
Rotavirus	High	Long	Moderate	High	No

Viruses present certain hazards, not only due to their interactions with host tissues, but also because they are much harder to detect and culture than bacteria, meaning their presence can often go unnoticed. Due to the inability of viruses to replicate and reproduce their genome without a host, viruses cannot be cultured as simply as bacteria can be, and require tissue cultures to facilitate sufficient growth for detection, which is not always possible and can be expensive. The use of tissue culture systems increases the time, labour, expertise and need for expensive equipment relative to bacterial cultures. In addition, certain viruses such as some adenoviruses are difficult to culture, with others not being possible to grow under laboratory conditions, such as human norovirus and hepatitis A virus.[122] Other methods, such as plaque assays, can be used to grow adenoviruses, but these require a 10-day incubation period. The polymerase chain reaction (PCR) method can be used to detect viral particle genomes rapidly, but still requires the use of cell cultures, limiting its implementability.

Further, due to the small size of viruses relative to other microbes, they are not able to be filtered out and require chemical, rather than physical, removal. This means that fine filters, such as those used in water bottles to help disinfect water when away from a dependable water source, are ineffective for removing viruses. Chlorination is typically employed, but some viruses are resistant to this, and the composition of the water affects the ability of the chlorine to inactivate the viruses. It has been found that the effectiveness of chlorination varies with water composition, making it difficult to correlate

results obtained from studies using distilled water spiked with one specific target virus to their practical counterparts.[123] Note, chlorination works by damaging the viral capsid proteins, as opposed to UV radiation which is thought to disinfect viruses by both damaging capsid proteins as well as the viral genome.[122] However, there is no known "silver bullet" treatment for viruses in water, with adenoviruses being almost five times more resistant to UV at 254 nm than other enteric viruses.[124] Further, enteroviruses have been identified as being more resistant to chlorination than reoviruses and adenoviruses, thus if the former is not present in water after chlorination, it can be assumed that the latter two will have also been removed.[104]

Adenoviruses are associated with many clinical illness, including respiratory illnesses such as pneumonia, conjunctivitis, cystitis and gastroenteritis.[125] Adenoviruses are excreted through faeces, making it possible for the virus to enter the water system and cause illness through ingestion, inhalation or direct contact with eyes, and are commonly found in swimming pools, river water and other surface water sources, waste water and oceans.[125] The presence of adenoviruses in water which can infect humans are likely to be the result of water contaminated with human sewage, rather than waste from other animals.[126] There have been reports of adenovirus outbreaks due to contaminated drinking water which lead to gastroenteritis due to inadequate disinfection,[127–129] as well as studies showing that adenoviruses were detectable in conventionally treated and disinfected drinking water in South Africa[130] following coagulation with slaked lime, flocculation, sedimentation, carbonation, filtration and chlorination; and Korea following sedimentation, filtration and chlorination,[131] implying they are resistant to such methods.

Adenoviruses contain double stranded DNA, which allows the genome to be more easily repaired by the host machinery once the virus has infected the host's cells, meaning it has the ability to remain active and cause disease, unlike some other water-borne single-stranded viruses which cannot be repaired by the host and thus are not pathogenic. This may give rise to the greater ability to survive for longer observed for adenoviruses in water compared to enteroviruses and hepatitis A virus,[132] as well as improved thermal stability and resistance to UV irradiation.

Noroviruses also have high clinical significance as they can cause gastroenteritis, entering private water systems, such as wells, by faecal contamination from infected humans. These viruses are also moderately resistant to chlorine, so cause significant concern. Studies have shown that noroviruses can be inactivated by UV irradiation and with photocatalysis using TiO_2, though Lee et al.[133] found that the improvement of the inactivation was only slightly better with TiO_2 present. However, the study used a suspension of TiO_2 particles under a 254 nm UV lamp for only 5 minutes, meaning that there is the possibility that photocatalysis could provide an even more significant advantage over SODIS alone for removing noroviruses if the reactor system and photocatalytic material employed are enhanced. Noroviruses are more susceptible to UV inactivation than adenoviruses,[133] which is possibly due to norovirus genomes being made up of ssRNA, unlike the dsDNA of adenoviruses, which can help the genome repair and lead to replication inside the host, as well as the differences in capsid structure.

Harding et al. highlighted the resistance of murine norovirus against SODIS, a well as SODIS enhanced with citric acid from limes, where insufficient inactivated was achieved, relative to inactivation below detectable levels for *E. coli*.[57] Murine norovirus is a type of norovirus that effects mice, not humans, but can still be used to suggest how human noroviruses may respond to SODIS. This suggests photocatalysis is an important route to explore with respect to determining which treatment types are effective against more resistant pathogens.

The high resistance of viruses to chlorination, as well as the high infectivity, highlights the need for more intensive methods of disinfection which can also be applied in rural contexts, such as photocatalysis. The structure of the protein capsid and possibility for genome repair likely give such viruses an advantage during disinfection processes. Further, as discussed in Section 1.2.1 on SODIS, UV irradiation utilised during SODIS can cause inhibition of ATP generation,[23] thus disrupting the metabolic system of the affected cell. However, viruses do not have their own metabolic function or cell membranes, relying on host cells instead, which could possibly contribute to the observed resistance of certain viruses to SODIS, since this mode of UV inactivation is not possible. Thus, the disinfection of viruses will largely be due to exogenous formation of ROS species which

can damage the capsid or viral genome, as endogenic inactivation processes will be less important than for bacteria, which are more susceptible. As a result, viral inactivation will depend more heavily on the composition of the water being treated.[11]

1.3.3.3 Protists

Some of the most hazardous and robust pathogens are protists, with those of concern to water safety presented in Table 1.6:

Table 1.6: Waterborne Protists of concern, as listed by the WHO[91]

Protistic Pathogen	Health Significance	Persistence in Water Supplies	Resistance to Chlorine	Relative Infectivity	Important Animal Source
Acanthamoeba spp.	High	May multiply	Low	High	No
Cryptosporidium parvum	High	Long	High	High	Yes
Cyclospora cayetanensis	High	Long	High	High	No
Entamoeba histolytica	High	Moderate	High	High	No
Giardia intestinalis	High	Moderate	High	High	Yes
Naegleria fowleri	High	May multiply	Low	Moderate	No
Toxoplasma gondii	High	Long	High	High	Yes

Most of the species presented in Table 1.6 are examples of coccidian (unicellular protozoan) parasites that infect the epithelial cells of the intestinal tract, thus with the potential to cause significant illness in humans. One of the most notorious classes of pathogens in the field of water treatment is *Cryptosporidium*, due to its persistence in water sources and ability to cause serious illness, either in the form of intestinal or respiratory cryptosporidiosis, which in some cases can be fatal. Intestinal infection typically causes diarrhoea, fever, weight loss and nausea, whereas respiratory infection leads to a cough, sore throat, fever and inflammation.[134]

Cyrptosporidium species which are known to cause diseases in humans include *C.parvum, C.hominis, C.canis, C.fellis, C.muris* and *C.melagridis*, with *C.parvum* being most commonly studied. One of the key characteristics of *Cyrptosporidium* species which allows them to be so resistant to many water treatment methods is the formation of oocysts as part of their standard life cycle. Oocysts are the hardy, thick-walled stage of the life-cycle of coccidian parasites, and also the stage that is formed inside the gut, and thus shed

in the faeces of people infected with such parasites. It is these oocysts which typically contaminate water supplies. Another key property of these parasites which can increase their prevalence is the fact that they are zoonotic, meaning they can pass between species, with water-borne transmission from livestock to humans being particularly common and threatening to rural communities with freely roaming livestock.[135]

C.parvum oocysts have multi-layered walls consisting of lipids, proteins and glycans,[136] which makes them resistant to inactivation through chlorination (at dosing safe to drink), but studies show that they may be susceptible to inactivation through UV irradiation. However, studies suggest that this would require UVC or UVB[137] radiation, which suggests that SODIS would be inefficient (no UVC can pass through the ozone layer, and only 1% of solar radiation at sea level is UVB). Further, it has been suggested that UV irradiation is only successful when the *C.parvum* oocysts have not bound to other organic pollutants. Therefore, laboratory-based testing under ideal conditions may give a false indication of the effectiveness of such a treatment. Despite the resistance to chlorination and, in some cases, UV, a study by Shen et al. demonstrates how polymeric metal-free photocatalysts can be used to inactivate *Cryptosporidium* in water,[138] which is very promising.

A study conducted by McGuigan et al.[139] found that SODIS was effective against *C.parvum* oocysts under simulated sunlight and a constant temperature of 40 °C. However, in order to achieve complete inactivation, 10 hours of the SODIS treatment was required, which is infeasible in terms of typical sunlight availability, and is longer than the standard recommended time of 6 hours, which means some users may not attempt to conduct the treatment for long enough, especially if they are unaware that the oocysts are present. It has also been suggested that DNA repair process may start after exposure to UV, and thus the inactivation may not be permanent.[140] Hence, the study by McGuigan et al suggests that the mechanism of SODIS can be effective, but would require enhancements in order for it to be suitable in practice and render the oocysts completely deactivated and unable to repair. This is supported by a study conducted by Méndez-Hermida[141] which found that removal of *C.parvum* oocysts was significantly enhanced by the presence of titania immobilised on plastic films, as performed under

natural sunlight in Spain.

Giardia are another type of protozoan pathogen which can cause gastroenteritis. Their life-cycle alternates between a swimming trophozoite and an infective, resistant cyst (note: *Giardia* produce cysts which are non-replicative, as opposed to oocysts which contain zygotes). The walls of this cyst are less complex than the oocyst of *Cryptosporidium*, but are nevertheless more robust than the trophozoite phase. The cyst walls consist of cell wall proteins (CWPs), which are lectins that bind to curled fibrils of the β-1,3-GaINAc polymer. Comparisons of the structural components of the (oo)cyst walls of *Giardia* and *Cryptosporidium*, as summarised by Samuelson et al.,[136] are presented in Table 1.7 and Figure 1.9. (Note: CWP = cyst wall proteins, OWP = oocyst wall proteins, POWP = possible oocyst wall proteins).

Table 1.7: Structural components of the (oo)cyst walls of *Giardia* and *Cryptosporidium*

Component Type	*Giardia*	*Cryptosporidium*
Sugar polymer(s)	β-1,3-GaINAc	None
Lipids	None	Acid-fast lipids
Proteins	CWP1 to CWP3	Cys- and His-rich OWPs
	GaINAc-binding lectins	POWPs
		Ser- and Thr-rich thethers
Abundant gycans	2 very short N-glycans	GaINAc- and fucose-rich O-glycans

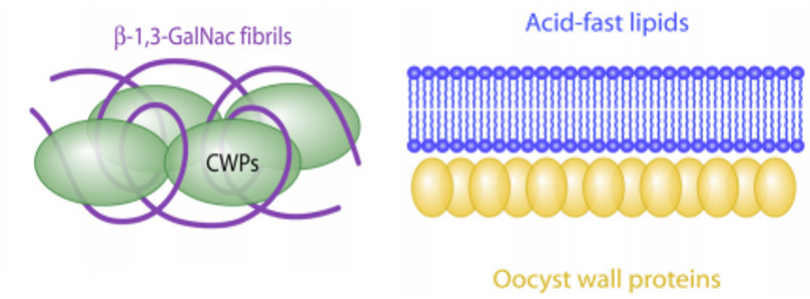

Figure 1.9: Structure of wall of *Giardia* cyst (left) and *Cryptosporidium* oocyst (right), reproduced from reference,[136] presented with permission from The American Society for Microbiology.

A study conducted by Lonnen et al.[142] which compared the susceptibility of certain bacteria, fungi and protozoa to SODIS and solar photocatalysis using TiO_2 found that the

cysts of protozoan pathogen *Acanthamoea polyphaga* were resistant to both treatments, as well as the spores of *Bacillus subtilis* (a bacterium). This shows the importance of the spore/(oo)cyst phases for pathogens that are able to form them for their survival in unfavourable conditions, and confirms that certain microbes require more vigorous treatment to be removed. This also demonstrates the importance of developing and testing novel high performance photocatalysts to investigate whether more promising results can be obtained, as the extent of ROS species which can be produced during SODIS alone are often ineffective against the hardy shells of protist cysts and spores.

1.3.3.4 Fungi

Fungal contaminants are frequently over-looked when assessing the parameters for safe drinking water, yet still have the potential to behave as pathogens and cause harm to humans. Many guideline documents, including those from the WHO, do not include comprehensive lists of fungal species of concern, as for the other classes of pathogens, despite the presence of fungi in water distribution systems and the associate health risks being documented within the literature.[143] Within Europe alone, more than 400 different fungal species have been reported to be found in groundwater, surface water and drinking water, 46 of which were classified as Biosafety Level 2.[144] The European Union drinking water directive states that drinking water should be "free from any micro-organisms and parasites and from any substances which, in numbers and concentrations, constitute a potential danger to human health",[145] which fungi species would certainly be classified as, despite this document not including a list of pathogenic water-borne fungi; suggesting further attention should be given to how they respond to certain water treatment methods. Some water-borne fungi reported to have impacts on health include those summarised in Table 1.8, though this is not an exhaustive list.

Further, due to their ability to form large hyphal networks, produce spores or grow as single yeast-cells, they are able to maximise their nutrient uptake in a range of different environments, and have therefore been detected in surface, ground and tap water intended for human consumption.[146] Hence, it is important to consider fungi when developing water treatment systems, particularly for rural areas where contamination can occur more readily and there is less access to municipally treated water.

The numbers and diversity of fungi found in surface water have been reported to be higher than in ground and tap water,[143] which is thought to be due to the higher content of organic nutrients present, varying temperature and pH and increased water flow.[147,148] Hence, rural communities that obtain their drinking water from sources such as rivers and lakes should take more care when considering fungal removal. Indeed, a study by Patil and Borse[149] showed that 362 species of fungi were identified in fresh water samples across India, though there is no assessment of any pathogenicity of the isolated species.

Some fungi also pass through filtration and chlorination which takes place when treating tap water. These fungi that survive can contribute to the formation of biofilms, their presence in which is poorly understood in terms of interactions with other microorganisms.[143] Biofilms also help microbes survive thermal and chlorination shock, so it is extremely important to prevent the build up of these. Another important factor which contributes to the heath risks of certain fungi is their ability to release secondary metabolites. These are released to defend their habitat and suppress the growth of competitors, with some of which being toxic to animals. If present in high concentrations, these secondary metabolites may also pose health risks to humans as well as animals. Particularly for immunocompromised individuals, the presence of fungal cell wall components can lead to allergic reactions and infections, with others leading to poor taste or smell of water supplies.[148]

One study by Pereira et al.[162] found that, for a sample size of 9 different fungi species, bacteria and viruses are more easily removed from water after chlorination than fungi (when measured relative to *E. coli* and Polio 1, respectively), but *Cryptosporidium* oocysts were most resistant (*Giardia lamblia* cysts were comparable to fungi). Particularly resistant species were identified at genus level as *Cladosporium, Penicillium* and *Trichodema*. It is important to understand the structural components and adaptations of such fungi that allow for such high resistance to chlorine, in order to understand whether other possible water treatment methods, such as SODIS or photocatalysis, could be effective.

Table 1.8: Waterborne Fungi of concern, selected from a summary by Novak Babič et al.[144]

Fungal Species	Biosafety Level	Where found	Health Impacts	References
Exophiala dermatitidis	2	Glacier water Mineral water Groundwater Tap water	Cerebral infections Cutaneous infections Disseminated infections Keratitis Otitis Respiratory infections Subcutaneous infections	150–152
Exophiala oligosperma	2	Groundwater Surface water Tap water	Cerebral infections Cutaneous infections Onychomycosis Subcutaneous infections	150,153–155
Microsporum canis	2	Surface water	Tinea capitis Tinea corporis	156
Phialemonium obovatum	2	Tap water	Endocarditis Keratitis Peritonitis Subcutaneous infections Systemic infections	157
Rhinocladiella aquaspersa	2	Surface water Tap water	Chromoblastomycosis	155,157
Scedosporium apiospermum	2	Surface water Tap water	Cerebral infections Respiratory infections Subcutaeous infections Systemic infections	158
Stachybotrys ramosus	1	Surface water	Cutaneous infections Respiratory infections	149,159
Rhizopus spp.	1	Surface water	Cutaneous infections Respiratory infections Rhinocerebral infections Subcutaneous infections	158
Rhizomucor spp.	1/2	Surface water Tap water	Disseminated infections Systemic infections	160,161

Many fungi have their cell membranes encased in an outer rigid cell wall which contains complex polysaccharides known as chitin and glucans. Chitin helps to add structural strength and protection to fungi cells, and is present in the exoskeletons of certain insects and crustaceans. The regular crystallinity of the polymer adds to the strength of the cell wall, and has also attracted interest in terms of utilising the material to increase the Young's modulus of various functional materials.[163] *Scedosporium apiospermum* is an example of a fungus which contains chitin in its cell wall,[164] and has also been identified as an emerging pathogen in India.[165]

However, chitin is not present in all species. For example, *Cladosporium* cell walls are composed mainly of galactose, hexoses and some mannose.[166] *Cladosporium* also falls into a group known as "dark fungi", which are so named due to their cell walls containing melanin, which gives them extra resistance to UV radiation,[166,167] and would mean that SODIS alone would not be sufficient to remove these types of contaminants, and that some type of enhancement such as with photocatalysis would be required. Indeed, studies have shown that, under simulated solar radiation, the numbers of species for non-melanised cells were notably reduced (such as for *Alternaria alternata, Fusarium equiseti, F. oxysporum, F. solani, F. verticillioides* and *Candida albicans*[142,168–170]) as opposed to those containing melanin which were less susceptible.[146]

Another example of a melanin-containing dark fungus is *Exophiala dermatitidis*, which is listed in Table 1.8 as being able to cause a variety of health issues. Particularly dangerous is the ability of this fungus to infect the central nervous system, which can be fatal, with cases recorded in Asia amongst otherwise healthy individuals,[171] showing it is not only the immunocompromised that are at risk when fungi contaminate water supplies. It is thought that the melanin component of the cell walls adds to the pathogenicity of this fungus, as well as increasing its resistance to host defence systems.[171] *Exophiala dermatitidis* has also been identified as a producer of exopolysaccharide (EPS), which are associated with giving the fungus thermotolerance,[171] meaning the combination of high temperature and UV radiation present during SODIS that is usually very effective against bacteria is unlikely to remove this pathogen.

As is apparent from the above discussion, it is not uncommon to detect fungal species within drinking water, even after treatment in water cleaning facilities, some of which can be pathogenic, particularly to vulnerable and immunocompromised people. Due to this class of microbe typically being overlooked when defining water quality parameters and outlining contaminants of concern, there are little data available on the efficacy of traditional water treatment methods for a wide variety of fungi, especially considering their abundance in drinking water sources. Thus, it is important for research to address the efficacy of various water treatment methods for removing fungi, as well as the mycotoxins they can produce, which also have health consequences.

1.4 Water in India

India is rapidly urbanising, with cities expanding and increasing in population. Despite economic benefits this may bring, this development also has some drawbacks. An increasing density of population means an increase in waste produced, and thus more contamination to water. With the increase in contamination, as well as the increase in demand due to higher population, water treatment facilities are significantly strained. Many water sources in India are contaminated with biological and chemical pollutants, and over 21% of the country's diseases are water-related.[172] India covers 2.45% of the world's land area and contains 4% of water resources, but accounts for 16% of the world's population,[173] putting large strain on these resources. Thus, it is incredibly important to have good water management in order to provide for all inhabitants in a sustainable way.

As well as the need to provide clean water for human consumption, the rise in population and global demand for food means more water is also needed for agriculture. India is the world's largest consumer of groundwater, which supplies 60% of the country's irrigation supply. This high consumption can lead to depletion of aquifers, which are often associated with replenishing water sources. Due to high rates of extraction, it is predicted that aquifers in the north-west and south will be critically low by 2025.[174]

In Bangalore, one of India's most populous cities, 1400 million litres a day (MLD) of

waste water is produced, but only 500-700 MLD are treated by centralised water treatment facilities.[175,176] Daily, 62 million litres of sewage is generated in urban India, and there is only capacity to treat 37% of this.[175] This clearly demonstrates the scale of the water problem for urban India, where roughly a third of the urban population live in slums.[177]

In Mumbai, the most populous city in India with approximately 18.5 million residents, more than half the population live in slums. According to the WHO, primary barriers to accessing water in slums can be legal, institutional and political, as well as monetary and technical.[177] If a slum is notified, meaning it is recognised by the government, inhabitants are entitled to access city services, including connections to the water supply. However, in 2012, 59% of slum settlements in India were not notified, meaning even in urban India there exists a serious problem with access to clean piped water and sanitation.[177] This amounts to approximately 3 million people in Mumbai alone. Further, in 2014, the Bombay High Court issued an order to the city government to extend the access of Mumbai's water supply to residents living in non-notified slums in order to address the problem.[177] However, further legal barriers prevail, as the Bombay High Court does not have jurisdiction over land belonging to the central government, so not all slums will be able to benefit from this ruling, as this does not apply to, nor affect, any slums outside of Mumbai. This indicates that human rights movements are of extreme importance to highlight issues relating to a lack of equity, particularly surrounding water access.

The scale of the water problem is made even clearer when the rural population is also considered. As mentioned in Section 1.1, in 2018 66 % of India's population lived in rural areas,[8] and therefore may face greater water scarcity than non-affluent urban populations. It is estimated that 70% of India's surface water is not fit for consumption,[178] and 40 million litres of waste water enters rivers and other bodies of water daily, with only a fraction being adequately treated. This results in the loss of approximately a quarter of a million lives per year,[179] contributing the most of any other country to the global total discussed above in Section 1.1 of approximately 829,000. This is unacceptable, preventable and must drive further research to mitigate the issue and make progress towards solving the ongoing water crisis.

1.4.1 Key Contaminants

1.4.1.1 Microbial Contaminants

Particularly in the summer, *E. coli* is often detected in water. Data published on the Central Pollution Control Board website, following a survey of the water bodies (lakes, tanks and ponds) across various Indian states in 2016,[180] showed that many water bodies across India show significant contamination, including total coliform, faecal coliform and biological oxygen demand (BOD). This is a clear indication of contamination with sewage, which is one of the largest sources of water pollution in India.[181]

Table 1.9 below shows a list of Indian states, summarising the data from the above described survey. For reference, field work conducted as part of this Thesis took place in the state of West Bengal, listed at the bottom of the table. The data highlights the extent of contamination across all water bodies studied, showing areas of major concern for water quality.

Table 1.9: Water Quality Across Indian States (2016 study[180])

State	Number of Water Bodies	Total Coliform Percentage over 5000 MBN/100 mL	Faecal Coliform Percentage over 2500 MBN/100 mL	BOD Percentage over 3 mg/L
Andhra Pradesh	2	0	0	0
Assam	26	96	38	92
Bihar	4	50	75	50
Chandigarh	1	100	100	100
Chhattisgarh	2	0	-	100
Goa	8	75	75	88
Gujarat	23	0	0	83
Haryana	2	-	-	50
Himachal Pradesh	5	0	0	40
Jammu and Kashmir	20	-	-	85
Jharkhnd	3	-	-	33
Karnataka	105	67	62	93
Kerala	18	0	0	61
Lakshadweep	1	100	100	-
Madhya Pradesh	26	0	0	100
Maharashtra	11	0	0	100
Manipur	18	0	-	56
Meghalaya	9	33	56	67
Mizoram	2	-	-	50
Odisha	8	50	38	100
Pondicherry	2	0	0	50
Punjab	3	0	0	97
Rajasthan	16	0	0	19
Tamil Nadu	8	50	38	100
Telandana	33	0	0	97
Tripura	8	0	0	75
Uttar Pradeshn	4	100	100	100
Uttarakhand	2	-	-	0
West Bengal	10	90	90	80

A study by Mukhopadhyay et al have found the presence of bacteria in well water used as a drinking water source in both urban and rural households,[182] including *E.coli*, faecal *streptococci* and saprophytes (microorganism that lives on dead or decaying organic matter), some of which show resistance to more than two different classes of antimicrobial agents. This indicates a point-of-source water treatment method could be beneficial to

reduce bacterial content from collected water.

Further, Schriewer et al.[183] studied 24 rural villages in Odisha, India, and found human contamination was observed in household storage of water, and animal contamination was found more frequently in water bodies from which water was collected. This shows there is a risk for exposure to animal faeces and zoontoic pathogens, and also shows the importance of ensuring water stored is kept free from further contamination, such as from hands during transport.

Due to the clear links between poor health and consumption of water contaminated with bacteria, it is clear efforts should be focused on improving the quality of water intended for drinking purposes in a way that is effective and easy to carry out where municipal treatments are not available.

1.4.1.2 Chemical Contaminants

There are many routes for contamination of water bodies, many due to human activities. Surface water, such as lakes, rivers, ponds and wetlands provide much of the drinking water to the majority of the population. However, these waters are very susceptible to contamination, for example with fertilisers and pesticides from agriculture, as well as the release of sewage generated in urban areas into rivers and lakes.[184]

Groundwater sources, such as aquifers, can also become contaminated due to minerals and other naturally occurring materials found in soil and rocks, as well as leaking of septic systems that releases nitrates, oils, bacterial, detergents and viruses into the water stores underground.[184] Heavy metal contamination is a particular issue for groundwater in India, with Figure 1.10 summarising some of the major contaminants. These can be released from natural processes, as well as from industrial processes and plumbing systems.

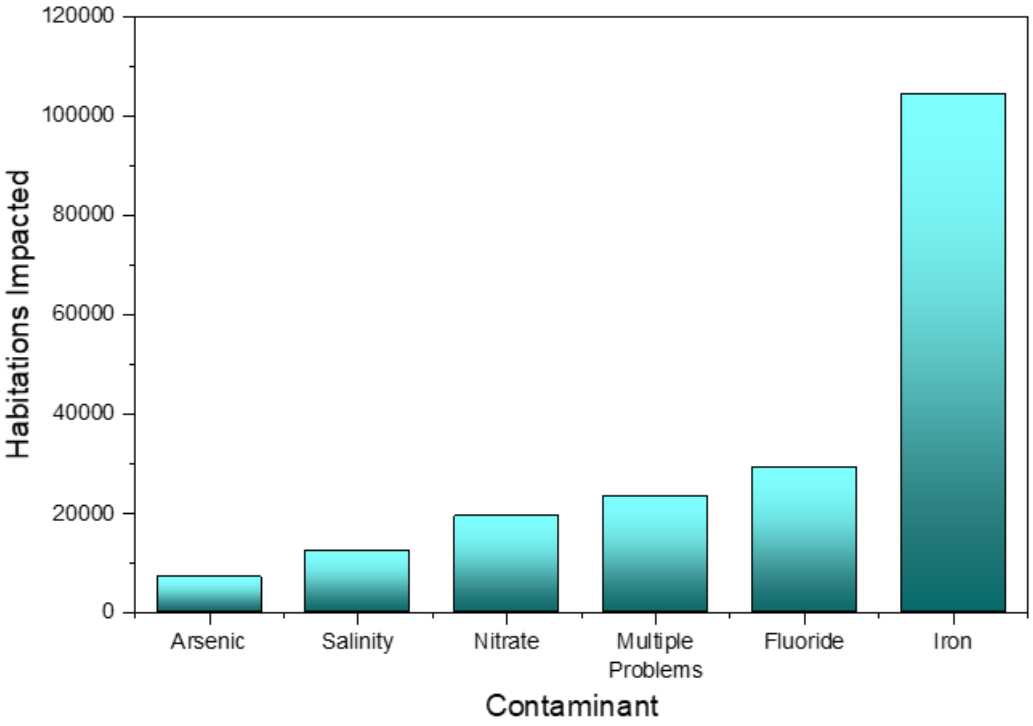

Figure 1.10: Plot adapted from WaterAid report[185] on drinking water quality in India, showing the number of habitations affected by water quality problems.

These contaminants can lead to serious health issues, such as skeletal and dental problems and cancers.[184] Excessive fluoride concentrations (>4.0 mg/L) have been detected in India,[186] with roughly two thirds of all states facing acute fluorosis problems, with 25 million people presently affected, and 66 million at risk of developing fluorosis.[187] The presence of arsenic is also a large problem in India, and can lead to arsenic poisoning, stomach pain, nausea, numbness in the hands and feet, partial paralysis and blindness.[186] The toxicity of arsenic also depends on its oxidation state, with As(III) being more than ten times more toxic than As(V).[188] This is a clear indication that water resources need to be more carefully protected, and water treatment systems need to become more widespread, affordable and efficient.

These contaminants cannot be removed from water through photocatalysis alone, which targets the breakdown of organic contaminants, so for regions where these mineral contaminants are particularly problematic, a treatment system with multiple steps will be necessary.

As well as significant mineral contamination, water bodies are also affected by organic man-made compounds which enter the water stream. Sources of particular significance include:[186]

- Pesticides. These are designed to interact with chemical processes within the pest's bodies, and can have unwatned interactions with non-targeted living organisms. These can cause damage to the liver and nervous system.
- Volatile organic chemicals (VOCs), such as adhesives and fuel additives, which can lead to cancers, central nervous system disorders, liver and kidney damage, reproductive disorders and birth defects.
- Dyes from the textile industry, a large industry in India, are becoming more concerning.
- Compounds of emerging concern (CECs)

Contaminants of emerging concern, including per- and polyfluoroalkyl substances (PFAS), are some of the largest threats to drinking water sources. These chemicals have useful properties such as being hydrophobic, lipophobic and are extremely persistent in the environment due to the strength of the C-F bond, and can enter surface water bodies through direct dumping, as well as percolating into ground water sources if disposed of in a dug ditch. Examples of materials that contain chemicals which would fall into the PFAS class include Teflon, fire-fighting foam, water repellent coatings and stain resistant fabrics.[189] They have been detected in all environmental media, including air, surface water, groundwater, soil and food.[190] Human exposure to PFAS has been linked to high cholesterol, decreased vaccination response and immune suppression, reduced fertility, thyroid disorders, pregnancy-induced hypertension and preeclampsia, testicular and kidney cancer.[189] The high presence of the materials in water sources, as well as the potentially severe health consequences associated with exposure indicates a more robust method of water treatment is required to remove these contaminants.

Another example of a chemical industry causing contamination to water is with the pulp and paper industry, which leads to the release of heavy metals as well as organic chemicals. This causes rises to biological and chemical oxygen demand (BOD and COD) and

TDS measurements. There are 406 registered pulp and paper generating mills in India, leading to the release of millions of tons of toxic waste water annually.[191] This again highlights the need for improved waste management and more responsible disposal of industrial waste, as well as the importance of water treatment facilities that are equipped to deal with the higher presence of chemical contamination observed with today's level of anthropogenic activities.

A study by Saha et al[192] investigated the presence of different endocrine disrupting chemicals (EDs) in Indian water sources, finding that 100% of the rivers and soils samples contained EDs. A map showing the locations of water samples is shown in Figure 1.11, indicating that this is a widespread issue, not limited to one small region.

Figure 1.11: Map showing the location of all sample points for the study conducted by Saha et al.,[192] where W indicated a surface water sample, S is a soil sample, and GW is a groundwater sample, presented with permission from Springer Nature Publishing.

The EDs studied are summarised in Table 1.10 and are presented in order of descending concentration in river sources.

Table 1.10: Summary of EDs studied by Saha et al.[192]

ED Name	Molecular Formula	Main Sources	Percentage Occurrence
Bisphenol A (BPA)	$C_{15}H_{16}O$	Industrial use	100
Di-n-butyl phthalate (DBP)	$C_{16}H_{22}O_4$	Industrial chemical	100
4-tert octylphenol (OC)	$C_{14}H_{22}O$	Industrial use	100
4-nonylphenol (NP)	$C_{15}H_{24}O$	Industrial use	100
Methyl paraben (MeP)	$C_8H_8O_3$	Food additives	95
Propyl paraben (PrP)	$C_{10}H_{12}O_3$	Food additives	95
Triclosan (TCS)	$C_{12}H_7Cl_3O_2$	Personal care products	90
Benzyl butyl phthalate (BBP)	$C_{19}H_{20}O_4$	Industrial chemical	75
Di-(2 ethylhexyl)phthalate (DEHP)	$C_{24}H_{38}O_4$	Industrial chemical	70
Triclocaban (TrC)	$C_{13}H_9Cl_3N_2O_2$	Personal care products	55
Butyl paraben (BuP)	$C_{11}H_{14}O_3$	Flavouring agents	45

The presence of phenolic compounds such as EDs is problematic as they, like the PFAS discussed above, are resistant to breakdown and thus stay in water courses for a long period of time if no targeted removal process is put in place. As discussed above in Section 1.2.1, this could have serious health consequences and efforts should be made to mitigate this.

1.4.2 Current State of Water Treatment

Centralised, municipal water treatment facilities in urban India which are managed by the government can provide clean water, though this supply is vulnerable to contamination, as access to water is limited for people who live in non-notified slums, forcing people to tap into the city water pipes illegally.[177]

A 2011 report by the Central Pollution Control Board on the status of water treatment plants in India found that conventional treatment consists of a sequence of alum addition, coagulation, flocculation, sedimentation, filtration and chlorination.[173] However, it also revealed a lack of uniform operation across treatment plants, and that alum dosing equipment was found to not be operation in many of the plants. Also, for open filters exposed to direct sunlight, algae would often grow resulting in the need to frequently clean filters. Further, the filter backwash water was required to be treated before being

discharged. The report advised that better training of water treatment plant operators should be brought in, as well as regular inspections of equipment to prevent failure. However, even with prescribed improvements, there is not a high enough capacity of all treatment plants to provide water for the whole population, highlighting the importance of decentralised treatments.

Insufficient municipal water treatment results in many urban households having their own means of treatment. This typically includes the use of chlorination tablets or reverse osmosis (RO) units (it is also common to see these units in restaurants and other public buildings). RO is currently the only in-home treatment method capable of desalination, though these units only treat 25-50% of the input water, with the rest wasted.[193]

In slums, a lack of access to clean water means that people are forced to purchase bottled water from street vendors, which can be very costly (estimated at more than 40 times the standard municipal water charge paid by residents of notified slums in 2014[177]). This can also result in less water being gathered and consumed than is necessary for maintaining health and hygiene.

In rural areas where access to bottled water may be limited or too expensive, water is required to be collected. Household water treatment, including boiling, filtration, solar disinfection and chlorination have been shown to be effective in reducing the prevalence of disease and thus their use is encouraged. According to a study by Rosa and Clasen in the state of Maharashtra for three rural villages, 74% of people surveyed claimed to use some form of household water treatment method year round, with boiling being the most common.[194] Initiatives such as women's self-help groups have been shown to improve adoption and upkeep of a household-scale water treatment method.[195]

It is clear that improved infrastructure and provision of water treatment is needed, with encouragement, financial support, installation and maintenance coming from bodies such as local governments or NGOs to help make the use of water treatments more widespread and improve the efficacy and ease of use of these.

1.5 Aims, Objectives and Novelty of This Research

This section will summarise the above theory and literature review to clearly outline the specific aims of the study:

- To develop high-functioning photocatalysts with the intent of deploying them in rural India for water-treatment at a household scale, as a type of enhanced SODIS. This will require improving the visible light activity, as well as the overall efficiency and rates achievable.
- To keep the costs of the photocatalysts low, by using abundant and accessible materials.
- To ensure the catalysts are stable, safe (non-toxic) and re-usable.
- To improve the physical adhesion of catalyst materials to supports, to mitigate the ongoing issue of catalyst entering the water system.
- To use convenient support materials for catalyst adhesion, factoring in the need for high surface area to enhance reaction rates, as well as ease of handling, separating and regenerating.
- To conduct tests in both laboratory and field settings, in order to bridge the gap between academic knowledge and practical implementation. This will involve using genuine water samples and testing them under sunlight. It will also involve some social science to gauge uptake and continued use likelihood.

The novelty of this study is in the application of developed photocatalysts specifically for the purpose of enhanced SODIS, rather than an industrial treatment step, whereby field testing is performed and societal opinions considered. The field testing under genuine conditions will give an invaluable insight into key practicality issues to address, and the view of the treatment method by the communities it is designed for, not simply academic interest.

Chapter 2

Instrumentation and General Experimental Techniques

This Chapter describes many of the experimental techniques that were frequently used for the collection of data required for this Thesis.

2.1 Preparation of Catalyst Coatings

Due to the nature of this research exploring different types of catalyst support materials and morphology, simple coating methods such as dip-coating, spin-coating or doctor blading were not always appropriate, for example when using glass beads or glass chips (as discussed in detail in Chapter 4). For this purpose, an immersion coating technique was used for the preparation of all films on any support morphology to ensure consistency. This type of coating method, whereby the P25 TiO_2 particles are suspended in a sol system, was first presented in the literature by Balasubramanian et al,[196] and the method followed here is outline by Odling et al.[97] Though other support materials were briefly explored, this Thesis will focus on the use of glass in different forms, so the procedure outlined here applies largely to such coatings.

1. **Etching**: For smooth glass surfaces, such as soda-lime beads or slides, etching is an important first step to enhance adhesion to the glass surface which is often too smooth to ensure good contact between the surface and the catalyst coating. First, a solution of potassium bifluoride (10 mg mL^{-1}) is prepared, taking extreme caution due to the highly corrosive nature. The glass is then placed into a plastic,

sealable container and the etching solution poured over the top. This is left for four days with occasional agitation. It is important to note that during this process, the operator should always have access to calcium gluconate gel in case of any contact between the etching solution, which can for a by-product of hydrofluoric acid, and the skin. This should not be conducted without another suitably trained individual present.

2. **Cleaning**: Once the glass has been exposed to the etching solution for four days, the solution is decanted and added to calcium carbonate to neutralise. The glass is then rinsed with de-ionised water and sonicated for 15 minutes, before draining the eater and repeat this step with ethanol. The glass is then dried at 100 degrees for 30 minutes.

3. **Further Treatment**: After thoroughly cooling to room temperature, the final chemical pre-treatment step can be conducted. For this, a solution of $TiCl_4$ (40 mM) is prepared and again poured over the glass in a sealable container and heated to 70 °C for 30 minutes. This step is typically used in the fabrication of dye-sensitised solar cells, but is also useful here to activate the glass surface further to allow for improved bonding of the TiO_2 to the surface. This in turn helps to prevent charge recombination at the glass-catalyst interface.[197] The cleaning steps in water and ethanol should then be repeated, followed by drying. Once dried, the treated glass can then finally be transferred to a muffle furnace for heating to 500 °C for 30 minutes.

4. **Coating**: Once the glass support is suitably treated and cooled, the catalyst coating can then be applied. Firstly, a suspension of the catalyst powder must be prepared. To do so, the titanium butoxide, $Ti(OBu)_4$, is added (1 mL) to a mix of n-butanol (20 mL) and HCl (0.23 mL, 37%) whilst stirring vigorously. After this, the catalyst of choice (e.g. commercially available P25 TiO_2 or synthesised novel nanoparticle materials) can then be added (0.667 g) whilst maintain vigorous stirring. The suspension should be stirred overnight and sonicated prior to coating to prevent any aggregation. The support material is then immersed in the suspension for 5 minutes, before being removed and drying at 150 °C to remove solvent. The films are then sintered to enhance adhesion between the particles and the support.

For TiO_2 this is performed at 500 °C for one hour, but different materials may have other optimal heating temperatures. Following sintering and cooling, this process is repeated such that there are 3 layers of catalyst in order to achieve a sufficiently thick film for testing.

2.2 Photocatalytic Testing

Following the synthesis of a material and its subsequent immobilisation onto a suitable support, novel catalysts must be tested for their performance under various light conditions in order to assess their suitability for various applications. This has largely been performed using UV-Vis spectroscopy to follow the fall in concentration of a model pollutant during treatment, but has also included microbiology tests.

Depending on the stage of characterisation for the material, the scale, and thus experimental set-up, of the photocatalytic testing can be adjusted. For initial screening on the smallest scale, a glass slide is used for the support and a cuvette is used as the reaction vessel, such that it can be transferred directly to a UV-Vis spectrometer for analysis. See Section 2.2.3 for further details on experimental set-up.

For testing, this research focused on the use of LEDs, with some tests using a solar simulator lamp. The LEDs used were manufactured by Intelligent LED Solutions, and were individual bulbs, as opposed to arrays. The solar simulator used was an AAA SLB300A lamp by Sciencetech, consisting of a xenon arc lamp fitted with a filter to replicate the solar spectrum at an air mass factor of atmosphere 1,5, and irradiance of 1000 Wm^{-2} (a standard used for solar cell testing). The spectral outputs for the lights used are shown below in Figure 2.1, and were measured using an Ocean Optics Photodetector with Ocean Optics SpectraSuite software.

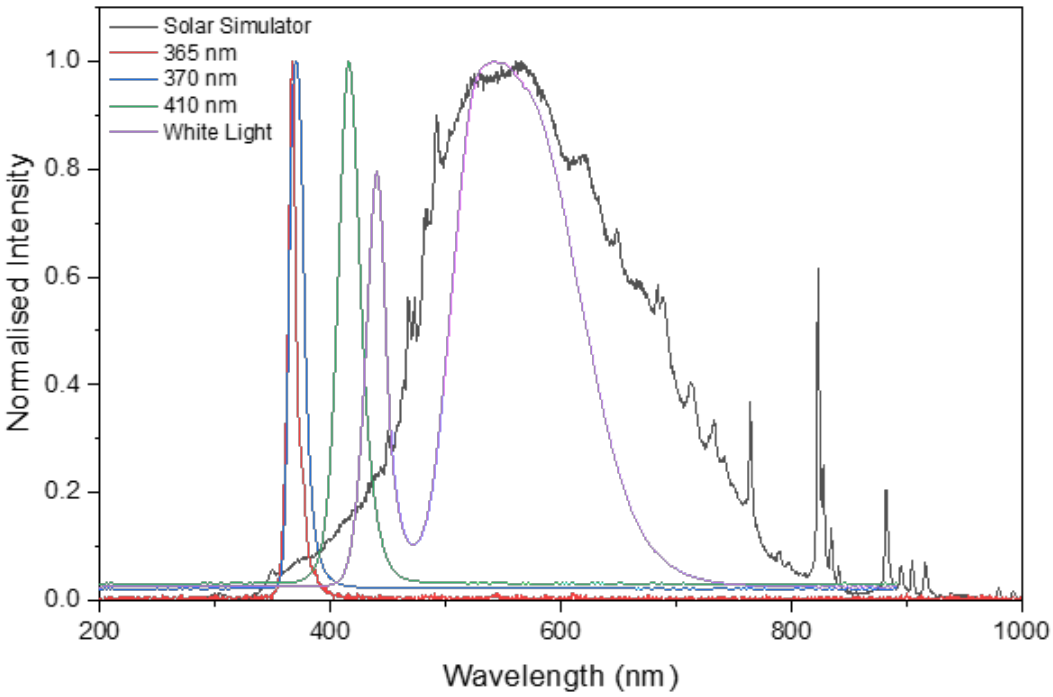

Figure 2.1: Normalised spectral outputs of all light sources used throughout this Thesis, measured using an Ocean Optics Photometer.

For all testing, LEDs were used at 0.8 A and 5 V (4 W). The intensities are listed in Table 2.1 for a distance of 5 cm away from the light. These were measured using a Thorlabs compact USB Power Meter (model PM16-122) and Optical Power Monitor GUI software.

Table 2.1: Intensity of all LEDs used throughout this Thesis, measured using Thorlabs compact USB Power Meter (model PM16-122).

LED		Intensity
UV	365 nm	1.62
	370 nm	0.46
Visible	410 nm	1.73
	White Light (5000 K)	1.20 (measured at 535 nm)

2.2.1 UV-vis Absorption Spectroscopy

The primary mode of tracking the fall in concentration of a known pollutant was to use UV-visible absorption spectroscopy. These measurements were taken using a Shimadzu UV-Pro 1800 instrument using UV-Pro software. The wavelength range scanned was adjusted depending on the sample being used.

UV-vis absorption spectroscopy allows for the concentration of a sample to be evaluated according to the Beer-Lambert Law:

$$A = \varepsilon cl \tag{2.1}$$

Where A is the absorbance of light by the material,ε is the molar extinction coefficient, c is the concentration of the solution and l is the path length of light through the sample (always 1 cm here).

The sample will absorb light depending on its concentration and how the particular molecule can interact with the photons it is irradiated with during the scan, which is described by ε. A typical plot returns the absorbance against the wavelength scanned, and from this the wavelength at which the peak with the maximum absorbance is located can be determined (defined as $\lambda_{\max}$). The absorbance at the $\lambda_{\max}$ can be recorded, and the change of absorbance at this position plotted against time in order to determine the rate of photocatalytic degradation.

The samples were exposed to light for 3 hours with measurements taken at 30 minute intervals (unless otherwise stated), including a 30 minute period in the dark to allow for equilibrium of surface adsorption to be achieved. This also allowed for confirmation that any fall in concentration was due to photocatalysis, and not adsorption alone.

The change in absorbance is given as A_t/A_0 where A_t is the absorbance at a given time point and A_0 is the initial absorbance. Since A is directly proportional to the concentration, this ratio will also corresponds to the change in concentration of the test pollutant in the water sample as the treatment proceeds.

For this Thesis, all solutions for model test molecules were made up to concentrations that have been identified to be within the linear region of the absorbance-concentration relationship, such that the Beer-Lambert Law holds. This is done *via* dilution calibration

tests, whereby the absorbance is measured for the same sample at different concentrations to demonstrate a linear relationship between absorbance and concentration, as performed by Zaitoon et al[198] for 4-chlorophenol. This, as well as context for water pollution levels, was used to determine the concentrations used for testing. For example, 4-chlorophenol has been found in the environment at concentrations between 150 μg/L to 200 mg/L,[199] thus an intermediate concentration of 20 mg/L (156 μM) was chosen, which is within the linear range.

2.2.2 Test Metrics and Data Analysis

Once testing of the catalysts had been performed, the data must be analysed to quantify the relative performance of each material under the different conditions investigated.

2.2.2.1 Langmuir-Hinshelwood Kinetic Model

For heterogeneous catalysis reactions, the Langmuir-Hinshelwood model (LHM) is commonly applied to quantify the reaction kinetics. This ultimately gives the equation that will frequently be used throughout this Thesis to determine the pseudo first order rate constant for each material tested:

$$-\ln\frac{C_A}{C_{A0}} = k_{app}t \tag{2.2}$$

Thus, from a plot of time against -$ln(C_A/C_{A0})$, the value for k_{app} can be estimated from the slope, which should be linear if the LHM holds.

2.2.2.2 Degradation Efficiency

As well as looking at the behaviour throughout the whole treatment process, as can be done using the above equation for the pseudo first order rate constant, the degradation efficiency can also be determined by comparing the final concentration of pollutant to that of the initial test solution. Thus, this is simply a percentage loss of the contaminant

and is given by:

$$DE = \left(1 - \frac{C}{C_0}\right) \times 100 \tag{2.3}$$

2.2.2.3 Determination of Photocatalytic Mechanism

Simple measurements can be performed to assess the dominant mechanism for the breakdown of pollutants in water; identifying whether holes, electrons or hydroxyl radicals are the main driver of the advanced oxidative mineralisation process.

These experiments are typically known as scavenging reactions, as they involve adding a chemical to the standard test solution (e.g. 4-chlorophenol) which readily react with the reactive oxidation species (ROS), effectively removing it from the test solution. In this way, it can be determined whether or not this ROS was the main driver of the photocatalysis reaction by comparing the DE to the standard test solution. If the DE or first order rate constant is much lower with the scavenger present, it is likely this ROS was responsible for the main mechanism of photocatalytic degradation.

For scavenging hydroxyl radicals, tert-butanol was used, and for holes methanol is used as it a strong electron donor so reacts readily with holes. For assessing the importance of photoexcited electrons, purging with nitrogen is performed to remove oxygen, as thus prevent the reaction of electrons with O_2 to form ROS superoxide.

2.2.2.4 Stability Testing

Tests were performed to assess the stability, re-usability and longevity of the synthesised photocatalysts. This involved testing the material and monitoring the degradation of a target pollutant (e.g. rhodamine B or 4-chlorophenol) over the course of treatment using UV-vis absorption spectroscopy.

The tests were conducted over the course of three hours under illumination, with the materials being reused following this treatment period. The material would be tested,

rinsed and reused with no calcination to regenerate in-between runs. This was repeated for 5 cycles, following which calcination would take. The purpose of the calcination was to fully regenerate the catalyst, and to burn off any remaining contaminants that may remain on the surface, taking up active sites on the catalyst. Calcination temperatures and durations vary for different materials, and are therefore stated in the specific experimental sections for each chapter where it is used.

After calcination, the tests would be repeated, again for another 5 repeats with only rinsing in-between runs. In total, three cycles of this reuse followed by calcination were conducted.

After the tests were completed, the degradation efficiency for each run was calculated, such that the change in performance could be tracked over the course of re-use testing.

2.2.3 General Set-up for Photocatalysis Testing

2.2.3.1 Glass Slide System

For initial screening of immobilised novel materials, a glass slide was used for simplicity. The method for this testing procedure was based on the process outlined by Odling et al.[200] The slide was coated in the catalyst following the above procedure, and placed into a cuvette containing the sample solution, typically 4-chlorophenol (156 μM). The cuvette could then be used as the reaction vessel and then directly placed into the chamber of the UV-vis spectrometer for ease of conducting the measurement. A sample holder was produced in order to keep the cuvette steady, as well as ensure consistent spacing between the lights and the sample for all measurements. The set-up for the experiment is shown in Figure 2.2.

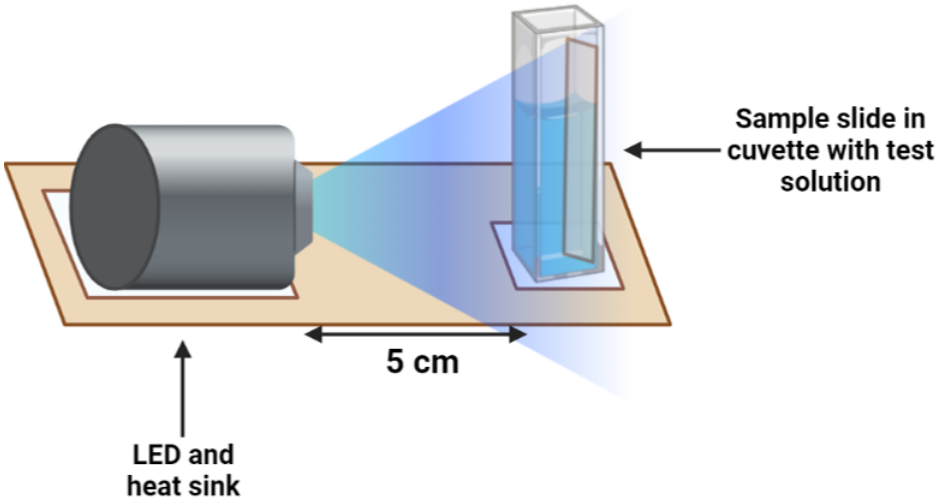

Figure 2.2: Schematic showing how the photocatalytic testing experiment was conducted with the material coated on a glass slide and using a cuvette as the test vessel.

2.2.3.2 Glass Chips and Beads System

For materials that performed well during initial screening, scaled up experiments were performed on glass beads and chips, in order to more closely represent the system that would be used in practice.

The coated glass substrate was placed into a glass dish such that it forms a mono-layer (25 g of beads/chips were used to achieve this) and 30 mL of the sample solution added to the dish. It is important to note that the beads/chips required rinsing with deionised water prior to testing in order to remove any excess catalyst from the surface and prevent scattering of light from any leached particles, which would render the absorption spectroscopy results in accurate. Further, this would also change the surface area available for reaction which would also alter the results.

The LED was placed above the dish at a height of 5 cm, as shown in Figure 2.3.

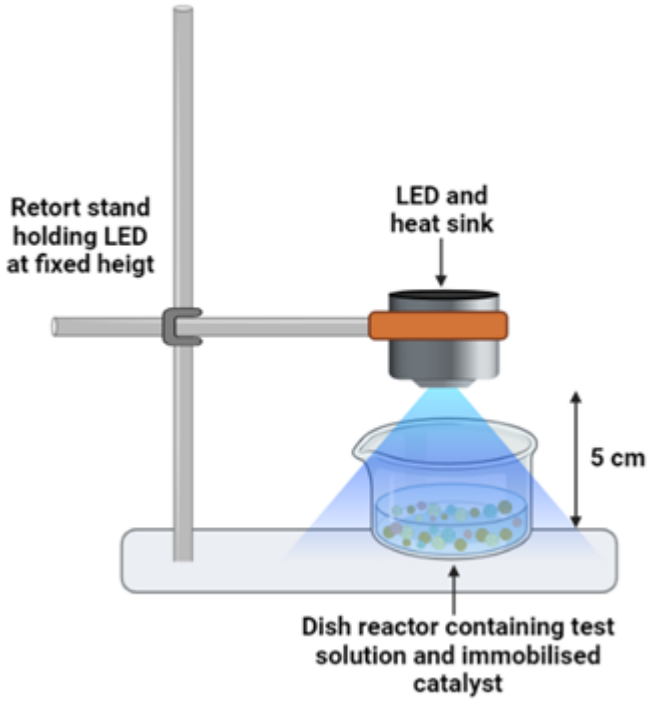

Figure 2.3: Schematic showing how the photocatalytic testing experiment was conducted with the material coated on glass chips and using a dish as the test vessel.

2.2.3.3 Microbiological Testing

Initial tests were conducted to assess the efficacy of the photocatalysts for the removal of *E. coli*, since this is commonly used in water quality testing as an indicator of faecal contamination.

The following summarises the information for the strain of *E. coli* used for testing in this Thesis: Deposited name: *Escherichia coli* (Migula) Castellani and Chalmers. Designation: EMG 2:K (lambda). Genotype: K-12 wild type.

Prior to use in experiments, the freeze-dried *E. coli* powder first requires re-hydrating and growing up. To do this, all equipment to be used was first autoclaved at 121 °C and 1 bar of pressure for 15 minutes. Nutrient broth (from Sigma, 13 g/L) was made up in sterile deionised water. Once cooled from the sterilisation process, the freeze-dried *E. coli* sample could be added. This was done by adding 1.5 mL of room temperature broth to the vial of *E. coli* and then transferring this to three sterile test tubes (0.5 mL in each). Each of the tubes was then made up to 5 mL, covered and incubated overnight

at 37 °C. After incubation, the solution becomes turbid, indicating successful growth.

Following this, the *E.coli* solution was then transferred to small Eppendorf tubes for long term storage in the freezer (-4 °C) in a 1:1 ratio with sterile 90% glycerol. This could then be used to spike water used for disinfection experiments.

Before beginning the experiment, Petri dishes with nutrient agar had to be prepared. For this, Brilliance *E.Coli* Coliform Selective Medium (from OXOID) was used (28 g/L). This was poured into the Petri dishes when molten and left to cool to form the solid gel onto which the samples could be spread.

One day prior to beginning the experiment, the *E.coli* must be regenerated from storage in the freezer. This was done by adding 50 μL of the stored solution onto a Petri dish and incubating overnight at 37 °C. To run the experiment the following day, *E.coli* from the Petri dish was scraped off and added to 50 mL of water. This was then diluted to achieve a concentration of magnitude 10^6 colony forming units per millilitre (CFU/mL). The water sample would then be added to a dish according to the set-up shown in Figure 2.3 which contained 15 g of catalyst-coated glass chips.

Measurement would be taken at 30 minute intervals (including after a preliminary period of 30 minutes in the dark) by taking 200 μL of the spiked sample and spreading on a Petri dish. Serial dilutions would also be made for the sample taken at each time point to ensure the number of colonies on the Petri dish was quantifiable. Serial dilutions were made by taking 0.5 mL of the sample and adding to an aliquot of 4.5 mL sterile 0.8% NaCl solution. This would yield a solution that was 10x more dilute than the test sample. This process was continued to achieve dilutions of 10^5 times diluted. Again, each of these diluted samples were spread onto Petri dishes by spreading 200 μL of the solution.

All dishes were then incubated overnight before counting the resulting colonies. Dishes with more than 150 colonies were not included in the data set as the error was too high. Once all of the colonies were counted, the data was converted into units of CFU / mL. To do this, Equation 2.4 is used:

$$\text{CFU / mL} = \frac{\text{number of colonies} \times \left(\frac{1\text{mL}}{\text{sample volume in mL}}\right)}{\text{dilution factor}} \tag{2.4}$$

2.3 Materials Characterisation

2.3.1 Diffuse Reflectance Spectroscopy (DRS)

UV-vis diffuse reflectance spectroscopy is a useful tool for estimating the band gap, E_g, of semiconductor materials, which is an important parameter to elucidate due to it underpinning much of the semiconductor's properties. This utilises the principle that, when the sample is irradiated with light, it will absorb light corresponding to the transition of electrons from the valence band to the conduction band, with this energy change corresponding to the optical band gap. Light can reflect off of a surface either as specular or diffuse reflectance, where specular reflectance occurs for smooth surfaces and is dependent on the angle of irradiation, and diffuse reflectance occurs on rough, irregular surfaces and can cause scattering in many directions. Due to the samples here being nanopowders, here the reflectance will be diffuse, leading to the light scattering from the sample needing to be collected by use of an integrating sphere.

Since the technique measures the reflectance of incident light, when the sample absorbs photons as the scan proceeds, there will be an increase in absorption and thus a drop in reflectance. The value of the band gap can therefore be extracted by a Tauc plot, which utilises the Kubelka-Munk function[201,202] , F(R∞):

$$F(R_\infty) = \frac{(1 - R_\infty)^2}{2R_\infty} = \frac{K}{S} \tag{2.5}$$

Where R_∞ is the reflectivity of the sample as a percentage, K is the absorption coefficient and S is the scattering coefficient at a particular wavelength of incident light. The Kubelka-Munk function assumes diffuse illumination of the sample, and that the sample

is an infinitely thick and opaque layer. For nanomaterials with a sample thickness of a few millimetres, this can be considered a reasonable assumption. From this, the Tauc plot can produced from the following equation:

$$(F(R_\infty)h\nu)^{1/n} = A(h\nu - E_g) \tag{2.6}$$

Where h is Planck's constant ($6.626\text{x}10^{-34}$ Js), ν is the frequency of incident light (s^{-1}), A is the absorption constant, and n describes the type of band gap the semiconductor possess, with n=0.5 for direct transitions and n=2 for indirect transitions. Direct transitions occur when there is no change in the momentum during the electronic transition, only a change in energy. An indirect band gap results in a change in momentum in order to be traversed, where momentum is conserved through the involvement of a phonon. Figure 2.4 demonstrates the two band gap types.

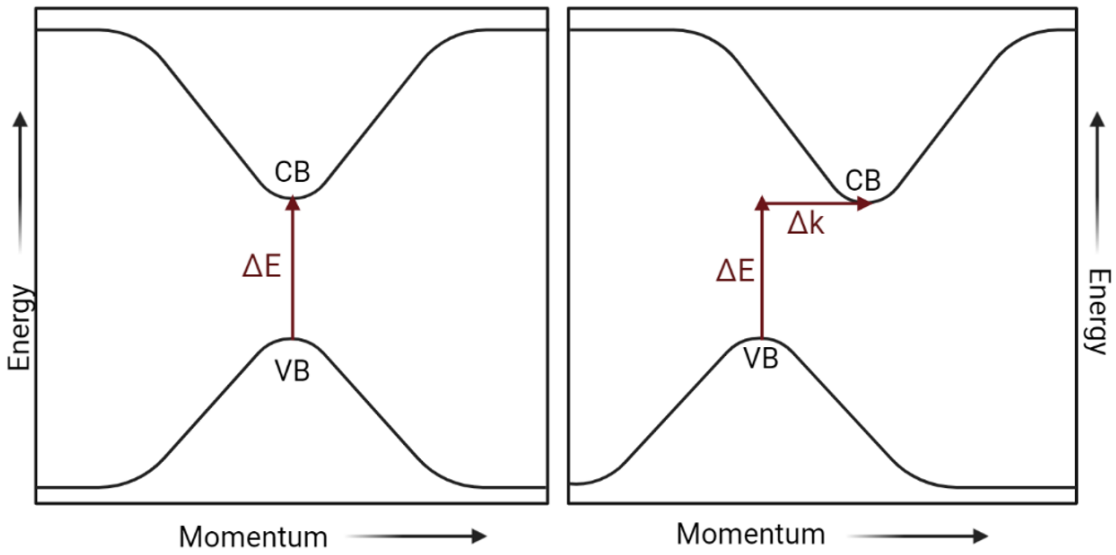

Figure 2.4: Schematic showing the difference between direct (left) and indirect (right) band gaps and the associated energy and momentum transfers.

By plotting $(F(R)h\nu)^{1/n}$ as a function of hν (which gives the photon energy in electron volts), the band gap can be extrapolated from the linear region of the plot, as illustrated in Figure 2.5b.

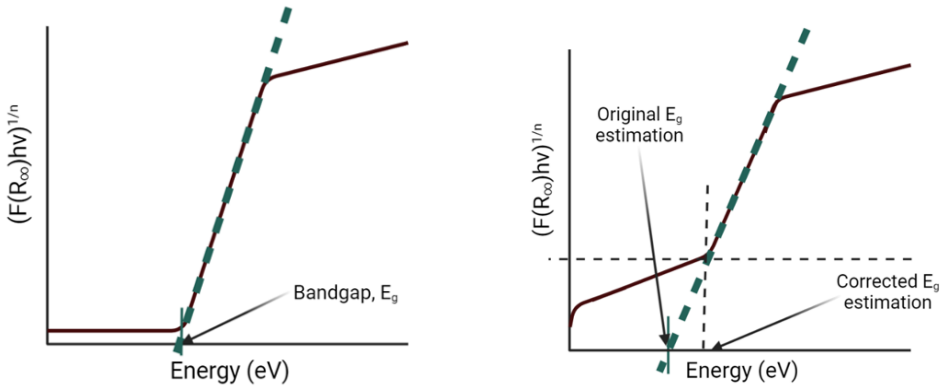

(a) How the band gap is extrapolation from the Tauc plot

(b) Correction applied in the case of a significant absorption onset

Figure 2.5: Schematic illustrating how to extract band gap information from Tauc Plots.

The band gap can be calculated by taking the values of the gradient (m) and y intercept (c) from the linear fitting conducted (performed throughout this Thesis using Origin Lab software). Thus, we can utilise the equation of a straight line to solve for the x intercept, which represents the band gap:

$$\begin{aligned} y &= mx + c \\ x &= \tfrac{(y-c)}{m} \end{aligned} \tag{2.7}$$

Once x is obtained, the associated error can also be calculated using the uncertainties in the values of c and m from the linear fit using the following method:

For a function $y = f(x, z, w...)$, the error, Δy, is given as:

$$(\Delta y)^2 = \left(\frac{\delta y}{\delta x}\right)^2 (\delta x)^2 + \left(\frac{\delta y}{\delta z}\right)^2 (\delta z)^2 + \left(\frac{\delta y}{\delta w}\right)^2 (\delta w)^2 \tag{2.8}$$

In this case the expression is $x = (y - c)/m$, where x is the intercept on the x-axis that corresponds to the optical band gap, y is the value on the y axis which here is 0 (and therefore so is the associated error), c is the y intercept of the line of best fit, and m is the slope of the line of best fit, which gives the following error expression:

$$\left|\frac{\Delta x}{x}\right| = \left|\sqrt{\left(\frac{\Delta c}{c}\right)^2 + \left(\frac{\Delta m}{m}\right)^2}\right| \tag{2.9}$$

$$|\Delta x| = |x| \left| \sqrt{\left(\frac{\Delta c}{c}\right)^2 + \left(\frac{\Delta m}{m}\right)^2} \right| \tag{2.10}$$

In some cases where there is a large onset of absorption, as shown in Figure 2.5b, a correction will have to be made to more accurately determine the band gap.[203] This typically occurs if there are multiple states close to the valence band edge, leading to a broader onset of absorption. In this case, the way in which the band gap is extrapolated must be adjusted to correct for this, as demonstrated in Figure 2.5b.

Measurements were made on powder samples using a JASCO V-670 spectrophotometer with an integrating sphere attachment. A non-absorbing white reference material is used for the background measurement and to dilute samples in. In this case, the powders were mixed with $BaSO_4$, which was also used to run the background scan. Scans were made between 200 and 1100 nm.

2.3.2 Mott-Schottky Analysis

Mott-Schottky (MS) analysis is useful in semiconductor characterisation, as it allows the flat band potential (EFB) to be measured, from which the location of the bottom of the conduction band can be estimated. This helps to elucidate the band gap architecture of a material, and thus explain its photocatalytic performance. This is an electrochemical technique which involves a three-electrode set-up and a supporting electrolyte. The samples were coated onto a conductive FTO slide and used as the working electrode, while a platinum wire is used for the counter electrode, and an Ag/AgCl electrode used for the reference. In this case, 0.5 M Na_2SO_4 was used as the electrolyte. The set-up used is shown below in Figure 2.6.

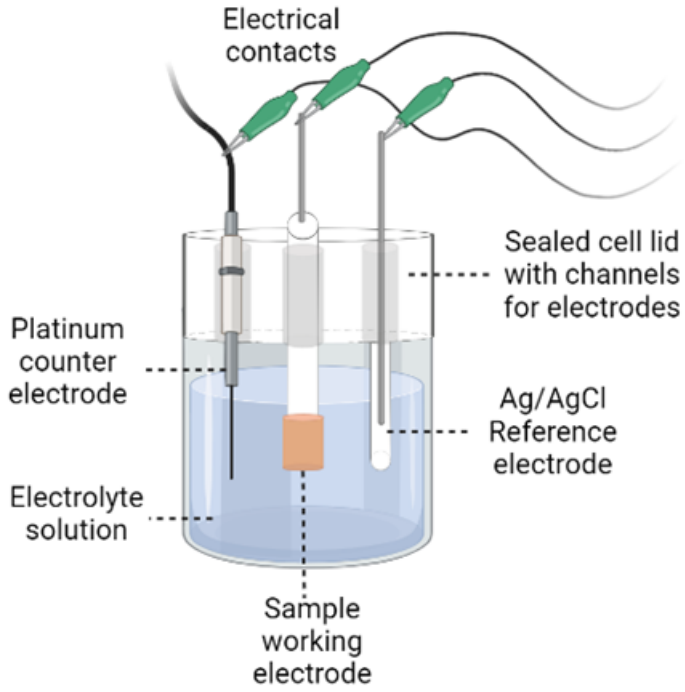

Figure 2.6: Schematic showing how Mott Schottky Testing was conducted using a three-electrode set-up.

The measurements were performed using Frequency Response Analysis (FRA) software with a Metrohm Autolab PGSTAT30 potentiostat instrument, whilst scanning at 1.5 kHz between -1.0 V to 1.0 V. Once the data was collected, the flat band potential EF was determined by performing a fit analysis of the linear region and using the corresponding fit data to calculate the intercept on the x axis. This can then be approximated as the bottom of the conduction band.

The measurement investigates the capacitance of the space charge region (CSC) between the semiconductor and electrolyte, which occurs when there is an exchange of charge carriers to achieve an equilibrium between the Fermi levels of both the semiconductor and the electrolyte (known as EF (redox)) such that the levels match, which causes bending of the bands of the semiconductor and a build-up of charge carriers at the surface, as shown in Figure 2.7. The width of the space charge region, d, is given by the Equation 2.11:

$$d = \frac{\varepsilon\varepsilon_0}{C_{SC}} \tag{2.11}$$

Where ε is the dielectric constant of the semiconductor material investigated and ε_0 is the permittivity of free space ($8.854\text{x}10^{-12}$ Fm^{-1}). If the electrochemical potential of the electrolyte solution differs from the Fermi level of the semiconductor, there will be band-bending and a depletion layer form. The band bending in the semiconductor is determined by the chemical potential of the electrons in the semiconductor and the difference between the chemical potentials of the redox species in the electrolyte solution. The flat band potential is a property of a semiconductor-electrolyte interface, which describes the potential at which there is no space charge region at the junction between the electrolyte and the semiconductor, which occurs when then Fermi levels of the semiconductor and electrolyte match, such that there is no band bending. This can be achieved by controlling an external electrode potential.[204]

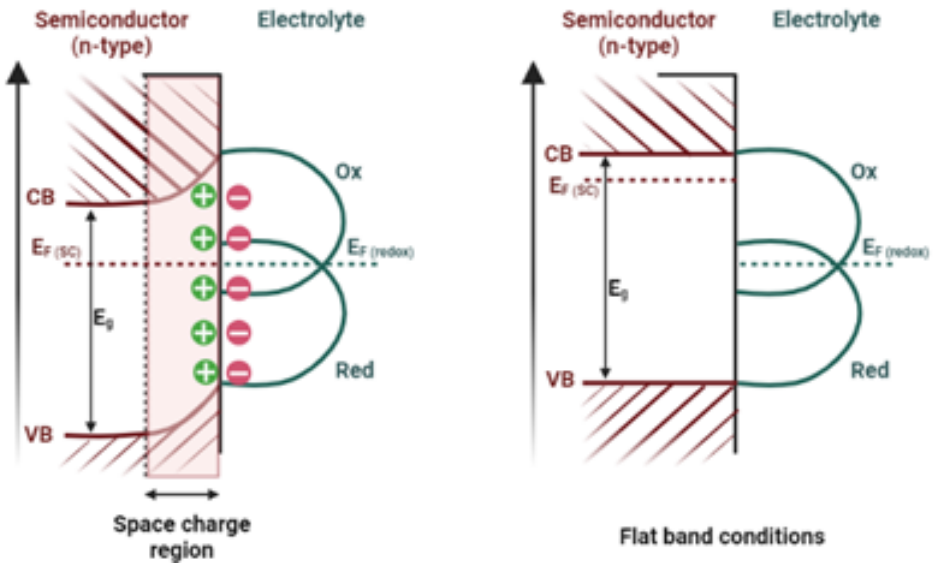

Figure 2.7: Schematic showing how bands bend during Mott Schottky testing to achieve the flat band condition.

At fixed frequencies, the potential is scanned, which will alter the size of the space charge region until eventually the potentials match and the space charge region disappears, leading to no more band-bending, achieving the flat band conditions. The potential at which this occurs can be extrapolated from a plot of the potential against the inverse square of the capacitance of the space charge region. The dependence of the CSC on the applied potential is given by the Mott-Schottky relationship shown in Equation 2.12.

$$\frac{1}{C_{SC}^2} = \left(\frac{2}{e\varepsilon_0\varepsilon N_D}\right)\left(E - E_{FB} - \left(\frac{k_b T}{e}\right)\right) \tag{2.12}$$

Where e is electronic charge (-1.603x10^{-1}9 C), ND is the charge carrier, kB is the Boltzmann constant (1.38x10^{-23} m^2 kg s^{-2} K^{-1}) and T is the temperature in Kelvin.

As deduced from the Mott-Schottky relationship, the inverse square of CSC is linearly proportional to the applied potential, E, and thus a linear slope will be observed for this system. As shown in Figure 2.8 (based on the figure in[204]), for n-type semi-conductors, as worked with throughout this Thesis, there is a positive slope exhibited from the scan, and the flat band potential is close to the bottom of the conduction band. For p-type semiconductors, there is a negative slope and the flat band potential is near the top of the valence band.

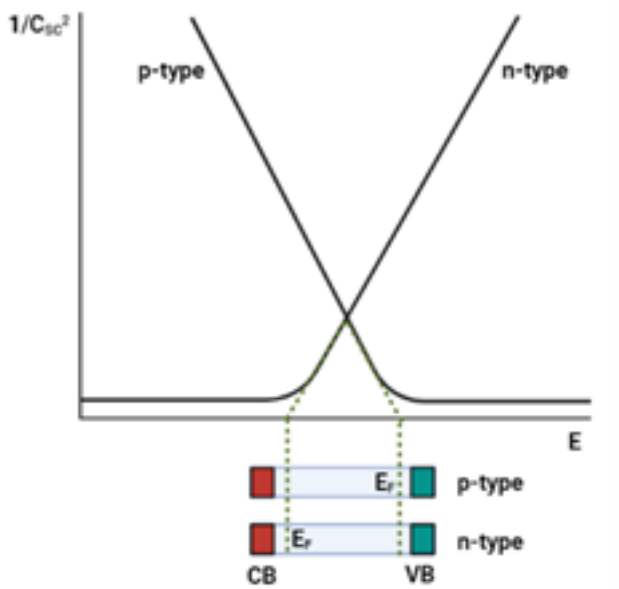

Figure 2.8: Schematic showing how the values for the conduction band or valence band can be extracted from Mott Schottky analysis for n-type and p-type materials, respectively.

As in Section 2.3.1, Equation 2.10 can be used to find the error in the flat band potential.

2.3.3 X-Ray Diffraction (XRD)

Determining the crystal structure of a material is very helpful for explaining the photocatalytic performance of, and identifying, the product of a novel synthesis route. To do

this, X-ray diffraction can be performed, whereby X-ray beams with wavelengths similar to the spacing between crystal planes are shone on the sample (either in powder of film form). The incident beams can then interact with diffracted and reflected beams, leading to interference patterns that can be interpreted to learn about the crystal spacing. Bragg's Law is used to obtain this information, which can be expressed through Equation 2.13 as:

$$n\lambda = 2d_{hkl}sin\theta \tag{2.13}$$

Where h, k and l are Miller indices which define the crystal plane and θ is the angle of incidence of the X-ray beam. Figure 2.9 shows how this is used in practice.

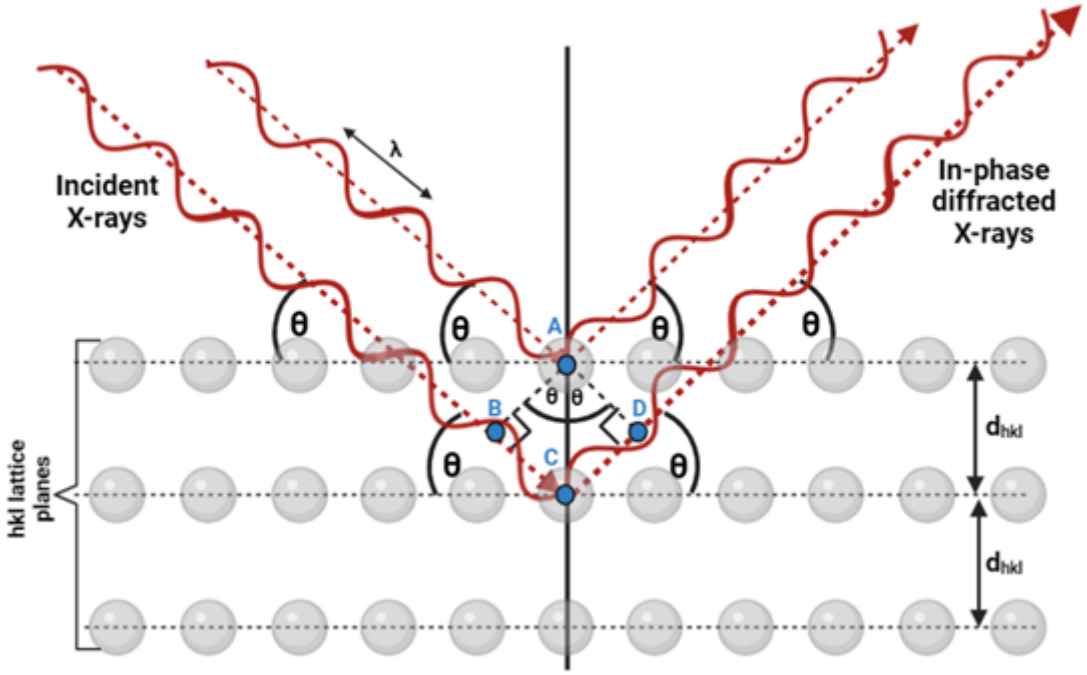

Figure 2.9: Schematic showing how Bragg scattering is used for conducting XRD analysis.

All XRD measurements taken for this Thesis were obtained using a Bruker D2 PHASER diffractometer using Cu Kα radiation and settings 30 kV and 10 mA. Measurements were taken between 5-90° with step size 0.05° and time per step of 0.82 seconds. All powders were ground down before placing on a silicon sample holder. For glass slides, a Teflon sample holder was made.

2.3.4 Inductively Coupled Plasma Optical Emission Spectroscopy (ICP-OES)

For determining the bulk chemical composition of a sample, ICP-OES spectroscopy can be used. This requires the sample to be prepared in solution form and then injected into the spectrometer.

The measurement is used to determine the concentration of select elements in the sample by exciting the sample to extremely high temperatures, forming a plasma, and then measuring the wavelength of light emitted by the sample, which is characteristic of the element present.

Measurements were taken using a PerkinElmer Optima 5300 DV ICP-OES instrument. Solutions of samples were prepared by adding some of the powder sample (0.05 – 0.5 g) to concentrated H_2SO_4 (96%, 10 mL). The sample then required heating to 300°C in order for the samples to dissolve. Once dissolved, the solution was allowed to cooling before adding 1 mL of the acid solution to 9 mL of deionised water. This dilution process was repeated once more by transferring 1 mL of the diluted sample to 9 mL of deionised water to achieve a sample solution within the correct concentration range for the instrument detection. A solution to use for the reference was prepared in the exact same way, excluding the addition of any powder sample (i.e. just the diluted acid).

2.3.5 Scanning Electron Microscopy (SEM)

SEM measurements were conducted in order to evaluate the morphology of the photocatalytic materials as well as the surface composition *via* energy dispersive X-ray spectroscopy (EDS) analysis.

This measurement technique uses a beam of electrons which is focused onto the sample. When these electrons reach the sample, this results in backscattered electrons, secondary electrons and X-rays to be emitted from the sample. Backscattered electrons results from elastic scattering from a few microns deep within the sample, whereas secondary electrons originate from inelastic scattering from the atoms of the sample at a depth of a few nanometers. The secondary electrons can therefore give high resolution information

about the topographic nature of the sample, helping to elucidate the morphology. The backscattered electrons can be useful for determining the elements present, and thus the chemical composition, as these are sensitive to differences in atomic number.[205] X-rays which are released as a result of electron bombardment are characteristic to the elements present in the sample and can thus also be used to learn about the composition. A schematic of the operation of the SEM instrument is shown in Figure 2.10.

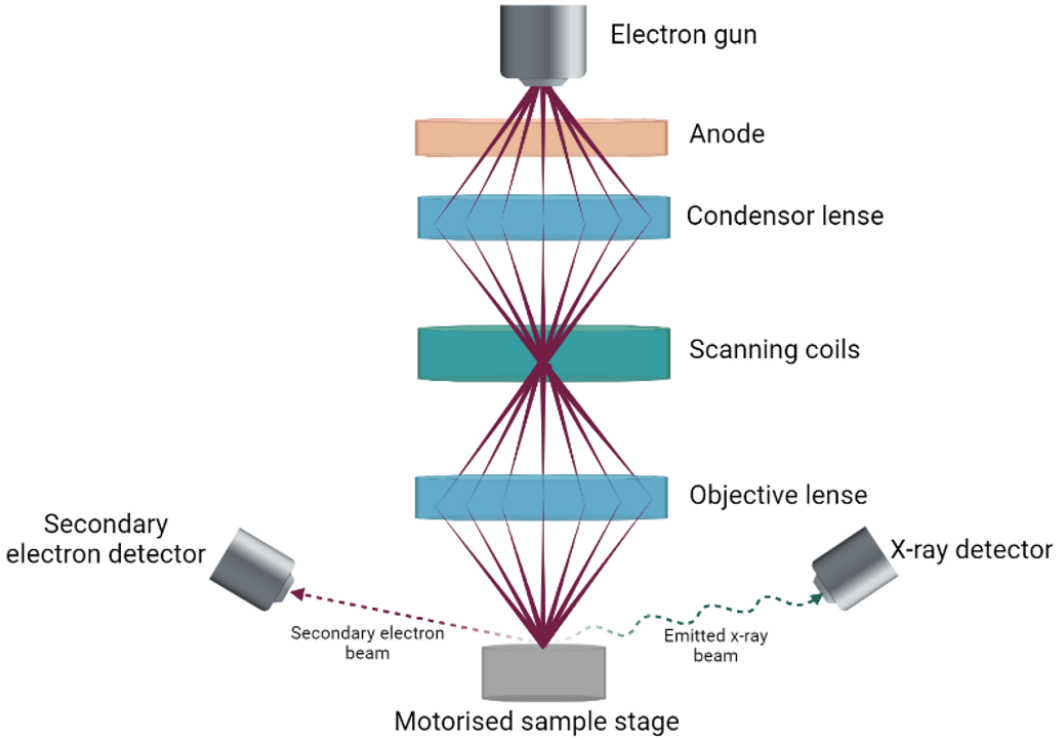

Figure 2.10: Schematic of a scanning electron microscope

Due to restrictions caused by the Covid-19 pandemic, instrumentation used for SEM measurements differed for Chapters 5 and 6.

For Chapter 5, SEM measurements were conducted in the School of Geosciences at the University of Edinburgh using a Carl Zeiss SIGMA HD VP Field Emission Scanning Electron Microscope with a Schottky thermal field emitter as the electron source, operated at 15 kV accelerating voltage using secondary imaging. SEM-EDS measurements were made using the same instrument and an Oxford Aztec Energy dispersive X-ray analysis system. For this analysis, samples were analysed as thin films on glass slides and coated with carbon to achieve a conductive surface.

For Chapter 6, SEM measurements were conducted in the School of Physics at the University of Edinburgh using a Ziess Crossbeam 550 FIB-SEM instrument operated at 1 kV accelerating voltage with secondary electron imaging. SEM-EDS measurements were made using the same instrument and an Oxford Instruments X-Max 150 EDS detector. Samples were analysed as powders coated with a sputtered layer of platinum.

2.3.6 X-ray Photoemission Spectroscopy (XPS)

XPS was used for estimating both the valence band position and the surface composition of the synthesised photocatalyst samples.

Due to restrictions caused by the Covid-19 pandemic, instrumentation used for XPS measurements differed for Chapters 5 and 6, though in both cases the samples were measured in powder form.

For Chapter 5, XPS measurements were conducted at the University of St Andrews using a monochromatised ($\Delta\varepsilon < 300$ meV) Scienta 300 X-ray photoelectron spectrometer with X-ray source Al Kα (1486.6 eV).

For Chapter 6, XPS measurements were conducted at Harwell Institute using a Thermo Fisher K-Alpha+ high-throughput X-ray Photoelectron Spectrometer instrument with monochromated Al Kα micro-focused X-ray source. The instrument was fitted with a 180° double focussing hemispherical analyser-128-channel detector, with kinetic energy range 100-4000 eV.

Chapter 3

Field Work at the Indian Institute of Technology Kharagpur, 2019

3.1 Introduction

To widen access to safe potable water in rural areas, many novel photocatalysts have been developed and presented in the literature, with the potential to be used in conjunction with simple solar disinfection (SODIS) techniques, showing successful removal of a range of contaminants. However, it is often the case that investigations into new photocatalytic systems are limited to laboratory tests, which are generally conducted under idealised conditions that do not take into account many practical limitations of real-world conditions. To address this need, photocatalyst materials were taken to The Indian Institute of Technology Kharagpur (IIT KGP) for preliminary field tests, such that they could be conducted under natural sunlight using real water sources from rural villages in India. This would allow the results of previous successful laboratory tests on a novel photocatalysts to be verified. It was found that SODIS can be significantly enhanced with the addition of photocatalysts, with an enhanced titania-based material showing better performance under solar irradiation relative to titania alone, consistent with previous lab studies. The study also highlighted areas for further optimisation, desirable to achieve before the technology can be most-effectively implemented.

Successful novel photocatalysts based on TiO_2 were previously developed and tested within the Robertson Group at The University of Edinburgh, including C–$TiCl_4$–TiO_2,[206]

$BiVO_4$–TiO_2,[207] BiOI–TiO_2[200] and $Bi_4Ti_3O_{12}$–TiO_2.[97,208] These offer enhanced photocatalytic activity over un-modified titania, with the most promising of these under laboratory conditions being the $Bi_4Ti_3O_{12}$–TiO_2 co-catalyst system (BTO–TiO_2), which can be attributed to its good stability and the presence of the heterojunction band architecture, which can reduce the extent of charge recombination. Following the thorough laboratory-based testing of the BTO–TiO_2 co-catalyst system as a thin layer coated on glass beads,[208] it was imperative that field tests should be conducted to confirm its suitability for water treatment in practice. For this purpose, real-world testing of the photocatalytic beads was conducted using water from rural villages in the vicinity of the Indian Institute of Technology Kharagpur (IIT KGP), where the analysis following treatment took place, in the Indian state of West Bengal, over March and April of 2019.

Rather than a rigorous quantitative analysis of the comparison between TiO_2 and bismuth titanate, which already exists in the literature[97,208] the aim of this study was to provide an assessment of catalyst performance when used outdoors under natural sunlight to treat contaminated water of practically useful volumes, when coupled with a simple and inexpensive SODIS-type reactor set-up, in order to act as a qualitative proof of concept for photocatalytic water treatment on a point-of-source personal-use scale. Further, this study aimed to provide useful insights into how best to build on the current system and optimise it further.

3.2 Experimental

3.2.1 Summary of Sample Names and Abbreviations

All water samples were collected from villages in the vicinity of IIT KGP, in the Kharagpur subdivision within the district of Paschim Medinipur, West Bengal, that are used daily for drinking purposes. Five samples were identified as being valuable for testing, as listed in Table 3.1 and shown in Figure 3.1.

Water from sources Well 1, Well 2, Time Water and Social Tap Water does not receive any treatment before being used for drinking, and as such the consumption of this water is a cause for concern regarding health.

Table 3.1: Summary of sample names for this Chapter.

Sample Name	Description
Well 1 (W1)	Water from a well in the village of Porapara, which was situated in an open space with dry ground close to freely roaming livestock. The well was open at ground-level, exposing it to contamination. The walls of the well were not bricked-lined, but the soil was densely packed (depth ca. 15 m, diameter ca. 1 m).
Well 2 (W2)	Well water from a village along the boundary wall of IIT KGP, also open and close to livestock, situated in a grassy field. The walls of the well were brick-lined (depth ca. 15 m, diameter ca. 2.3 m) and the opening was above ground level.
Time Water (TW)	Water from a tube well (TW), situated near a toilet block, agricultural land (a possible source of pesticides) and a pond (depth ca. 20 m, diameter ca. 0.1 m).
Social Tap Water (STW)	Water from a government-controlled tap which was only turned on for limited times during the day, known as 'time' or 'social' tap water. The water supplying the tap is sourced by ground water which is pumped up and stored in overhead water tanks.
Campus Water (CW)	Water from a tap on the campus, which undergoes thorough treatment on the campus itself, though may become contaminated by bacteria growing in old pipes. Treatment includes aeration, filtration and oxidation.

Figure 3.1: Images of the water sources used throughout this investigation.

3.2.2 Photocatalytic Bead Preparation

The TiO_2 and BTO-TiO_2 coated beads were prepared according to the procedures outlined by Odling et al.[208] and summarised in full in Section 2.1 of Chapter 2

3.2.3 Photocatalytic testing

Testing involved filling 3 plastic bottles (500 mL capacity polyethylene terephthalate (PET) produced by Indian beverage company Bisleri) with the relevant water sample and exposing to sunlight for 3 hours. The following treatment methods were tested using each of the aforementioned five water samples:

- BTO–TiO_2 catalyst in 500 mL water.
- TiO_2 catalyst in 500 mL water.
- No catalyst, only exposure of the 500 mL of water to the same sunlight and temperature conditions (SODIS) to act as a control.

For the conditions with the catalyst present, 45 g of beads were used in each bottle (each bead weighing approximately 40 mg, with approximately 0.2 mg of catalyst per bead). This gave approximately 0.2 g of immobilised catalyst per 500 mL of water in the system. After each set of treatments, the bottles were thoroughly cleaned using water and detergent, with each bottle also being flushed with some of the water sample to be treated before each new test began in order to prevent cross-contamination.

In order to investigate the effects on the duration of sunlight exposure, an additional test was performed using water from Well 2 (chosen for its high bacterial colony count). This was done following the same set-up as described above for 3 hours, but conducted in triplicate, such that samples could be removed and tested after 1 hour, 3 hours and 5 hours of sunlight exposure (see Figure 3.2). Each of the test conditions was repeated at least three times.

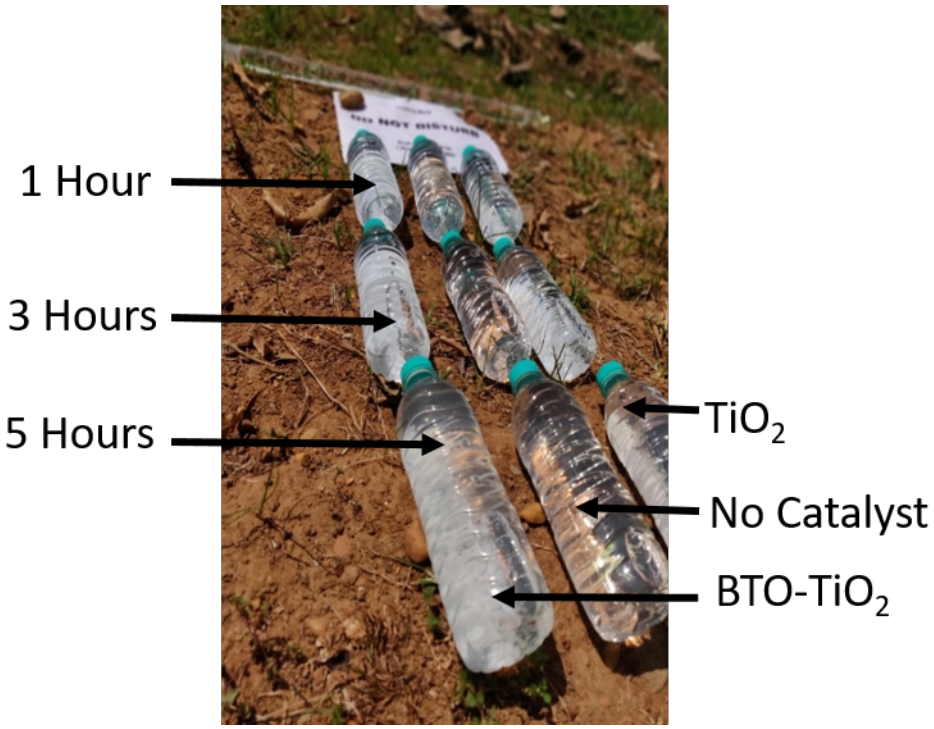

Figure 3.2: Image to illustrate the way in which the bottles were set-up throughout the investigation.

3.2.4 Sample Analysis

All of the water samples were characterised before and after treatment using bacterial culture counts to assess the extent of contamination, as well as measurements of the total dissolved solids (TDS), conductivity and salinity to gain insight into the nature of contamination pathways, and general water quality in different areas. The bacterial culture counts were obtained by taking 40 μL of each sample and spreading it onto a Petri dish containing a non-selective nutrient agar medium ('Nutrient Agar M001' produced by HI-MEDIA). This was performed a maximum of 1 hour after the treatment was completed and the samples were removed from exposure to sunlight in order to mitigate the effects of any further bacterial growth or death that could occur during dark storage and thus falsely affect the results. The Petri dishes were then covered and sealed with paraffin wrap before placing in an incubator at 37 °C overnight. Following this, the Petri dishes were removed from the incubator and the colonies counted, which indicated the extent of contamination in general, rather than tracking one specific species, since a non-selective nutrient agar medium was used. This number was then converted to colony forming units per mL (CFU mL^{-1}). All equipment that had to be re-used was sterilised using ethanol

and also autoclaved, with all Petri dishes being single-use. This limited contamination to reduce fluctuations in colony counts due to external factors.

For the solid contamination parameters, all measurements were obtained using the Waterproof PCSTestr 35 pH/conductivity/TDS/salinity/temperature Tester by Electric Burst. These measurements were trivial to collect, by simply filling a beaker with the sample to be tested, inserting the multimeter and taking the reading. The meter was cleaned with distilled water in between measurements. The analysis was performed three times, once for each of the experimental repeats.

3.2.5 Mass Transport Investigation

An additional laboratory study was performed to support the findings from the field work in India, which tested the effect of agitating the water to reduce mass transport limitations. This was performed by filling two 500 mL PET bottles with 4-chlorophenol (160 μM) and 45 g of BTO–TiO_2 beads. Both bottles were placed on their side and illuminated from above with a 370 nm LED at 0.5 V and 2.5 A. The bottles were illuminated for 5 hours, with UV-vis absorption measurements taken every 30 minutes over a wavelength range of 200–400 nm. One bottle was left stationary for the duration of the treatment, whereas the other bottle was rotated every 15 minutes to mix the water sample.

3.3 Results and Discussion

3.3.1 Solid Content Parameters - TDS, salt and conductivity

According to the WHO, TDS levels should not exceed 1000 ppm for potable water,[91] and are optimum between 300 and 600 ppm[92] above which the water will be too hard and unpalatable, and significantly below this range the content of essential minerals may be too low (e.g. below around 100 ppm), with the extremes of both cases having the possibility of leading to poor health. The TDS, values for all of the water samples fell below the upper limit for causing health risks, though complaints were made that some of the water was too hard and unpleasant to drink. As expected, it was observed throughout this study that the photocatalysis treatment did not significantly alter the TDS, salt or

conductivity values for any of the water sources (Table 3.2), and though the safety of the water remains the main priority, concerns over palatability are nonetheless useful to bear in mind when considering developing a water treatment system.

The values presented in Table 3.2 are the averages over the repeat tests with their accompanying standard error, determined according to Equation 3.1.

Table 3.2: Average values and standard error of physiochemical properties of the water samples used in this study prior to any treatment

Water Sample	Well 1	Well 2	Tube Well	Social Tap Water	Campus Water
TDS (ppm)	45 ± 1	349 ± 6	545 ± 7	232 ± 5	214 ± 1
Conductivity (μS)	63 ± 0.5	490 ± 9	767 ± 9	326 ± 6	302 ± 1.4
Salt (ppm)	36 ± 1.5	236 ± 3	373 ± 5	157 ± 3	146 ± 1

$$s_x = \frac{s}{\sqrt{n}} \tag{3.1}$$

where s_x is the sample standard error, n is the number of repeat measurements, and s is the sample standard deviation, calculation according to Equation 3.2:

$$s = \sqrt{\frac{1}{n-1}\left[\left(\sum_{i=1}^{n} x_i^2\right) - n\bar{x}^2\right]} \tag{3.2}$$

Although photocatalysis cannot be used to reduce hardness of water, these quick and easy measurements were conducted to give a set of parameters for understanding more about the context of the water content and social attitudes towards it, as highlighted by members of the local community commenting that they didn't like the flavour of the hard water available. Despite this treatment method alone not being able to reduce these concerns, it is important to keep them in mind for designing a system which may be taken on board in the future.

3.3.2 Bacterial Content

One of the most useful and important metrics for monitoring water quality is the bacterial content, as the presence of pathogens has the potential to cause serious illness, with poor sanitation being highlighted as a significant issue in India.[209,210] According to the WHO,[104] there should be no *E. coli* present in any 100 mL sample. Their guidelines

for safe drinking water state: *"Ideally, drinking-water should not contain any microorganisms known to be pathogenic... ". "The detection of Escherichia coli provides definite evidence of faecal pollution... ".* Indian legislation on water quality follows this guidance, stating that *E. coli* or thermotolerant coliform bacteria should not be detectable in any 100 mL sample. Further, per 100 mL, treated water in a distribution system should also have the total coliform bacteria present be undetectable.[211]

The number of bacterial counts after 3 hours treatment for each sample location are presented in Table 3.3, where the data were calculated for the raw counts in the Petri dish (40 μL of sample) and then converted to CFU mL^{-1}. The associated error values were calculated according to the same formulae above (Equations 3.1 and 3.2).

Table 3.3: Bacteria Counts in CFU mL $^{-1}$ for all sites before and after treatment Error is calculated as standard error. Note that 'No Catalyst' here refers to SODIS only as the treatment.

Sample	Well 1	Well 2	Campus Water	Tube Well	Social Tap Water
Raw	2150 ± 400	4625 ± 913	483 ± 102	2100 ± 475	342 ± 242
No Catalyst	500 ± 123	381 ± 64	283 ± 196	200 ± 25	v513 ± 238
BTO-TiO_2	192 ± 71	88 ± 36	67 ± 42	338 ± 238	63 ± 38
TiO_2	488 ± 288	213 ± 73	83 ± 71	288 ± 238	438 ± 288

This data indicates that all five of the water sources studied contained significant bacterial contamination, making them unsuitable for human consumption. The Campus Water (CW) and Social Tap Water samples show lower, but still detectable, numbers of colony forming units per millilitre (CFU mL^{-1}). For CW, this suggests that the pipes supplying water to the campus are likely to contain substantial bacterial growth leading to recontamination, since the water flowing through the pipes has undergone extensive treatment, both before entering the campus and after with aeration, filtration and oxidation employed.

The general efficacy of each treatment type for each water source, as presented in Table 3.3, shows that the modified BTO–TiO_2 catalyst is the most effective at removing bac-

teria on average. This is consistent with the reported laboratory studies, indicating that these tests provide a good prediction of real-world solar performance.

Treatment with the BTO–TiO_2 catalyst shows the least amount of spread in results after the 3 hours in sunlight, as well as a decrease in colony counts for all samples relative to the raw value, which was not found for any other treatment methods. Though this indicates promise for implementation, further enhancement to the materials or the method is desirable to fully remove all remaining bacteria. We note that since a selective nutrient medium was not used, the colonies formed were not necessarily all *E. coli*, as other bacteria, pathogenic or otherwise, may also be found in naturally occurring water.

Due to photocatalysis being largely non-selective in its disinfection mechanism, the raw number of bacteria can be used as an indication of the effectiveness of the treatment method employed here in general, without the need to culture only one type of microbe, such as *E. coli*. Indeed, there is opportunity for further research into selective disinfection methods such that the rate of removal of specific types of bacteria can be increased,[212] however this is beyond the scope of this preliminary, proof-of-concept study.

3.3.2.1 Time interval Testing

In terms of effectiveness of each treatment type for photocatalytic inactivation of bacteria, the same results as those indicated in Table 3.3 can also be seen with the bacterial inactivation over time in Figure 3.3, where the BTO–TiO_2 catalyst is shown to give a faster rate of bacterial removal relative to the other treatment methods. However, it was observed that none of the treatments performed could consistently achieve complete bacterial disinfection, as reflected by the average colony counts never reaching zero, as shown by Table 3.4 which contains the data used to produce Figure 3.3.

Table 3.4: Average bacteria counts for each treatment type on W2B for 1, 3 and 5 hours of treatment, given here in CFU/mL

Time (hours)	No Catalyst	BTO-TiO_2	TiO_2
0	4625 ± 914	4625 ± 914	4625 ± 914
1	492 ± 79	175 ± 63	313 ± 88
3	381 ± 64	88 ± 36	213 ± 73
5	58 ± 36	33 ± 22	50 ± 25

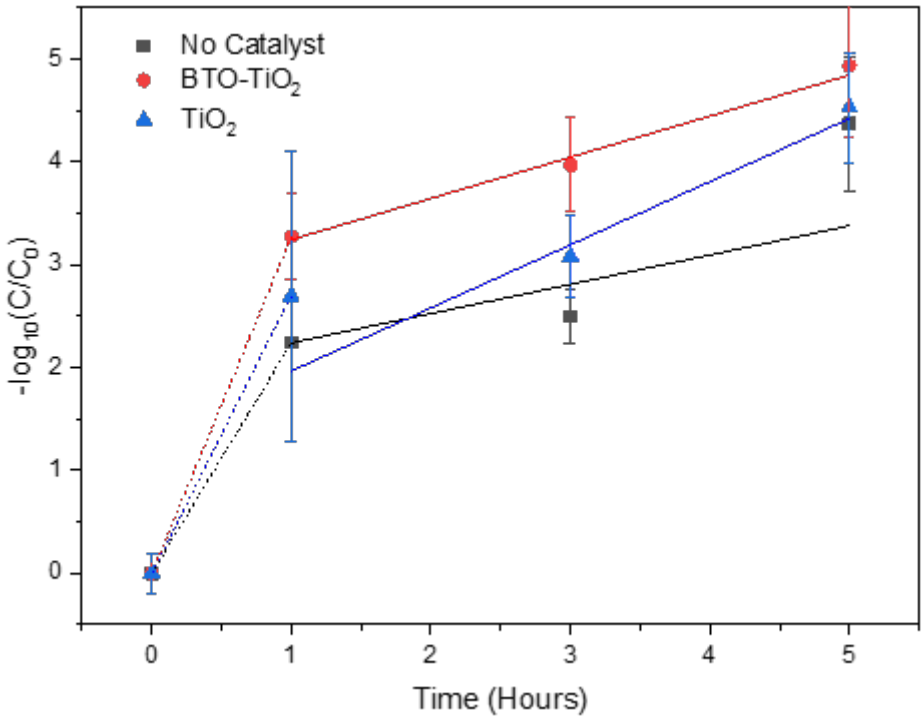

Figure 3.3: Linearised rate of disinfection for Well 2 water, showing two linear regions. Note that here, concentration C refers to colony forming units in one millilitre (CFU/mL).

The above Figure appears to have two linear regions, from 0 to 1 hours, and from 1 to 5 hours. Though this cannot be robustly confirmed due to the period between 0 and 1 hours having only two sample points, the apparent change in rate of bacterial removal after 1 hour does suggest a slowing of the inactivation rate after this point.

It is also interesting to note that, according to the Centers for Disease Control and Prevention (CDC),[213] the acceptable level of heterotrophic bacteria for potable water is below 500 CFU/mL. It can be seen from the above data that this is achieved for all treatment types after 5 hours, but achieved for the treatment types with catalyst present

after just 1 hour. This suggests that the faster rate of bacterial inactivation for photocatalysis compared to SODIS alone can help to increase the practicality, and possibly therefore the acceptability, of this treatment type.

Note, the error bars for Figure 3.3 were calculated *via* propagation of the errors arising from the raw bacterial count values, using the following equations:

For $y = ln(x)$, the error in y is given by:

$$\Delta y = \frac{1}{x}\Delta x \tag{3.3}$$

In this case, $y = ln\frac{N}{N_0}$, so x is $\frac{N}{N_0}$. Thus, the error on x, Δx, can be determined using the following expression:

$$\Delta x = x\sqrt{\left(\frac{\Delta N}{N}\right)^2 + \left(\frac{\Delta N_0}{N_0}\right)^2} \tag{3.4}$$

Hence, by inputting the standard error values for N (the colony counts at each time interval for each treatment type) and N_0 (the initial colony counts prior to any treatment), the error for x (N/N_0) can be determined, substituted into Equation 3.3 for the error in y, and thus an error quantified with which to determine error bounds for Figure 3.3.

3.3.3 Mass Transport Investigation

It can also be seen in Figure 3.3 that there is a slight deviation from the expected behaviour of pseudo-first-order rate kinetics. This is likely to be due to mass-transport limitations that arise from the large volume of water relative to the surface area of exposed catalysts, exaggerated by the lack of any stirring or agitation. Slow diffusion of living bacteria from the top of the bottle towards the catalyst at the bottom will effectively create a layered system of disinfected and non-disinfected water. It is possible that a bilayer of inactivated bacteria close to the catalyst surface and still viable bacteria floating nearer to the top of the bottle was induced, as shown in Figure 3.4.

Figure 3.4: Mass transport schematic, illustrating how two layers of water may form close to and far away from the catalyst layer.

This highlights the need to adjust the practical set-up of the treatment system, such that the extent of photocatalytic inactivation can be maximised. To elucidate the mechanism behind these kinetics for the treatment process, an investigation was subsequently conducted under laboratory conditions to compare the degradation of persistent contaminant 4-Chlorophenol (4-CP) *via* BTO–TiO_2 coated glass beads in 500 mL PET bottles under a 370 nm LED (the emission spectrum for the LED is shown in Section 2.2 of Chapter 2) when the bottle was turned every 15 minutes and when the bottle was stationary. The data for this investigation is shown below in Figure 3.5.

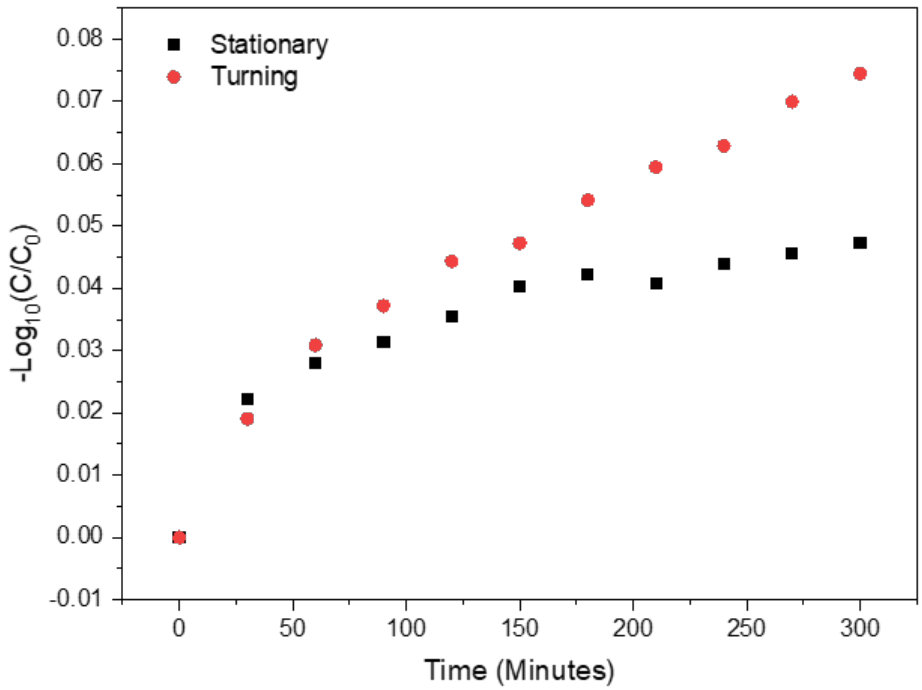

Figure 3.5: Plot showing the rate of removal of 4-CP from water for stationary and turning bottles.

From the slopes in Figure 3.4, the first order rate constants were calculated to more accurately evaluate the effect of agitation of the solution. The results of these calculations are shown in Figure 3.6.

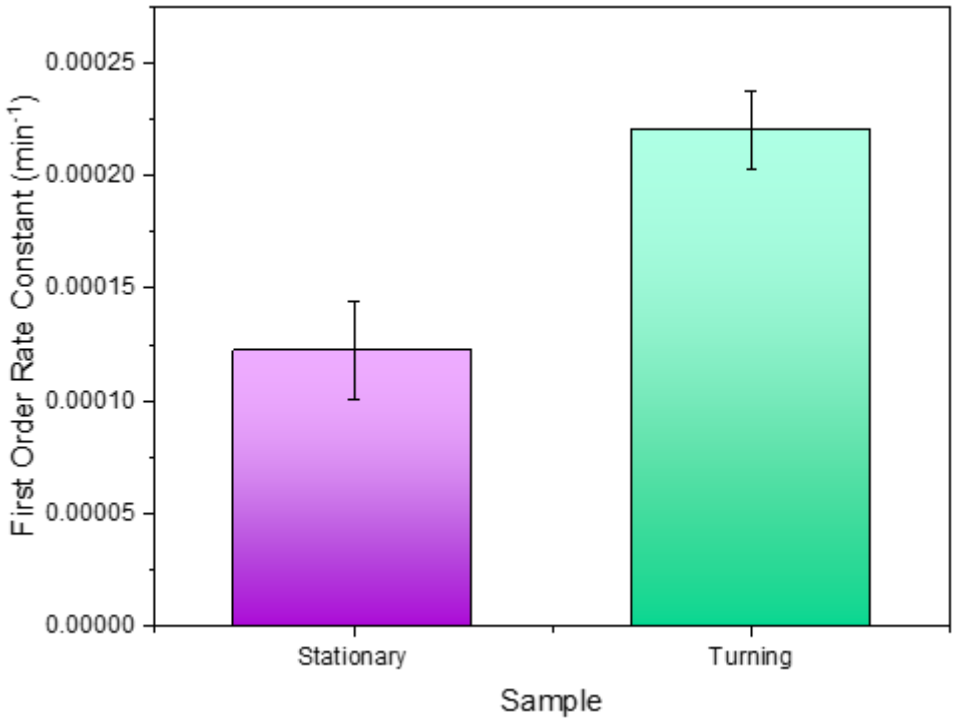

Figure 3.6: First order rate constants for the treatment systems with stationary and turning bottles.

Here it can be seen that turning the bottle results in a rate constant 1.8 times that of the stationary system. Hence, it is apparent that regularly turning the bottle enables the photocatalytic degradation of contaminants to proceed with reduced mass-transport limitations, whereas the stationary bottle led to a plateau of disinfection similar to that seen in the field studies. Based on these results, it appears that this mass-transport problem could be rectified by turning the bottle at regular intervals during the real-world treatment period, further enhancing the rate of treatment observed for the photocatalytic process.

This is important to develop into further test systems and protocols. It should also be noted that, because a non-selective growth medium was used throughout this investigation, the treatment may not have been consistently successful for all microorganisms within the water samples, with some species being more resistant to the treatment than others. Indeed, there are plans for more thorough screening of bacterial content and the

efficacy of the treatment against certain microorganisms as future work relating to this investigation. However, the increase in rate of degradation shown for 4-CP when turning the bottle does suggest that mass transport limitations do play a significant role, which can be overcome with simple reactor system modifications.

3.3.4 Other Practical Observations

Another crucial aspect of the study was to highlight areas necessary for further improvement before the treatment method will be ready for implementation in rural villages. Indeed, this study allowed the main limits to practicality associated with photocatalysis as a treatment method for rural villages to be more clearly identified, such that further work can be made in eradicating such barriers.

During the study it was clear that the catalyst material was becoming darker in colour (Figure 3.7), turning from the original pristine white to a light brown colour, most likely from the build-up of transition metal deposits or carbonaceous material from the water sources. Throughout this study, the same regeneration technique was used as in previous laboratory studies, whereby the beads were rinsed in distilled water and calcinated in a furnace at 500 °C for 1 hour after each use. In doing so, any remaining contaminants could be removed from the photocatalyst's active sites, meaning the beads remained active for the duration of the study and compatibility between runs could be ensured.

Figure 3.7: Colour difference between pristine, unused beads, and those which had been used in testing multiple times

However, it is unlikely that such a cleaning method could be implemented without also

developing the necessary infrastructure to service the villages. This could lead to more rapid deterioration of the catalyst films, resulting in the need to replace the beads more frequently, which would have a negative impact on the required cost-effectiveness of the technology.

Further, the beads also began to show significant loss of coating as the investigation continued, with some beads appearing completely clean and without a coating at all by the end of the study. Although the treatment process did not notably seem to become slowed relative to the start when the beads were in their optimum condition, this does suggest that improved methods need to be developed for adhering catalyst films to the support for systems that are intended for prolonged use. These stability questions highlight the largest practical issue raised by this investigation, and emphasise the need to improve catalyst adhesion and regeneration methods before further field testing can take place.

For successful implementation to be feasible, further chemical enhancements are desirable to improve the visible light efficiency of the catalyst, such that the rate of disinfection can be increased without the need to add more of the catalyst beads, which would increase the cost and weight of the system. Although the glass beads provide a suitable surface area available for the catalytic reaction to occur, the low mass of catalyst compared with that of the bead leads to a bulky and heavy system that would be hard to mass produce. For this reason, different support materials and structures should be investigated to improve the practicality of the system, in tandem with improved adhesion methods to reduce the extent of catalyst flaking.

3.4 Conclusions

Through this investigation, it was found that all treatment methods were able to reduce bacterial content to some extent, verifying SODIS and solar photocatalysis as viable techniques for improving the safety of water in rural areas with intense sunlight exposure. It was also found that the use of our photocatalyst materials provided an enhanced treatment ability relative to the simple SODIS technique and relative to standard titania, as

indicated by overall lower bacterial content and faster disinfection rates shown in Tables 3.3 - 3.4 and Figure 3.3.

Although it was observed that the complete removal of all bacteria could not be achieved after exposure to sunlight for up to 5 hours, this can be attributed to mass-transport limitations incurred by using large volumes of water, which highlights the need to optimise the operation of the treatment system, as well as just the catalyst material, in order for the removal of contaminants to be as effective as possible.

All of the results gained from this investigation provided valuable insights into the viability of photocatalysis as a point-of-source decentralised waste water treatment method, and have identified crucial areas for development that can help to further optimise this method. Though it is clear further work is required, the study supports the notion that photocatalysis can indeed be a practical option for water disinfection when the necessary system optimisation measures are made. The prospect of further investigation is extremely timely as the increase in global population puts even more strain on existing water sources.

Chapter 4

Support Materials and Improving the Adhesion of Photocatalysts

This Chapter focuses on the importance of the choice of support material used to immobilise a nanopowder photocatalyst onto for the application of water treatment. To explore this, first an overview of different support materials and relevant pre-treatment methods from the literature is given, before then presenting new data from a study conducted to explore the effects of different glass substrates and coating methods for improving adhesion and the lifetime of the resulting catalyst coatings.

4.1 Literature Review and Background

Although much work remains to fully assess the influence of the many contributing factors associated with different catalytic supports, this Chapter aims to shed some light on the current state of the field. Commonly used support materials will be examined to give an overview of some of the more frequently employed methods for catalyst film fabrication, as well as their most significant advantages and disadvantages. A further discussion is provided in more detail by Porley and Robertson[214] for the interested reader.

4.1.1 Glass

Glass is a substrate commonly used in photocatalysis research due to the desirable properties of stability and high temperature resistance. Not only the choice of support material,

but also the structure of that support, is a factor that can greatly affect the kinetics and activity of the catalytic reaction responsible for the degradation of pollutants. For glass, structures explored often throughout the literature include slides,[206,215] beads[97,216–218] hollow beads[219,220] and fibres.[221]

In a study conducted by Fernández et al.[222] to compare glass, quartz, stainless steel foil and a nanoparticle suspension of titania, it was found that immobilisation significantly slowed the rate of degradation. For a test molecule of malic acid, the suspension form of the catalyst totally degraded the pollutant in 30 minutes (5 mg of P25 titania for 7.46 μmol of pollutant), whereas titania on quartz took 1 hour, and 3 hours for glass and stainless steel. This strongly implies that the available surface area is extremely important for determining the activity, but also that the nature of the surface itself has a clear significance. A further factor to consider when immobilising catalysts is that heat is often required to improve adhesion. This heating process means that the support-catalyst interface does not remain inactive and diffusion of ions from the support into the titania film becomes possible, often with an inhibitory effect on the photocatalytic activity.[222,223] For the titania film samples on glass in the study above,[222] sodium and silicon ions were detected through XPS, meaning that heating close to the melting point of the glass allows the diffusion of these ions into the titania. In the same study, heating with stainless steel led to Fe^{3+} and Cr^{3+} being detected.

Despite the advantages of quartz, stemming from a reduced capacity for migration of ions in the support material into the catalyst coating which can alter the performance, glass slides are more widely used as a research-phase support for titania for photocatalysis on account of their lower cost. Glass is readily available in various structures and makes a convenient support for structural analysis of any new photocatalytic material developed, for example through X-ray diffraction or SEM where the flat surface of a glass slide is ideal for probing the nature of the material.

A common issue faced by researchers making films of catalyst materials on glass is that of poor adhesion. It is commonplace to incorporate a pre-treatment stage into the catalyst preparation process, in order to prevent significant flaking and improve the activity

of the films by adjusting the surface chemistry of the glass substrate. Samsudin et al.[224] described several techniques for surface modification of glass, including gamma irradiation, chemical surface oxidation, plasma treatment and UV/ozone oxidation, to introduce functional groups with minimal alteration of bulk properties. Indeed, several of these methods first used in research on glass are now widely applied to other supports.

Chemical surface oxidation methods include etching, for example by immersing the glass in potassium bifluoride,[208] though this must be conducted with extreme caution due to the formation of hydrofluoric acid as a by-product. Furthermore, sulfonation can also help enhance the photocatalytic activity of titania by improving adhesion and film quality, as well as reducing the ability of Na^+ ions to cross from the glass into the film. This was demonstrated by Wu et al.[223] through the insertion of a self-assembled monolayer (SAM) of terminating bifunctional alkoxysilane on one end and sulfonate ($-SO_3H$) groups on the other, in between the glass substrate and titania film. The alkoxysilane group forms bonds to the surface *via* exposed hydroxyl groups, where the sulfonate group bonds to the titania particles, forming a molecular bridge and improving adhesion. Another simple and effective method for preparing the surface of glass for film deposition is to mechanically roughen the surface with abrasive paper.

As well as chemically or mechanically etching the glass surface, another commonly utilised method of preparing glass to use as a support for thin films for many applications, not just photocatalysis, is exposing the glass to UV light, often referred to as UV/ozone treatment (see Figure 4.1). This technique often employs bench-top instruments that emit UV light of around 250 nm, which cleaves bonds of organic molecules on the surface, helping to clean it and prepare the surface for coating. They also produces a strong emission around 185 nm, converting molecular oxygen to ozone, which is highly oxidising and can attack other small molecular fragments, as well as oxidise the surface to functionalise it. This is often found to be preferred over wet chemical techniques (though sometimes is used in conjunction with them), since it is a much more practically simple technique that does not require any complex chemical processing, and is thus quicker and easier to employ. UV/ozone treatment can give precise control over the modification process without the need for any hazardous chemicals often used in wet chemistry techniques,

and can be conducted in various gases at room temperature.[224]

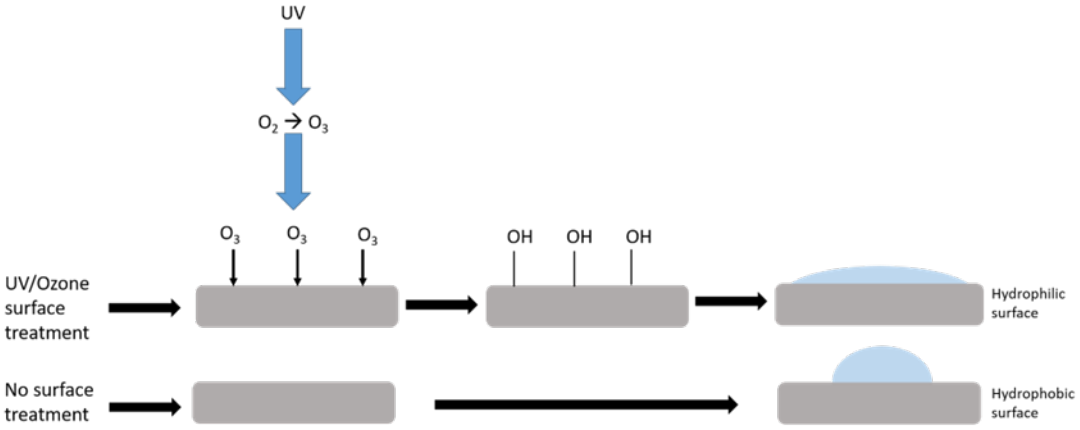

Figure 4.1: Schematic to illustrate the mechanism of functionalisation achieved via UV/ozone surface treatments

Further to this, there also exist examples of plasmas being directly used for enhancing the effect achieved by a UV/ozone treatment. Although plasma treatment is more intensive and achieves a prepared surface in a shorter amount of time, it also requires a vacuum where UV/ozone does not. This means more specialist equipment is required, and can therefore be more expensive and less accessible. Yamamoto et al.[225] conducted a study into how the hydrophilic and hydrophobic properties of glass can be altered using plasma treatments. They found that plasma treatment allowed for excellent hydrophilic properties, though with a limited lifetime. Thus, it is important to introduce the catalyst coating rapidly after plasma treatment while the surface modifications are still present.

As well as physical and chemical modifications to the surface conducted during the laboratory preparation process, another promising option is to use commercially available FTO glass (fluorine-doped tin oxide glass), which was demonstrated by Odling et al.[206] to improve adhesion of a titania paste with significantly less flaking than that of glass, without requiring any further pre-treatment other than cleaning and a simple UV/ozone step. However, one disadvantage of using FTO glass is that is it much more expensive than plain glass (by approximately 40 times, as listed by scientific supplier Sigma Aldrich). It is also unnecessary to have a conductive surface for photocatalysis.

Once the glass is sufficiently pre-treated, the choice of coating method must then be

made. As with most substrates, the method chosen for obtaining layers of the given catalyst on glass vary largely depending on the structure of the substrate involved. For example, many studies, such as by Odling et al.,[206] employ doctor blading to create smooth films, though this can only be performed on flat glass surfaces, not complicated structures including glass fibres, beads, tubes etc. Doctor blading involves applying a paste or slurry of the catalyst material onto the glass slide surface following the cleaning and pre-treatments stages. The paste is then smoothed out across the surface, for example by using a glass rod to push the paste across evenly. This is a technique frequently used for its simplicity. Commercial semiconductor catalyst pastes are available, so one would simply have to pre-treat the glass slide and apply the desired paste, without the need for complex chemical processing. As well as using commercially available pastes, this technique can be customised for specific materials research needs, by preparing one's own paste, or slurry, and applying that to the slide in the same way.

Other methods of preparing catalyst films on glass include dip-coating and spin-coating, as well as simple immersion techniques. Examples of these can be found widely across the literature, where slight alterations are made to account for different material and substrate requirements. Immersing the glass support material into a suspension of catalyst nanoparticles, such as P25 titania, is a simple way of coating complex structures. For example, Odling et al.[208] utilised this method when coating large quantities of glass beads with titania. In this study, the use of this simplistic technique then allowed for further material modifications to be made using the sequential ionic layer adsorption reaction (SILAR) technique to enhance the visible light activity of plain titania. Such methods are versatile and simple to perform without the need of expensive laboratory equipment. However, it should be noted that the requirement to produce a large enough quantity of the catalyst suspension will lead to more solvent waste than many other coating techniques. This is certainly something to be aware of and consider, especially when trying to utilise photocatalysis for an environmental benefit.

Another method which can be used to prepare catalyst films on glass, as well as other support types, is to use a sol-gel process. This is one of the most widely used techniques for the synthesis of various functional coating films.[226] Relatively low processing tem-

perature, ease of coating homogeneous multicomponent oxide films over a large surface, and good control of the composition and properties of the final material are some of the benefits allowed by this technique.[227] The method involves the preparation of a sol (colloidal suspension of very small particles) and is often performed in conjunction with a dip-coating technique. The thickness of the films resulting from this is often proportional to the viscosity of the sol (which in turn is dependent on the water content). Hence, a higher viscosity is often desirable to reduce the number of dip and annealing cycles required,[196] though this must be performed with caution, as too high a viscosity can lead to films being non-uniform and flaky. More detail on the chemistry behind the sol-gel process is given in Chapter 6.

Another set of methods which can be used in conjunction with glass substrates is that of vapour deposition, both chemical and physical. For large, flat surface areas (e.g. glass slides), physical vapour deposition (PVD) techniques such as magnetron sputtering can be used. However, if a more complex substrate structure such as glass beads, or a customised intricate design for increasing surface area is used, chemical vapour deposition (CVD) is preferred. CVD is an excellent method for achieving high crystallinity, mechanical stability and strong film adhesion, as well as being easily scaled up for industrial uses.[228] As with the majority of commonly used methods to obtain films of titania on glass, CVD produces amorphous layers which can be converted into the crystalline form via calcination. An example of CVD used to produce films designed for photocatalysis was presented by Karches et al.,[229] who used a specially-designed circulating bed plasma-CVD reactor to obtain titania coatings on glass beads. Although these methods have clear benefits for film quality and customisability, as well as reducing the extent of chemical processing and solvent waste involved compared to some of the above methods, they are often less commonly used as they require expensive specialist equipment which makes them less accessible.

4.1.2 Titanium

For titania, or titania-based photocatalysts, one of the more practically simple options for obtaining a film would be to start with a titanium metal support and oxidise the

surface to produce the titania layer, rather than attempting to adhere pre-formed titania to a surface, as is the case for other supports. Thus, titanium offers a straightforward option for titania preparation; eliminating the need for complex chemical preparation and syntheses to coat a different inert surface. A traditionally used method of preparing oxidised films from a support is anodisation (see Figure 4.2).

Anodisation, so named due to the metal to be oxidised forming the anode within an electrochemical cell, is a common method of titania production from titanium and produces porous or nanotube arrays. The titanium substrate is first cleaned and then introduced into an electrolytic solution, where an external potential is applied across the electrodes. After anodisation, the substrate is dried and annealed to obtain crystalline anatase TiO_2.[230–232] The anodisation conditions (e.g. electrolyte, pH, applied potential, time duration and temperature) affect the morphology of the nanostructures that result from this coating method. One prominent example is the use of electrolytes which contain fluoride ions, as these encourage the formation of nanotube arrays (NTAs), whereas other electrolytes tend to results in the formation of more compact layers of titania[233] (see Figure 4.3). The voltage applied influences the morphology of formed nanostructures, with the time the potential is applied for affecting the length of the NTAs.[234]

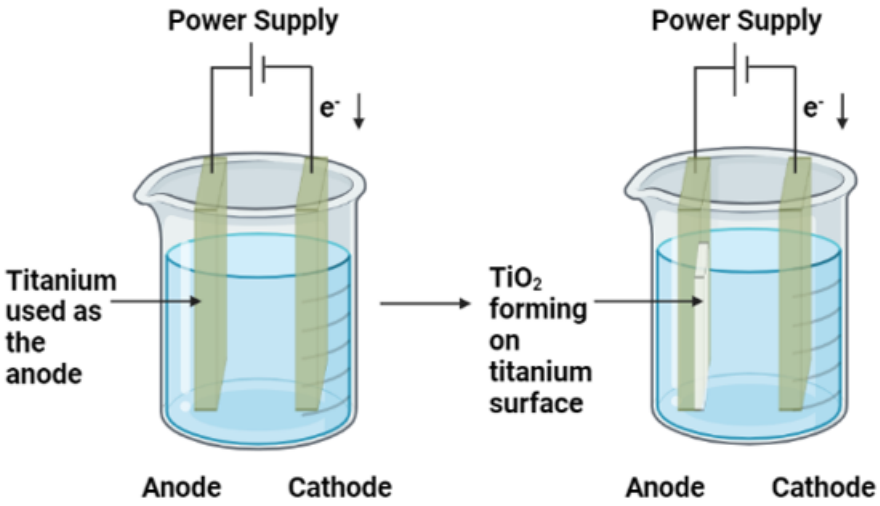

Figure 4.2: Schematic diagram of the anodisation process, demonstrating how the metal oxide layer builds up on the anode when connected to a power supply

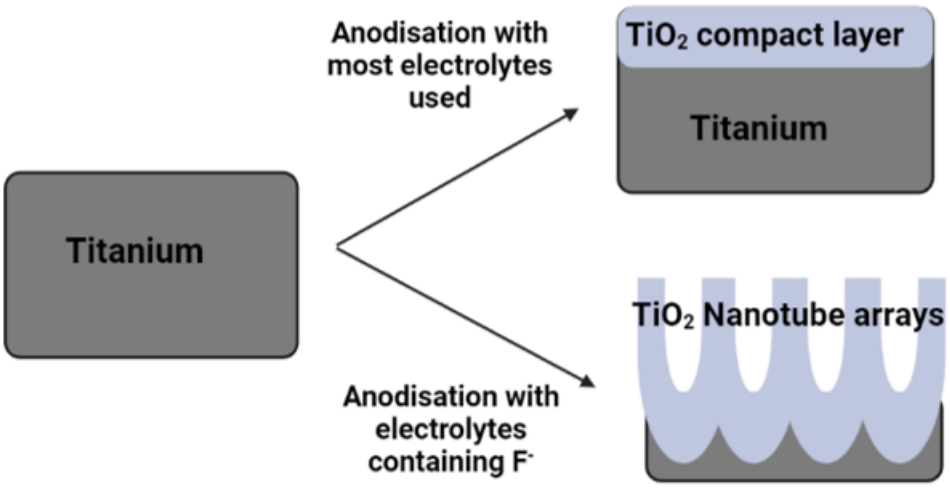

Figure 4.3: Schematic diagram showing how the metal surface forms nanotube arrays with the presence of F^- ions, as opposed to a simple top layer

4.1.3 Stainless Steel

Though there are clear practical benefits for direct oxidation of titanium, using stainless steel as a support is a cheaper alternative, and is thus widely used when a metallic support is required or preferred. The composition of elements used to make up stainless steel, also known as the grade, significantly influences the physical and chemical properties, and hence the suitability of each grade for certain applications. An example is shown below in Table 4.1 for grade 304 stainless steel, which has the following composition:

Table 4.1: Grade 304 stainless steel percentage composition data from.[235]

	C	Mn	Si	P	S	Cr	Mo	Ni	N
Min						17.5		8.0	
Max	0.07	2.0	0.75	0.045	0.030	19.25		10.5	0.10

This grade has good oxidation resistance and can withstand temperatures of up to 870 °C,[235] and as a result has been used as a support in photocatalysis research.[236,237] However, despite the robustness of stainless steel having clear advantages for the lifetime of the support, this property can also lead to problems in activating the surface for optimising the coating process. As discussed above, titania coatings often present poor adhesion to the support surface employed, with stainless steel being no exception. Thus, pre-treatments must be used to provide the required means of tackling this issue, which

include methods such as conversion coating, hydroxylation or the use of adhesion promoters.

One of the most commonly used methods for metallic surfaces is electrophoretic deposition (EPD) from a suspension of the catalyst material. This highly versatile wet chemistry technique can be used to form ceramic films from a colloidal suspension in an organic solvent, by the action of an applied electric field, with the standard set-up shown in Figure 4.4. Due to their natural surface charge, the titania particles move to the stainless steel cathode and form a layer. Its applications are wide due to the ease of tunability, meaning the qualities of the resulting film can be adjusted, such as thickness and porosity. This technique is also able to be used widely due to the simplicity of the practical apparatus, and the fact that deposition can be achieved on any shape of electrode, which is of clear benefit when trying to find the best support structure.[238]

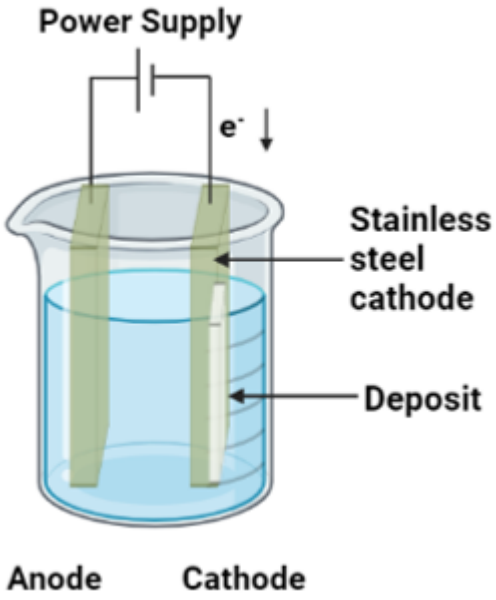

Figure 4.4: Schematic diagram demonstrating the EPD set-up

One drawback of using EPD is that the voltage required is dependent on the particle size of the catalyst in the suspension. P25 titania is often used in such suspensions, which contains nanoparticles of approximately 21 nm in diameter, meaning they are small enough that they should not easily fall out of suspension. Where this is not the case (above 20 μm), the mobility of the particles and the potential difference applied

must be sufficient to counter the effect of gravity that would lead to the particles settling out before reaching the electrode they must coat.[238] One way to try to address this is to leave the suspension stirring overnight and sonicate it to achieve homogeneity, and run the experiment over short lengths of time to avoid this becoming an issue.

As well as being very widely used in film preparation on glass, sol-gel and dip-coating methods are also utilised for stainless steel supports. There are extensive examples of sol-gel methods throughout the literature with slight alterations to the components to suit various applications.[239–244] A simple method for coating metals was conducted by Coto et al.,[221] by dip-coating a porous 'foam-like' nickel structure with a binder. In their study, they used polyacrylonitrile to act as a binder to improve adhesion of the catalyst to the metallic support and reduce flaking. However, it was found that comparisons to samples prepared on fibre glass gave much higher rate constants than the catalysts on the nickel foam support.

4.1.4 Plastics

Plastics are not as commonly used as glass, titanium or stainless steel as substrates in photocatalysis research, but could actually provide an excellent support for photocatalysis on the basis of the desirable properties of being low cost, lightweight and easy to shape to increase surface area. Many researchers have moved away from using plastics due to negative connotations associated with the adverse environmental impact caused from their over-use. However, using waste materials such as old bottles as supports for photocatalysts would be a useful way to re-purpose single-use plastics, particularly ones which are not widely recycled.

Initially, plastics were used as containers for the water treated through solar disinfection (SODIS) before combining with photocatalysis, by simply filling a plastic bottle with contaminated water and irradiating it for up to a day, as introduced by Acra[245] and discussed in Chapter 1. In order to tackle the drawbacks of simply using plastic bottles for SODIS alone, Meichtry et al.[246] coated the walls of plastic bottles with titania prior to filling them with contaminated water and exposing to solar irradiation. Their

method consisted of filling a plastic bottle with a titania suspension, shaking to achieve a homogeneous coating, draining then drying at room temperature for 24 hours. It was found that the activity within the bottle coated with titania was similar to that of a bottle containing titania coated on various glass supports, but used a smaller quantity of catalyst.

This study by Meichtry et al.[246] influenced other researchers to adapt this simple immersion technique for coating plastics with P25 titania, for example de Barros et al.[247] and de Melo Santas et al.[248] Where the immobilisation method employed by de Barros et al. also used PET plastic bottles as a support, de Melo Santas et al. provide examples of other plastics, such as polystyrene. In their paper, de Melo Santas et al. utilised waste polystyrene from used food packaging as a support for titania to remove food dyes from water using photocatalysis.

Interestingly, in the same study by de Barros et al.,[247] it was found that attempting to improve adhesion by carefully scratching the surface of the PET with an abrasive material in fact lead to the formation of poor quality films, where the grooves caused accumulation of titania in certain regions on the surface. This resulted in flaky, inhomogeneous films, whereas not conducting any surface modification treatments was preferable in this case. For the unmodified PET surfaces, it was found that the immobilised titania did indeed act to remove the test pollutant of paracetamol, which was not observed for the control test with just UV. This supports the idea that SODIS can be useful for bacterial pollutants, but a photocatalyst is particularly advantageous when aiming to also remove potentially harmful molecular contaminants. It was observed that repeating the immobilisation process 5 times achieved the optimum photocatalytic rate.

As well as the commonly used immersion techniques, researchers have also employed thermal fixation methods to adhere catalyst powders such as P25 titania to the surface of plastics. For example, Altin et al.[249] used polystyrene balls as a support, which they heated with P25 titania in crucibles at 162 °C, whereby the glass transition point of the polystyrene (150 °C) was passed. This meant that the surface softened and allowed the titania to adhere, with remaining loose powder being sieved off. Although photocat-

alytic degradation of bacteria and reduction of Cr(VI) was observed in this study, which presents an extremely simple and practical method of coating plastic supports with photocatalyst materials, it was also found that this method led to the formation of an uneven surface with titania aggregation. Although many thermal methods can be utilised for preparing catalyst coatings on plastics, the low melting point of many plastics can pose problems for coatings prepared using other methods, such as immersion techniques. The requirement to anneal such prepared films limits the possibility of using certain support materials that cannot themselves withstand the necessary high temperatures of around 500 °C. For this reason, cold methods can be used to synthesize anatase titania at temperatures below 100 °C, opening up the possibilities of using materials such as plastics and fabrics, which have benefits of being lightweight and flexible, with more versatility.

Plastics are an excellent option for catalyst supports where the requirement to be lightweight is of high importance, and many of the coating techniques that they allow for are practically simple and affordable. However, there still exists the problem of their instability, both in terms of low temperature resistance and in terms of monomer leaching, which limits the choices of coating methods available, with hazardous syntheses posing issues for real-world applicability as well as reducing willingness to use these on both research and industrial scales.

4.1.5 Textiles

Another less frequently used, but very promising, class of support materials for photocatalysts is that of textiles. These are an extremely versatile class of substrates, with many different preparation methods available, depending on the application. For example, textiles may be produced from naturally occurring materials, such as wool or cotton, or man-made synthetics for achieving specific material properties. One benefit of using textile supports is the naturally high surface area nature of their surfaces on account of the weaving process used in their formation. This acts to improve adhesion and increase the area available for the disinfection reaction to take place, even on supports of simple geometries. In addition, many are cheap and widely accessible, making them strong candidates to use for research in enhancing water purification using immobilised

photocatalysts. Common practical methods employed to adhere the catalyst material to a textile support include sol-gel methods,[250–253] in-situ synthesis,[88,254] electrostatic assembly[255] and pad-dry-cure methods.[256,257]

Despite the roughness of such supports, many groups still opt to conduct preliminary pre-treatment steps to functionalise the surface for further enhancement to the extent of adhesion. There have been examples throughout the literature of treatment methods including the use of plasmas treatments (radio-frequency and microwave plasma, as well as using UV irradiation to generate highly oxidising oxygen species which causes scission of C-C bonds, allowing for C-O or C-N bonds to form, making the surface more hydrophilic[257,258]) to prepare synthetic textiles, in order to enhance the loading of titania by wet chemistry techniques (Bozzi et al.[258] and Kiwi and Pulgarin[257]). This is an excellent example of the application opportunities using textiles as a catalyst support allows for, which is discussed in detail in a review by Dastjerdi and Montazer.[259]

Many coating procedures can be performed by immobilising the catalyst already prepared in powder form to the surface. However, in-situ synthesis methods are also frequently employed for coating, with one such example given by Danwittayakul et al., where a study was conducted into photocatalysis with ZnO on cellulose and polyester fibres to enhance the SODIS process.[88] Rather than attempt to directly adhere the ZnO particles to the surface of the fabrics, they first deposited a seeding layer by dipping the fabrics into a dispersion of ZnO nanoparticles followed by heating at 90 °C. ZnO nanoparticles were then synthesised on top of the seed layer by incubating equimolar concentrations of zinc acetate dihydride and sodium hydroxide in ethanol at 60 °C for 3 hours. The final step in preparing the catalyst was to then achieve ZnO nanorods to improve the surface area available. These were grown from the seeded nanoparticles for 20 hours in a chemical bath consisting of zinc nitrate and hexamethylenetetramine (HMT) at 90 °C. Finally, the samples were then annealed at 90 °C overnight.

It is interesting to note that, when the catalyst system using polyester was tested under real sunlight conditions, 98% degradation of the bacteria was achieved in just 15 minutes, whereas control experiments with only SODIS and no photocatalyst took at least

90 minutes to achieve the same degradation. This is a great example of how fabrics can make excellent supports for photocatalysts, and how a combined system with SODIS has the potential to achieve enhanced rates of degradation, thus improving the accessibility of potable water in rural areas.

Other synthesis routes include the versatile technique of sol-gel, which is also frequently applied to textile coating processes, with Landi et al. utilising this method in two works,[251,252] based on a study conducted by Diaz et al.[250] The sol-gel method has also been utilised in conjunction with other coating methods, such as the pad-dry-cure technique, as described by Colleoni et al.[260] In general, pad-dry-cure methods involve immersing a textile in a solution bath to apply a desired treatment coating (for example, this can be used in the clothing industry to apply coatings to enhance durability and water-proofing), passing it through padded rollers to squeeze the textile, allowing it to dry, then curing at an elevated temperature. The procedure adapted for use by Calleoni et al. was based on immersion of the fabrics into prepared sols before passing through a two-roll laboratory padder. The textiles were then left to dry, during which time the excess solvent could evaporate and the sol-gel polymerisation process could take place. The textiles were thoroughly dried at 60 °C before finally curing at 120 °C for 5 minutes. Although this adds an extra step to the usual sol-gel process, including the pad-dry-cure technique to the coating procedure helps to improve the extent of catalyst adhesion, and by rolling through the padders, excess material is removed, which can act to reduce the extent of flaking or the presence of inhomogeneous films.

Other notable studies using textiles for supports include those by Wang et al.[261] and Fan et al.,[262] where carbon and nitrogen were used in catalysis. Wang et al. explored the use of cotton as a support for titania modified with C_3N_4 to improve its visible light activity[261] (see Figure 4.5). An interesting finding from this study was the improvement in adsorption capacity of the test pollutants to the catalyst introduced by coating it onto the cotton, compared to the same material in nanoparticular suspension form. This is particularly significant since adsorption capacity limits the rate of reaction, so if this can be increased, the photocatalytic activity of the system has the potential to be notably improved. Another observation made by Wang et al. was that there was almost no

change in the photocatalytic activity in recyclability tests for up to 4 cycles of repeated use. They attributed this to the electrostatic interaction between the cotton and catalyst film, increasing the stability of the film.[261]

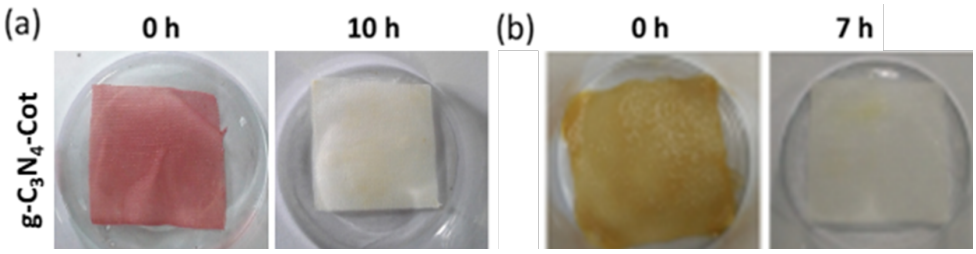

Figure 4.5: Digital images to show the successful degradation of (a) red wine and (b) coffee by C_3N_4 on cotton achieved after exposure to irradiation for 10 hours. Reproduced from[262] with permission from Elsevier Publishing.

Fan et al. also reported excellent photocatalytic degradation of Rhodamine B (RhB) when using graphite-like carbon nitride as a catalyst on cotton.[262] Due to the difficulty in modifying titania to successfully degrade pollutant under visible light, Fan et al. attempted to move away from titania by using g-C_3N_4 (band gap = 2.7 eV), which has also been used frequently in photocatalysis research. In this study, benefits of using textiles as supports were discussed, including good moisture absorption, air permeability, durability and, in some cases, biodegradability. These are very desirable properties for support materials, particularly the possibility of biodegradability as movements must be made to reduce the environmental impact of industrial process, with water purification being no exception.

4.1.6 Support Summary

A plethora of support materials and structures exist and are employed by a range of research groups, making it impossible for the above discussion to be completely exhaustive. Rather, it describes some of the most commonly used materials for the study of photocatalysis, though many more are becoming common place. Where once the default material for immobilising photocatalysts would have been considered to be glass, it is now very clear that many more possibilities exist, all with varying advantages and disadvantages which define the suitability of each support for a given application. Indeed,

many groups now chose to develop their own materials to use as supports, with the freedom to customize and tune the properties to fit their exact needs. An example of this using an infrequently employed material which shows great promise was presented by Kete et al.[263] In their study they investigated a photocatalytic reaction for water purification using an Al_2O_3 porous monolith foam (10 pores per inch) as the support for a TiO_2 catalyst, which allowed for excellent surface area availability and catalyst adhesion.

Some of the main properties of each support focused on in this Chapter are summarised below in Table 4.2.

Table 4.2: Support summary.

Support Material	Advantages	Disadvantages
Glass	Low cost (relative to other glass-type supports such as FTO or quartz)	Heavy when scaled up
	High temperature resistance	Fragile
	High chemical resistance	Ion diffusion causing film contamination can occur
	Ease of surface analysis when flat (e.g. glass slide)	Surface preparation required, can be extensive depending on the structure/roughness of the substrate
Titanium	High temperature resistance	High cost (relative to stainless steel)
	High chemical resistance	Limits coating through anodisation to titania-based materials
	Allows for surface oxidation	
	Malleable for geometry adjustment	
	Little surface preparation needed	
	Non-fragile	
Stainless Steel	Low cost	Requires extensive surface preparation
	Malleable for geometry adjustment	Ion diffusion causing film contamination can occur
	High temperature resistance	
	High chemical resistance	
	Non-fragile	
Plastics	Low cost	Poor temperature resistance
	Lightweight	Microplastic and monomer leaching
	Easily shaped for specific needs	May require extensive surface preparation
	Non-fragile	
Textiles	Low cost (though cost will vary depending on the nature of the textile e.g. how bespoke it is)	Poor temperature resistance
	Lightweight	Microplastic leaching from synthetic textiles
	Versatile morphology	
	Less surface preparation required relative to other materials e.g. stainless steel	

From the above discussion and summary, it is clear that all possible supports have both advantages and disadvantages for use in photocatalysis, with these being highly context and application dependent. The choice of support has a large effect on the performance of the overall photocatalytic treatment system, with no single substrate standing out as the most convenient for all contexts. For the context of this research, focusing on water treatment in rural areas, qualities such as long-term stability, ease of handling, low costs and the robustness of the resulting film are key.

Preliminary tests were conducted to evaluate at the use of stainless steel and plastics as supports, all of which yielded poor adhesion. Stainless steel meshes were coated using electrophoretic deposition as well as dip coating techniques, with and without chemical etching to prepare the surface. In all cases, the coatings were very flaky. Similarly for the plastic trials, PET bottles were used with an immersion technique similar to that used for the glass beads, as outlines in Chapter 2), but this gave very uneven coatings which would easily peel off. Figure 4.6 show examples of poor quality coatings.

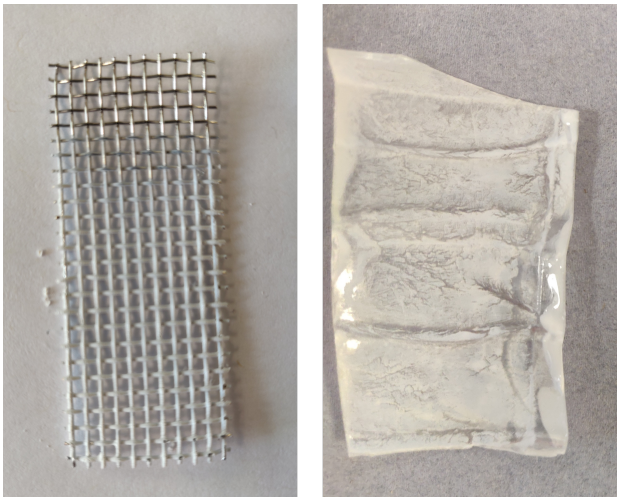

Figure 4.6: Images showing poor film qualities of TiO_2 on stainless steel (left) and PET plastic (right). It can be seen that areas of the coating on the stainless steel mesh have fallen off and are visible next to the substrate.

Therefore, due to the convenience and greater understanding of how to achieve better quality films, this Chapter will focus on the use of glass as a support, and explore the effects of changing the structure of the glass substrate to address common issues such as poor adhesion when the surface is too smooth.

As presented above and in Chapter 3, glass beads have been used previously and provide a good starting point due to the high surface area offered. However, the glass beads themselves add to the overall cost of the treatment method, which needs to be as low as possible for widening access to safe water in less affluent areas. The beads also have a very smooth surface, which does not constitute good adhesion of catalyst films and thus requires extensive chemical etching, adding to the costs and complexity of preparation.

Thus, a material with a similarly high surface area as round beads, but with a naturally less-smooth surface and lower costs is desired. As such, this research focuses on the application of used glass bottles ground into chips, such that waste can be upcycled and used again, increasing sustainability and reducing costs. Due to the nature of grinding down the bottles to form the glass chips, the surface is left rough, which has the potential to be a better surface for coatings to adhere to than the smooth surface of soda lime glass beads.

The glass chips were provided by locally-based water treatment company Dryden Aqua, who turn used glass (e.g. from glass recycling points) into water filtration media. The filtration process utilises a chemical coating to reduce any biofouling on the glass surface, but the glass provided for this work did not possess any coatings, and was simply ground down into small chips. The appearance of these chips with and without catalyst coating is shown in Figure 4.7.

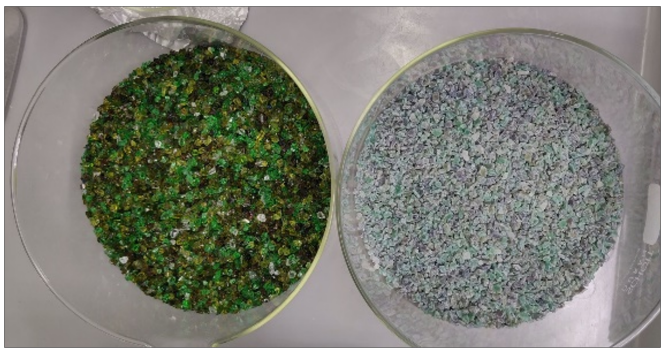

Figure 4.7: Image to show the appearance of the glass chips used in this study, without (left) and with (right) catalyst coating.

The use of glass beads or chips also addresses an important question for the usability of photocatalysis for water treatment: scalability. Where it may be harder to increase the capacity of treatment where glass slides, or indeed other substrates such as metal meshes

or plastic sheets, are used, the high surface area and easy customisation of a system using beads or chips provides another advantage for this support type.

4.2 Experimental

4.2.1 Initial Tests on the Importance of Chemical Etching for Different Substrates

The process used here for etching of glass substrates and subsequent coating via immersion in a catalyst suspension is presented in Chapter 2.

The photocatalytic activity was then tested according to the procedure outlined in Section 2.2 of Chapter 2 using 30 mL of 4-chlorophenol (156 μM) as the test pollutant under 370 nm.

The change in concentration of 4CP was tracked using UV-Vis absorption spectroscopy on a Shimadzu 1800-UV instrument, as described in Section 2.2.1 of Chapter 2.

Following this, the robustness of the films was tested by placing the coated glass substrates into an ultrasonic shaker for 5 minutes to simulate aggressive long-term use, before repeating the photocatalytic testing to evaluate if there was any change to activity.

4.2.2 Film Adhesion Modifications

In order to improve the adhesion between the titania coating and the glass substrate surface, silica was used (both as a layer on top of the glass, and mixed into the nanoparticle suspension) to act as a binder between the two materials. The coatings containing SiO_2 were formed by preparing suspensions of the catalyst and adding an appropriate quantity of silica solution. Firstly, tetraethyl orthosilicate (TEOS) was added to ethanol and stirred to form the silica solution. At the same time, a photocatalyst suspension was formed by adding powder P25 TiO_2 (ca. 6.67 g) to butanol (200 mL), 37% HCl (2.5 mL) and $Ti(OBu)_4$ (10 mL) whilst stirring vigorously overnight. To this suspension, SiO_2 was added to form separate suspensions of the 10% SiO_2 in TiO_2 and 50% SiO_2 in TiO_2

to be poured over the glass chips for coating.

The coating process involved pouring the necessary suspension over the glass chips and leaving them immersed for 5 minutes, before removing the excess and drying the chips at 150 °C. Following this, the chips were then annealed at 500 °C after each layer, until the coatings as shown above in Figure 4.8 were achieved. Note, for consistency, each material had 3 layers, so in the cases where there are not 3 different materials used, either 2 or 3 layers of the catalyst were used to maintain the same level of film thickness.

The photocatalytic activity was then tested according to the procedure outlined in Section 2.2 of Chapter 2 using 30 mL of RhB (6 μM) as the test solution. Tests were conducted under UV light at 370 nm. The change in concentration of RhB was tracked using UV-Vis absorption spectroscopy on a Shimadzu 1800-UV instrument.

Following this, the robustness of the films was tested by placing the coated glass chips into flasks containing deionised water, which were then placed on a shaker plate for 15 hours at 220 RPM. The chips were then collected, the resulting loss of coating rinsed away, and the activity measured as above using RhB under 370 nm for 3 hours.

4.2.3 Microbial Testing

Testing was conducted with *E. coli* according to the procedure outlined in Section 2.2.3.3 of Chapter 2.

4.2.4 Summary of Sample Names and Abbreviations

A summary of the names given to all coating methods used in the proceeding discussion for glass chips is given below in Table 4.3.

Table 4.3: Summary of sample names for this Chapter.

Name	Description
NT	Non-treated glass chips. No pre-treatment used, only the catalyst coating applied after cleaning.
PT	Pre-treated glass chips. The etching process used for the glass beads as presented in Section 2.1 of Chapter 2 was used here on the chips before adding the coating.
B10T	1 base layer of silica, followed by a mixed layer of 10% silica in the catalyst, followed by a top layer of just the catalyst
B10	1 base layer of silica, followed by a mixed layer of 10% silica in the
10	No silica base, but a 10% mix of silica in the catalyst
B50T	1 base layer of silica, followed by a mixed layer of 50% silica in the catalyst, followed by a top layer of just the catalyst
B50	1 base layer of silica, followed by a mixed layer of 50% silica in the catalyst
50	No silica base, but a 50% mix of silica in the catalyst

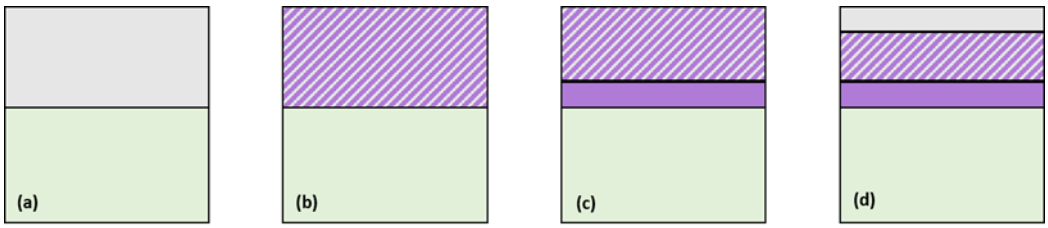

Figure 4.8: Illustration of catalyst coatings on the glass chips. Left to right: (a) catalyst alone, (b) mixed coating of catalyst and silica, (c) silica base with a mixed coating of catalyst and silica, and (d) a silica base with mixed coating of catalyst and silica, followed with a top layer of plain catalyst.

4.3 Results and Discussion

4.3.1 Initial Tests on the Importance of Chemical Etching for Different Substrates

Prior to the studies including application of silica to the glass chips to improve adhesion, an initial test was performed to see if it would be necessary to perform the same level of chemical etching to the chips as is required for the glass beads, or whether the chips could reasonably be used without this chemically intensive and dangerous step. To do this, glass chips were etched in the same way as glass beads, as covered in Chapter 2 and then exposed to aggressive mechanical shaking to simulate repeated use over a long period of time. For this purpose, the samples were immersed in water and placed in an ultrasonic shaker for 5 minutes, which quickly caused some of the catalyst coating to be removed. It was found that adhesion of P25 titania onto the glass chips was comparable for both

the clean, non-treated surface and the etched chips, indicating that it would not be necessary to undergo the potentially hazardous, four-day etching process for minimal benefit.

It can be seen in Figure 4.9 that the removal of the model contaminant 4CP after the 3 hour period of illumination under UV light was affected mostly by sonication for the glass beads, despite these having been chemically etching. The chips did not seem to show as significant a difference in performance when etched or not, following a period of sonication.

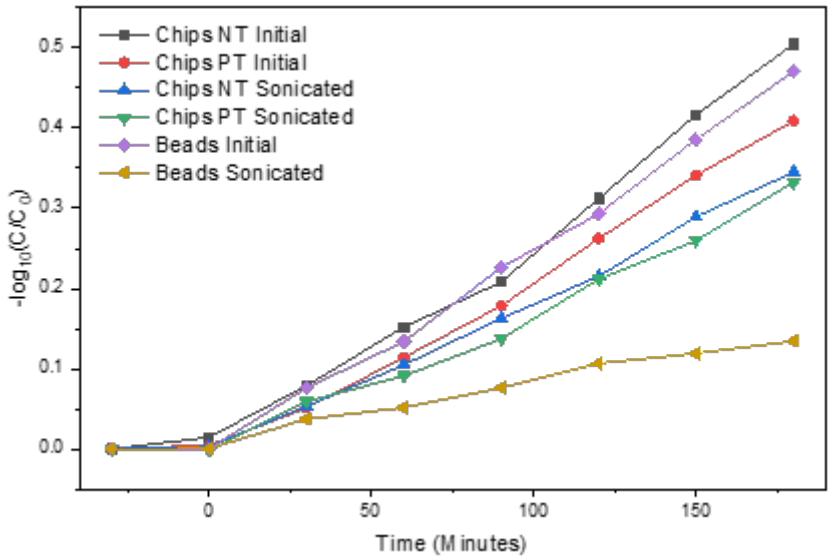

Figure 4.9: Rate of fall in normalised concentration of 4CP under 370 nm LED illumination. NT refers to 'non-treated' and PT refers to 'pre-treated'.

To evaluate the performance differences between the beads and chips, as well as the need to pre-treat the chips, the percentage loss of the model pollutant was determined, also referred to as the degradation efficiency (outlined in Section 2.2.2.2 of Chapter 2). This data, along with the percentage difference between concentration loss before and after damage to the coatings, is shown in Figures 4.10 and 4.11, respectively.

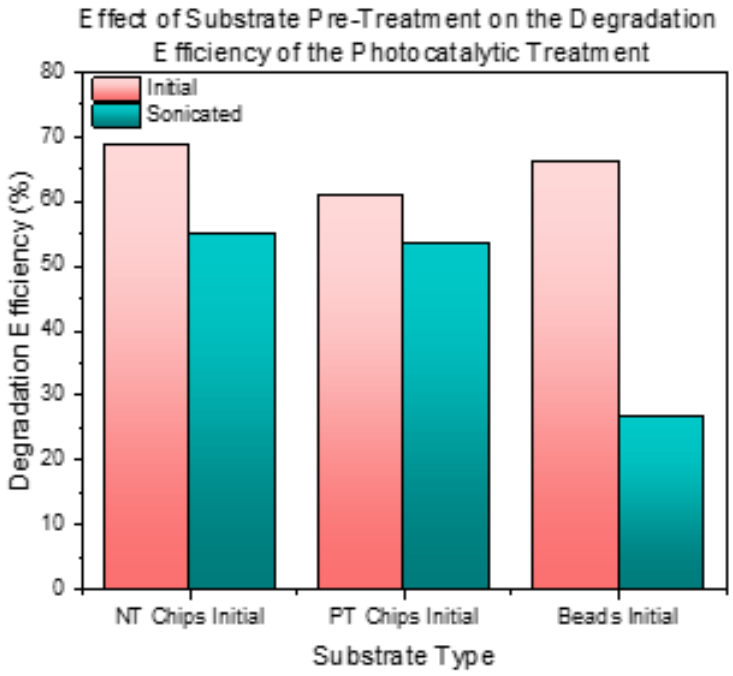

Figure 4.10: Degradation efficiency for the different treatment types under 370 nm LED illumination, before and after sonication. NT refers to 'non-treated' and PT refers to 'pre-treated'.

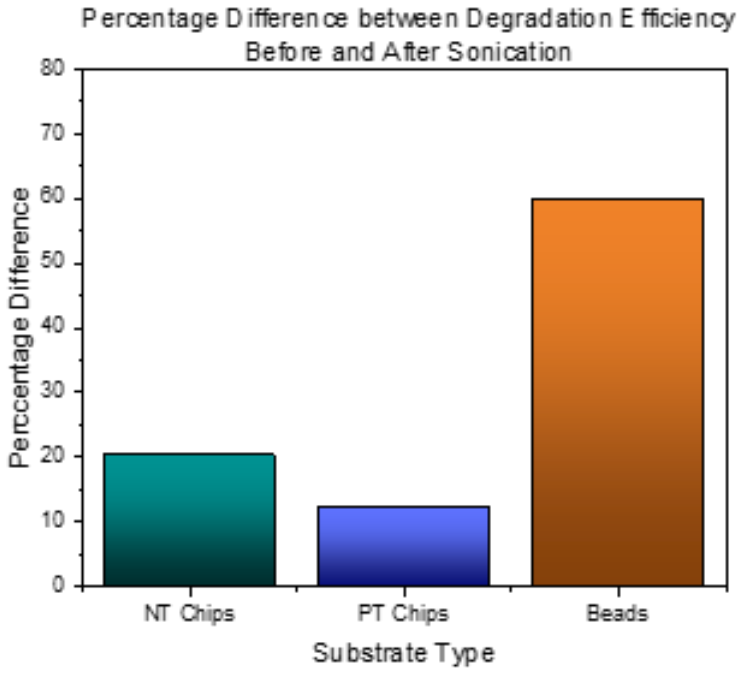

Figure 4.11: Percentage difference between initial and final degradation efficiencies. NT refers to 'non-treated' and PT refers to 'pre-treated'.

It is clear that the rougher surface of the glass chips relative to the smooth glass beads

increases the robustness of the film adhesion and prevents as significant an extent of loss of films, with little difference after sonication for the pre-treated and non-pre-treated chips. This is very promising as it eliminates the need for lengthy chemical etching, reducing the time and chemicals required for preparation, as well as costs, and increases safety. This suggests that chips could provide an excellent substitute for glass beads for photocatalysis in rural areas.

4.3.2 Film Adhesion Modifications

Following the initial results presented above, further testing was conducted to attempt to improve the adhesion to the chips further, without the need for chemical etching. Though the chips already showed promise over the beads, flaking of the catalyst film could still be observed, which is crucial to reduce in order to increase the safety of using this method for water treatment in practice.

In order to achieve this, various modifications were performed using silica mixed with the catalyst powder, in order to improve chemical binding to the glass surface. The different coating types containing SiO_2, as listed in Table 4.3, were prepared and tested for their initial performance, and then again after shaking over-night to mimic extended long-term use. In this case, a shaker plate was used rather than the ultrasonic shaker, since a less aggressive method which could be used over a longer period was desired for the follow-up study, in order to more closely mimic real use conditions. A different model pollutant was also used in order to assess whether similar behaviour would be observed for different chemical contaminants; in this case Rhodamine B was used.

As shown in Figure 4.12, it was generally observed that the higher content of SiO_2 enhanced activity, with the SiO_2 base + 50% SiO_2/TiO_2 (B50) mixture performing best. This was promising as it showed that mixing the catalyst with silica did not damage the activity, but could even enhance it in some cases, likely due to less catalyst loss in rinsing and a smoother coverage on the substrate surface.

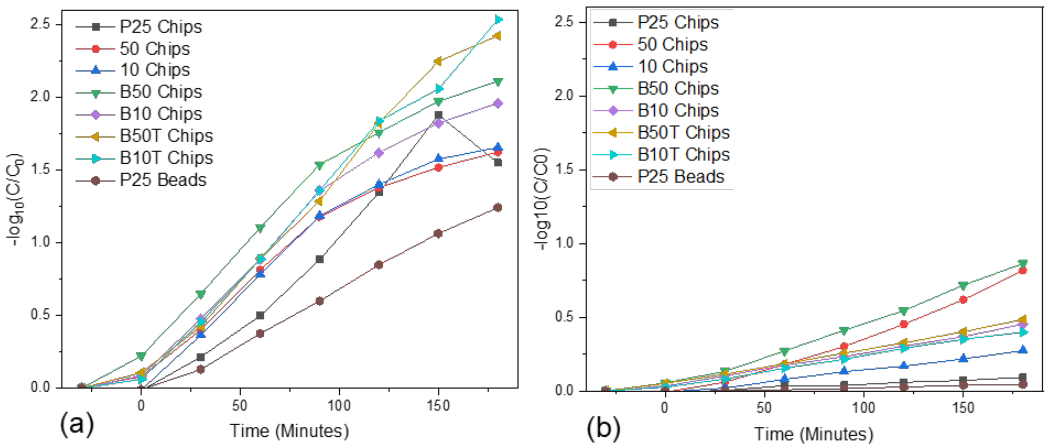

Figure 4.12: Rate of fall in concentration of RhB during treatment under 370 nm LED illumination, (a) before, and (b) after 220 RPM shaking.

This study was further proof that the chips require a less chemically aggressive and time-consuming treatment method to improve adhesion relative to the glass chips, which here were fully etched prior to coating and shaking overnight. Even with a harsher etching process, the beads showed the largest change in photocatalytic activity against RhB between the initial performance and that after accelerated degradation. This can also be made clear in Figure 4.13, which shows the rate constants calculated for the treatment.

These studies show that the mixture of 50% SiO_2 in TiO_2 gave enhanced immobilisation relative to the 10% mixture, and the P25 coating on glass beads after etching. It also showed that the extra top coating of P25 on its own with no SiO_2 was not necessary, and the simpler preparation method of simply using the 50% SiO_2-TiO_2 suspension for all three layers of catalyst coating was both the highest performing, and most convenient to prepare. The effect of the base layer of SiO_2 is less conclusive here, with the performances of the 50 and B50 samples being very similar when the errors in the rate constant calculations are taken into account. The base coat seems to provide more improvement in the immobilisation for the 10% SiO_2-TiO_2 coatings, perhaps because the lower amount of SiO_2 leads to more of the catalyst coating being able to flake off, so small changes to the system may be made more apparent than in the systems with higher content, where the base coating is less important.

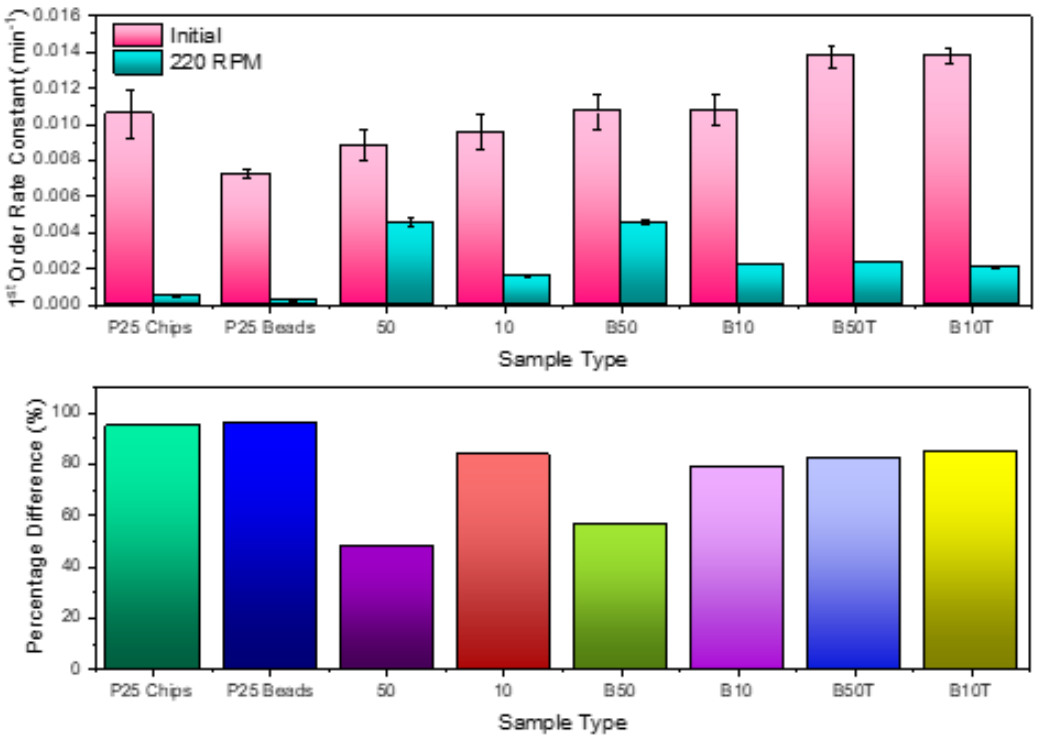

Figure 4.13: Top: Comparison of rate constants for each different coating type before and after shaking. Bottom: percentage difference between initial rate constants and rate constants after film damage. Tests conducted under 370 nm LED illumination.

This study was also repeated with a novel material (given the sample name ZnFeO-B-2), the synthesis, characterisation and possible applications for which is presented in Chapter 5. Even with the more complex chemical system, the same general behaviour was observed, with the 50% SiO_2-catalyst mixture giving the best activity, as shown in Figure 4.14.

In this case, the SiO_2 base with 50% SiO_2/TiO_2 mix seemed to perform best, though the adhesion did not seem as strong for the enhanced material as plain P25, as can be shown by the shaking at 220 RPM removing most of the coating, and another trial at 120 RPM being performed to improve the clarity of the results.

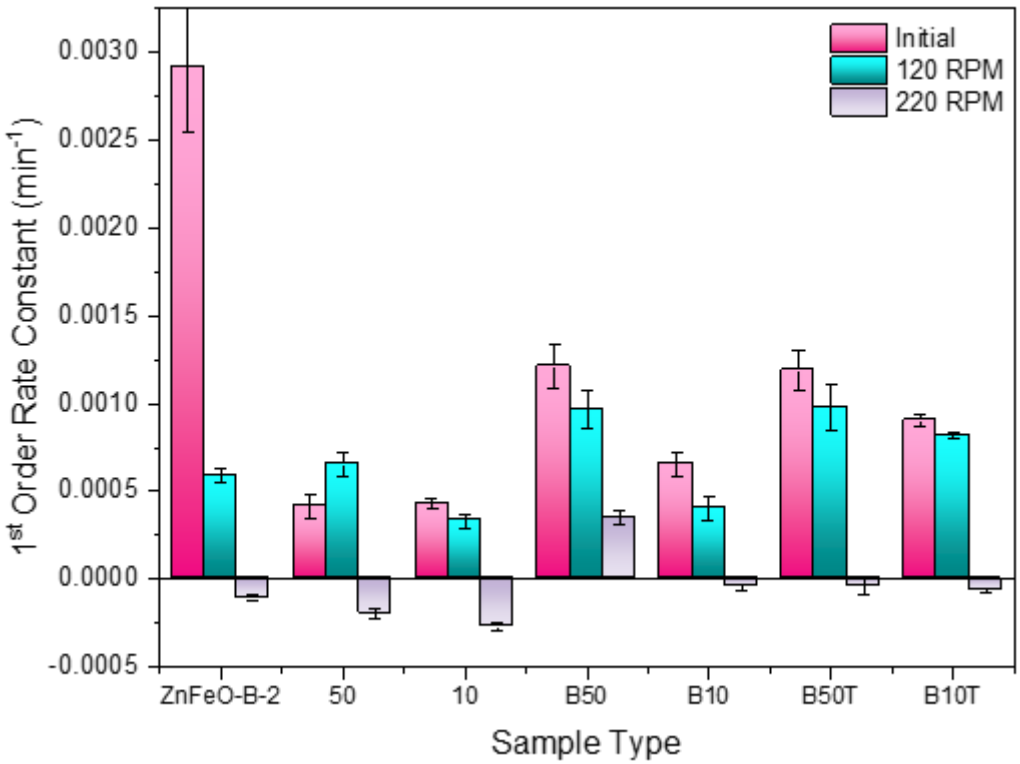

Figure 4.14: Comparison of percentage loss of RhB after 3 hours under 370 nm LED irradiation for each different coating type of the enhanced material ZnFeO-B-2 before and after shaking.

This demonstrates that, although the addition of SiO_2 allowed for significant improvements to the catalyst adhesion, and by extension the lifetime of the coatings, the specific method of improvement employed should be tailored to the catalyst system used in order to optimise fully.

4.3.3 Microbial Testing

Due to the ideal application of this product being in rural regions where the primary contaminants of concern are pathogenic as well as chemical, it was important to test the substrate types for their efficacy in removing bacteria. This is important as bacterial systems are more complex and can lead to differing behaviours than those observed during chemical testing.

It was found that the quantity of glass chips affected the ability of the catalyst to inactivate the bacteria, with 15 g providing a better performance than the original 30 g, as

shown in Figure 4.15.

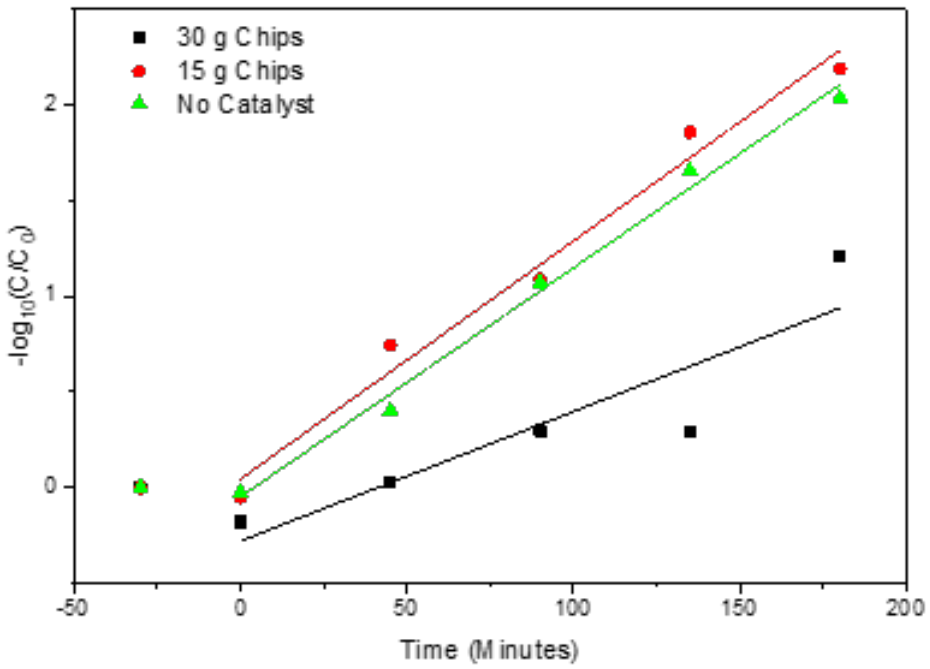

Figure 4.15: Rate of loss of *E.coli* for different quantities of glass chips under 410 nm LED illumination. Note that here, concentration C refers to colony forming units in one millilitre (CFU/mL).

It was seen that 30 g of glass chips coated with P25 TiO_2 performed worse than the condition with the light and no catalyst. This is likely to be due to the bacteria becoming shielded from the light due to the uneven surface of the chips, forming pockets where the bacteria could avoid exposure to light. Thus, with more than a monolayer of chips present, there would be more surfaces for the bacteria to shield from the light, relative to the surfaces available for inactivation. Therefore, when the quantity of bacteria was reduced to 15 g, successful disinfection was more clearly observed, as the bacteria could come in to contact with the surface of the catalyst, which was mostly exposed to light, with few shadowed areas.

This emphasises the importance of system optimisation, and also shows that adding more catalyst can sometimes be detrimental, as can also be the case for slurry reactors.[264–266] It should also be noted here that Figure 4.15 represents data collected under 410 nm irradiation which was collected as part of a study discussed in Chapter 5 on visible light

catalysts. All further bacterial studies presented in this Chapter were collected under 370 nm irradiation to better analyse the behaviour of P25 TiO_2, which is known to perform best under these conditions.

Following the results presented in Figure 4.15, a study was conducted to compare the behaviour of 15 g of coated beads to 15 g of coated chips under UV light. The aim of this was not to assess whether or not the catalyst itself can inactivate bacteria; this is explored in Chapters 5 and 6 in detail. For this study, the purpose was exclusively to evaluate whether the move from beads to chips would cause any disruption to the inactivation of bacteria during the treatment process. For the system with 15 g of either chips or beads coated with P25 TiO_2, it was found that there was little significant difference between the two substrates, as shown in Figure 4.16. It should also be noted that this experiment was conducted under UV light which has bactericidal activity, which explains why the control condition with no catalyst also provides good inactivation, which was not observed to as high a degree in Chapters 5 and 6 where studies were conducted under visible light irradiation.

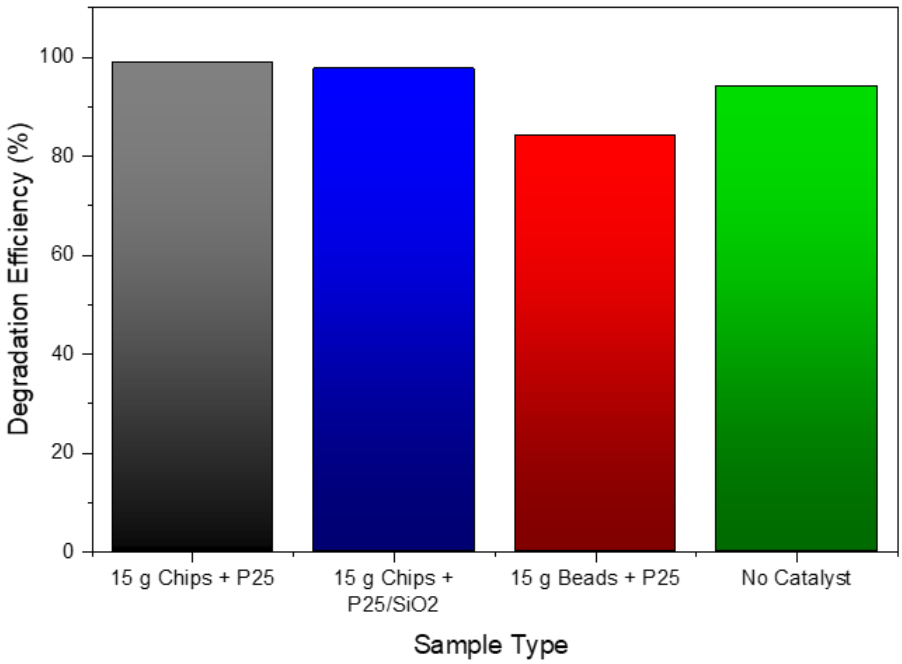

Figure 4.16: Degradation efficiency for removal of *E.coli* for glass beads and glass chips under 370 nm LED illumination.

This is encouraging, as it confirms that using the chips for bactericidal water treatment

as well as the removal of chemical contamination in rural areas would likely have a similar performance to the system with the beads studied in the field tests covered in Chapter 3, but in a more cost-effective and sustainable way with no real loss in performance.

4.4 Conclusions

As outlined in the above study and accompanying literature review, there is no one-size-fits all solution to finding the best substrate for photocatalytic water treatment. Given the broad range of applications within this one field, and different choices of catalyst material that may be required, changes to the support material, structure, pre-treatment and coating processes will have to be made.

Glass is one of the most convenient substrates to use for materials development research on account of its ease of allowing for various analysis techniques to be conducted, such as X-ray diffraction (XRD). Titanium metal has been popular for the ability to anodise the surface to form a TiO_2 layer directly, rather than needing to adhere a coating. However, this could be expensive and dangerous to prepare, which again limits scalability to rural areas. Other metals such as stainless steel have also been investigated, but often chemical adhesion can be difficult and requires adhesion promoters, such as those used in improving the contact between paints and the metal bodies of cars, but these adhesion promoters could be destroyed in the photocatalysis process, as well during annealing at high temperatures during catalyst preparation. Titanium and stainless steel show excellent temperature resistance and exhibit significantly lower interactions with the catalyst layer than is often observed with an inhibitory effect for glass, as well as being less fragile when used in more complex geometries that would allow for the dual action of photocatalysis and micro-filtration.

Similar properties are observed for plastics and fabrics, which also allow for an industry based on used and waste materials to be built, which can allow for a significant environmental benefit if the issues of microplastic leaching can be overcome (this is something that is also a significant issue for synthetic fabrics).

This study showed that transitioning the focus from glass beads to a practical, high-surface area solid support is possible and successful in the form of upcycled glass chips from used bottles. This could be a viable option for reducing costs and preparation time required, which is very attractive for taking photocatalysis from lab-based research to larger scale, practical implementation and still being affordable.

Given that the catalyst coatings show increased robustness when combined with an SiO_2 base layer, topped with a 50% SiO_2/TiO_2 mix, it would suggest that this extra step could eliminate the need for other lengthy steps, such as chemical etching of glass beads, as well increase the lifetime of the catalysts without reducing activity. Considering the higher cost of glass beads relative to the chips, as well as the requirement to use the more involved and dangerous process of etching, makes this substrate very impractical for use in rural areas.

Thus, the benefits provided by the glass chips combined with the addition of silica can significantly outweigh the minor reduction in activity seen for bacterial inactivation, considering it is likely to reach acceptable levels within an acceptable time frame - SODIS can take between 6 to 48 hours, depending on weather conditions , so an enhancement on the time required and the extent of water treatment will make the process worth using, given that the costs incurred will be much reduced by switching to glass chips as the substrate. Despite the clear improvement in adhesion and good performance against both chemical and pathogenic contaminants shown for the 50% SiO_2/TiO_2 coating method, some flaking was still observed, as evidence by the drop in activity after shaking overnight at 220 RPM. Though this was much more robust than other coating types, further improvements could be made to ensure safe adhesion for applications where access to high-power centrifuges or micro-filtration is not available. Further exploration into different ways to prepare the glass surface and mix with silica could be explored as part of future studies into improving adhesion of nano-powder catalysts onto glass substrates.

Chapter 5

Material Development for Solar Photocatalysis: TiO_2 and Zinc-Iron Oxide Composites

This Chapter focuses on the synthesis of visible-light activated catalysts, and some of the difficulties faced when attempting to modify titania to extend its high-performance photoactivity across the whole solar range.

5.1 Literature Review and Background Theory

Over the past twenty years, the possibility of harnessing the Sun for water treatment using photocatalysts has slowly become closer, but never quite achieved on a practical scale for rural use. At the same time, the water crisis threatens to worsen, and the need for a robust and accessible water treatment system becomes even more important. It is a frequent issue in the field that a lack of standardised testing and characterisation makes comparisons between materials difficult, and therefore assessing the applicability of a novel material intended for decentralised water treatment under solar irradiation is far from simple.[267] Here, the difficulties that have prevented this from becoming a reality thus far, despite a wealth of research and many materials being developed, are discussed.

One way to attempt to improve solar activation of photocatalysts is to improve visible light harvesting, and thus not simply depending on the UV portion, such that a larger

part of the solar spectrum can be utilised. However, it is a common occurrence that when a catalyst is developed with good visible light activity, this is often at the cost of good UV light activity. Many studies have developed photocatalysts as enhanced TiO_2 materials, and do demonstrate a significant improvement of activity within the visible region of light, but show either no improvement in the UV, or even a drop. This can often tip the scales and results in TiO_2 still performing better under solar light, despite the synthetic efforts to improve TiO_2.

A review article by Rengifo-Herrera et al[268] discussed this phenomenon relating to nitrogen-doping of TiO_2, suggesting this arises from the shift in formation of highly reactive $\cdot OH$ to O_2^- radicals. In N-modified TiO_2 materials, visible light can photo-induce electrons from N 2p mid-gap states to the conduction band, which poses enough redox potential to reduce molecular oxygen to form superoxide radicals. However, the photoinduced holes from the mid-gap states do not have positive enough redox potential to oxidise water and generate $\cdot OH$ radicals (according to the reactions outlined in Section 1.2.2.1 of Chapter 1). This leads to the predominant ROS species being superoxide, which is less reactive than $\cdot OH$. It is often discussed that more states in the band gap caused by oxygen vacancies can lead to a smaller effective gap, and therefore lower energy photons required for inducing photocatalysis, thus meaning visible light can be utilised.[268–270] However, it is also possible that these extra states could be detrimental if they prevent the key redox potentials for production of ROS being accessed, making $\cdot OH$ formation thermodynamically unfavourable.

As well as having lower oxidative power than $\cdot OH$, forming O_2^- as the main ROS present can be detrimental as it is very short-lived and unstable in aqueous media often undergoing further reactions to form H_2O_2.[271] Thus, it could be argued that substituting photocatalytic sites that can generate non-selective and highly reactive OH radicals under UV with sites that can generate more selective and less powerful radicals such as O_2^- under visible light, does not help to improve the photoactivity under the whole solar spectrum, despite being able to technically utilise more wavelengths present.

An alternative method to doping, as discussed in Section 1.2.2.2 of Chapter 1, is the

formation of a heterojunction between two semiconductor materials with different band gaps. This could be very powerful for improving solar light activity, as charge recombination can be reduced without necessarily removing the ability of TiO_2 to form ·OH.

To investigate this phenomenon further and assess if a simple, low-cost synthesis route to form a heterojunction can be found, this Chapter will focus on the synthesis, characterisation and testing of a class of materials produced with the aim of forming a composite of a zinc-iron oxide with P25 TiO_2. Similar attempts to this have also been reported in the literature previously,[272,273] whereby the products indeed showed very good improvement in the visible region, but a worsening in the UV. These two studies used $Zn(NO_3)_2$ and $Fe(NO_3)_2$ as starting materials for the formation of $ZnFe_2O_4$. Another study by Dhiman et al[274] used different starting materials, and looked at the activity of the $ZnFe_2O_4$ material on its own, without combining with TiO_2 and found good visible light activity for removing dye from solutions. For the study presented here, the synthetic route from Dhiman et al was used to prepare $ZnFe_2O_4$, then modifying to combine with TiO_2, to compare the effects.

Some studies reported the addition of such transition metal oxides could lead to enhanced solar spectral activity, though this has involved assistance from photo-Fenton system (addition of H_2O_2), such as a study by ThanhThuy et al on $ZnSe/TiO_2$ nanocomposites.[275] Another example of a high-performing photocatalyst made as a composite from TiO_2 and a transition metal oxide was presented by Wang et al.[276] as a core-shell nanostructure of a silver-coated magnetic Fe_3O_4-TiO_2 material, though this can largely be attributed to the presence of the silver nanoparticles allowing for surface plasmon resonance. A more simple and low-cost system is required for the specific application to water treatment in rural India, which this Chapter will focus on exploring.

5.2 Experimental

5.2.1 Summary of Sample Names

The samples studied in this Chapter are presented in Table 5.1. More detailed descriptions of the synthesis routes are given in Section 5.2.2. The names are given to indicate

the synthesis route type (e.g. A if autoclaved, R if refluxed, B if stirred with base) and the number indicates the percentage of $ZnFe_2O_4$ was intended to be present with respect to P25 TiO_2.

Table 5.1: Summary of samples made for this Chapter and their assigned names

Sample Name	Description
ZnFeO-A-0	Zinc-Iron oxide, no TiO_2 present. Autoclaved during synthesis. Oxalic acid used to catalyse synthesis. Isolated in 71% yield.
ZnFeO-A-5	P25 added to precursor solutions used to form ZnFeO-A, following otherwise the same procedure (5% $ZnFe_2O_4$ in P25). Isolated in 35% yield.
ZnFeO-A-2	P25 added to precursor solutions used to form ZnFeO-A, following otherwise the same procedure (2% $ZnFe_2O_4$ in P25). Isolated in 33% yield.
ZnFeO-A-8	P25 added to precursor solutions used to form ZnFeO-A, following otherwise the same procedure (8% $ZnFe_2O_4$ in P25). Isolated in 11% yield.
ZnFeO-R-2	P25 added to precursor solutions used to form ZnFeO-A (2% $ZnFe_2O_4$ in P25). No autoclaving, instead reflux. Isolated in 28% yield.
ZnFeO-B-2	P25 added to precursor solutions to form ZnFeO-A (2% P25). No autoclaving or reflux. Basic conditions, no oxalic acid (1 mL NH_3 in 50 mL H_2O). Isolated in 29% yield.
ZnFeO-B2-2	P25 added to precursor solutions to form ZnFeO-A (2% P25). No autoclaving or reflux. Basic conditions, no oxalic acid (0.5 mL NH_3 in 50 mL H_2O). Isolated in 24% yield.
BTO-TiO_2	Bismuth titanate composite material prepared by previous member of the Robertson research group at The University of Edinburgh (more details in Chapter 3). Included here as a comparison for novel visible-light activate materials.

5.2.2 Synthesis

$ZnFe_2O_4$ synthesis was conducted according to the method described by Dhiman et al, and is summarised briefly here: $Zn(SO_4)_2.7H_2O$ (1 mmol) and $(NH_4)_2Fe(SO_4)_2$ (2 mmol) were mixed together in a 3:1 mix of ethylene glycol and water (to make a total of 40 mL solvent). To this, oxalic acid (3 mmol) was added, also in the same solvent, before transferring to a Teflon-lined hydrothermal synthesis autoclave and heating for 24 hours at 120 °C. The product was retrieved through centrifugation, washed with ethanol and dried at 80 °C overnight, before annealing at 400 °C for 2 hours. This product was named ZnFeO-A-0 (0.1700 g, 71% yield).

Following this, a combined material was synthesised to produce 5% $ZnFe_2O_4$ in TiO_2; called ZnFeO-A-5 (1.6700 g, 35% yield). This was produced in the same way as above, but with 1.6 g P25 added to the precursor solution, prior to addition of oxalic acid. P25 was dispersed thoroughly by sonication.

The content of $ZnFe_2O_4$ was adjusted by making materials at 2% and 8%, named ZnFeO-A-2 (1.6021 g, 33% yield) and ZnFeO-A-8 (2.1566 g, 11% yield), respectively.

A simplified version of the original synthesis was conducted by replacing the autoclave step with a room pressure reflux at 120 °C overnight, which was named ZnFeO-R-2 (1.3401 g, 28% yield).

Another synthesis route, named ZnFeO-B-2 (1.1061 g, 24% yield), was performed by following the same 3 steps as outlined above, but rather than adding oxalic acid, a solution of 1 mL NH_3 in 50 mL de-ionised water was dropped in slowly whilst stirring. The suspension was then stirred for a further 30 minutes at room temperature and pressure, before centrifuging the product and cleaning in ethanol. A final synthesis was included with 0.5 mL NH_3 in 50 mL, which was named ZnFeO-B2-2 (1.4210 g, 29% yield).

Films on glass slides and glass chips were produced according to the procedures outlined in Section 4.2.2 of Chapter 2.

5.2.3 Characterisation

XRD, Diffuse reflectance, Mott-Schottky, ICP-OES, XPS, SEM were all conducted according to the relevant sections in Chapter 2.

5.2.4 Chemical Photocatalytic Testing and UV-vis Spectroscopy

Tests were conducted on glass slides and glass chips according to the procedures outlined in Section 2.2 of Chapter 2, using 4-CP (156 μmol) as the model pollutant. Lights used for the experiments in this Chapter include: 370 nm, 410 nm, and white light LEDs, as well as a solar simulator lamp. The emission spectra for these lights are shown in Section 2.2 of Chapter 2.

5.2.5 Microbial Photocatalytic Testing

The procedure outlined in Section 2.2.3.3 of Chapter 2 was used for these experiments, beginning with the contaminated water sample being exposed to the catalyst in the dark for 30 minutes before irradiating with the different light sources for 2 hours. Measurements were taken every 20 minutes.

5.2.6 Mechanistic Studies

Tests were conducted according to Section 2.2.2.3 of Chapter 2 for determining the dominant mechanism for photocatalytic decontamination.

5.2.7 Stability Testing

To investigate the stability of the catalysts, 25 g of glass chips coated with ZnFeO-R-2 and ZnFeO-B-2 were used to treat 30 mL of the dye Rhodamine B (RhB) (10 μM) under 370 nm, multiple times in succession. Typically, to ensure full regeneration, all catalysts are calcinated at 400 °C to remove any remaining organics taking up active sites on the surface, leading to fowling. In this case, the catalysts were used 5 times in a row with only rinsing in deionised water in between uses. After the 5th use, the catalysts were calcinated to check if they would return to their original activities. This was repeated for 3 cycles, totalling 16 successive uses.

5.3 Results and Discussion

5.3.1 XRD

The XRD pattern of ZnFeO-A-0 (no P25 present) was similar to that found in the literature, which the synthesis was based on.[272] This was promising and showed that the method was reproducible.

Figure 5.1 shows the ZnFeO-A-0 XRD pattern for the sample synthesised in this work, as well as the literature data from the study by Nugent et al.,[272] alongside the known XRD pattern for this material (ICED card number 01-089-1012). Peaks at 37° and 46° seem to be missing from both the data collected here and the pattern observed in the study by Nugent et al, though these are weak peaks and thus the XRD patterns suggest that the desired product is likely to have been synthesised in both cases.

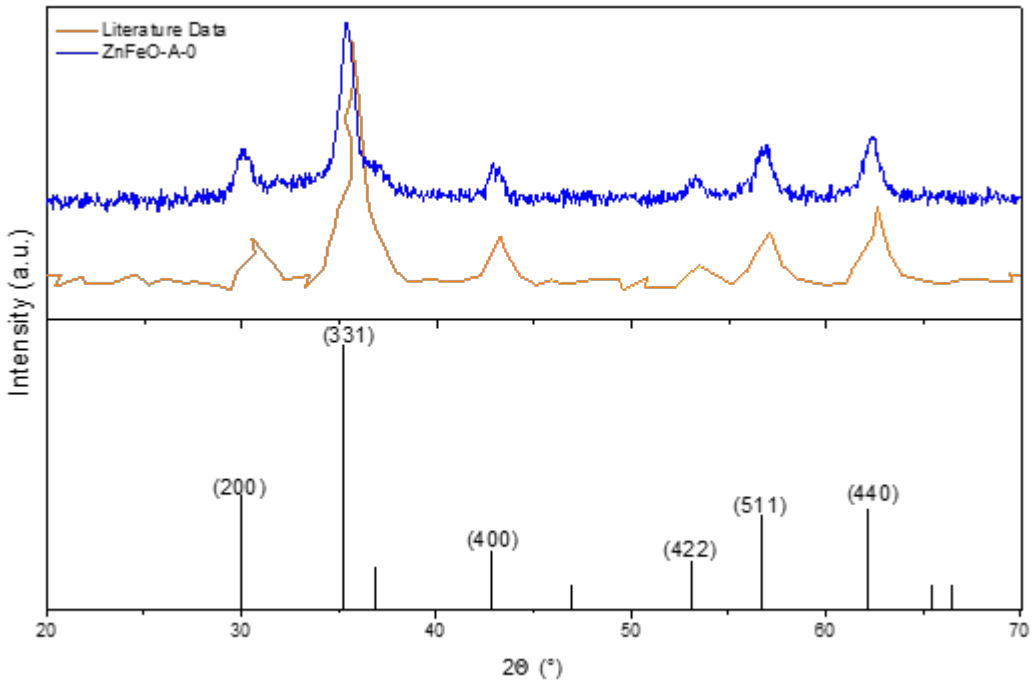

Figure 5.1: XRD pattern for $ZnFe_2O_4$. Literature data presented is from the study by Nugent et al.[272]

XRD traces are shown for all synthesised materials in Figure 5.2, where the dominant pattern observed is for that of P25 TiO_2.

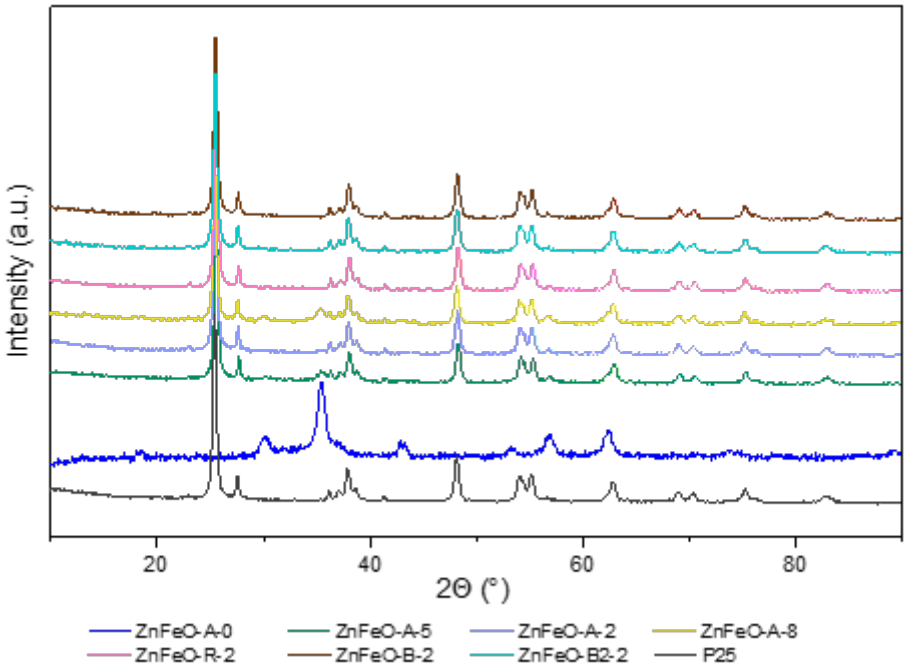

Figure 5.2: XRD patterns for all Zn/Fe-P25 composite products.

Faint peaks corresponding to ZnFeO-A-0 were visible in the XRD pattern for ZnFeO-A-5 and ZnFeO-A-8 for the peak at 36°, and very faintly for ZnFeO-A-2. There are also peaks observed for all samples (though very faint) for the $ZnFe_2O_4$ peak at 58° (as well as the overlapped peaks for the $ZnFe_2O_4$ and P25 peaks at 62° which could further support the presence of the two semiconductors being present).

This data is very interesting as it suggests that the spinel was likely formed during the synthesis of ZnFeO-A-0 alone, but when the combined material is produced, some of the synthesised products seem to show very little $ZnFe_2O_4$ character. This could suggest a few different possibilities: the two semiconductor materials are both present in crystalline form, but with the $ZnFe_2O_4$ in a very small relative quantity; or the material is present as an amorphous coating on the surface of the P25 particles, coated completely by P25; or that the Zn and Fe are taken up as dopants into TiO_2 as opposed to forming the metal oxide semiconductor, where the presence of Zn and Fe could alter the states within the gap, or shift the conductance band down, which may be possible whether in spinel form or not. It is also a possibly to have synthesised products with a combination of all three of these situations, giving rise to the differing patterns observed for each synthesis route.

5.3.2 ICP-OES

ICP-OES analysis was performed in order to investigate the bulk ratio of the component elements in the synthesised products, to further assist in understanding how different synthesis methods using the same precursor materials gave such differing photocatalytic activities. The ratios obtained are presented in Table 5.2 for a selection of the products, where the raw data and the corrected data taken the reading for the blank sample (aqueous acid solvent with no sample) into account are shown.

Table 5.2: Summary of ICP-OES data collected for selected samples synthesised for this Chapter. Note that the wavelengths used for detecting Ti, Zn and Fe were 368.519 nm, 206.200 nm and 238.204 nm, respectively. Data presented is corrected to account for the concentration of each element in a blank sample of just solvent.

Sample	Ti (mg/L)	Zn (mg/L)	Fe (mg/L)	Approx. Ti:Zn:Fe Ratio
ZnFeO-A-0	N/A	0.641	0.709	0:1:1
ZnFeO-A-2	1.193	0.0407	0.0509	100:3:4
ZnFeO-R-2	0.903	0.0271	0.214	100:3:24
ZnFeO-B-2	1.398	0.0467	0.0777	100:3:6

It is surprising here that the expected ratio of 1:2 for Zn:Fe was not observed for the products of any of the synthesis routes, particularly for sample ZnFeO-A-0 which had an XRD (Section 5.3.1) trace that matched data from literature for $ZnFe_2O_4$. This could possibly suggest that the synthesis route used does not produce pure $ZnFe_2O_4$, but rather a material both amorphous and crystalline character, giving it an overall ratio of 1:1 between Zn and Fe. This demonstrates the clear importance of thorough characterisation of a newly-synthesised material, in order to fully understand its structure and function, and thus the breadth of its applicability in various water treatment contexts.

According to the quantities of each material added during the synthesis, $ZnFe_2O_4$ was expected to be present as 2% of P25 TiO_2. This would give a ratio of 1:50 for Zn:Ti, where 1:30 is consistently observed. This suggests an addition of closer to 3% of Zn, which could be due to incomplete incorporation of the P25 into the final composite material due to an inhomogeneous mixture of the reagents.

It is also interesting that there seems to be more variation in the Zn:Fe and Fe:Ti ratios relative to that for Zn:Ti, which remains more consistent. Perhaps this can shed some light on the synthesis mechanism, and how it may be more finely controlled for further optimisation. It may be that there is a preferential reaction of the Zn precursor with the P25 TiO_2 over Fe, and that this takes place more favourably than the reaction of Zn with Fe under these reaction conditions.

5.3.3 SEM

It was clear from SEM images (shown in Figure 5.3) that the morphology of the synthesised ZnFeO-A-0 product was indeed the desired nanorod structure presented in the literature.[272] This further supports the notion that the same product was made as in the literature.

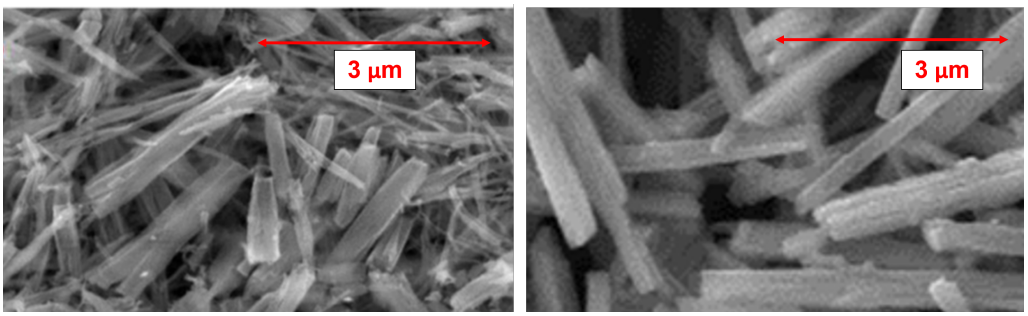

Figure 5.3: SEM images for $ZnFe_2O_4$. Left is from the literature[272] and right is from this study (ZnFeO-A-0).

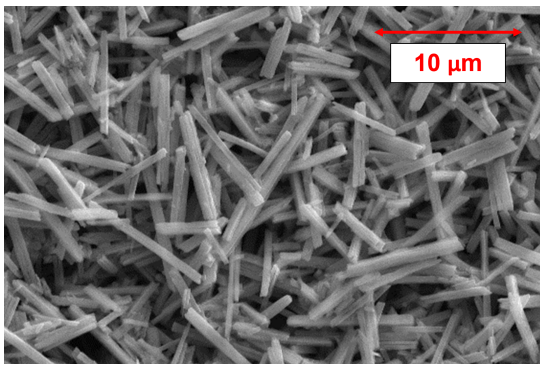

Figure 5.4: The same SEM image for the $ZnFe_2O_4$ product synthesised in this study as shown in Figure 5.3, but at a lower magnification for clarity.

The elemental analysis data for a selection of the synthesis products is shown in Table 5.3.

Table 5.3: Summary of SEM EDS data collected for selected samples synthesised for this Chapter. Note that the data presented are the average values taken from across multiple sites used to repeat the measurements across the material surfaces.

Sample	Atomic % Ti	Atomic % Zn	Atomic % Fe	Approx. Ti:Zn:Fe Ratio
ZnFeO-A-0	N/A	20.57	28.89	0:5:7
ZnFeO-A-2	32.85	0.12	0.25	1000:4:8
ZnFeO-R-2	32.89	0.063	0.32	1000:2:10
ZnFeO-B-2	32.23	0.17	0.60	1000:5:19

The expected ratio for Zn:Fe of 1:2 was again not consistently observed for the different samples, but was closest for sample ZnFeO-A-0, and for ZnFeO-A-2 of the combined materials, showing that it is not easy to control the ratios of Zn to Fe in the final product via this synthesis route.

Again, the expected ratio for 2% addition was not observed, with the Zn:Ti ratio being an order of magnitude lower than expected. This differs from the results observed through ICP-OES, which is a bulk measurement technique as opposed to surface analysis achieved through SEM. This could suggest that there is a variation in presence of the material from the surface layer to deeper within the material.

5.3.4 XPS

From the XPS data collected for sample ZnFeO-A-2, the valence band edge was calculated to be 3.11 $\pm$ 0.12 eV, as shown in Figure 5.5, where the error is calculated from the linear fitting using Equation 2.10. For all other samples, reliable data could not be collected.

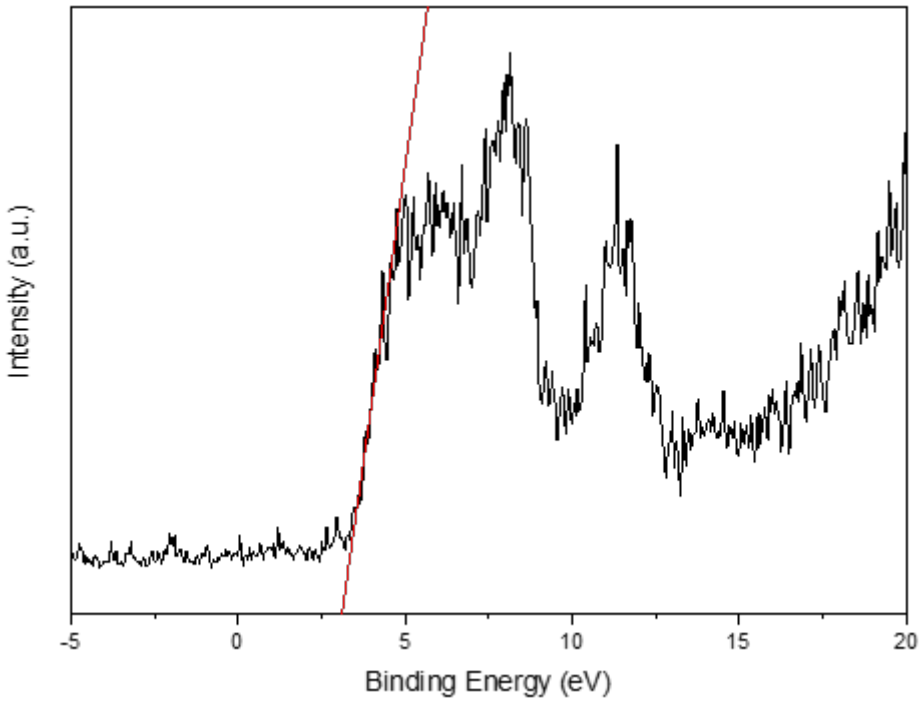

Figure 5.5: XPS data for the extrapolation of the valence band edge or ZnFeO-A-2.

Analysis of the elemental composition was also performed during the XPS measurements. The plots for Ti, Zn and Fe are shown in Figures 5.6, 5.7 and 5.8, respectively, though these cannot be analysed quantitatively due to the noisy data obtained for Fe and Zn, likely due to them being present in low concentrations.

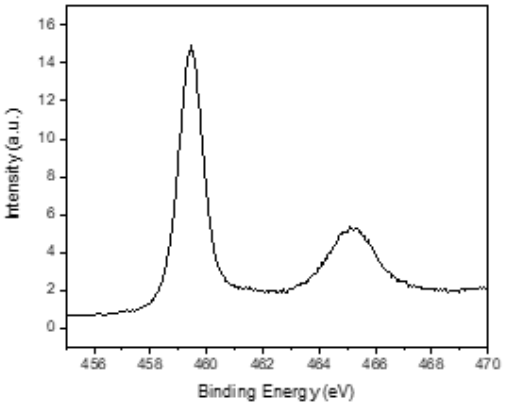

Figure 5.6: XPS data for Ti

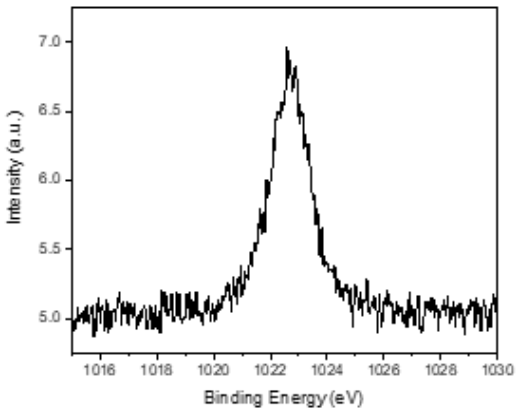

Figure 5.7: XPS data for Zn

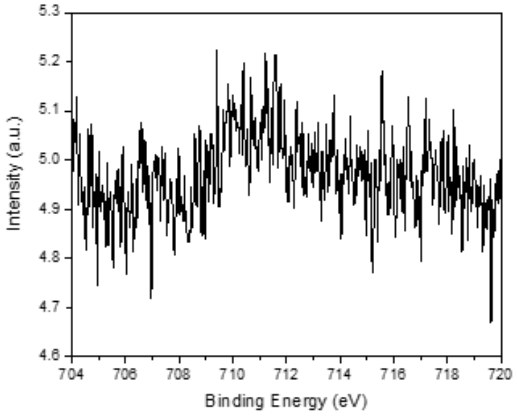

Figure 5.8: XPS data for Fe

Though the XPS data was not as directly enlightening as other characterisation methods, it can still be used as a further check for the valence band estimations. This can be done by comparing with the data obtained for the band gap estimated from DRS, and the conduction band edge from Mott-Schottky analysis, to see if the valence band edge estimated mathematically from comparing these two is similar to the experimental value obtained for ZnFeO-A-5. This is detailed further in Section 5.3.7.

5.3.5 Diffuse Reflectance Spectroscopy

The promising samples, ZnFeO-R-2 and ZnFeO-B-2, were analysed using DRS, and both shown to appear similar to P25 TiO_2. In contrast, the sample with no P25, ZnFeO-A-0, appeared very different. The data collected from the UV-visible diffuse reflectance spectroscopy was converted into Tauc plots, shown in Figures 5.9, 5.10 and 5.11, with linear fits sowing how the estimates for the band gaps were extrapolated.

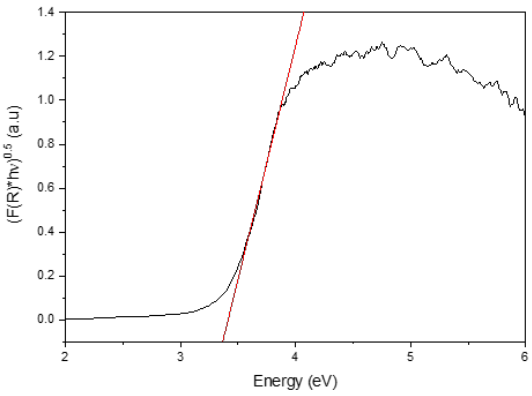

Figure 5.9: Tauc Plot for ZnFeO-R-2

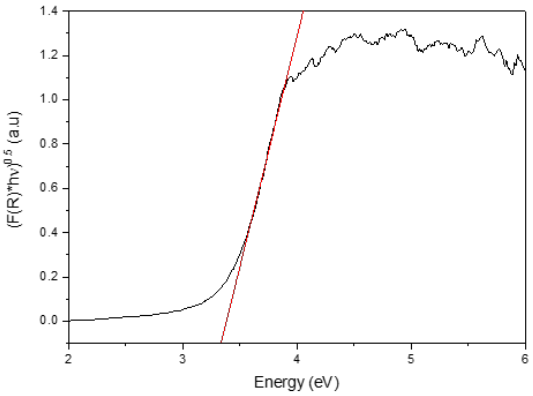

Figure 5.10: Tauc Plot for ZnFeO-B-2

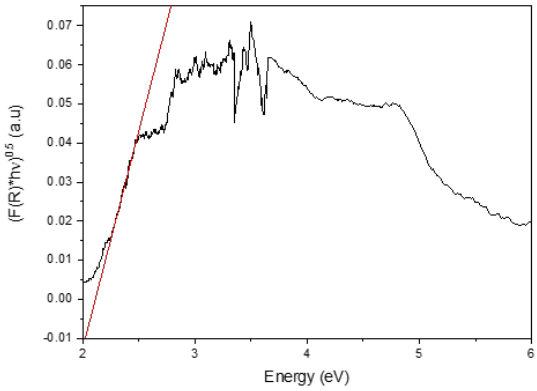

Figure 5.11: Tauc Plot for ZnFeO-A-0

Based on the linear fits performed, the band gaps were estimated and shown in Table 5.4 as:

Table 5.4: Band gap estimations based on associated Tauc plots.

Sample	Estimated Band Gap (eV)	Corresponding Wavelength (nm)
ZnFeO-A-0	2.06 ± 0.01	603
ZnFeO-R-2	3.43 ± 0.07	362
ZnFeO-B-2	3.38 ± 0.07	368

The values for the errors associated with each band gap estimate were calculated using Equation 2.10 from Section 2.3.1 of Chapter 2.

Interestingly, the composite materials ZnFeO-R-2 and ZnFeO-B-2 appear to have band gaps larger than that of TiO_2 at 3.2 eV, suggesting less visible light harvesting. Despite

this, the visible light performance is clearly significantly higher for the composite materials, and the spinel on its own, ZnFeO-A-0, has a band gap in the visible region of 2.06 eV, which corresponds to a wavelength of approximately 600 nm.

A heterojunction is typically indicated by the presence of two clear and distinct linear regions, from which two band gaps can be determined, appearing as a step in the Tauc plot where the gradient changes. No clear second step was observed in the Tauc plot traces, which indicates that possibly a heterojunction was not formed, but that the Zn and Fe are altering the photocatalytic activity in other ways. However, the lack of characteristic heterojunction structure in the Tauc plots could also simply be due to the low concentration of the spinel present relative to P25, or indeed a mix of both situations.

5.3.6 Mott-Schottky Analysis

As outlined in Section 2.3.2 of Chapter 2, Mott-Schottky analysis allows an estimation of the conduction band to be made by measuring the flat band potential of an n-type semiconductor. Measurements were made for samples ZnFeO-A-0, ZnFeO-A-2, ZnFeO-R-2, and ZnFeO-B-2 at a frequency of 2 kHz and scanning between -1.50 V and 0 V. The results are shown in Figures 5.12 and 5.13 (due to the onset of the change in capacitance not beginning until after 0 V, the trace for ZnFeO-A-0 is shown separately on Figure 5.13).

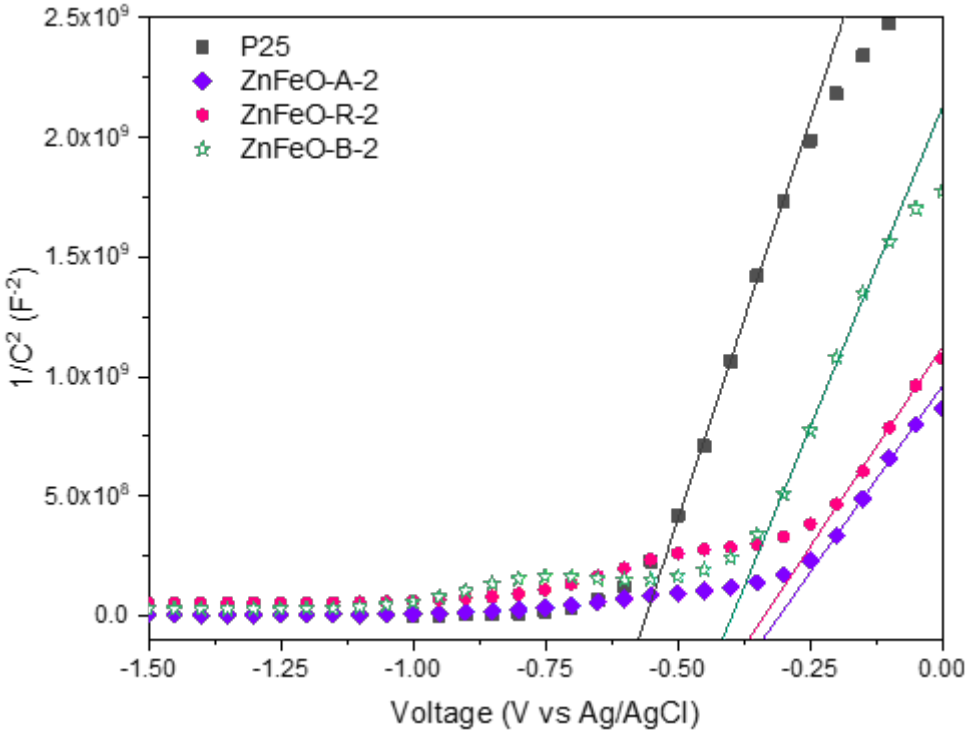

Figure 5.12: Mott-Schottky plot for samples ZnFeO-A-2, ZnFeO-R-2 and ZnFeO-B-2.

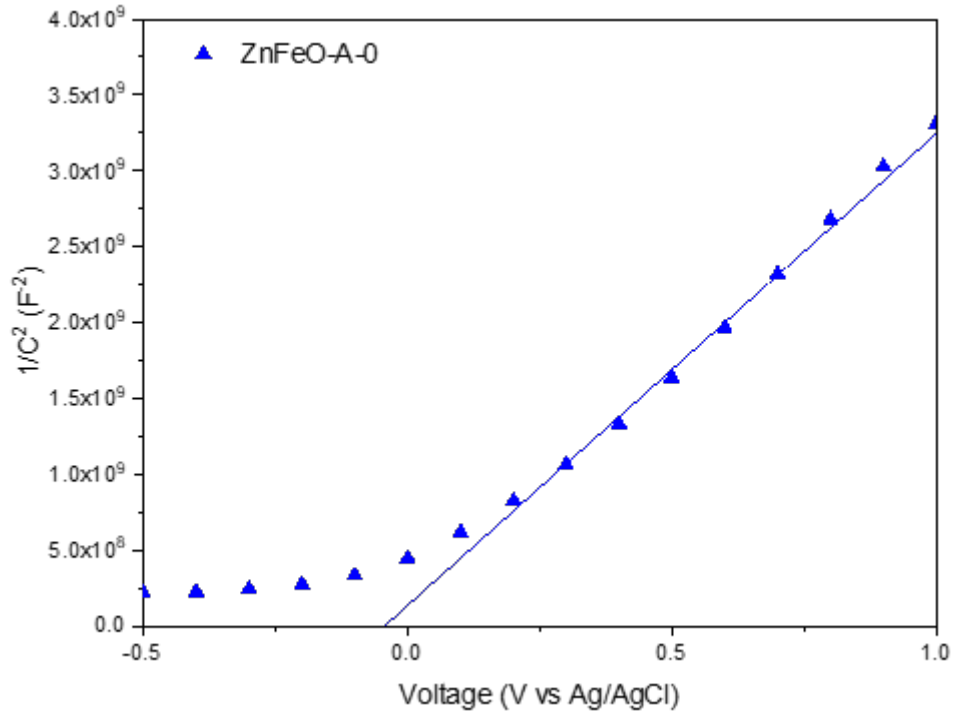

Figure 5.13: Mott-Schottky plot for sample ZnFeO-A-0.

The Mott-Schottky data collected here is typical for n-type semiconductor materials, as characterised by the positive gradient in the linear region of the plots. This indicates

that the majority charge carriers are electrons. For n-type materials, the flat band is located approximately 0.1 V anodically (i.e. more positively) from the conduction band minimum ($E_{CB,M}$) , which has been used to obtain estimates for $E_{CB,M}$ here, and is presented alongside the summary of the Mott-Schottky results gathered in Table 5.5. The errors are calculated in the same way as in Section 2.3.1 Chapter 2 using Equation 2.10.

Table 5.5: Summary of flat band potential and associated calculated values.

Sample	Flat band potential (E_{FB}) (V)	Error in E_{FB} (V)	Anodic shift relative to P25 (V)	Estimated $E_{CB,M}$ (V)
P25 TiO_2	-0.560	0.014		-0.460
ZnFeO-A-0	-0.044	0.017	0.516	0.044
ZnFeO-A-2	-0.308	0.009	0.252	-0.208
ZnFeO-R-2	-0.336	0.016	0.224	-0.236
ZnFeO-B-2	-0.397	0.015	0.163	-0.297

These materials appear to have flat bands which are shifted anodically relative to P25 TiO_2, which would correspond to a lower conduction band, as expected from the decreased band gap observed from the DRS results. This could explain poorer performance in the UV region, due to a reduction in the driving force for electron injection. This could suggest why we see improved activity in the visible region relative to P25, where more light absorption can now occur, meaning more charge carriers may be released, but worse overall performance, as these charge carriers are less energetic.

5.3.7 Band Structure Estimations

By combining all of the above data, it is possible to predict the band architecture for these synthesised composites of a transition metal oxide and P25 TiO_2, where the band gap for TiO_2 alone is presented using literature data.[277] These band gaps are presented in Figure 5.14.

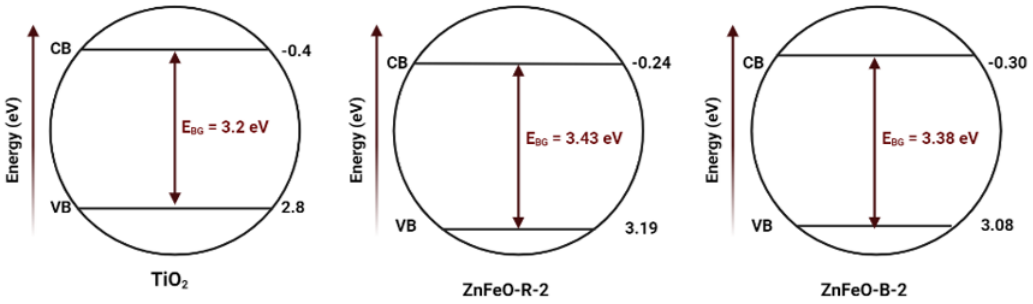

Figure 5.14: Estimates of band structures for ZnFeO-R-2 and ZnFeO-B-2, shown next to TiO_2 for reference.

Here, the band diagrams have been estimated for ZnFeO-R-2 and ZnFeO-B-2 by using the diffuse reflectance results to estimate the band gap, and the Mott Schottky results to estimate the location of the conduction band edge. The valence band edge is then calculated based on both of these values, and compared to the result from the XPS measurement of ZnFeO-A-5. In this case, the valence bad edge values are close (319 eV for ZnFeO-R-2 and 3.08 eV for ZnFeO-B-2, relative to the experimental value of 3.11 eV).

It is also important to note that the experimentally determined band gaps for the composite materials seem to be larger than P25, despite the performance suggesting otherwise. This is interesting and implies a much more complicated band architecture may be present, with many states in the gap, allowing for visible light to be harvested more efficiently.

These diagrams are not presented here as heterojunctions between a zinc-iron oxide and TiO_2, due to the lack of evidence for this type of band structure.

5.3.8 Chemical Photocatalytic Testing

For the initial screening tests to ascertain which materials, if any, performed well relative to commercial standard P25 TiO_2, samples were tested as thin films on glass slides using 4-chlorophenol (4CP) as the model pollutant. To understand the photocatalytic behaviour fully, this testing was performed under UV light (370 nm), visible lights (410 nm and a white light LED) and the full solar range using a solar simulator lamp (this was measured for the best performing materials only). The procedure used for these tests is summarised in Section 5.2.4, with more detail given in Section 2.2 of Chapter 2.

Plots were produced of the negative logarithm of the quantity C/C_0 against time, where C is the concentration of 4CP at a given time point, and C_0 is the initial concentration, in order to assess the first-order rate kinetics, as discussed in Section 2.2 of Chapter 2. Following this analysis, it was found that ZnFeO-R-2 and ZnFeO-B-2 were the most promising in terms of resulting activity and experimental practicality. The results are shown below in Figure 5.15.

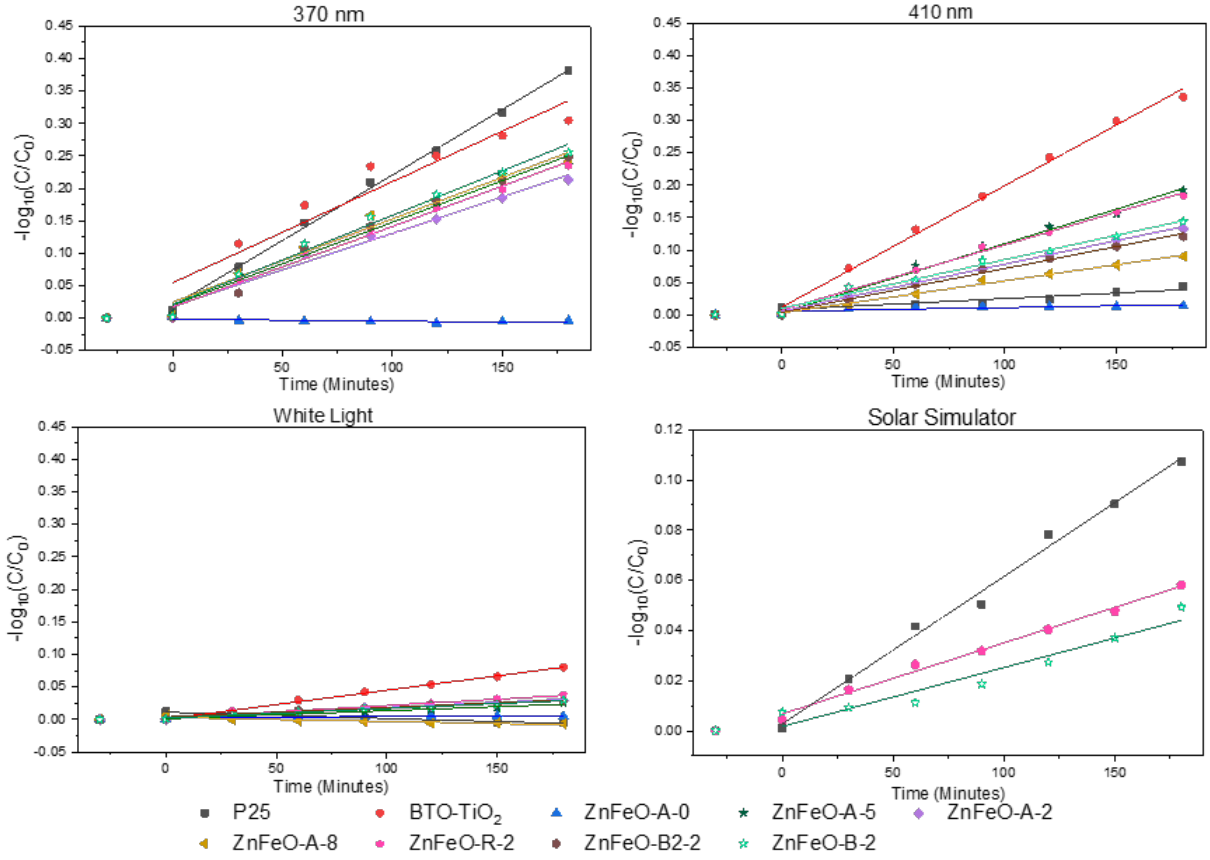

Figure 5.15: Rate of removal of 4-CP under different light source for all samples studied in this Chapter. Note that the linear fit begins at time = 0 minutes, and does not include the 30 minutes in the dark, such that the rate of just the active photocatalysis is found.

Interestingly, despite clear similarities between characterisation data acquired here and in the literature study by Dhiman et al[274] which reported very good photocatalytic activity under visible light, the ZnFeO-A-0 did not perform well under any of the light sources.

Following these tests, it was found that ZnFeO-R-2 and ZnFeO-A-2 were similar in activity and performed the best of all synthesised samples under the 410 nm light (excluding

BTO-TiO_2), though ZnFeO-A-2 has a more complex synthesis route, requiring the use of autoclaves. Thus, of the two, ZnFeO-R-2 would appear to be a better option when considering both performance and practicalities of use. Under 370 nm, ZnFeO-B-2 seemed to perform best, with ZnFeO-R-2 best under the white light. Therefore, due to combination of good performance and simple synthesis routes, ZnFeO-R-2 and ZnFeO-B-2 were taken forwarded for further testing, as opposed to pursuing the samples that require autoclaving.

ZnFeO-R-2 and ZnFeO-B-2 were then used for testing with the solar simulator, as shown in the bottom right plot in Figure 5.15. From these studies, it was found that ZnFeO-R-2 performed slightly better than ZnFeO-B-2, with both showing reasonable photocatalytic activity, but were outperformed by P25 TiO_2. This shows that, despite the increase in visible light activity relative to P25, the lowered activity in the UV means that P25 performs best under the combination of light within the solar spectrum as a whole.

The first order rate constants for ZnFeO-R-2 and ZnFeO-B-2 are shown below in Figure 5.16 for the different light sources.

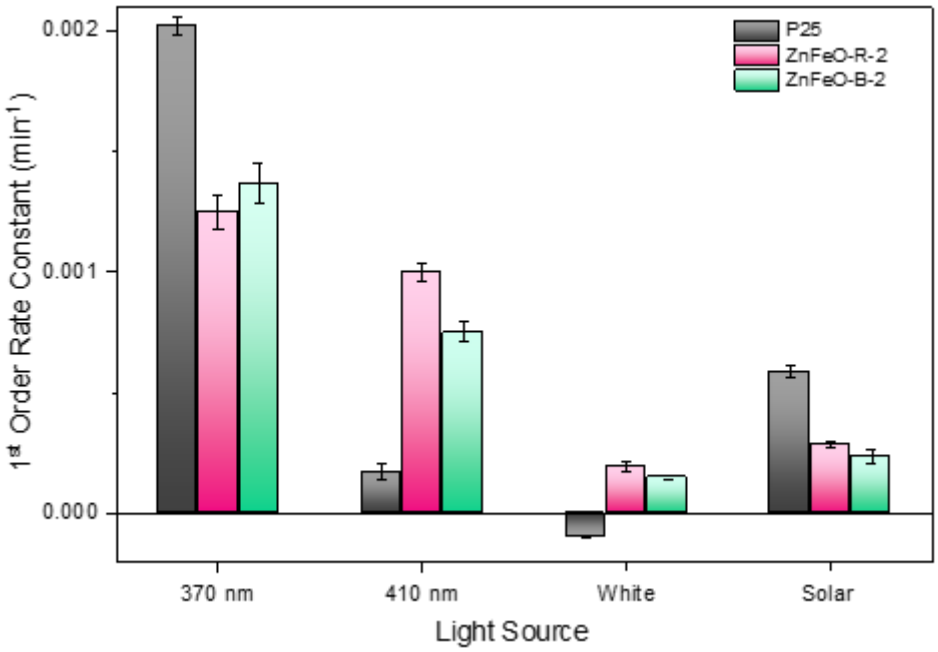

Figure 5.16: First order rate constants for P25, ZnFeO-R-2 and ZnFeO-B-2.

From this data, it can be seen that P25 clearly outperforms the composites under UV light, but significantly under-performs under visible lights.

5.3.9 Microbial Photocatalytic Testing

Moving forward with the most promising materials, ZnFeO-R-2 and ZnFeO-B-2, further studies into the efficacy of removing contaminants from water were conducted, this time focusing on microbial content. Here, non-pathogenic *Escherichia coli* was used as a model microbial contaminant, as the presence of *E. coli* is an indicator of faecal contamination, and as such is an important species to study for water treatment.

These studies were performed on a larger scale than the aforementioned chemical tests that were conducted on glass slides. Here, glass chips were used with 50 mL of spiked water, with testing performed under 410 nm, according to the procedure outlined in Sections 2.2.3.2 and 2.2.3.3 of Chapter 2. Each test was performed with three repeats.

Fluctuations were seen over the course of the experiments, as is expected when working with bacteria, but overall trends could be extrapolated, as shown in Figure 5.18, with Figure 5.17 being the same data linearised, but with the controls included for completeness (and removed from Figure 5.18 for clarity of identifying the trends). These controls showed the expected behaviour of very little change in bacterial colony counts, with some even increasing with time. Therefore, it is easier to compare the behaviour of the synthesised materials relative to P25 under lights with these omitted.

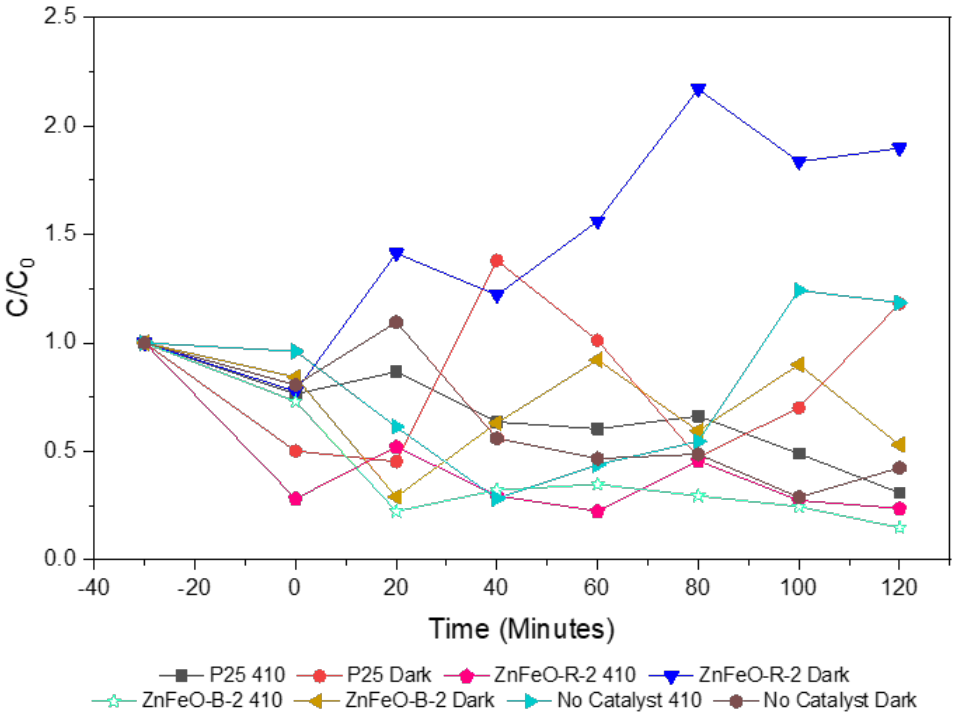

Figure 5.17: Removal of *E. coli* during the two hours of treatment, with both dark and light conditions presented. Testing performed under 410 nm LED irradiation. Here, 'C/C_0' refers to the CFU/mL at a given time point over the original value prior to treatment.

The same data is presented again below in Figure 5.18 with controls excluded for the data to be read more clearly.

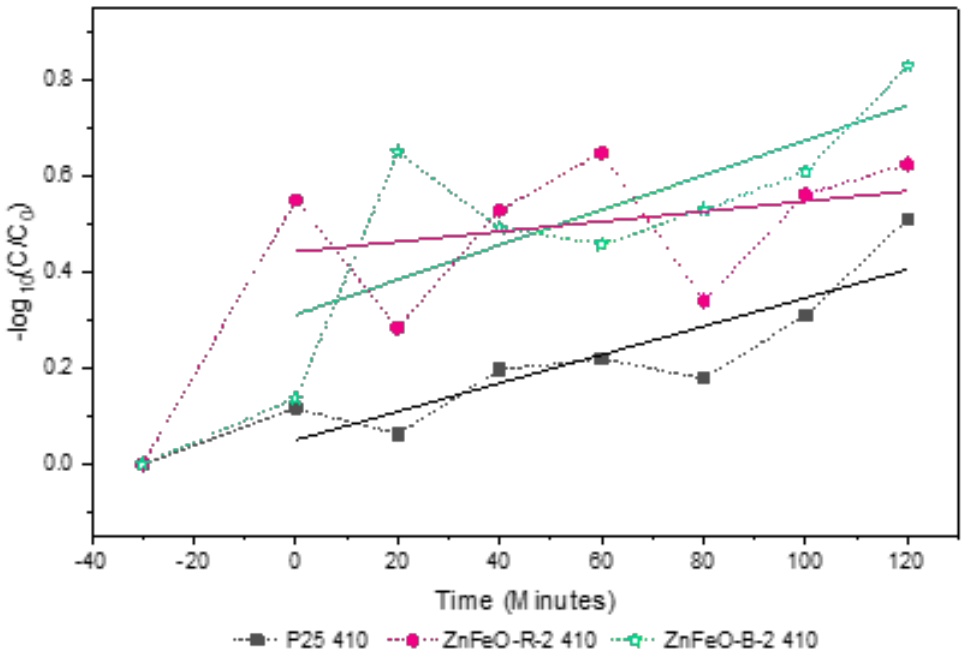

Figure 5.18: The same data from Figure 5.17 but with controls excluded for clarity. The solid lines shown represent the linear fits used to estimate the first order rate constants. Testing performed under 410 nm LED irradiation. Note that the linear fit begins at time = 0 minutes, and does not include the 30 minutes in the dark, such that the rate of just the active photocatalysis is found.

The first order rate constants for P25, ZnFeO-R-2 and ZnFeO-B-2 were calculated from the above plots for the removal of *E.coli* under 410 nm irradiation over the course of the two hour treatment are shown in Figure 5.19.

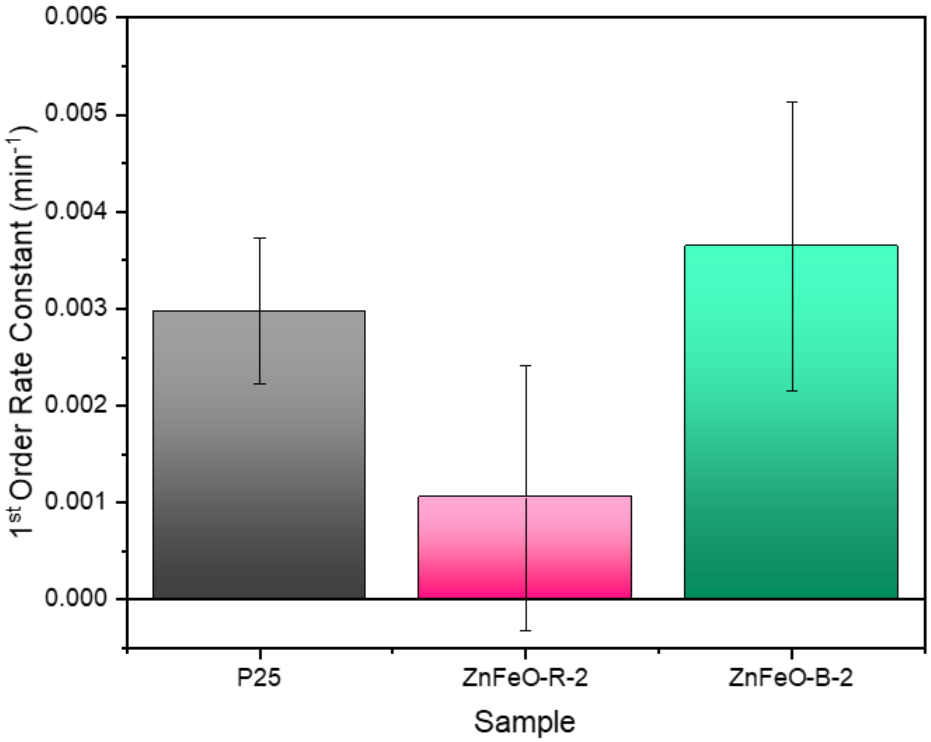

Figure 5.19: The first order rate constants obtained from the slopes presented in Figure 5.18. Testing performed under illumination with a 410 nm LED.

These results were promising in that they suggest a clear ability of the catalysts to remove microbial content under visible light, relative to P25, which is known to have bactericidal properties. However, these results do not conclusively confirm whether or not these materials perform better than P25, as they all showed a drop in CFU/mL on the same order of magnitude. Due to the high experimental uncertainty associated with biological systems, as shown with the large error bars in Figure 5.19, it can only be concluded with certainty that all materials can remove *E. coli* under visible light, though it can be tentatively interpreted as suggesting that the modified materials have the potential to perform better under visible light.

This provides an interesting opportunity for future work, whereby the study can be expanded to cover more test conditions and performed with a much higher volume of repeats for any further, more concrete conclusions to be drawn.

However, these data do provide a clear answer to the question: can these composite materials reasonably replace the P25 TiO_2 without a reduction in performance? Indeed, these results are consistent with the chemical studies presented above in indicating that

these materials can be as good as, if not better than, P25 under under visible light.

5.3.10 Mechanistic Studies

In order to elucidate the dominant mechanism behind the observed photocatalytic activity of these materials, scavenging and purging tests were conducted. This involved the addition of methanol (MeOH) and tert-butanol (t-BuOH) to 4-CP, used to scavenge for holes and hydroxyl radicals, respectively. Nitrogen was also bubbled through the 4-CP solution to purge oxygen from the system, and thus prevent photo-excited electrons from reducing molecular oxygen to form superoxide radicals.

The rate of removal of 4-CP with the addition of the scavenging and purging agents is shown for ZnFeO-R-2 in Figure 5.20 and for ZnFeO-B-2 in Figure 5.21.

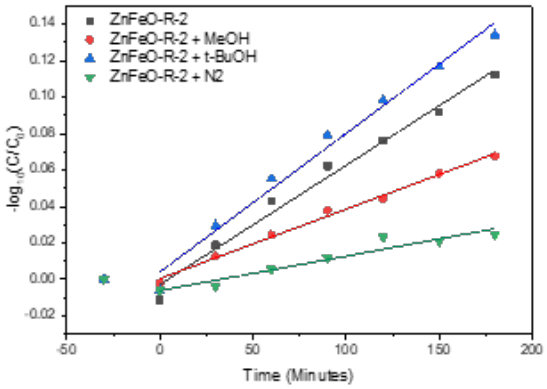

Figure 5.20: ZnFeO-R-2

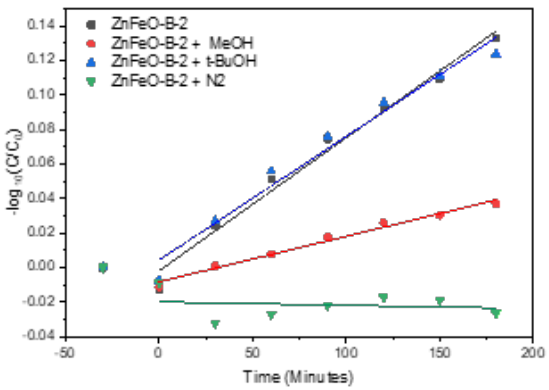

Figure 5.21: ZnFeO-B-2

The gradients obtained through these plots were then used to calculate rate constants, which are shown in Figure 5.22. Note that the linear fits begin at time = 0 minutes, and does not include the 30 minutes in the dark, such that the rate of just the active photocatalysis is found.

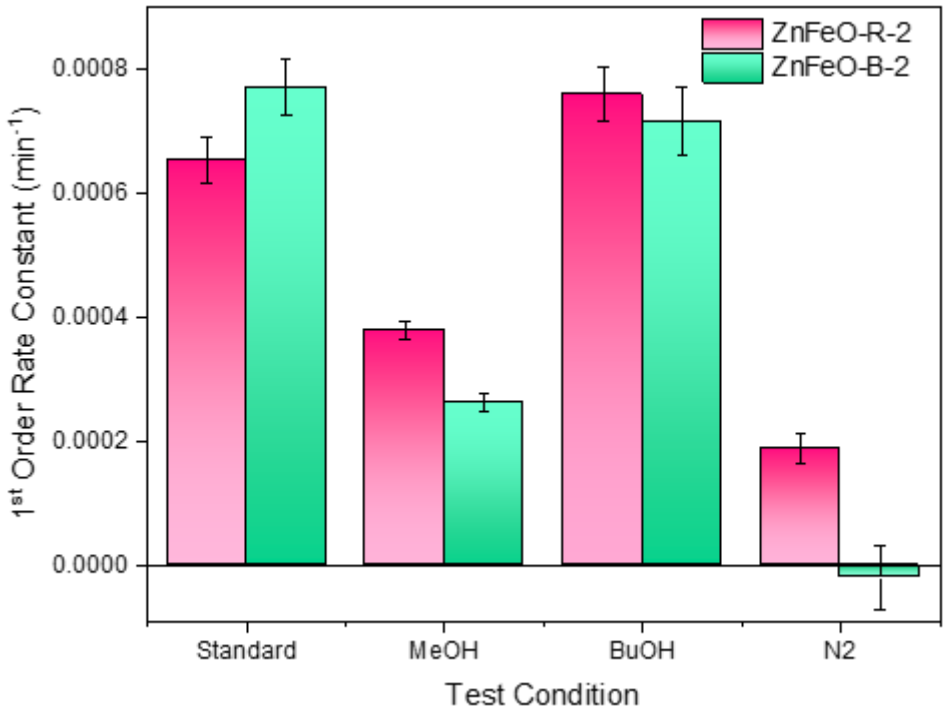

Figure 5.22: The first order rate constants obtained from the slopes presented in Figure 5.20 and 5.21.

For both ZnFeO-R-2 and ZnFeO-B-2, it was found that the addition of t-BuOH did very little to affect the observed rate, whereas the test condition with added MeOH showed a significant drop in the first order rate constant. This indicates that photoholes are more important to the mechanism than hydroxyl radicals, which also suggests the catalysis is largely surface driven, as opposed to any bulk action.

Purging with nitrogen also led to a significant drop in rate constant for both materials, which suggests photoelectrons are important to the mechanism, which was expected based on the result that holes were more important than hydroxyl radicals. This shows that there is clear photoexcitation occurring which is then being harnessed to breakdown organic contaminants present, and that this is likely to be due to the formation of predominantly O_2^-, rather than the more reactive $^{\cdot}OH$ radicals.

The overall trends for ZnFeO-R-2 and ZnFeO-B-2 are similar, but with slight variations. ZnFeO-R-2 seemed to show a slight increase in rate constant with the presence of t-BuOH, and ZnFeO-B-2 seems to show a very drop in rate constant in the presence of N_2, with an effective increase in concentration of 4-CP. This latter result can be attributed

to a complete loss of catalytic activity, alongside some evaporation occurring as a result of the flow of nitrogen, which in turn leads to an effective increase in concentration.

5.3.11 Stability Testing

An extremely important parameter for assessing the applicability of a photocatalytic material for use in water treatment, particularly in decentralised systems, is the stability and reusability of the material. Despite this, such studies are often missing from the literature, including in the aforementioned studies that showed successful trials with their $ZnFe_2O_4$-TiO_2 materials. As such, an experimental procedure was designed for this purpose, as outlined in Section 2.2.2.4 of Chapter 2, and tests were conducted in order to assess the applicability of the synthesised materials for use in decentralised water treatment in rural India.

Each of the two materials showed good reusability over the course of the investigation, with neither ZnFeO-R-2 or ZnFeO-B-2 showing a significantly better long-term function over the other. Variations were seen in which material had the highest degradation efficiency with each use.

There was a significant drop between the first and second uses in each cycle, but following this, the drop off between successive tests was smaller and seemed to plateau. After a period of calcination at 400 °C, the activity was largely regenerated, which was a positive sign for the long-term use of the materials. These results are presented in Figure 5.23, with stars showing the runs following calcination to regenerate the materials.

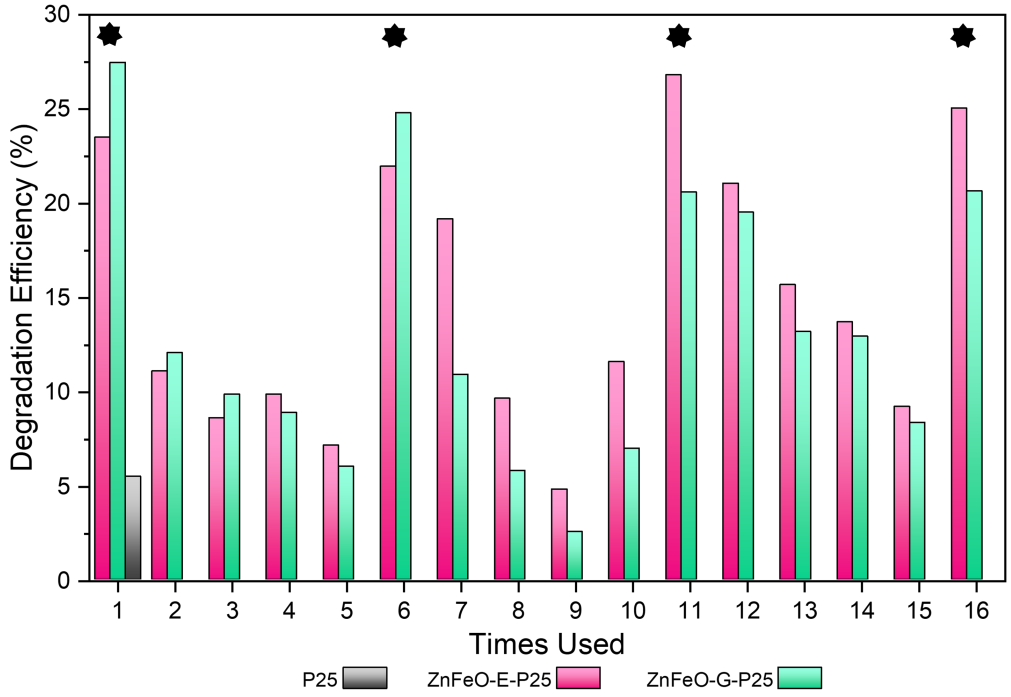

Figure 5.23: Degradation efficiency calculated at the end of consecutive 3 hour test runs to assess the stability and reusability of the catalyst materials. Star symbols indicate the runs following a period of calcination to regenerate the catalyst.

5.4 Conclusions

Composite materials of P25 TiO_2 and a zinc-iron oxide have been prepared. It is clear from the results of photocatalytic testing shown in Section 5.3.8 that BTO-TiO_2 outperforms the materials presented in this work, but it must be noted that the synthesis of this material is much more laborious. BTO-TiO_2 is produced via a SILAR synthesis route, which is very time consuming, labour-intensive and also results in large solvent waste. In contrast, the synthetic routes used here are very simple, particularly ZnFeO-B-2 which only requires stirring for 30 minutes. Hence, these benefits and drawbacks must be taken into account when deciding which material to deploy, and it could be argued that each material would be more suitable for different applications, with the ZnFeO/P25 class of materials being suitable for visible light-induced treatments, and BTO-TiO_2 possibly being more appropriate for UV or solar light-induced treatments.

It was found that the ZnFeO-A-0 material, despite having XRD and SEM data similar to that presented in the literature, did not show good catalytic activity under 410 nm

for the removal of model pollutant 4-CP. This is likely due to the original paper using visible dyes as the test material, which can be excited by visible light, and thus lead to dye-sensitisation and an over estimation of the success of the results.

When combined with P25 TiO_2, a significant improvement relative to both ZnFeO-A-0 and P25 TiO_2 alone was observed for 410 nm. However, this unfortunately led to a decrease in activity in the UV region relative to P25 TiO_2. This resulted in the overall performance under solar light also being lower than P25 TiO_2, despite the improvement in the visible region. This clearly demonstrates how successful TiO_2 is as a photocatalyst, and how difficult it is to achieve a modified material that provides sufficient improvement to outweigh the increased complexity in preparation, relative to simply using TiO_2 itself.

Despite the different quantities of Zn, Fe and Ti observed for the different synthesis products, sample ZnFeO-A-2, ZnFeO-R-2 and ZnFeO-B-2 all gave similar photocatalytic activities, as shown in Section 5.3.8, and thus this suggests that achieving the exact 2% $ZnFe_2O_4$ in TiO_2 heterojunction is not the only way to utilising zinc and iron for enhancing the visible light activity of TiO_2.

From the results presented in this Chapter, we can see that it is difficult to confidently determine the exact chemical structure due to conflicting results from different characterisation techniques. Due to the quantities used in synthesis, it was expected that Ti would be present in much higher quantities than Zn and Fe, which was observed, though with varying ratios for each synthesis attempt. This is partly expected due to differences in the techniques used, where ICP-OES measures the bulk material, but SEM and XPS can only measure the surface, with different penetration depths and thus will produce slightly different results for materials with non-uniform chemical distribution. With this in mind, some differences would be expected, but the anticipated ratio of 1:2 for Zn:Fe based on the desired chemical formula for the spinel of $ZnFe_2O_4$ was not observed clearly for any materials, with all characterisation methods showing different relative quantities of each constituent element. This shows the importance of using multiple characterisation techniques to avoid drawing any inaccurate conclusions.

Further, this Chapter highlights the importance of considering a balance between yield of the synthesis, ease of the synthesis, and the performance of the catalyst. The ZnFeO-A-2 product had a higher yield (see Section 5.2.2) and performance (see Section 5.3.8), but the synthesis was more complex and less practical due to the need for autoclaves. This suggests that the slightly lower performance and yields achieved for ZnFeO-R-2 and ZnFeO-B-2 may be acceptable if it means the product can be made more easily, and thus be a more widely accessible water treatment method.

Chapter 6

Material Development for Solar Photocatalysis: TiO_2 with Bismuth

This Chapter builds on the knowledge gained in previous studies discussed in this Thesis to further enhance photocatalytic activity *via* simple synthesis routes. As seen in Chapter 5, the previous synthesis attempt involved starting from commercial P25 and attempting to form a composite with another semiconductor material, in that case a zinc-iron oxide. In this Chapter, a different approach is used, whereby TiO_2 is synthesised *in situ*, in the presence of dopants, in order to alter the photochemical properties.

6.1 Literature Review and Background Theory

Following the success, both in the lab and in the field, of previously developed BTO-TiO_2,[208,278] further synthetic attempts were made in order to incorporate bismuth into the TiO_2 lattice, whilst removing the need for using the SILAR method. Many studies have been conducted on materials either based on, or modified with, bismuth for the application of photocatalysis. This has included using various bismuth-based semiconductor materials such as Bi_2O_3, Bi_2S_3, and metal oxides in the form $M(BiO_3)_n$, as well as many others discussed in a review of bismuth-based photocatalytic semiconductors.[279] Bismuth semiconductors are often studied in the context of forming photocatalysts with smaller band gaps than TiO_2, and thus increasing the visible light response. TiO_2 has a valence band composed of O 2p orbitals, whereas bismuth-based materials have valence bands made up of O 2p and Bi 6s hybrid orbitals, which has been reported to increase

mobility of photogenerated charge carriers, as well as decrease the band gap.[280,281]

One of the most frequently studied methods of enhancing photocatalytic performance is to form a heterojunction between two semiconductor materials with different band gaps in order to reduce charge recombination. Hence, one way to utilise bismuth to form a high-performing photocatalyst for solar activation is to form composites with TiO_2. This was the goal in forming bismuth titanate (BTO-TiO_2) which was field tested and shown to be promising (Chapter 3). Rather than starting with P25 TiO_2 and modifying it *via* SILAR or other synthetic means of forming a composite, this Chapter focuses on the *in situ* synthesis of TiO_2 in the presence of additives to form a modified material in fewer steps, simplifying the preparation process further.

For this Chapter, a sol-gel synthesis method was used, being widely studied and easy to perform at low temperatures, without the need for expensive equipment (e.g. autoclaves). The sol-gel process usually comprises a sequence of the following chemical and physical steps; (i) inorganic polymerisation (based on hydrolysis and polycondensation), (ii) gelation, (iii) ageing, (iv) drying, and (v) densification.[282] The first step often uses a metallo-organic precursor e.g. alkoxides ($Ti(OC_nH_{2n+1})_4$) in an organic solvent, typically the parent alcohol of the alkoxide. Water is used to promote hydrolysis and condensation, as shown in Figure 6.1.

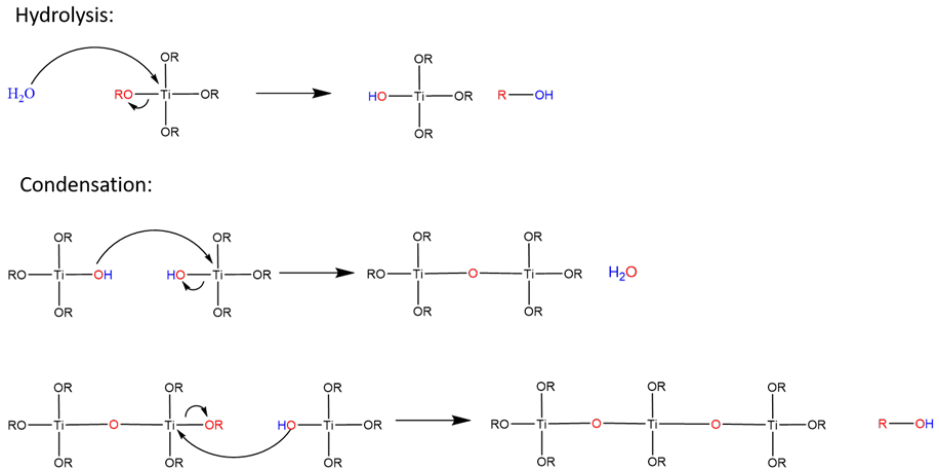

Figure 6.1: Sol-gel reactions leading to the formation of long chain gel structures.

A colloidal suspension of nanoparticles (a sol) can then form following these competitive reactions. These nanoparticles can then aggregate together to form a continuous 3D

network, known as a gel.[282] The precursor solution usually uses an alcohol with a low evaporation temperature as the solvent. Organic materials or other dopants can be used for chemical or surface modifications. In most cases, after dip-coating, samples are left to stand in a fume hood to allow excess solvent to evaporate, as well as any gas-phase by-products.[66] The nanoparticles that are produced through sol-gel methods are amorphous, and as such need calcinating at high temperatures to achieve crystallinity.[66]

Such wet chemistry techniques are excellent for allowing alterations to be made easily and at various stages in the research process, in order to explore the optimum components and conditions for producing materials with the target properties. The frequency of utilisation of sol-gel methods speaks to its success, usability and flexibility of processing, without the requirement for complex apparatus beyond that found in an average chemistry laboratory. However, it must also be held in mind that, like many other synthesis processes, sol-gel methods have their disadvantages, including solvent waste, the requirement of hazardous materials and potentially lengthy preparation time, though this can often be the case with alternative synthesis routes.

Several studies have been performed on the synthesis of various modified TiO_2 materials using a sol-gel route, with it typically being utilised for the convenient adjustment of parameters for allowing fine control of properties and allowing for the production of bespoke materials. A TiO_2-Bi_2O_3 material was prepared through a sol-gel route by Casados et al,[283] which involved adding bismuth nitrate to titanium isopropoxide, which was then added to propanol to form the gel. It was found that adjusting the quantity of bismuth nitrate added, that the composition of the product could be changed from TiO_2 to TiO_2 and bismuth titanate, bismuth oxide and bismuth titanate and just bismuth oxide. This leads to changes in optical properties and thus photocatalytic performance, and shows how the sol-gel process can be easily adapted for meeting various application criteria.

This was followed up with a subsequent study to form Bi-modified TiO_2 using a similar method,[284] whereby titanium tetraisopropoxide (TTIP) was mixed with propanol and stirred for 1 hour. Bismuth nitrate was then slowly added and nitric acid added to induce the gelation process. The gel was sonicated to form a gelled solution which was

used for spin coating. They found at lower concentration of bismuth nitrate, Bi could be incorporated into the TiO_2 lattice, but with higher content, bismuth titanate formed. It was also found that the addition of Bi reduced the band gap from 3.3 eV for plain TiO_2 to 2.7 eV, which the authors claim makes this a better candidate for solar photocatalysis than TiO_2 alone. They tested this by using Malachite Green carbinol base dye (MG) dye as a model pollutant and placing under simulated solar irradiation. This shows promise, but also highlights the need for more robust characterisation and analysis, as the effect of self-sensitisation with visible dyes is reported as a possible cause for incorrectly interpreting improved visible light performance as being down to a better visible light catalyst.

Another example of bismuth titanate synthesis through a sol-gel route is given by Madeswaran et al,[285] whereby bismuth nitrate is reacted with titanium butoxide, with glacial acetic acid and ethanolamine used as solvents and stabilising agent (to prevent $Bi(NO_3)_3$ reacting with water to form $BiONO_3$), respectively. The bismuth nitrate was dissolved in acetic acid with ethanolamine at 80 °C for 2 hours, before adding the titanium butoxide, forming a yellow-gold transparent solution that was used for spin-coating onto platinum-silicon substrates then drying at 400-600 °C for 1 hour.

Another study to form Bi-modified TiO_2 *via* a sol-gel route was conducted by Yi et al[286] in which they report on the photocatalytic behaviour of bismuth titanate composites with variable Bi/Ti ratios. For their synthesis, again bismuth nitrate was used to incorporate Bi into the system. It was dissolved in nitric acid, water and ethanol. Titanium butoxide as dissolved in ethanol, before the bismuth nitrate solution was added drop-wise. The mixture was then transferred to a Teflon-lined autoclave and heated at 180 °C for 15 hours, then filtered, dried and sintered at 450 °C for 4 hours. It was found that the material showed good activity under irradiation of 447 nm. This hydrothermal process is often utilised to obtain smaller particles, and can thus increase the performance of the catalyst, but may not be suitable for materials developed for the specific application of water treatment in rural areas, as this could limit the practicality of preparing new material as a local enterprise, and would require dependence on other chemical manufacturers.

One method of achieving finer control of particle size without the need for a hydrothermal

method is to perform a reverse-micelle sol-gel synthesis. This typically leads to a smaller variation in particle size and can be used to synthesise smaller nanoparticles, which can be difficult to achieve through a sol-gel synthesis alone.[287] The reverse micelle process is performed by forming a microemulsion of water in oil, leading to a thermodynamically stable dispersion of the two immiscible phases by the addition of a surfactant, as shown in Figure 6.2. The synthesis of the nanoparticles can then take place in the water micelles, which essentially create micro-reactors and prevent the particles from aggravating and forming particles that are too large.

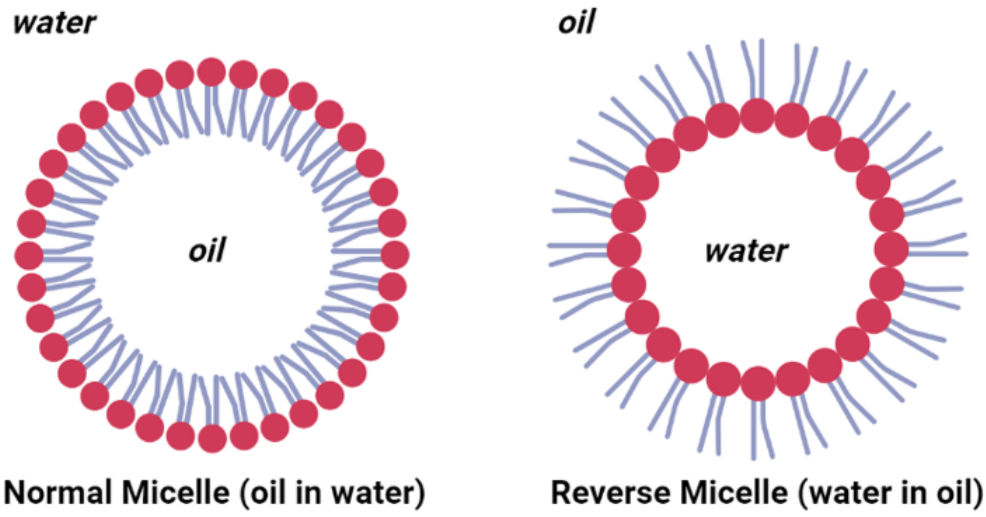

Figure 6.2: Difference between a normal micelle and a reverse micelle.

The material properties are heavily influenced by parameters including the content of water, solvent and surfactant, as well as the presence of a co-solvent. The relative ratios of each of these components can have a significant effect on the resulting material product, though there is some debate in the literature as to what the exact effects and reasoning behind these are.

There have been several cases in the literature of reverse micelle sol-gel (RMSG) procedures being employed for preparation of photocatalytic nanoparticles. Despite this, there still appears to be debate surrounding the best relative ratios of organic solvent, surfactant, water and precursor material to use in order to achieve the optimum conditions for synthesis.

6.2 Experimental

6.2.1 Synthesis

Bi-TiO_2-RMSG-1 (no P25) (0.4906 g, 41% yield): Cyclohexane (60 mL) and Triton-X 100 surfactant were mixed together at 50 °C for 30 minutes. Following this, an aqueous solution of $Bi(NO_3)_3.5H_2O$ ($1.63x10^{-4}$ mol, 10 mL) and HCl (37%, 0.6 mL) was first sonicated then added slowly to the organic solution. This was stirred for a further 15 minutes before adding titanium tetraisopropxide (TTIP) ($1.32x10^{-2}$ mol, 4mL) drop-wise and stirring at 50 °C for 2 hours. Isopropyl alcohol (40 mL) was added to quench the reaction, and the product obtained through centrifugation (5 minutes, 4400 RPM). The sample was then washed in ethanol 2 times (retrieved each time using a centrifuge at 4400 RPM for 20 minutes) before drying overnight at 80 °C. Once dry, the product was ground to a fine powder and annealed at 500 °C for 2 hours. A suspension was then prepared in the usual way, and films on glass slides prepared for initial testing.

Bi-TiO_2-RMSG-2 (P25) (0.6128 g, 51% yield): Same as above, but with the addition of P25 (0.05 g) to the aqueous solution of $Bi(NO_3)_3.5H_2O$ ($1.63x10^{-4}$ mol, 10 mL) and HCl (37%, 0.6 mL).

Plain TiO_2-RMSG synthesis (0.4743 g, 45% yield): 60 mL cyclohexane and 2 mL Triton-X were stirred for 30 minutes at 50 °C. After this time, 10 mL of water containing 0.6 mL of 37% HCl was added and stirred for a further 15 minutes to form an emulsion. TTIP was then added (4 mL) drop-wise, and the system stirred for 2 hours at 50 degrees before adding 40 mL IPA to quench the reaction. Product centrifuged and washed then dried overnight at 80 degrees before sintering at 500 °C for 2 hours.

6.2.2 Characterisation

XRD, DRS, Mott-Schottky, ICP-OES, XPS, SEM were all conducted according to the relevant sections in Chapter 2.

6.2.3 Chemical Photocatalytic Testing

First, glass slides and chips were coated with each material according to the procedure outlined in Section 2.1 of Chapter 2. An initial test of the photocatalytic activity was performed on glass slides according to the procedure outlined in Section 2.2.3.1 of Chapter 2, using 4-chlorophenol (156 μM) as the test pollutant under 370 nm, 410 nm and a white light LED (all spectra given in Section 2.2 of Chapter 2). The change in concentration of 4CP was tracked using UV-Vis absorption spectroscopy on a Shimadzu 1800-UV instrument, as described in section 2.2.1 of Chapter 2.

Following initial screening on the glass slides, chips were used for tests at a larger scale, following the procedure outlines in Section 2.2.3.2 of Chapter 2.

6.2.4 Microbial Photocatalytic Testing

For testing with *E.coli*, experiments were conducted as described in Section 2.2.3.3 of Chapter 2, in the same way as in Chapter 5.

The testing using *Geobacillus stearothermophilus* was conducted following the same general procedure, with illumination from the 410 nm LED, the mass of catalyst-coated glass chips still being 15 g and volume of water spiked with bacteria being 50 mL.

The spore suspension used was supplied from Excelsior Scientific (ATCC 7953) at a concentration of order of magnitude 10^6 CFU/mL. For the experiment, a concentration of 10^4 CFU/mL was needed to be comparable to the *E.coli* measurements conducted previously. Therefore, 0.5 mL of the spore suspension was added to the 50 mL of sterile de-ionised water, before adding to the dish containing the catalyst and conducting the experiment as normal, taking 0.5 mL for serial dilutions and using 50 μL for spreading on the Petri dishes.

The nutrient media used here was Luria-Bertani (LB) broth (supplied by Sigma), which was made by adding 10 g of the LB powder to 400 mL of deionised water and autoclaving in the same way as used in the *E.coli* methodology. Once autoclaved, the molten solution was poured into Petri dishes (roughly 4 mL per dish) and left to set.

After spreading the sample on the media, the dishes were wrapped in Parafilm to prevent drying and placed in the incubator at 60 °C overnight, before counting the colonies and converting to CFU/mL.

The methodology for using the T4 bacteriophage virus differed to that for testing with bacteria, as a host bacteria was required for the virus to grow. For this purpose, K-12 *E.coli* was used. To prepare the Petri dishes for sampling, a two layer approach was needed. The bottom layer was made up using 25 g/L of agar (supplied by Merck) and 15 g/L of LB broth, which was then autoclaved and poured into the dishes in a thin layer. On top of this, the second layer was made by mixing 5 g of agar and 25 g of LB then autoclaving. Once autoclaved, the media was kept molten by storing in a water bath at 40 °C. The *E.coli* K-12 then needed to be mixed with the media before pouring onto plates, in order for the virus to have a host. To do this, 4 mL of the molten media was taken, and 200 μL of *E.coli* solution was added, before pouring over the solidified bottom layer of agar/LB. This was left to set before using in the experiment.

The *E.coli* suspension used was prepared by scraping an inoculation loop across the surface of a dish with *E.coli* colonies and adding this to a solution of LB broth and incubating at 37 °C overnight, which formed a turbid solution. This was refreshed on the morning of the experiment by adding 2.5 mL of the *E.coli* suspension to 7.5 mL of sterile LB broth and incubating again for 1 hour.

The virus solution used (provided by the James Hutton Institute) contained roughly 10^8 PFU/mL of the T4 bacteriophage, so for a solution of 10^4 PFU/mL, 50 μL of the suspension was added to 50 mL of sterile water, which was then poured into the dish containing the catalyst in the same way as for the bacterial experiments.

The serial dilutions were made in the same way as previously, but this time using TM buffer rather than the 8% NaCl solution. TM buffer (so named as it contains tris(hydroxylmethyl)aminomethane, 'Tris', and magnesium) was made as follows: 10 mM $MgSO_4$, 10 mM 'Tris', 5 μM $CaCl_2$ in distilled water, adjusted to pH 7.4 by adding

7% HCl drop-wise.

To check for virus growth, the dishes were split into six sections: three for one dilution, and three for another dilution. This way, three repeats could be made without using too many dishes and wasting resources. To add the sample to the dishes, a 5 μL drop was added in each of the sections. If the virus was functioning, it would infect and inactivate the *E.coli*, leaving a clear spot on the surface of the media known as a plaque. Therefore, the viral content can be assessed by counting the presence of blank spots were *E.coli* has been removed. This is known as the plaque assay method.

6.2.5 Mechanistic Studies

Tests were conducted according to Section 2.2.2.3 of Chapter 2 for determining the dominant mechanism for photocatalytic decontamination.

6.2.6 Stability Testing

These tests were performed using 4-CP under 410 nm light, following the same pattern of testing outlined in Section 2.2.2.4 Chapter 2. Briefly, the samples were used 5 consecutive times without regeneration, only rinsing. After the fifth use, the samples were calcinated at 500 °C for 1 hour, before repeating the testing for 5 more uses. This was repeated to give three complete cycles of testing.

6.2.7 Summary of Sample Names

A summary of synthesis attempts is given in Table 6.1. Reverse-micelle sol-gel synthesis is abbreviated as RMSG for all below sample names and throughout the proceeding discussion. Attempts focused on trying to develop bismuth titanate, by synthesising TiO-2 *in situ* in the presence of $Bi(NO_3)_3$. Several attempts were made, with many samples showing an improvement relative to P25 TiO_2 in the visible light region, but not under UV.

Table 6.1: Summary of samples made for this Chapter and their assigned names.

Sample Name	Description
TiO_2-RMSG	Reverse Micelle Sol-gel. Plain TiO_2. No P25 present. White appearance (not as bright as P25). Isolated in 45% yield.
Bi-TiO_2-RMSG-1 (no P25)	Reverse Micelle Sol-gel with no P25. Peach coloured powder. Isolated in 41% yield.
Bi-TiO_2-RMSG-2 (P25)	Reverse Micelle Sol-gel. Same as Bi-TiO_2-RMSG-1 (no P25) but with addition of P25 during synthesis. Peach colour powder, lighter than samples with no P25. Isolated in 51% yield.

The best performing material found, Bi-TiO_2-RMSG-2 (P25), was developed by a reverse micelle sol-gel (RMSG) route. This synthesis largely focused on the preparation of TiO_2 *in-situ*, rather than starting from P25 TiO_2 and trying to mix with another semiconductor (as with SILAR or the ZnFe/TiO_2 materials explored previously). Thus, it would be a more appropriate control to use TiO_2 synthesised in the same way as the Bi-TiO_2 materials to assess whether the additive is beneficial or not, rather than P25 TiO_2.

The synthesis, testing and characterisation for the following materials will be presented in the proceeding discussion: Bi-TiO_2-RMSG-1 (no P25), Bi-TiO_2-RMSG-2 (P25) and TiO_2-RMSG.

6.3 Results and Discussion

6.3.1 XRD

The Bi-TiO_2 materials exhibit XRD powder patterns that can be entirely assigned to TiO_2 peaks, as shown in Figure 6.3, which includes experimental powder XRD traces, as well as literature data for anatase (ICSD card number 21-1272) and rutile (ICSD card number 21-1276). Interestingly, the modified materials with bismuth present seems to facilitate the formation of the anatase phase, whereas the plain TiO_2 material contains only rutile peaks. This could explain why the typical phenomenon of observing a worsening of photocatalytic performance under the whole solar spectrum relative to titania

alone is not as pronounced in this material as for the ZnFe/TiO_2 materials, and others presented in the literature.

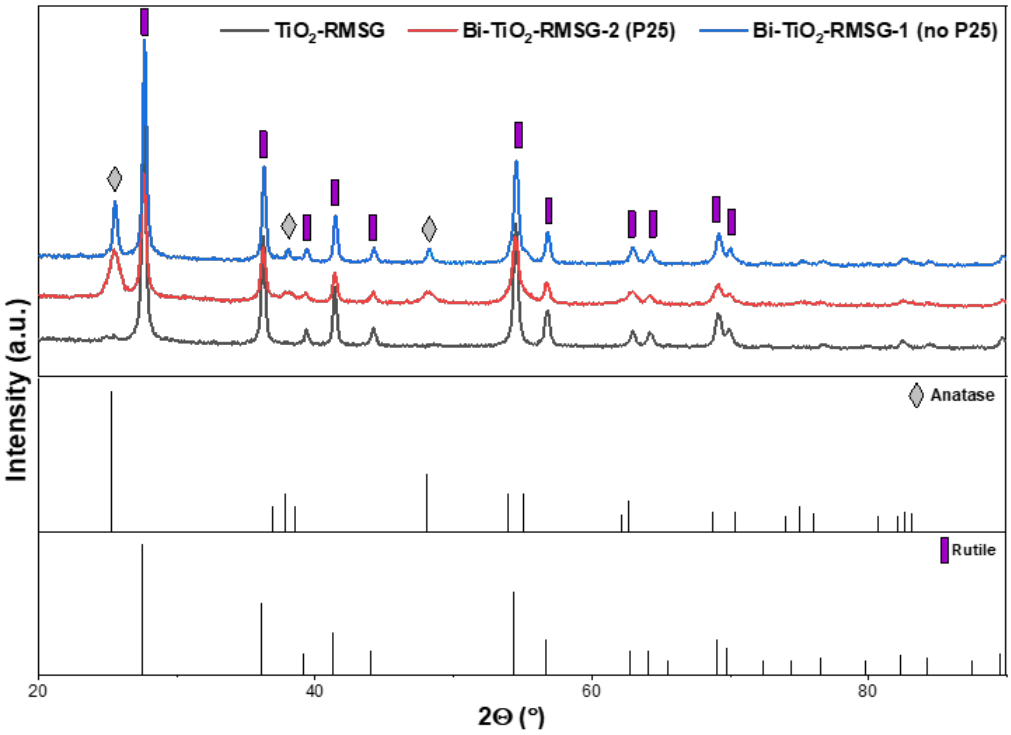

Figure 6.3: XRD patterns for TiO_2-RMSG, Bi-TiO_2-RMSG-2 (P25) and Bi-TiO_2-RMSG-1 (no P25).

P25 is made up of 80% anatase and 20% rutile, so in its XRD pattern, anatase peaks will dominate (as seen in Figure 5.2 in Chapter 5). However, in the material here containing P25, Bi-TiO_2-RMSG-2 (P25), the anatase peaks are not notably stronger than for the material with no P25, Bi-TiO_2-RMSG-1 (no P25). This is likely to be due to the low relative proportion of P25 to the synthesised TiO_2.

Further, the lack of any clear peaks for crystal structures containing bismuth, such as bismuth oxide or bismuth titanate, suggest that either the material has been incorporated into the structure as an amorphous coating on the surface of TiO_2, or the Bi is simply taken up as an impurity in the TiO_2 lattice.

6.3.2 ICP-OES

The samples were analysed using ICP-OES to investigate the composition of the bulk materials. The results are shown below in Table 6.2, with the data adjusted to take

account of the measurement of the blank sample, as in Chapter 5.

Table 6.2: Summary of ICP-OES data collected for selected samples synthesised for this Chapter. Note that the wavelengths used for detecting Ti and Bi were 368.519 nm and 206.170 nm, respectively. Data presented is corrected to account for the concentration of each element in a blank sample of just solvent.

Sample	Ti (mg/L)	Bi (mg/L)	Approx. Ti:Bi Ratio
TiO_2-RMSG	50.152	-0.099	
Bi-TiO_2-RMSG-1 (no P25)	23.869	1.143	20:1
Bi-TiO_2-RMSG-2 (P25)	29.438	1.07	30:1

As shown in Table 6.2, the Bi measured in the TiO_2 sample is lower than the blank sample, which suggests that, within a reasonable error caused by measurement fluctuations, the Bi content is negligible, as expected. The Bi content is lower for the sample synthesised in the presence of P25, which is to be expected as there is additional TiO_2 content, with the quantity of $Bi(NO_3)_3$ added to the synthesis for both Bi-TiO_2-RMSG-1 (no P25) and Bi-TiO_2-RMSG-2 (P25) being the same.

The bismuth content is higher than expected based on the ratio of reagents added ($1.32x10^{-2}$ mol Ti from TTIP and $1.63x10^{-4}$ mol Bi from $Bi(NO_3)_3.5H_2O$, giving a theoretical ratio close to 100:1). The higher experimental ratio suggests that the Bi is more efficiently taken up in the synthesis, but the TTIP is in slight excess, suggesting the quantity could be reduced for similar results, with lower synthesis costs.

The ICP results further suggest that a bismuth titanate material was not made, as these typically have chemical formulae with more bismuth than titanium, such as $Bi_{12}TiO_{20}$ or $Bi_4Ti_3O_{12}$, which is not the case here.

6.3.3 SEM

In order to evaluate how the synthesis method affects the morphology of the photocatalyst nanoparticles, SEM images were taken of the synthesised TiO_2, Bi-TiO_2-RMSG-1 (no P25) and Bi-TiO_2-RMSG-2 (P25) samples, as well as commercial P25 TiO_2.

It was found that, though small particles of the order of magnitude of tens of nanome-

tres could be observed, for these samples synthesised *via* the RMSG route, the particles tended to aggregate into larger clumps. However, it must be noted here that the small particles visible for these samples may be due to the presence of platinum on the surface, due to the coating applied to prepare the samples for imaging. If this is the case, then the RMSG synthesis route appears to produce particles on the micrometer scale.

Images of P25 TiO_2 were taken to compare morphology and particle size of the synthesised products. These are shown in Figures 6.4 and 6.5.

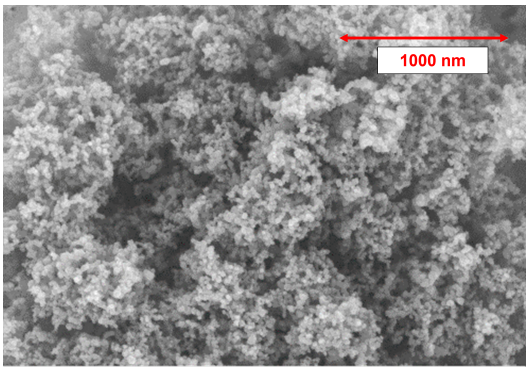

Figure 6.4: SEM image of P25.

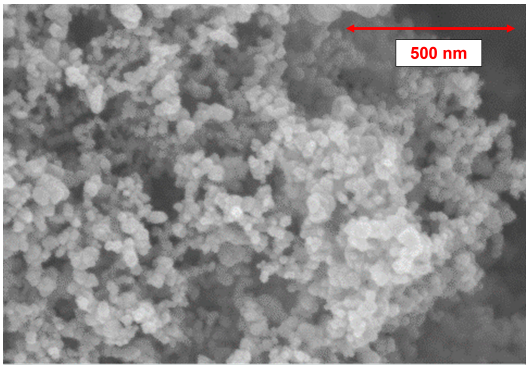

Figure 6.5: SEM image of P25.

Images of TiO_2-RMSG are shown in Figures 6.6 - 6.9, where small particles within the aggregates can be seen.

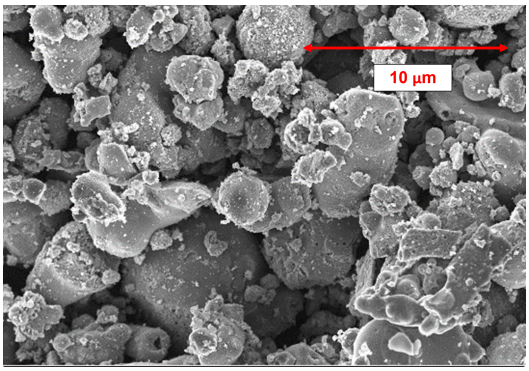

Figure 6.6: SEM image of TiO_2-RMSG.

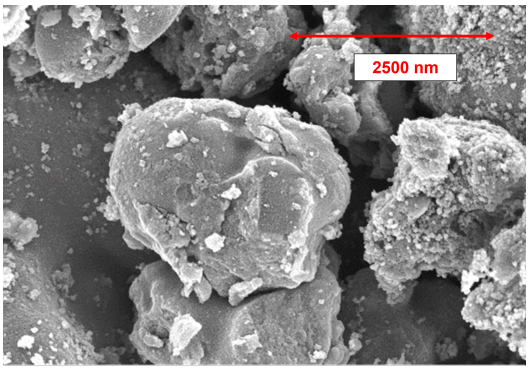

Figure 6.7: SEM image of TiO_2-RMSG.

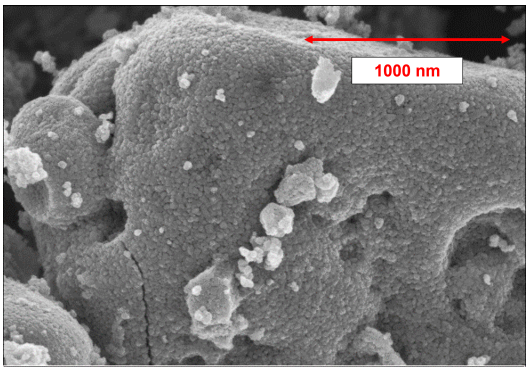

Figure 6.8: SEM image of TiO_2-RMSG.

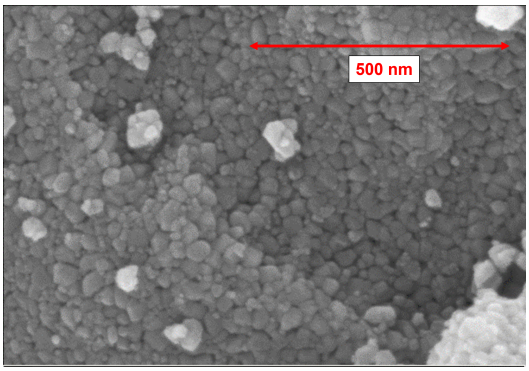

Figure 6.9: SEM image of TiO_2-RMSG.

Images of Bi-TiO_2-RMSG-1 (no P25) are shown in Figures 6.10 - 6.13.

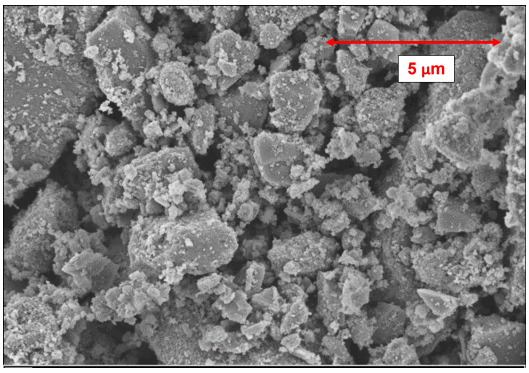

Figure 6.10: SEM image of Bi-TiO_2-RMSG-1 (no P25).

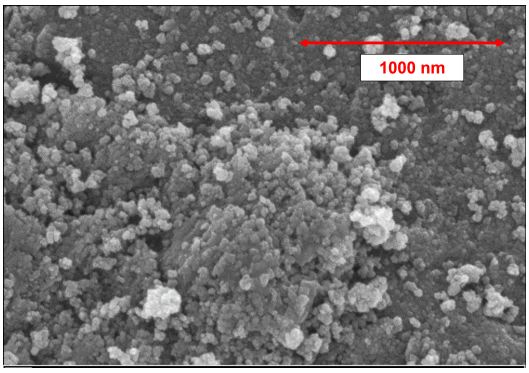

Figure 6.11: SEM image of Bi-TiO_2-RMSG-1 (no P25).

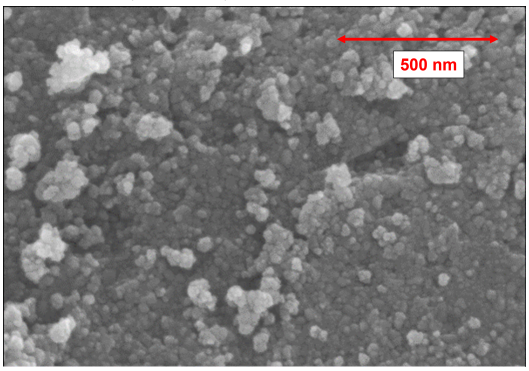

Figure 6.12: SEM image of Bi-TiO_2-RMSG-1 (no P25).

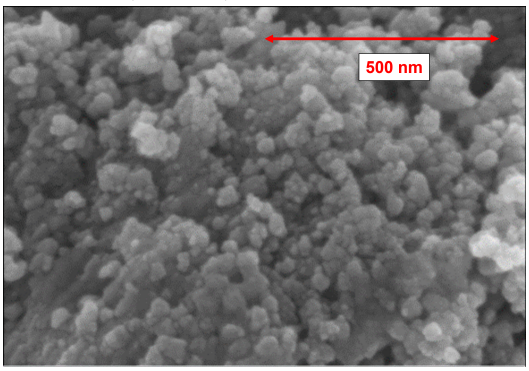

Figure 6.13: SEM image of Bi-TiO_2-RMSG-1 (no P25).

Images of Bi-TiO_2-RMSG-2 (P25) are shown in Figures 6.14 - 6.17.

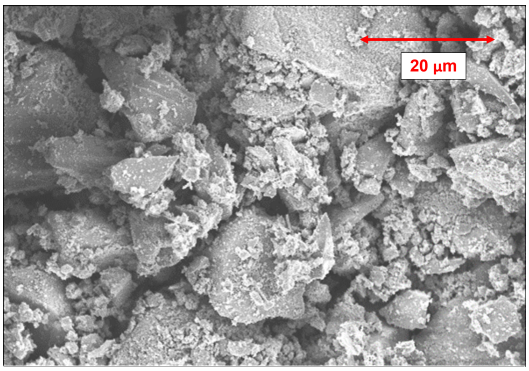

Figure 6.14: SEM image of Bi-TiO_2-RMSG-2 (P25).

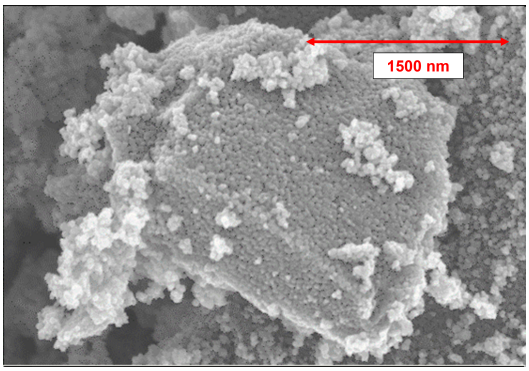

Figure 6.15: SEM image of Bi-TiO_2-RMSG-2 (P25).

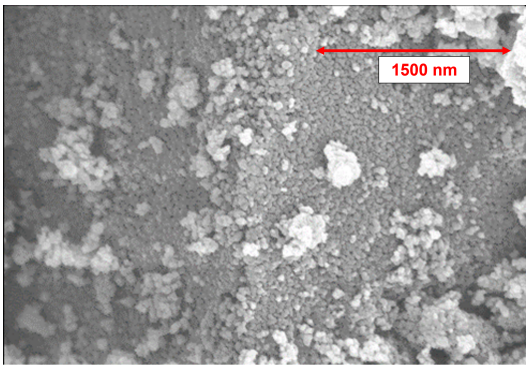

Figure 6.16: SEM image of Bi-TiO_2-RMSG-2 (P25).

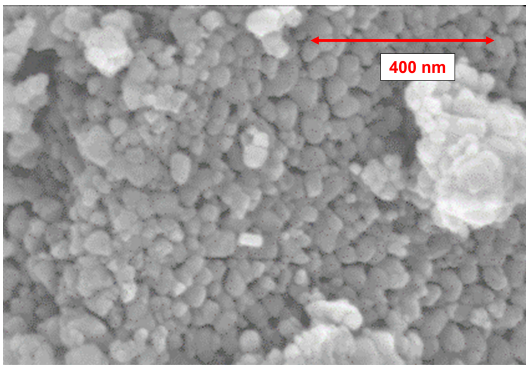

Figure 6.17: SEM image of Bi-TiO_2-RMSG-2 (P25).

It can be seen from the collected SEM images that these materials have a tendency to cluster more tightly than P25, which appears as a loose powder. This will act to reduce the effective surface area available for reaction, and could explain why P25 still seems to perform best under simulated solar light, despite the clear improvement to photoactivity under visible light. However, this may have benefits in terms of recapture of any leached particles and reducing any health concerns relating to small nanoparticles.

There also seems to be a large variation of approximately an order of magnitude in aggregate size (1 – 10 μm), for all RMSG products. The addition of P25 to the synthesis for the Bi-TiO_2-RMSG-2 (P25) sample does not seem to affect the morphology significantly relative to other RMSG products, with large aggregates of smaller particles also appearing.

Further, the SEM images appear similar for each of the products, suggesting the P25 is not on the surface of the Bi-TiO_2-RMSG-2 (P25) clusters. If the P25 is indeed covered

by the formation of RMSG particles around it, this could explain why the UV activity is not higher than P25 on its own, as the P25 is not itself exposed to light, but its presence could help to improve charge transfer and reduce recombination, giving it an advantage over the Bi-TiO_2-RMSG-1 (no P25) sample with no P25.

This could suggest that the P25 added to the synthesis may form a seed site for the formation of further TiO_2 particles, thus forming a composite particle. This could help to explain why the Bi-TiO_2-RMSG-2 (P25) sample has such a significantly improved performance relative to the Bi-TiO_2-RMSG-1 (no P25) sample, which was otherwise prepared in the same way.

To evaluate the chemical composition further, elemental analysis (*via* energy-dispersive X-ray spectroscopy, EDS) was also performed during the SEM measurements, with multiple measurements taken for each sample to account for variations at different measurement sites. TiO_2 and P25 were consistent with the measurements taken at the different locations on the same site, but there was some variation for the bismuth-modified samples so in this case, more sites were used to confirm the results. The results are presented in Table 6.3 below.

Table 6.3: Summary of SEM EDS data collected for selected samples synthesised for this Chapter. Note that the data presented are the average values taken from across multiple sites used to repeat the measurements across the material surfaces.

Sample	Atomic % Ti	Atomic % O	Atomic % Bi	Approx. Ti:O:Bi Ratio
P25	39.25	60.75		2:3:0
TiO_2-RMSG	38.17	61.57		5:8:0
Bi-TiO_2-RMSG-1 (no P25)	37.17	62.58	0.22	300:500:1
Bi-TiO_2-RMSG-2 (P25)	35.62	64.19	0.18	300:540:1

Interestingly, the Bi content recorded here is much lower than that observed using ICP-OES, suggesting that the distribution of Bi is not uniform across the whole particle. Considering that SEM penetrates to a depth of roughly 1 micron, it cannot be conclusively

stated that the bismuth is mostly contained within the particles, and the discrepancy could be due to any overlapping EDS peaks which obscure the bismuth detection and make it hard to unambiguously disentangle the results. The Bi content is slightly lower here for the Bi-TiO_2-RMSG-2 (P25) sample, which is consistent with the results from ICP-OES.

The ratio of Ti to O is mostly consistent for the samples, around 0.6, though some variations are seen, with the Bi-TiO_2-RMSG-2 (P25) having the lowest oxygen content. It is interesting to note that none of the samples here produced the expected result of 1:2 (0.5) for Ti:O, as it would be for a true TiO_2 sample. Since this was also the case for the commercial P25 sample, it can be assumed that this is due to measurement uncertainty, but trends can still be reliably evaluated.

The presence of the aggregates leading to the presence of larger clusters could prove advantageous for water treatment in rural areas, where the removal of any leached nanoparticles could prove extremely difficult without access to expensive microfilters or centrifugation. As discussed above, studies have suggested that particles from 250 nm and above show lower toxicity than particles at 20 nm scale. Some of the aggregates observed are even larger, on the scale of tens of micrometres, which could help to mitigate any adverse health effects if any particles leach off and are inhaled or consumed. This, it could be argued, is worth the dip in activity relative to P25 as concerns over negative health impacts, whether strictly a concern at this concentration, would still limit interest from possible users or investors when trying to implement the treatment method in practice.

Due to the large particles being made up of smaller constituents, this leads to a porous surface, meaning that the activity is not completely diminished by the presence of larger particles. Further, in an environment where more sophisticated technologies and higher funding is available that would allow finer nanoparticles to be extracted from water, such as in municipal water treatment facilities, the products of these RMSG syntheses could be ground down using a ball mill to break the aggregates up. This would expose the smaller constituent particles, increasing surface area and thus possibly lead to higher activities, though further testing would be needed to check this.

6.3.4 XPS

XPS measurements revealed some very interesting data pertaining to the composition of the synthesised materials, particularly with respect to the bismuth content.

For both Bi-TiO_2-RMSG-1 (no P25) and Bi-TiO_2-RMSG-2 (P25), bismuth was observed as Bi^{3+}, Bi^{4+} and as metallic bismuth. This could help to explain why no peaks were seen for bismuth titanate in the XRD patterns for these materials, as the bismuth is changing oxidation state during the synthesis, so not enough remains when reacting with the titanium source (in this case TTIP) to form this material in high enough quantity to be observed. The results of the quantitative composition analysis are shown in Table 6.4.

Table 6.4: Summary of XPS data collected for selected samples synthesised for this Chapter.

Sample	Atomic % Ti	Atomic % O	Atomic % Bi	Approx. Ti:O:Bi Ratio
P25	21.43	59.61		1:3:0
TiO_2-RMSG	29.19	56.41		1:2:0
Bi-TiO_2-RMSG-1 (no P25)	28.57	55.65	0.49	290:550:5
Bi-TiO_2-RMSG-2 (P25)	29.19	58.42	0.74	290:580:7

These ratios can be further expanded to show the breakdown of oxidation states that contribute to the total presence of each element, as shown in Table 6.5.

Table 6.5: Oxidation states detected for each element through XPS analysis.

	Titanium		Bismuth		
Sample	% Ti IV	% Ti III	% Bi IV	% Bi III	% Bi 0
P25	100	0	0	0	0
TiO_2-RMSG	100	0	0	0	0
Bi-TiO_2-RMSG-1 (no P25)	95	5	63	8	29
Bi-TiO_2-RMSG-2 (P25)	95	5	69	13	18

It was found that Bi-TiO_2-RMSG-1 (no P25) had the most metallic Bi present, though the ratios for each of the two bismuth-containing materials was quite similar. The results obtained here were most in line with those obtained *via* SEM, rather than ICP-OES, which is expected due to the measurement techniques being more similar (i.e. surface rather than bulk measurements), though it should be highlighted that the penetration depth for XPS is less than that for SEM, at around 1 nm. This could explain the small difference in ratio between Ti and Bi for SEM and XPS, though this could also be down to errors in measurements.

Valence band estimations could also be made *via* XPS, with the results shown in Figures 6.18 to 6.21 and summarised in Table 6.6. The errors are calculated based on the propagation of errors on the slope and intercept from the linear fit.

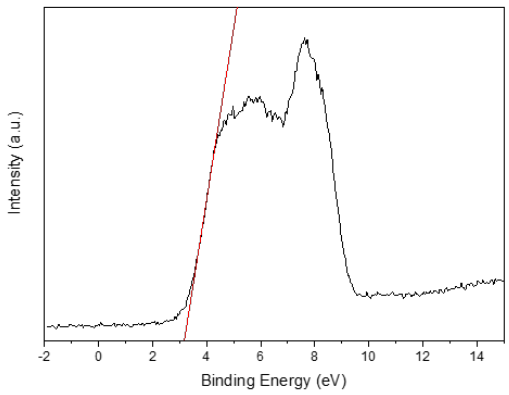

Figure 6.18: XPS plot for P25

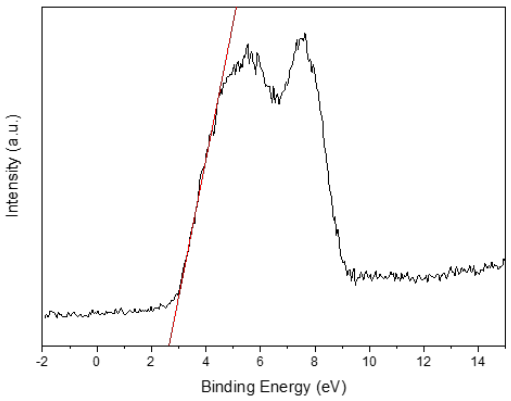

Figure 6.19: XPS plot for TiO_2-RMSG

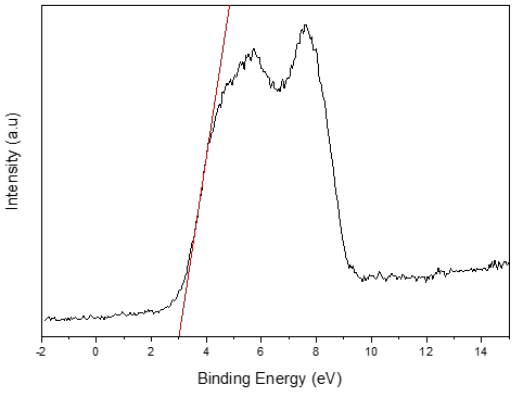

Figure 6.20: XPS plot for Bi-TiO_2-RMSG-1 (no P25)

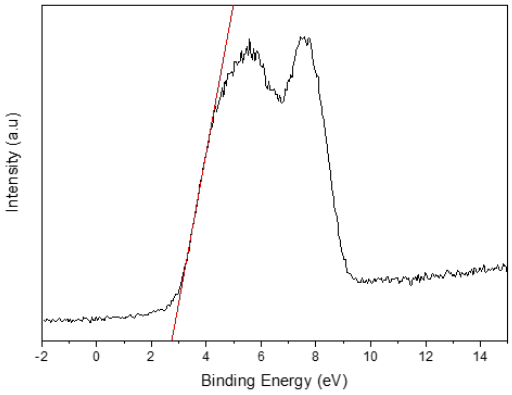

Figure 6.21: XPS plot for Bi-TiO_2-RMSG-2 (P25)

Table 6.6: Valence band estimations from XPS analysis on NHE scale.

Sample	Estimated Valence Band (eV)
P25	3.18 ± 0.10
TiO_2-RMSG	2.64 ± 0.25
Bi-TiO_2-RMSG-1 (no P25)	3.00 ± 0.15
Bi-TiO_2-RMSG-2 (P25)	2.74 ± 0.09

Interestingly, the product with a valence band most similar to P25 is Bi-TiO_2, though there is also a slightly larger tail shown in the plot from which the valence band value was measured, which could lead to an inaccurately large calculated value. The trace for TiO_2-RMSG appears to have less of a tail than the other synthesised products, suggesting the presence of bismuth is altering the states present around the valence band, and thus the photoactivity that can result. Further, it from this analysis it would seem that the valence bands for all products here are quite deep, and should thus be able to oxidise hydroxide (redox potential at -2.17 eV vs vacuum).

6.3.5 DRS

As shown in Figures 6.22 - 6.24, a clear difference can be observed between the plain TiO_2-RMSG material and the two materials containing bismuth, in that the modified materials show distinct tails, indicating more states added in the gap. This also had to be taken into account when measuring the estimated band gap from the linear regions in the Tauc plots, with corrections applied according to the procedure outlined in Section 2.3.1 of Chapter 2.

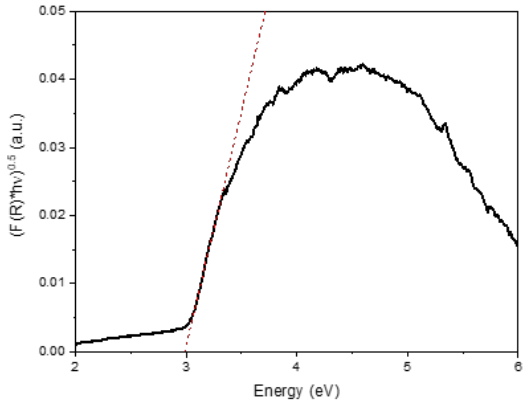

Figure 6.22: Tauc Plot for Bi-TiO_2-RMSG-1 (no P25)

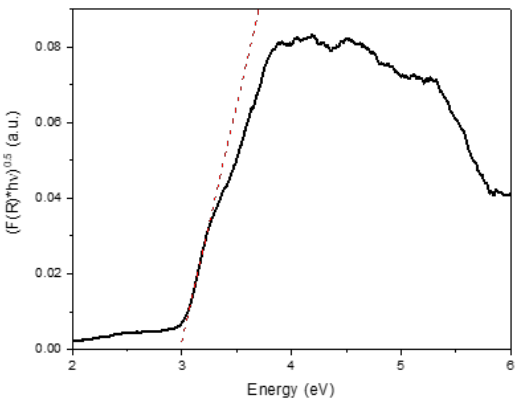

Figure 6.23: Tauc Plot for Bi-TiO_2-RMSG-2 (P25)

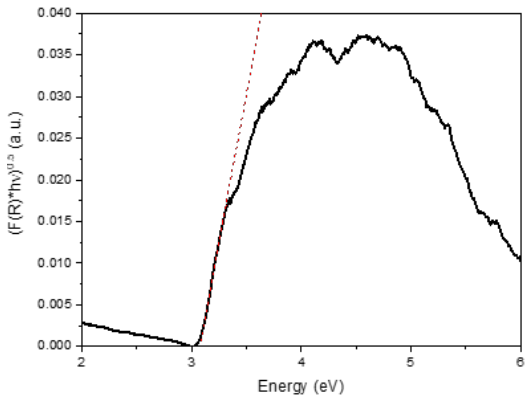

Figure 6.24: Tauc Plot for TiO_2-RMSG

The calculated band gaps based on the Tauc plots are summarised in Table 6.7, with the error calculated in the same way as in Chapter 5 using Equation 2.10.

Table 6.7: Band gap estimations based on associated Tauc plots.

Sample	Estimated Band Gap (eV)	Corrected Band Gap (eV)	Corresponding Wavelength (nm)
TiO_2-RMSG	3.01 ± 0.002		405
Bi-TiO_2-RMSG-1 (no P25)	2.98 ± 0.002	3.05 ± 0.002	407 - 417
Bi-TiO_2-RMSG-2 (P25)	2.98 ± 0.003	3.03 ± 0.003	410 - 417

For the corrections, y was taken as 0.004 for Bi-TiO_2-RMSG-1 (no P25) and 0.006 for Bi-TiO_2-RMSG-2 (P25). With the corrections taken into account, there does not appear to be a significant altering of the band gap size when adding bismuth, though the extra states added may explain the difference in visible light harvesting.

6.3.6 Mott-Schottky Analysis

Electrochemical tests were performed to probe the flat band potential of these materials, in order to obtain an estimate for the position of their conduction bands. The results for a scan at 1.5 kHz from -1 V to 0 V is shown below in Figure 6.25.

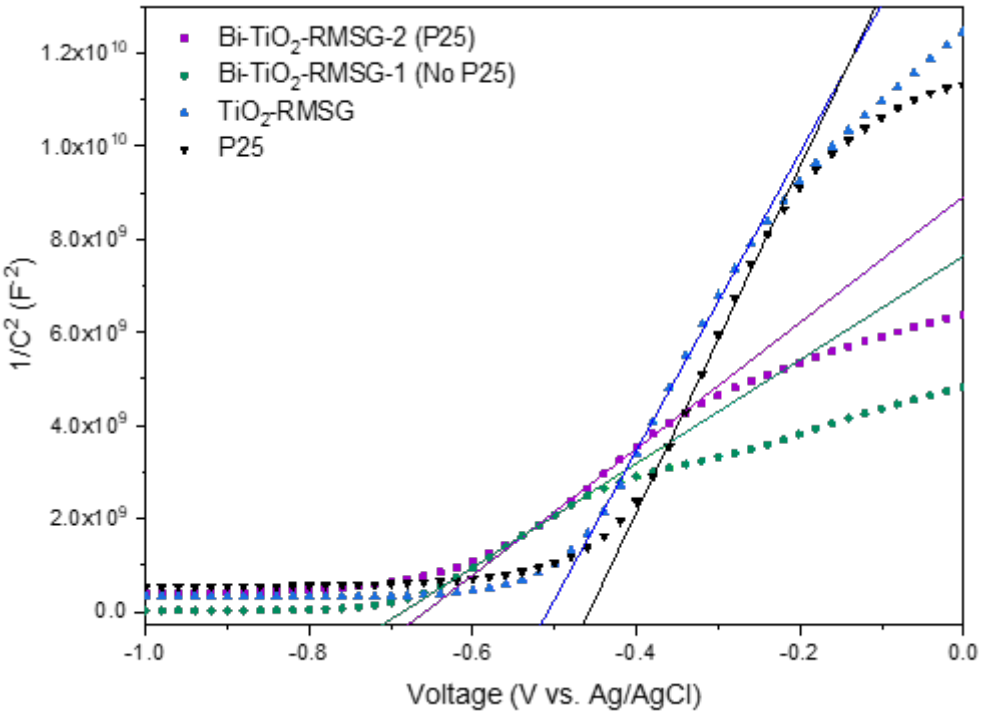

Figure 6.25: Mott-Schottky plots for P25, TiO_2-RMSG, Bi-TiO_2-RMSG-2 (P25) and Bi-TiO_2-RMSG-1 (no P25).

From the plot it can be deduced that these materials are all n-type semiconductors, due to the characteristic positive slope exhibited, and that the conduction bands of all of the synthesised materials are cathodically shifted (i.e. more negative) relative to P25 TiO_2. Unlike the ZnFe/TiO_2 materials presented in Chapter 5, this would suggest a greater driving force for electron transfer relative to P25. These materials do perform well, and have shown the highest activity under visible light observed throughout the entire work for this Thesis. However, a small reduction in simulated solar performance was still observed, which could be due to disruptions to the lattice increasing charge recombination.

Impurities in the material can also shift the Fermi level (EF), which represents the electron population and determines conductivity. If the EF shifts higher, electrons can reach the CB more easily, leading to the production of more photoelectrons. The addition of

bismuth into the TiO_2 system would therefore act as an impurity and give rise to the different in band structure for the plain TiO_2-RMSG sample. This may explain why the visible light activity is improved, despite the CB being raised, as the effective gap becomes smaller. This is also demonstrated by the valence band XPS measurements and optical gap determined via DRS.

It is also interesting to see two distinct trace shapes from the Mott Schottky plots, with the plain TiO_2 materials appearing to have similar behaviour and flat band potentials, and the bismuth-modified materials also showing similar behaviour to each other. This confirms the bismuth is responsible for altering the electronic properties of the semiconductors. The results are summarised in Table 6.8.

Table 6.8: Summary of flat band potential and associated calculated values.

Sample	Flat band potential (E_{FB}) (V)	Error in E_{FB} (V)	Cathodic shift relative to P25 (V)	Estimated $E_{CB,M}$ (V)
P25 TiO_2	-0.458	0.010		-0.358
TiO_2-RMSG	-0.508	0.013	0.05	-0.408
Bi-TiO_2-RMSG-1 (no P25)	-0.658	0.012	0.20	-0.558
Bi-TiO_2-RMSG-2 (P25)	-0.685	0.008	0.23	-0.585

The errors are calculated in the same way as in Section 2.3.1 of Chapter 2 using Equation 2.10.

The conduction band indicates the ease of oxidation, so the shift in the CB minimum relative to P25 TiO_2 can help explain the different activities. The electrons in the CB of Bi-TiO_2-RMSG-2 (P25) appear to be more energetic and will lead to the semiconductor being oxidised more readily, providing more electrons for oxidation of contaminants, which the mechanistic studies found to be the dominant mode for mineralisation. Hence, this material performs best of all samples.

6.3.7 Band Structure Estimations

In the same way as in Chapter 5, all of the above data can be combined to predict the band architecture for these bismuth-TiO_2 composites, as presented in Figure 6.26.

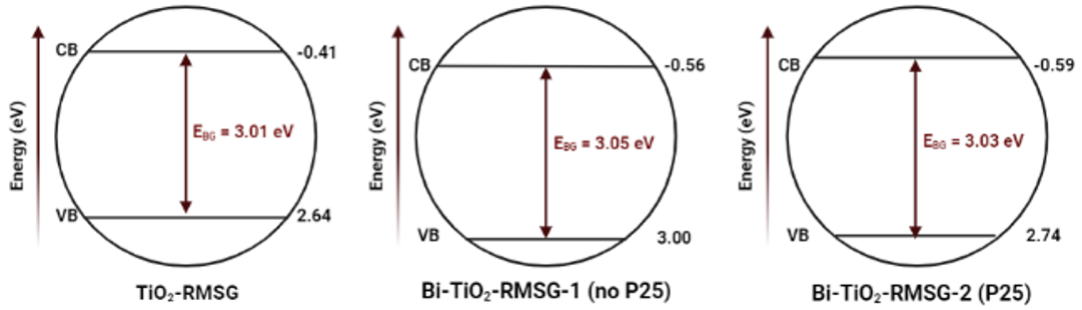

Figure 6.26: Estimates of band structures for TiO_2-RMSG, Bi-TiO_2-RMSG-1 (no P25) and Bi-TiO_2-RMSG-2 (P25).

In the above diagrams, there are some discrepancies with the values shown for the valence band, conduction band and band gap, obtained from the XPS, Mott-Schottky and DRS analysis, respectively.

It is likely the majority of this error comes from the DRS measurements for the band gap, on account of the tail in absorption which increases the complexity in extrapolating the correct data.

These diagrams have been produced to show the band gaps without the presence of a heterojunction, though the presence of one may also help to explain the lack of consistency between the calculated values from different methods and why they don't coincide with each other. This could also be due to the presence of more complicated electronic structure, with more states present in between the gap due to the presence of bismuth, which could allow for lower energy visible light photons to be absorbed, and making the effective band gap measured appear smaller.

6.3.8 Chemical Photocatalytic Testing

The results for the tests conducted for the materials on glass slides with model pollutant 4-CP are presented below for all of the four light conditions (365 nm, 410 nm, a white light and a solar simulator lamp). The results for these tests are shown in Figure 6.27.

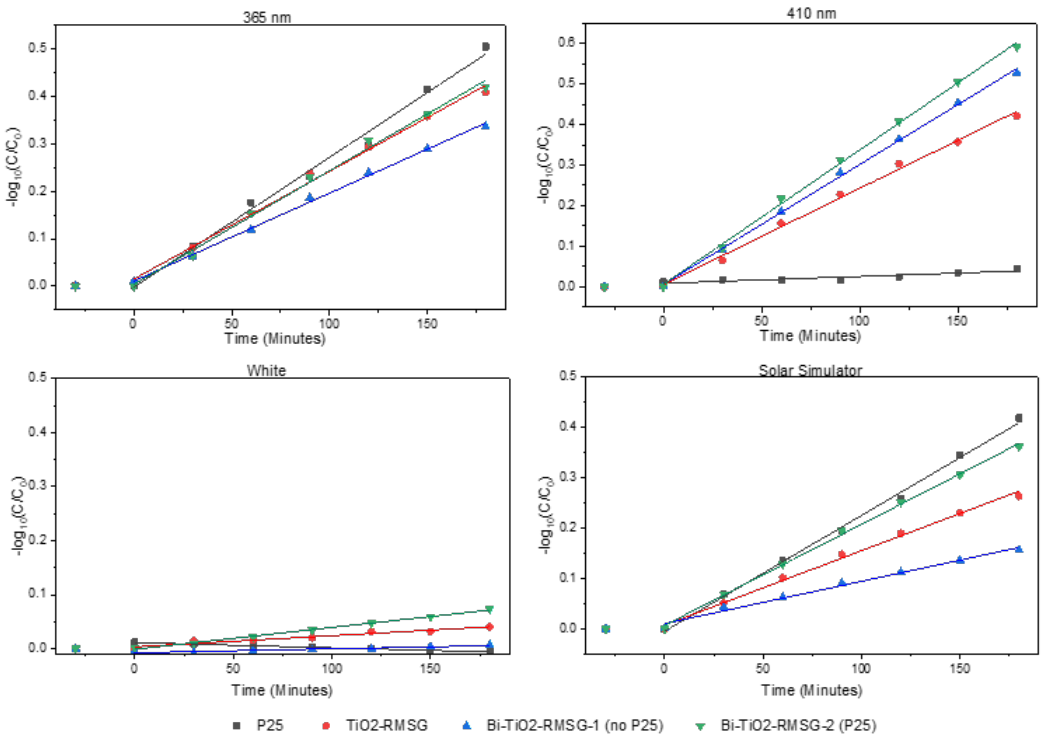

Figure 6.27: Rate of change in 4-CP concentration over the course of 3 hours treatment under different light sources for P25 TiO_2, TiO_2-RMSG, Bi-TiO_2-RMSG-1 (no P25) and Bi-TiO_2-RMSG-2 (P25). Note that the linear fit begins at time = 0 minutes, and does not include the 30 minutes in the dark, such that the rate of just the active photocatalysis is found.

From these plots, the first order rate constants could be estimated. These are shown in Figure 6.28.

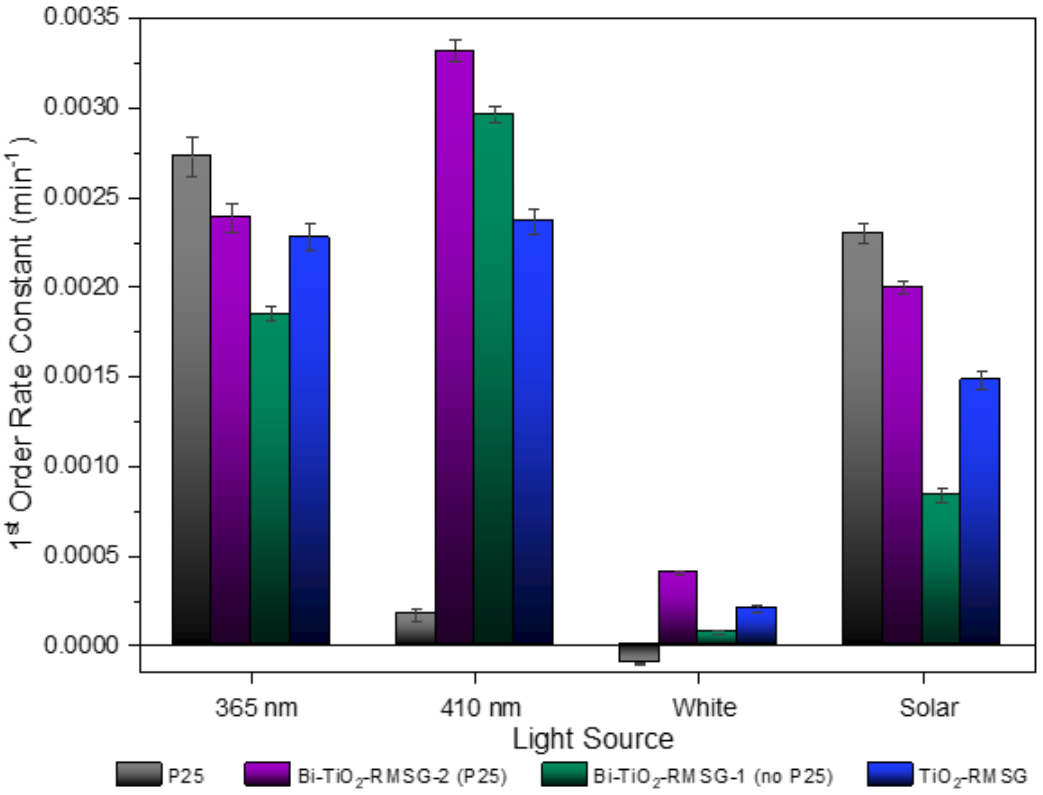

Figure 6.28: First order rate constants under different light sources.

Of all modified materials, Bi-TiO_2-RMSG-2 (P25) consistently had the highest first order rate constant under each light source. This material outperforms all of the other RMSG materials under all lights, and P25 under 410 nm and the white light. P25 appeared to have a slightly higher activity under UV and solar simulation, as is often the case for materials prepared with additives or dopants in TiO_2. However, the extent to which Bi-TiO_2-RMSG-2 (P25) is improved relative to P25 under visible light is much higher than the difference between Bi-TiO_2-RMSG-2 (P25) and P25 under UV light, suggesting that the solar simulator relationship observed here may vary more significantly for different weather types. In cases of higher cloud cover, resulting in lower intensities of UV light reaching the catalyst surface, it is possible that this material may also outperform P25 under solar conditions.

6.3.9 Microbial Photocatalytic Testing

Following the same protocol as the studies conducted with *E.coli* following used in Chapter 5 for the ZnFe/TiO_2 materials, preliminary tests were conducted to evaluate the ability of the bismuth-containing catalysts to remove bacterial contamination.

The percentage loss of *E. coli*, also referred to as the degradation efficiency, is presented in Figure 6.29, where it can be seen that all conditions with catalysts present remove more bacteria relative to the condition with no catalyst, only light. The materials containing bismuth appear to outperform the titania catalysts without bismuth.

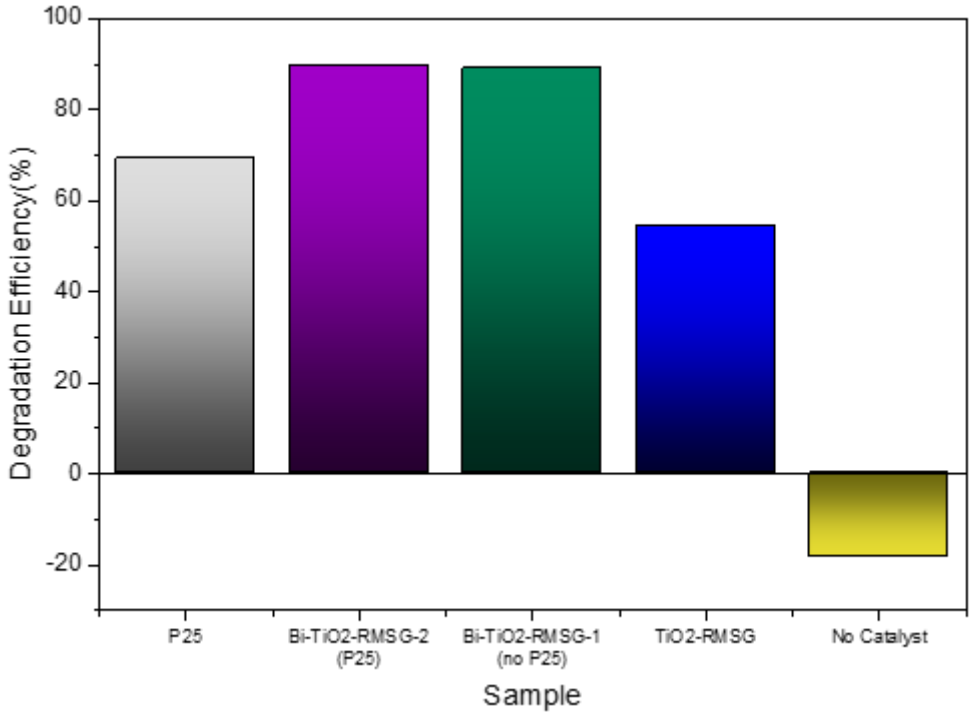

Figure 6.29: Degradation efficiency of the different catalysts studied in this Chapter for the removal of *E. coli* under 410 nm LED irradiation.

These results are very promising and suggest that the synthesised materials are capable of removing bacteria from water under visible light irradiation. These data alone cannot confirm that the materials can consistently remove bacteria to a greater extent than P25 TiO_2, given that uncertainties can be large with biological systems, but one positive result which can be confidently stated is that the materials are photocatalytically active under these conditions. Each material was tested both in the dark and under the light, and for every test, the dark controls showed no significant removal of bacteria, or sometimes even an increase in bacteria, relative to the trial under 410 nm light. We can conjecture in this case that any significant fall in the bacterial colony counts for the 410 nm irradiated samples is due to photocatalysis and not purely a natural decline in viability of the *E.coli* over time.

Following these preliminary tests which suggest the catalysts can indeed act to inactivate bacteria in water, further studies were conducted to investigate the effect of the treatment on more microbial contaminants. For these studies, spores of bacterium *Geobacillus stearothermophilus* and the bacteriophage virus T4 were used to spike the test water in the same way the *E.coli* had been previously.

Geobacillus stearothermophilus was chosen as a surrogate for Cryptosporidium oocysts, as the spores formed are extremely hardy and difficult to remove by traditional treatment methods. *G. stearothermophilus* is a thermophilic, rod-shaped, Gram-positive which forms heat-resistant spores under stress, and is therefore hard to inactive by simple methods such as boiling which can readily remove bacteria such as *E.coli*. These spores themselves are safe to work with, being Biosafety Level 1 (BSL-1, where BSL-4 is the maximum level of contaminant) and thus do not pose a public health concern, and therefore provide a safe alternative for investigating the ability of the treatment method for removing spores and oocysts.

Indeed, these spores present a significant decontamination challenge, as described by Watanabe et al.[288] who studied a range of spores including, *Bacillus coagulans*, *Bacillus subtilis*, *Bacillus cereus*, *Bacillus licheniformis*, and *G. stearothermophilus*, and found that all spores other than *G. stearothermophilus* were easily inactivated by heat treatment. They were able to remove them through a high-pressure treatment with CO_2 (30 MPa of pressure at 95 °C for 120 minutes).

It was found that the photocatalytic treatment as it was set-up had little effect on the spores, and no significant removal was seen relative to the control tests. Data is shown for these studies in Figure 6.30.

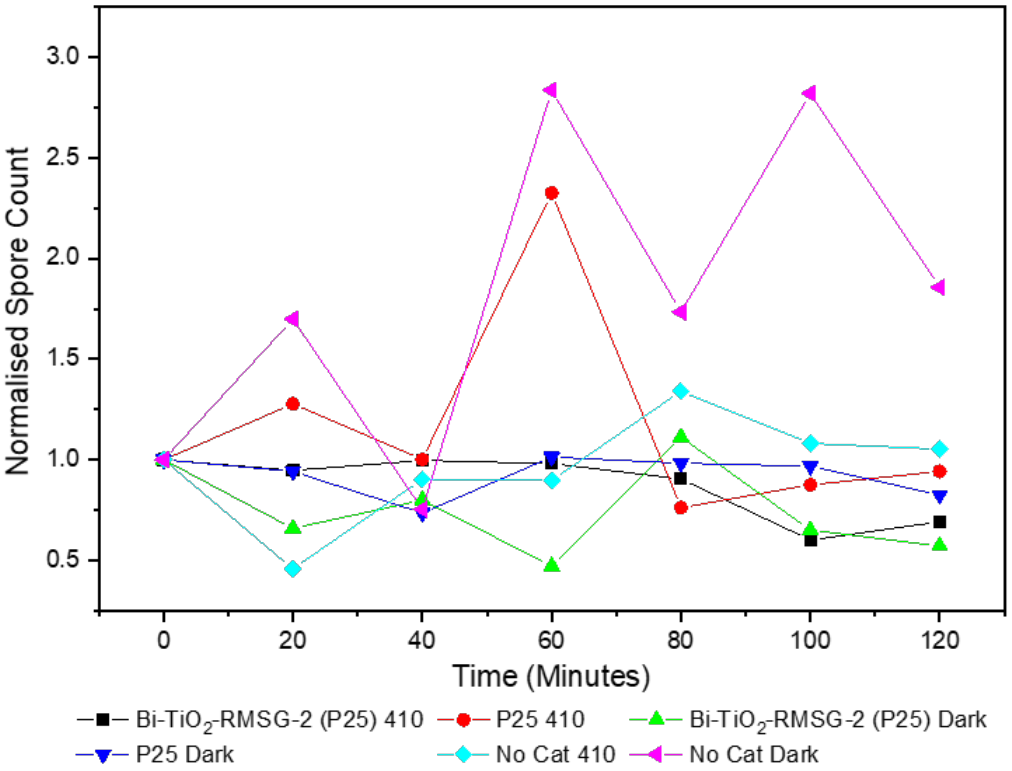

Figure 6.30: Change in normalised concentration of *G. stearothermophilus* spores present during treatment under 410 nm light over the course of 2 hours.

As seen in Figure 6.30, the counts for CFU/mL fluctuate for all test conditions, with no condition presenting a clear improvement to removal of the spores relative to another.

However, several studies have presented results indicating photocatalysis can remove spores and oocysts from water, so the result of this investigation would suggest that the limitation lies in the practical set-up, rather than with the material properties. In other studies, it is often the case that more advanced set-ups are used, such as free nanoparticle suspensions with mechanical stirring or lamps with higher power used. In this case, the visible light LEDs used were operated at a power of around 4 W, which is significantly lower than most in the literature.

Further, this presents an opportunity to explore how to optimise the system for practical usage in rural areas as opposed to industrial scales were more sophisticated set-ups may be employed. It is essential that the material be immobilised, which could be a large reason for the lack of inactivation over this time period and under these lights. Further

studies should be conducted to build on the results presented in Chapter 4 and further optimise the catalyst-substrate system.

If optimisation is possible and can result in an inactivation of such resistant spores, this bismuth-doped TiO_2 material could present an excellent opportunity for not only removing the spores, but the bacteria themselves. The bacteria form spores when stressed as a defence mechanism, which commonly occurs during boiling or exposure to UV light. Therefore, if a low-temperature treatment using visible light can be used, this could prevent the bacteria forming as many spores and thus be easier to remove completely. It should be noted that the process of oxidative inactivation would also lead to some stress, but likely less than when paired with UV light or when boiling.

Following on from the studies with the spores, a further investigation was conducted on the removal of T4 phage from water. In this case, inactivation was observed for the two conditions with photocatalyst present, with the bismuth-doped material performing slightly better after three repeats, as shown in Figure 6.31, where Bi-TiO_2 is used to denote Bi-TiO_2-RMSG-2 (P25).

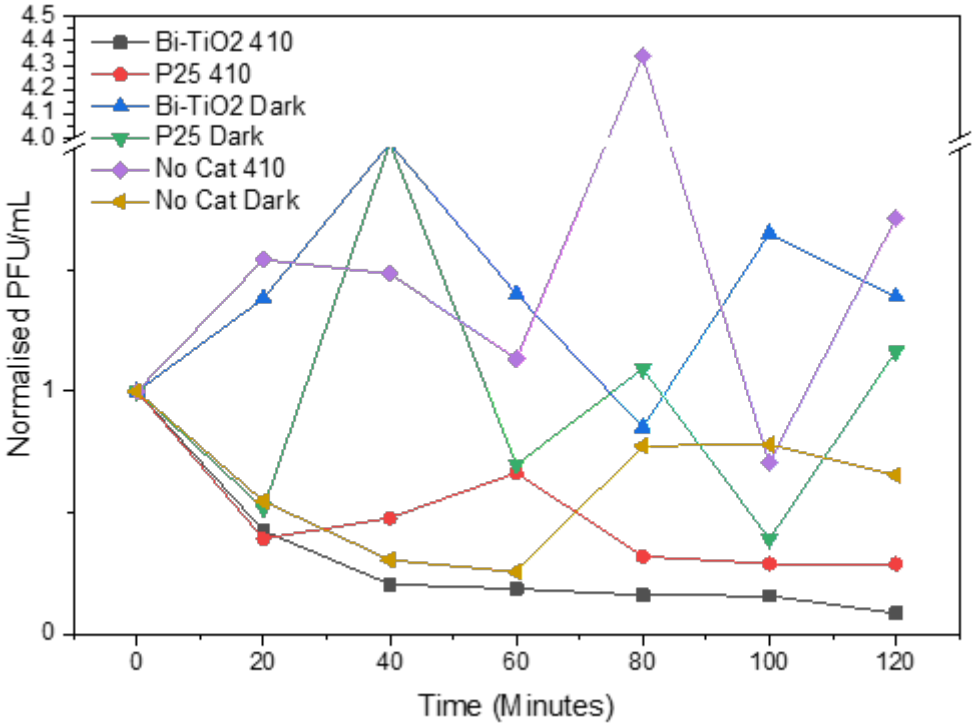

Figure 6.31: Change in concentration of T4 virus under 410 nm by Bi-TiO_2-RMSG-2 (P25).

The above results, excluding the control runs for clarity of seeing the photocatalytic inactivation data, were used to produce linearised changes in T4 plaque counts. This is presented in Figure 6.32.

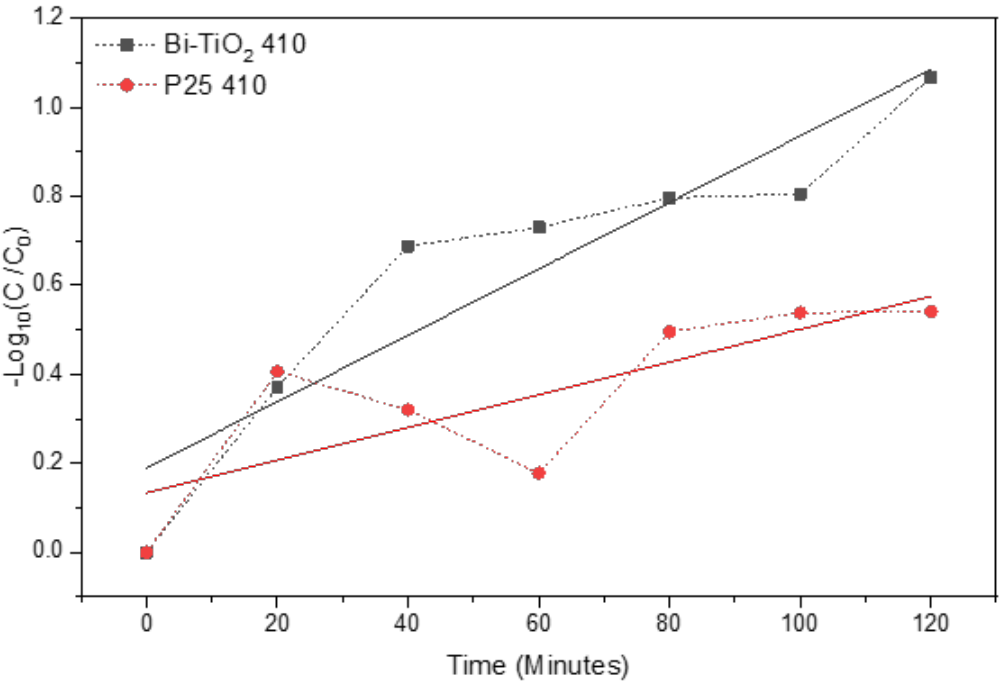

Figure 6.32: Rate of removal of T4 virus under 410 nm by Bi-TiO_2-RMSG-2 (P25) with controls removed.

The degradation efficiencies achieved are also presented for ease of comparison in Figure 6.33.

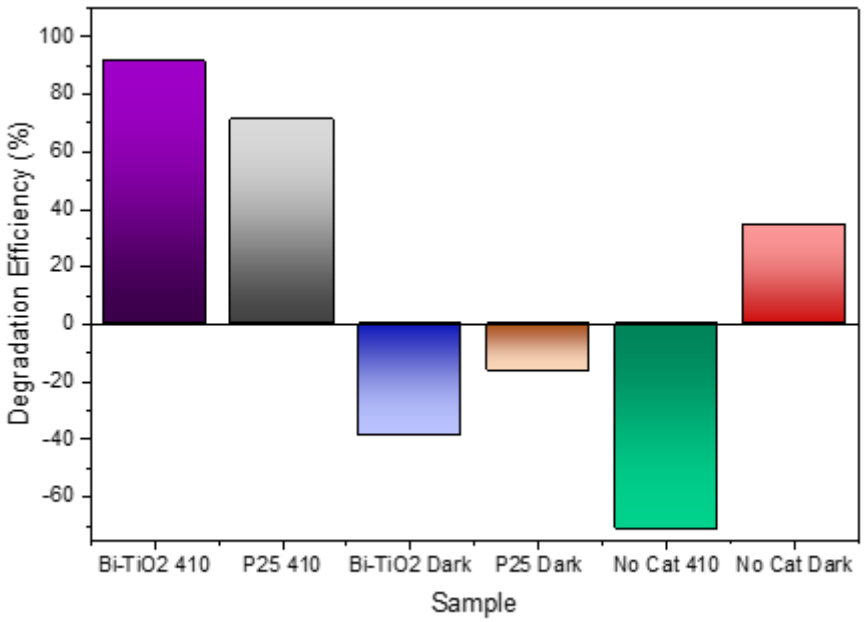

Figure 6.33: Degradation efficiency of the different catalysts studied in this Chapter for the removal of T4 phage virus under 410 nm LED irradiation. Note that the linear fit begins at time = 0 minutes, and does not include the 30 minutes in the dark, such that the rate of just the active photocatalysis is found.

There is a much more clear trend in the data here, in contrast to the spore experiments, which suggests that the photocatalytic treatment was successful to remove the T4 bacteriophage under these conditions. The experiment could certainly benefit from further optimisation, as PFU/mL came down from 10^7 PFU/mL to 10^5 PFU/mL, but this is still higher than desired. Perhaps simply running the treatment for longer could be sufficient, but other optimisations such as adjusting the concentration of catalyst, altering the catalyst-substrate system, occasional agitation (as was found to be successful following field tests, as presented in Chapter 3).

The counts were collected as an average between three plaques during one experiment, the averaged over three repeats (so 9 total plaques to count). Figure 6.34 shows how the measurements were made, with an example of this in practice shown in Figure 6.35, and explained in further detail by the schematic in Figure 6.34.

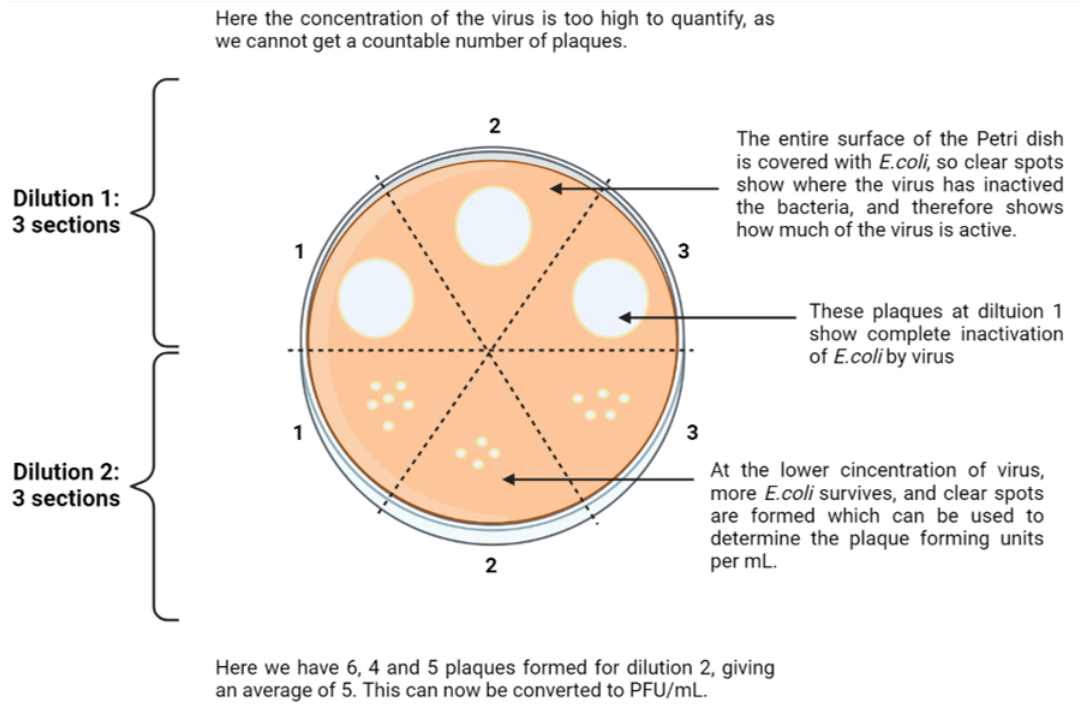

Figure 6.34: Schematic of how the plaque assay method is used to determine the concentration of active virus, by the removal of a host bacteria.

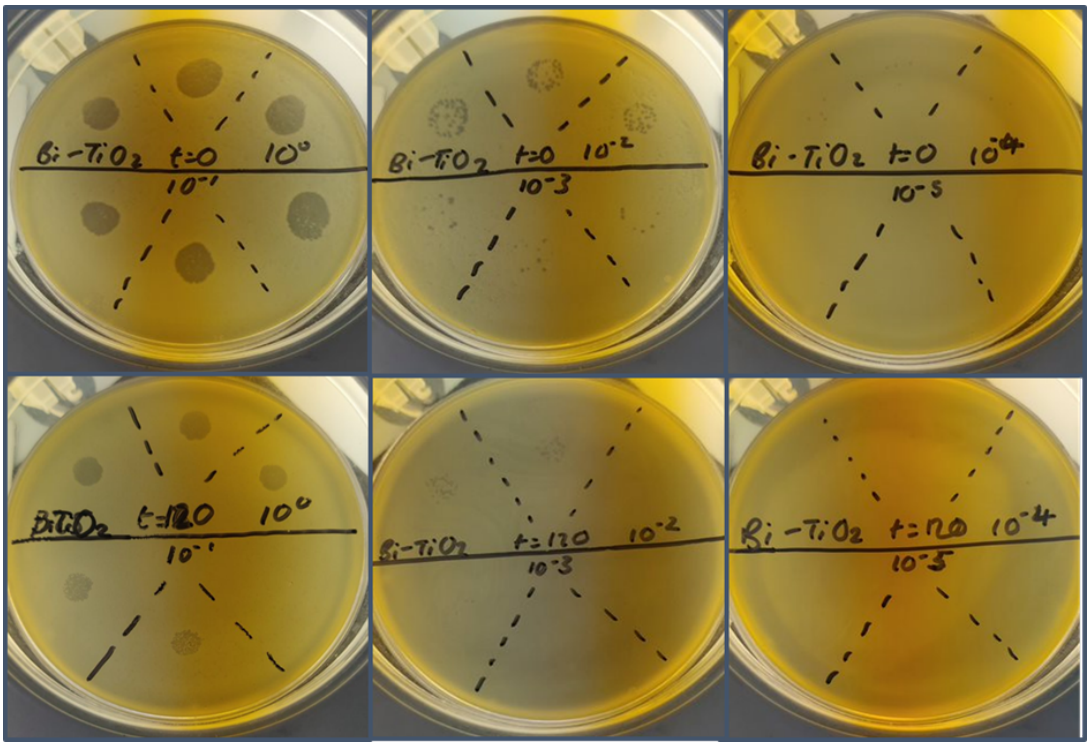

Figure 6.35: Images showing the formation of plaques where T4 viruses multiplied and inactivated the *E.coli* host. Note, in the image, 10^0 indicates no dilution (stock solution), and 10^{-1} is a 10x dilution, 10^{-2} is a 100x dilution, and so on.

Here it can be shown that, for each plate, two dilution samples can be analysed with three drops added per dilution. At the beginning of the experiment (t=0), the T4 phage has killed all *E.coli* present on the agar, and thus we see clear spots of active virus which is too high a concentration to be quantified. For the same time point with further dilution, we see a countable number of plaques forming, with the 1000x dilution being easiest to count, with 6, 8 and 6 spots in each section for the t=0 plate (the 10,000x dilution here has plaque counts 4, 4 and 2, and the 10,0000x dilution has zero plaques). After 120 minutes, we can see there are fewer plaques formed, as the virus has been inactivated and thus less *E.coli* is cleared from the plate.

The first order rate constants of the catalysts were calculated and are presented in Figure 6.36.

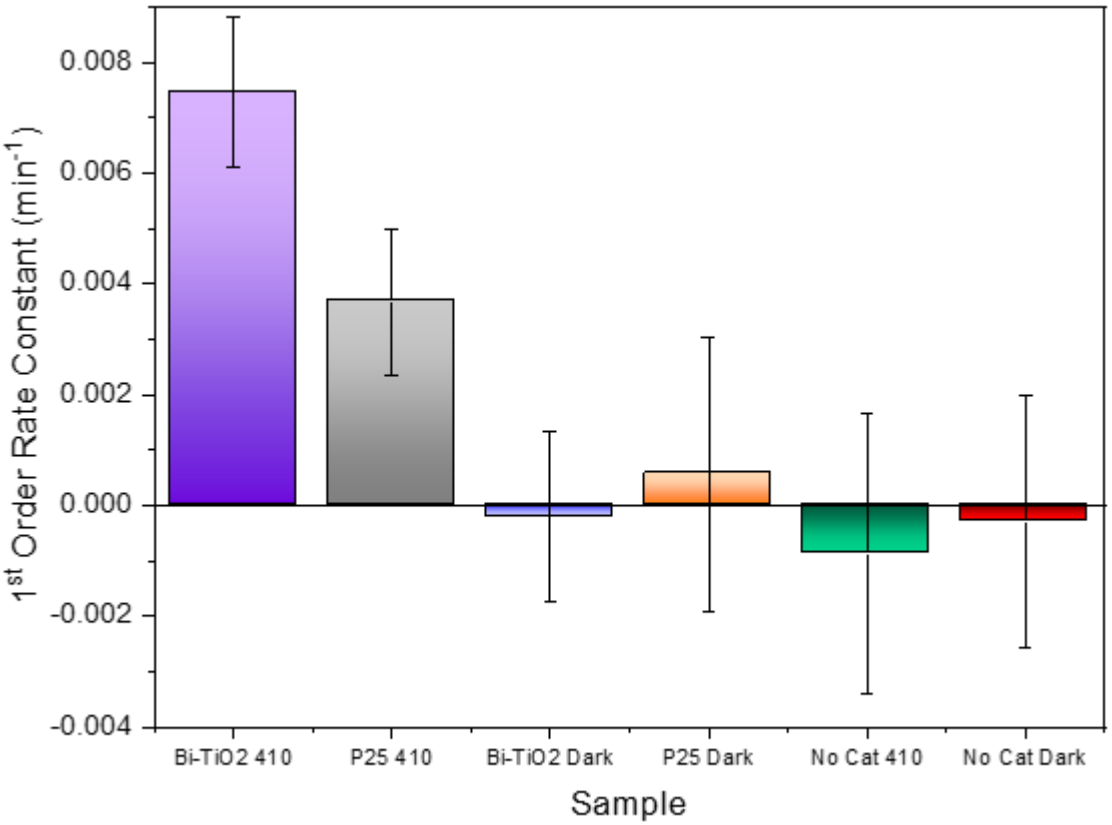

Figure 6.36: First order rate constants under different light sources for the removal of T4 virus by Bi-TiO_2-RMSG-2 (P25).

Though complete removal of neither microbe was achieved under these conditions, combing all of the results of these studies with the chemical tests and results presented across the literature suggests that this material could be a good option for photocatalytic removal of a range of contaminants in water with some optimisations to the practical system employed. This is an exciting opportunity for further studies to focus on.

6.3.10 Mechanistic Studies

As was the case with the ZnFe/TiO_2 materials in Chapter 5, the addition of methanol and purging of oxygen with nitrogen had the greatest effect on the photocatalytic performance relative to the initial measurement, for tests conducted under 410 nm with 4-CP. The additional of tert-butanol only slightly reduced the activity of Bi-TiO_2-RMSG-2 (P25), and seemed to increase the activity for Bi-TiO_2-RMSG-1 (no P25) and TiO_2-RMSG. It would suggest that, for the removal of 4-CP, the mechanism depends mostly on the excited holes and electrons directly, rather than the formation of hydroxyl radicals. The effect of the additional agents on the rate of removal of 4-CP over the course of treatment

is shown in Figures 6.37 to 6.39. Note that the linear fit begins at time = 0 minutes, and does not include the 30 minutes in the dark, such that the rate of just the active photocatalysis is found.

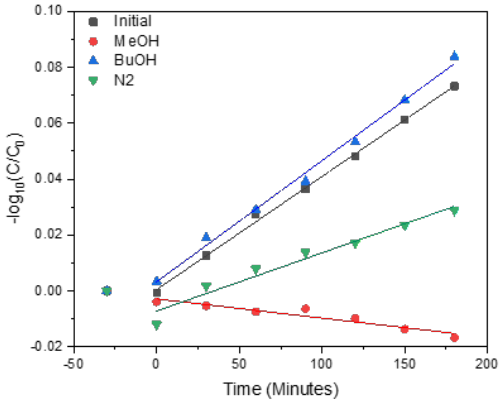

Figure 6.37: Rate of Change in concentration of 4-CP for Bi-TiO_2-RMSG-1 (no P25) under 410 nm irradiation.

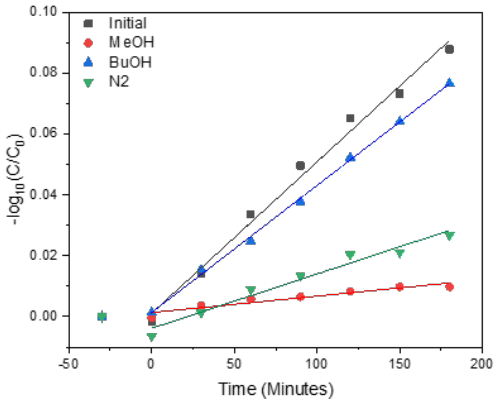

Figure 6.38: Rate of Change in concentration of 4-CP for Bi-TiO_2-RMSG-2 (P25) under 410 nm irradiation.

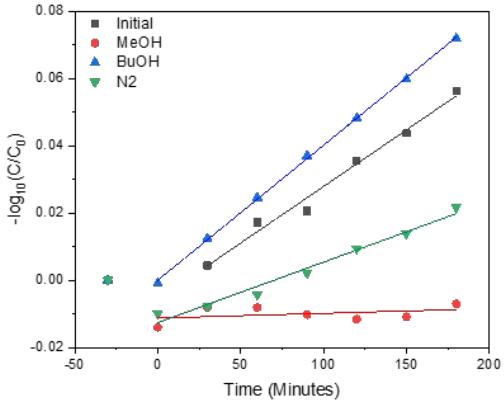

Figure 6.39: Rate of Change in concentration of 4-CP for TiO_2-RMSG under 410 nm irradiation.

Based on these rate plots, the first order rate constants under each condition can be calculated to further demonstrate how the presence of the additional agent changes the photocatalytic behaviour.

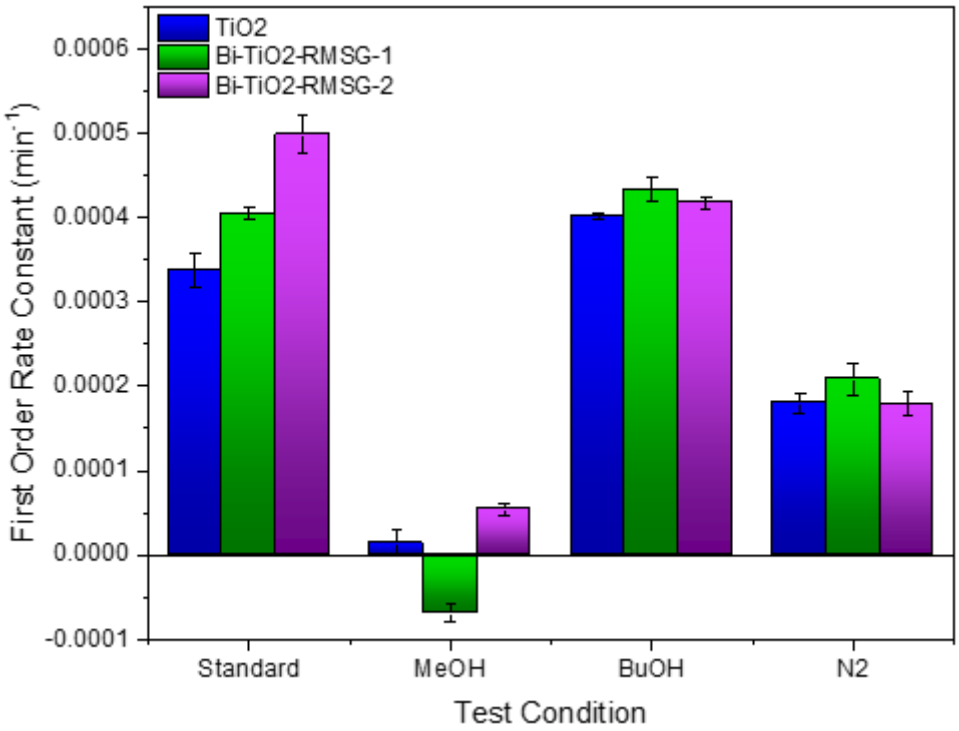

Figure 6.40: The first order rate constants obtained from the slopes presented in Figure 6.37 and 6.38.

6.3.11 Stability Testing

In order to assess the stability, longevity and reusability of the synthesised materials, consecutive repeats of the above methodology for photocatalytic testing were conducted, in the same fashion as presented in Chapter 5 and summarised in Chapter 2, using rhodamine B under 365 nm light. This is extremely important for evaluating the practicality of implementing this material in rural areas for solar water treatment. Results are shown in Figure 6.41, with stars marking the test runs performed following calcination.

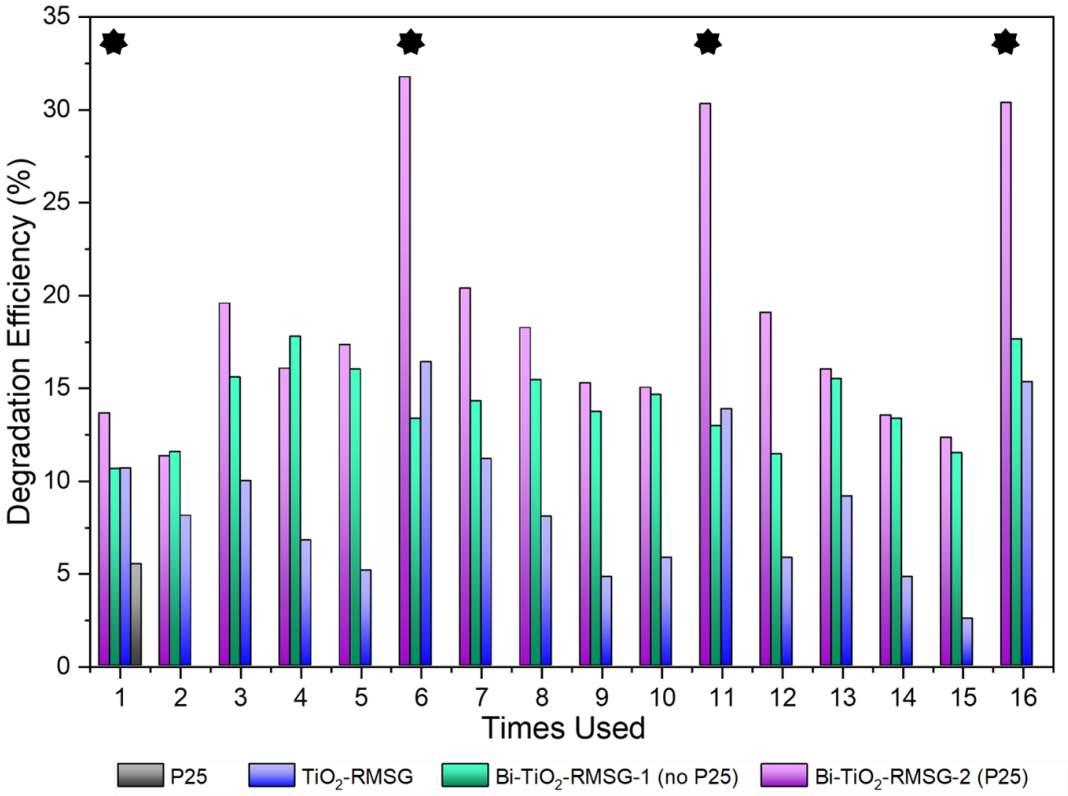

Figure 6.41: Degradation efficiency of the Bi-TiO_2-RMSG-2 (P25) catalyst following repeated use for 3 hour-long treatments to remove 4-CP from water. The stars indicate where tests were performed following calcination.

Surprisingly, the bismuth-modified materials showed a much smaller drop-off in activity with repeated use relative to the ZnFe/TiO_2 materials. This would suggest they can be used consistently without as regular regeneration being required, making them a more practical option.

Rather than a significant fall in activity after the first run, the activity after each use seems to fluctuation around a similar magnitude of percentage degradation, with increased activity also observed after some consecutive runs. This would suggest slight rinsing could be sufficient to extend the life of the catalyst.

It is also interesting to note that the degradation efficiency of the bismuth-modified materials never falls below the activity of P25 at its first use, suggesting that, even with losses and fluctuation over repeated use, this material could still provide significantly better removal of contaminates from water under visible light, and possibly under solar

irradiation depending on weather conditions, relative to P25.

6.4 Conclusions

In this Chapter, different synthesis attempts were presented for the development of bismuth-titania composites. All of these synthesis routes were based on the *in-situ* formation of TiO_2 *via* a reverse micelle sol-gel approach in the presence of bismuth nitrate.

These composite materials outperformed those presented in Chapter 5 under all lights studied, and appeared more robust and long-lasting, as well as following a faster synthesis relative to that for ZnFeO-R-2. However, these materials still did not lead to an overall improvement relative to P25 TiO_2 under the whole solar spectrum. It should be noted here that all testing was performed under simulated solar light, rather than the real-world conditions that could be used for testing in Chapter 3. Due to this, it is not possible to conclusively state which material is the best overall for use in rural areas when considering ease of preparation, longevity and efficacy, though it can be confidently stated that this material shows a significant improvement for visible light performance.

As in Chapter 5, the materials studied in this Chapter where characterised using XRD, ICP-OES, SEM, XPS, DRS and Mott-Schottky analysis. These techniques combined together helped to elucidate the chemical composition of the materials produced, and thus gain further insight into their performances. The peaks present in the XRD patterns could be completely assigned as TiO_2 peaks, showing a mixture of rutile and anatase, which may have helped the performance by forming a heterojunction in the same way as P25. This could suggest that the bismuth was taken up as an amorphous coating of the surface as opposed to being fully doped into the lattice. However, it should be noted that this XRD observation would only occur if the doping was not uniform, which seems likely given the variation across the different characterisation techniques.

The XPS data revealed multiple oxidation states of bismuth were present, again suggesting that bismuth titanate had not formed, but a mix of titania with a bismuth material, possibly with an uneven distribution. This can further be supported by the comparison

between compositional analysis via surface techniques (SEM and XPS) and bulk techniques (ICP-OES). ICP-OES data suggested a Ti:Bi ratio of 20:1 for Bi-TiO_2-RMSG-1 (no P25) and 30:1 for Bi-TiO_2-RMSG-2 (P25). In contrast, SEM-EDS and XPS results gave Ti:Bi ratios of roughly 300:1 for both materials, an order of magnitude difference. This suggests that the lower bismuth content on the surface is not representative of the bismuth present within the whole material.

The lack of uniformity in bismuth distribution may be the reason for a heterojunction not being observed in DRS or Mott-Schottky measurements. Finer control of the synthesis conditions may alter this, and provides an opportunity for further study, to investigate whether this fine-tuning of morphology could aid the photocatalytic performance further.

As well as the material characterisations, photocatalytic tests were performed with 4-CP, as well as bacteria, viruses and bacterial spores, which give good insights into the overall performance. It was found that this material could remove the bacteria and viruses studied, as well as the chemical contaminants, but was less effective at removing the more robust bacterial spores. This suggests it could perform very well for removing microbial and chemical contaminants in rural water treatment systems, but that further investigations should be conducted to compare the performance to P25 under real-world conditions.

Finally, a very promising result for this material was the stability observed after repeated use testing. The degradation efficiency did not seem to significantly drop, and the performance was much better in this respect than the materials discussed in Chapter 5. Importantly, the performance of the prepared materials only dropped below the degradation efficiency observed for fresh P25 under the same light source (410 nm) towards the end of a reuse cycle, and always returned to a much higher performance following calcination.

Questions still remain for assessing the best synthesis route for this class of materials, and whether or not a reverse micelle sol-gel approach allows a high enough level of control for producing high-performing photocatalysts. That being said, the investigations performed

in this Chapter show how simple synthesis routes can produce materials with strong visible light performance, and is very motivating for finding a good candidate for water treatment in rural areas.

Chapter 7

Conclusions and Future Work

This Thesis has focused on the ways in which heterogeneous semiconductor photocatalysts can be utilised and enhanced in order to meet the demands of specific contexts; in this case decentralised water treatment in rural India.

Through field work presented in Chapter 3 to act as proof-of-concept tests for simple, solar driven photocatalytic water treatment with immobilised catalysts, it was determined that the presence of photocatalysts can increase bacterial inactivation of real world water samples. This is promising for ensuring drinking water can be delivered more quickly and with a higher extent of contaminants removed, all with a very simple set-up.

Following these tests, areas of improvement were highlighted, mainly with improving catalyst adhesion to a support which would allow easy removal of the catalyst from water with minimal leaching. This was the focus of Chapter 4, which showed that the addition of silica could act as a glue to prevent loss of the catalyst coating. Further, glass chips which were upcycled from used glass bottles show the potential to be an excellent, sustainable support material with little overhead costs.

As well as the practical aspects which had to be improved, chemical modifications were also explored in Chapters 5 and 6 in an attempt to improve photoactivity and utilise more of the solar spectrum. Though the materials used here were only able to improve activity in the visible region, some researchers have had success in improving the photocatalytic activity across the whole solar spectrum[289] or under UV illumination,[290] and

this is exactly what we should hope for when aiming to modify TiO_2. However, not all of these studies include evaluation of the stability, reusability and practicalities of synthesis and reactor set-up (a study by Admadpour et al. on $ZnFe_2O_4/TiO_2$ composites[291] did include some recycling tests, but only 5 cycles were performed). It is also much more practical for photocatalysis to be used in decentralised water treatment systems in rural areas as a form of enhanced SODIS if the nanoparticles must be immobilised on a solid support, not used as a slurry. In many studies, immobilisation is not performed, which will have a significant effect on the catalytic activity, and would alter the results presented.

Further, the synthesis routes used must also be carefully considered. Hydrothermal syntheses can produce excellent results, providing good control over morphology and thus material properties. Hence, many studies use autoclaves during the material development phase of their research, which delivers successful lab-based results, but may not provide an appropriate method for real-world use. In particular, such methods are limited by scalability, costs and access to sophisticated equipment. For some of the most water-stressed regions, this is unlikely to be easily set-up to provide a self-sustaining source of catalyst for household or village scale water treatment.

As of yet, there is no clear front-runner for a material to take solar photocatalysis from the lab to practical use in regions that could massively benefit from it. This only serves to highlight how difficult the task is, in terms of materials chemistry and engineering solutions. It is arguable that, due to the ability of TiO_2 to out-perform materials under solar light with significantly better visible light activities, a good route would be to improve the UV activity of TiO_2 through methods such as preventing charge recombination, and only seek to adjust the optical band gap to adjust visible light activity slightly, such that we don't reduce the driving force of the all-important photoelectrons and photoholes. This was the primary function of the previously developed BTO-TiO_2 material, which performed well but had a synthesis which was not particularly convenient. This motivated the materials developed in Chapter 6, highlighting that a natural step for further work would be to test the best performer, Bi-TiO_2-RMSG-2 (P25), under the same real world conditions used in Chapter 3.

As discussed previously, the Bi-TiO_2-RMSG-2 (P25) material was the best performer of those synthesised for this Thesis, with a straight forward synthesis route. Therefore, the better performance of P25 under idealised laboratory conditions with solar simulation may not translate to the field where the intensity and composition of light reaching the catalyst will vary, as well as the temperature. Hence, it would be pertinent to conduct further testing, and use these results to motivate further optimisation attempts.

The scope for synthetic alterations to further enhance the photocatalytic performance of titania-based composite materials is massive, be that by adjusting parameters such as the temperature and pressure of the synthesis, altering the quantities of reagents and solvents, or in fact changing those reagents and solvents used. The breadth of opportunity for enhancement is also expanded when the modes of improving adhesion to a solid support are further explored. This could prove the most fruitful way to bring us closer to a robust photocatalytic system for water treatment in rural areas, where it could be argued that the practicalities are the limiting factor to installation. Perhaps as researchers, it is time to focus more on the practicalities and implementation aspects to truly begin to start addressing the water crisis and meet SDG 6.

Chapter 8

Published Work

Work published during the completion of this Thesis is listed below:

Substrate and support materials for photocatalysis

V. Porley and N. Robertson, in *Nanostructured Photocatalysts*, ed. R. Boukherroub, S. Ogale and N. Robertson, Elsevier, Cambridge, 2020, ch. 6, 129-171.

Field testing of low-cost titania-based photocatalysts for enhanced solar disinfection (SODIS) in rural India

V. Porley, E. Chatzisymeon, B. C. Meikap, S. Ghosal and N. Robertson, *Environ. Sci.: Water Res. Tehnol.*, 2020, **6**, 809-816

Solar disinfection (SODIS) provides a much underexploited opportunity for researchers in photocatalytic water treatment (PWT)

B. Cowie, V. Porley and N. Robertson, *ACS Catal.*, 2020, **10**, 11779-11782.

Bibliography

[1] WHO, *Drinking-water Fact Sheet*, https://www.who.int/en/news-room/fact-sheets/detail/drinking-water, Accessed 2020-02-03.

[2] UN, *Goal 6: Ensure access to water and sanitation for all*, https://www.un.org/sustainabledevelopment/water-and-sanitation/, Accessed: 2020-05-04.

[3] E. Sanganyado and W. Gwenzi, Antibiotic resistance in drinking water systems: Occurrence, removal, and human health risks, *Science of the Total Environment*, 2019, **669**, 785–797.

[4] M. K. Viršek, M. N. Lovšin, Š. Koren, A. Kržan and M. Peterlin, Microplastics as a vector for the transport of the bacterial fish pathogen species Aeromonas salmonicida, *Marine pollution bulletin*, 2017, **125**, 301–309.

[5] A. A. Koelmans, in *Marine anthropogenic litter*, ed. M. Bergmann, L. Gutaw and M. Klages, Springer, 2015, ch. 11, pp. 309–324.

[6] UN, *Sustainable Development Goals*, https://sustainabledevelopment.un.org/?menu=1300, Accessed 2020-02-03.

[7] N. Pichel, M. Vivar and M. Fuentes, The problem of drinking water access: A review of disinfection technologies with an emphasis on solar treatment methods, *Chemosphere*, 2018, **218**, 1014 – 1030.

[8] WorldBank, *Rural population (% of total population) - India*, https://data.worldbank.org/indicator/SP.RUR.TOTL.ZS?locations=IN, Accessed 2020-04-30.

[9] WaterAid, *The Water Gap - The State of The WOrld's Water*, https://washmatters.wateraid.org/sites/g/files/jkxoof256/files/The%

20Water%20Gap%20State%20of%20Water%20report%20lr%20pages.pdf, Accessed 2020-04-30.

[10] EPA, *Waste Water Technology Fact Sheet - Ultraviolet Disinfection*, url-https://www3.epa.gov/npdes/pubs/uv.pdf, 1999, Accessed 2020-02-03.

[11] EAWAG, *SODIS manual - Guidance on solar water disinfection*, https://www.sodis.ch/methode/anwendung/ausbildungsmaterial/dokumente_material/sodismanual_2016_lr.pdf, Accessed: 2020-05-04.

[12] R. Meierhofer and G. Landolt, Factors supporting the sustained use of solar water disinfection—Experiences from a global promotion and dissemination programme, *Desalination*, 2009, **248**, 144–151.

[13] A. Acra, Z. Raffoul and Y. Karahagopian, *Solar disinfection of drinking water and oral rehydration solutions: guidelines for household application in developing countries*, Illustrated Publications, Beirut, 1984.

[14] A. Rose, S. Roy, V. Abraham, G. Holmgren, K. George, V. Balraj, S. Abraham, J. Muliyil, A. Joseph and G. Kang, Solar disinfection of water for diarrhoeal prevention in southern India, *Archives of disease in childhood*, 2006, **91**, 139–141.

[15] M. Boyle, C. Sichel, P. Fernández-Ibáñez, G. Arias-Quiroz, M. Iriarte-Puná, A. Mercado, E. Ubomba-Jaswa and K. McGuigan, Bactericidal effect of solar water disinfection under real sunlight conditions, *Appl. Environ. Microbiol.*, 2008, **74**, 2997–3001.

[16] E. Ubomba-Jaswa, M. Boyle and K. McGuigan, Journal of Physics: Conference Series, 2008, p. 012003.

[17] K. G. McGuigan, R. M. Conroy, H.-J. Mosler, M. du Preez, E. Ubomba-Jaswa and P. Fernandez-Ibanez, Solar water disinfection (SODIS): a review from bench-top to roof-top, *Journal of hazardous materials*, 2012, **235**, 29–46.

[18] A. Dessie, E. Alemayehu, S. Mekonen, W. Legesse, H. Kloos and A. Ambelu, Solar disinfection: an approach for low-cost household water treatment technology in Southwestern Ethiopia, *Journal of Environmental Health Science and Engineering*, 2014, **12**, 25.

[19] B. Sommer, A. Marino, Y. Solarte, M. Salas, C. Dierolf, C. Valiente, D. Mora, R. Rechsteiner, P. Setter, W. Wirojanagud *et al.*, SODIS- an emerging water treatment process, *AQUA(OXFORD)*, 1997, **46**, 127–137.

[20] P. Borde, K. Elmusharaf, K. G. McGuigan and M. B. Keogh, Community challenges when using large plastic bottles for Solar Energy Disinfection of Water (SODIS), *BMC public health*, 2016, **16**, 931.

[21] W. Heaselgrave, N. Patel, S. Kilvington, S. Kehoe and K. McGuigan, Solar disinfection of poliovirus and Acanthamoeba polyphaga cysts in water–a laboratory study using simulated sunlight, *Letters in applied microbiology*, 2006, **43**, 125–130.

[22] W. Heaselgrave and S. Kilvington, The efficacy of simulated solar disinfection (SODIS) against Ascaris, Giardia, Acanthamoeba, Naegleria, Entamoeba and Cryptosporidium, *Acta tropica*, 2011, **119**, 138–143.

[23] F. Bosshard, K. Riedel, T. Schneider, C. Geiser, M. Bucheli and T. Egli, Protein oxidation and aggregation in UVA-irradiated Escherichia coli cells as signs of accelerated cellular senescence, *Environmental microbiology*, 2010, **12**, 2931–2945.

[24] A. Villanueva, Photosensitization of bacteria to visible light by meso-substituted porphyrins, *J. Braz. Chem. Soc*, 1995, **6**, 123–125.

[25] A.-G. Rincón and C. Pulgarin, Field solar E. coli inactivation in the absence and presence of TiO2: is UV solar dose an appropriate parameter for standardization of water solar disinfection?, *Solar Energy*, 2004, **77**, 635–648.

[26] E. Ubomba-Jaswa, C. Navntoft, M. I. Polo-lópez, P. Fernández-Ibáñez and K. G. McGuigan, Solar disinfection of drinking water (SODIS): an investigation of the effect of UV-A dose on inactivation efficiency, *Photochemical and Photobiological Sciences*, 2008, **8**, 587–595.

[27] P. M. Oates, P. Shanahan and M. F. Polz, Solar disinfection (SODIS): simulation of solar radiation for global assessment and application for point-of-use water treatment in Haiti, *Water Research*, 2003, **37**, 47–54.

[28] F. Sciacca, J. A. Rengifo-Herrera, J. Wéthé and C. Pulgarin, Dramatic enhancement of solar disinfection (SODIS) of wild Salmonella sp. in PET bottles by H2O2

addition on natural water of Burkina Faso containing dissolved iron, *Chemosphere*, 2010, **78**, 1186–1191.

[29] A.-G. Rincon and C. Pulgarin, Bactericidal action of illuminated TiO2 on pure Escherichia coli and natural bacterial consortia: post-irradiation events in the dark and assessment of the effective disinfection time, *Applied Catalysis B: Environmental*, 2004, **49**, 99–112.

[30] M. Wegelin, S. Canonica, K. Mechsner, T. Fleischmann, F. Pesaro and A. Metzler, Solar water disinfection: scope of the process and analysis of radiation experiments, *Aqua*, 1994, **43**, 154–169.

[31] K. McGuigan, T. Joyce, R. Conroy, J. Gillespie and M. Elmore-Meegan, Solar disinfection of drinking water contained in transparent plastic bottles: characterizing the bacterial inactivation process, *Journal of applied microbiology*, 1998, **84**, 1138–1148.

[32] J. Asiimwe, B. Quilty, C. Muyanja and K. McGuigan, Field comparison of solar water disinfection (SODIS) efficacy between glass and polyethylene terephalate (PET) plastic bottles under sub-Saharan weather conditions, *Journal of water and health*, 2013, **11**, 729–737.

[33] C. Z. Yang, S. I. Yaniger, V. C. Jordan, D. J. Klein and G. D. Bittner, Most plastic products release estrogenic chemicals: a potential health problem that can be solved, *Environmental Health Perspectives*, 2011, **119**, 989.

[34] WHO, *Guidelines for drinking-water quality - chemical fact sheets - Antimony*, https://www.who.int/water_sanitation_health/dwq/chemicals/antimonysum.pdf, Accessed: 2020-05-04.

[35] P. Westerhoff, P. Prapaipong, E. Shock and A. Hillaireau, Antimony leaching from polyethylene terephthalate (PET) plastic used for bottled drinking water, *Water Research*, 2008, **42**, 551–556.

[36] E. M. Aghaee, M. Alimohammadi, R. Nabizadeh, S. Naseri, A. H. Mahvi, K. Yaghmaeian, H. Aslani, S. Nazmara, B. Mahmoudi, M. Ghani *et al.*, Effects of storage time and temperature on the antimony and some trace element release from

polyethylene terephthalate (PET) into the bottled drinking water, *Journal of Environmental Health Science and Engineering*, 2014, **12**, 133.

[37] E. Diamanti-Kandarakis, J.-P. Bourguignon, L. C. Giudice, R. Hauser, G. S. Prins, A. M. Soto, R. T. Zoeller and A. C. Gore, Endocrine-disrupting chemicals: an Endocrine Society scientific statement, *Endocrine reviews*, 2009, **30**, 293–342.

[38] C. Brede, P. Fjeldal, I. Skjevrak and H. Herikstad, Increased migration levels of bisphenol A from polycarbonate baby bottles after dishwashing, boiling and brushing, *Food Additives & Contaminants*, 2003, **20**, 684–689.

[39] M. B. Keogh, M. Castro-Alférez, M. Polo-López, I. F. Calderero, Y. Al-Eryani, C. Joseph-Titus, B. Sawant, R. Dhodapkar, C. Mathur, K. G. McGuigan *et al.*, Capability of 19-L polycarbonate plastic water cooler containers for efficient solar water disinfection (SODIS): Field case studies in India, Bahrain and Spain, *Solar Energy*, 2015, **116**, 1–11.

[40] EFSA, Scientific opinion on the risks to public health related to the presence of bisphenol A (BPA) in foodstuffs., *EFSA Journal*, 2015, **13**, 3978.

[41] M. Wegelin, S. Canonica, C. Alder, D. Marazuela, M.-F. Suter, T. D. Bucheli, O. Haefliger, R. Zenobi, K. McGuigan, M. Kelly *et al.*, Does sunlight change the material and content of polyethylene terephthalate (PET) bottles?, *Journal of Water Supply: Research and Technology—AQUA*, 2001, **50**, 125–135.

[42] P. Schmid, M. Kohler, R. Meierhofer, S. Luzi and M. Wegelin, Does the reuse of PET bottles during solar water disinfection pose a health risk due to the migration of plasticisers and other chemicals into the water?, *Water research*, 2008, **42**, 5054–5060.

[43] E. Ubomba-Jaswa, P. Fernández-Ibáñez and K. G. McGuigan, A preliminary Ames fluctuation assay assessment of the genotoxicity of drinking water that has been solar disinfected in polyethylene terephthalate (PET) bottles, *Journal of water and health*, 2010, **8**, 712–719.

[44] H. Gómez-Couso, M. Fontán-Sainz, K. G. McGuigan and E. Ares-Mazáz, Effect of the radiation intensity, water turbidity and exposure time on the survival of Cryp-

tosporidium during simulated solar disinfection of drinking water, *Acta Tropica*, 2009, **112**, 43–48.

[45] T. Joyce, K. McGuigan, M. Elmore-Meegan and R. Conroy, Inactivation of fecal bacteria in drinking water by solar heating., *Appl. Environ. Microbiol.*, 1996, **62**, 399–402.

[46] E. Ubomba-Jaswa, P. Fernández-Ibáñez, C. Navntoft, M. I. Polo-López and K. G. McGuigan, Investigating the microbial inactivation efficiency of a 25 L batch solar disinfection (SODIS) reactor enhanced with a compound parabolic collector (CPC) for household use, *Journal of Chemical Technology & Biotechnology*, 2010, **85**, 1028–1037.

[47] K. G. McGuigan, P. Samaiyar, M. du Preez and R. M. Conroy, High compliance randomized controlled field trial of solar disinfection of drinking water and its impact on childhood diarrhea in rural Cambodia, *Environmental science & technology*, 2011, **45**, 7862–7867.

[48] B. D. Bitew, Y. K. Gete, G. A. Biks and T. T. Adafrie, Barriers and Enabling Factors Associated with the Implementation of Household Solar Water Disinfection: A Qualitative Study in Northwest Ethiopia, *The American Journal of Tropical Medicine and Hygiene*, 2020, **102**, 458–467.

[49] N. N. Martínez, J. M. Ribera, S. Hausmann-Muela, M. Cevallos, S. M. Hartinger, A. Christen and D. Mäusezahl, The Meanings of Water: Socio-Cultural Perceptions of Solar Disinfected (SODIS) Drinking Water in Bolivia and Implications for its Uptake, *Water*, 2020, **12**, 442.

[50] M. D. Sobsey, C. E. Stauber, L. M. Casanova, J. M. Brown and M. A. Elliott, Point of use household drinking water filtration: a practical, effective solution for providing sustained access to safe drinking water in the developing world, *Environmental science & technology*, 2008, **42**, 4261–4267.

[51] A.-M. Altherr, H.-J. Mosler, R. Tobias and F. Butera, Attitudinal and relational factors predicting the use of solar water disinfection: a field study in Nicaragua, *Health Education & Behavior*, 2008, **35**, 207–220.

[52] Á. García-Gil, R. A. García-Muñoz, K. G. McGuigan and J. Marugán, Solar Water Disinfection to produce safe drinking water: A review of parameters, enhancements, and modelling approaches to make SODIS faster and safer, *Molecules*, 2021, **26**, 3431.

[53] A. Tamas and H.-J. Mosler, Why do people stop treating contaminated drinking water with solar water disinfection (SODIS)?, *Health education & behavior*, 2011, **38**, 357–366.

[54] W. E. Oswald, A. G. Lescano, C. Bern, M. M. Calderon, L. Cabrera and R. H. Gilman, Fecal contamination of drinking water within peri-urban households, Lima, Peru, *The American journal of tropical medicine and hygiene*, 2007, **77**, 699–704.

[55] S. K. Mani, R. Kanjur, I. S. B. Singh and R. H. Reed, Comparative effectiveness of solar disinfection using small-scale batch reactors with reflective, absorptive and transmissive rear surfaces, *Water research*, 2006, **40**, 721–727.

[56] M. Polo-López, P. Fernández-Ibáñez, E. Ubomba-Jaswa, C. Navntoft, I. García-Fernández, P. Dunlop, M. Schmid, J. Byrne and K. G. McGuigan, Elimination of water pathogens with solar radiation using an automated sequential batch CPC reactor, *Journal of hazardous materials*, 2011, **196**, 16–21.

[57] A. S. Harding and K. J. Schwab, Using limes and synthetic psoralens to enhance solar disinfection of water (SODIS): a laboratory evaluation with norovirus, Escherichia coli, and MS2, *The American journal of tropical medicine and hygiene*, 2012, **86**, 566–572.

[58] M. B. Fisher, C. R. Keenan, K. L. Nelson and B. M. Voelker, Speeding up solar disinfection (SODIS): effects of hydrogen peroxide, temperature, pH, and copper plus ascorbate on the photoinactivation of E. coli, *Journal of Water and Health*, 2008, **6**, 35–51.

[59] N. J. Ragab-Depre, Water disinfection with the hydrogen peroxide-ascorbic acid-copper (II) system., *Appl. Environ. Microbiol.*, 1982, **44**, 555–560.

[60] R. Reed, Solar inactivation of faecal bacteria in water: the critical role of oxygen, *Letters in Applied Microbiology*, 1997, **24**, 276–280.

[61] P. H. Gleick, Water and energy, *Annu. Rev. Energ. Env.*, 1994, **19**, 267–299.

[62] C. A. Scott, S. A. Pierce, M. J. Pasqualetti, A. L. Jones, B. E. Montz and J. H. Hoover, Policy and institutional dimensions of the water–energy nexus, *Energy Policy*, 2011, **39**, 6622–6630.

[63] A. M. R. Carrillo and C. Frei, Water: A key resource in energy production, *Energy Policy*, 2009, **37**, 4303–4312.

[64] J. A. Ibáñez, M. I. Litter and R. A. Pizarro, Photocatalytic bactericidal effect of TiO2 on Enterobacter cloacae: Comparative study with other Gram (-) bacteria, *J. Photoch. Photobio A*, 2003, **157**, 81–85.

[65] M. Gratzel, *Energy Resources Through Photochemistry and Catalysis*, Academic Press, New York, 1984, p. 217.

[66] H. Yamashita, M. Takeuchi, M. Anpo and H. Nalwa, *Encyclopedia of Nanoscience and Nanotechnology*, American Scientific Publishers, California, 2004, vol. 9, p. 669.

[67] J. Schneider, M. Matsuoka, M. Takeuchi, J. Zhang, Y. Horiuchi, M. Anpo and D. W. Bahnemann, Understanding TiO2 photocatalysis: mechanisms and materials, *Chem. Rev.*, 2014, **114**, 9919–9986.

[68] D. B. Miklos, C. Remy, M. Jekel, K. G. Linden, J. E. Drewes and U. Hübner, Evaluation of advanced oxidation processes for water and wastewater treatment–A critical review, *Water Res.*, 2018, **139**, 118–131.

[69] J. Marugán, J. Aguado, W. Gernjak and S. Malato, Solar photocatalytic degradation of dichloroacetic acid with silica-supported titania at pilot-plant scale, *Catal. Today*, 2007, **129**, 59–68.

[70] H. Yamashita, M. Takeuchi, M. Anpo and H. Nalwa, *Encyclopedia of Nanoscience and Nanotechnology*, American Scientific Publishers, California, 2004, vol. 6, p. 505.

[71] N. Serpone, D. Lawless, R. Khairutdinov and E. Pelizzetti, Subnanosecond relaxation dynamics in TiO2 colloidal sols (particle sizes Rp= 1.0-13.4 nm). Relevance to heterogeneous photocatalysis, *J. Phys. Chem.*, 1995, **99**, 16655–16661.

[72] S. Leytner and J. T. Hupp, Evaluation of the energetics of electron trap states at the nanocrystalline titanium dioxide/aqueous solution interface via time-resolved photoacoustic spectroscopy, *Chem. Phys. Lett.*, 2000, **330**, 231–236.

[73] Z. Huang, P.-C. Maness, D. M. Blake, E. J. Wolfrum, S. L. Smolinski and W. A. Jacoby, Bactericidal mode of titanium dioxide photocatalysis, *J. Photoch. Photobio A*, 2000, **130**, 163–170.

[74] R. Fagan, D. E. McCormack, D. D. Dionysiou and S. C. Pillai, A review of solar and visible light active TiO2 photocatalysis for treating bacteria, cyanotoxins and contaminants of emerging concern, *Mat. Sci. Semicon. Proc.*, 2016, **42**, 2–14.

[75] J. Podporska-Carroll, E. Panaitescu, B. Quilty, L. Wang, L. Menon and S. C. Pillai, Antimicrobial properties of highly efficient photocatalytic TiO2 nanotubes, *Appl. Catal. B-Environ.*, 2015, **176**, 70–75.

[76] Y. Wang, Q. Wang, X. Zhan, F. Wang, M. Safdar and J. He, Visible light driven type II heterostructures and their enhanced photocatalysis properties: a review, *Nanoscale*, 2013, **5**, 8326–8339.

[77] M. A. Albrecht, C. W. Evans and C. L. Raston, Green chemistry and the health implications of nanoparticles, *Green chemistry*, 2006, **8**, 417–432.

[78] H. Liu, L. Ma, J. Zhao, J. Liu, J. Yan, J. Ruan and F. Hong, Biochemical toxicity of nano-anatase TiO2 particles in mice, *Biological trace element research*, 2009, **129**, 170–180.

[79] L. Gonzalez, L. C. Thomassen, G. Plas, V. Rabolli, D. Napierska, I. Decordier, M. Roelants, P. H. Hoet, C. E. Kirschhock, J. A. Martens *et al.*, Exploring the aneugenic and clastogenic potential in the nanosize range: A549 human lung carcinoma cells and amorphous monodisperse silica nanoparticles as models, *Nanotoxicology*, 2010, **4**, 382–395.

[80] S. K. Loeb, P. J. Alvarez, J. A. Brame, E. L. Cates, W. Choi, J. Crittenden, D. D. Dionysiou, Q. Li, G. Li-Puma, X. Quan *et al.*, The technology horizon for photocatalytic water treatment: sunrise or sunset?, *Environ. Sci. Technol.*, 2019, **53**, 2937–2947.

[81] N. Vela, M. Calín, M. J. Yáñez-Gascón, I. Garrido, G. Pérez-Lucas, J. Fenoll and S. Navarro, Photocatalytic oxidation of six endocrine disruptor chemicals in wastewater using ZnO at pilot plant scale under natural sunlight, *Environmental Science and Pollution Research*, 2018, **25**, 34995–35007.

[82] J.-M. Herrmann, J. Matos, J. Disdier, C. Guillard, J. Laine, S. Malato and J. Blanco, Solar photocatalytic degradation of 4-chlorophenol using the synergistic effect between titania and activated carbon in aqueous suspension, *Catalysis Today*, 1999, **54**, 255–265.

[83] A. Vidal, A. Dıaz, A. El Hraiki, M. Romero, I. Muguruza, F. Senhaji and J. González, Solar photocatalysis for detoxification and disinfection of contaminated water: pilot plant studies, *Catalysis Today*, 1999, **54**, 283–290.

[84] S. Malato, J. Blanco, J. Cáceres, A. Fernández-Alba, A. Agüera and A. Rodrıguez, Photocatalytic treatment of water-soluble pesticides by photo-Fenton and TiO2 using solar energy, *Catalysis Today*, 2002, **76**, 209–220.

[85] A.-G. Rincón and C. Pulgarin, Use of coaxial photocatalytic reactor (CAPHORE) in the TiO2 photo-assisted treatment of mixed E. coli and Bacillus sp. and bacterial community present in wastewater, *Catalysis today*, 2005, **101**, 331–344.

[86] S. Gelover, L. A. Gómez, K. Reyes and M. T. Leal, A practical demonstration of water disinfection using TiO2 films and sunlight, *Water research*, 2006, **40**, 3274–3280.

[87] E. Duffy, F. Al Touati, S. Kehoe, O. McLoughlin, L. Gill, W. Gernjak, I. Oller, M. Maldonado, S. Malato, J. Cassidy *et al.*, A novel TiO2-assisted solar photocatalytic batch-process disinfection reactor for the treatment of biological and chemical contaminants in domestic drinking water in developing countries, *Solar Energy*, 2004, **77**, 649–655.

[88] S. Danwittayakul, S. Songngam and S. Sukkasi, Enhanced solar water disinfection using ZnO supported photocatalysts, *Environmental technology*, 2020, **41**, 349–356.

[89] A.-G. Rincón and C. Pulgarin, Solar photolytic and photocatalytic disinfection of water at laboratory and field scale. Effect of the chemical composition of water and

study of the postirradiation events, *Journal of Solar Energy Engineering*, 2007, **129**, 100–110.

[90] J. Zhao, L. Bowman, X. Zhang, V. Vallyathan, S.-H. Young, V. Castranova and M. Ding, Titanium dioxide (TiO2) nanoparticles induce JB6 cell apoptosis through activation of the caspase-8/Bid and mitochondrial pathways, *Journal of Toxicology and Environmental Health, Part A*, 2009, **72**, 1141–1149.

[91] WHO, *Guidelines for drinking-water quality, Fourth Edition including the first adenndum*, https://www.who.int/water_sanitation_health/publications/drinking-water-quality-guidelines-4-including-1st-addendum/en/, Accessed: 2020-04-20.

[92] WHO, *Total dissolved solids in Drinking-water*, https://www.who.int/water_sanitation_health/dwq/chemicals/tds.pdf, Accessed: 2020-04-20.

[93] EMA, *Guideline on the Environmental Risk Assessment of Medicinal Products for Human Use*, https://www.ema.europa.eu/en/documents/scientific-guideline/guideline-environmental-risk-assessment-medicinal-products-human-use-first-versio en.pdf, Accessed: 2020-04-20.

[94] J. C. Espíndola and V. J. Vilar, Innovative light-driven chemical/catalytic reactors towards contaminants of emerging concern mitigation: A review, *Chemical Engineering Journal*, 2020, 124865.

[95] K. Helwig, C. Hunter, M. McNaughtan, J. Roberts and O. Pahl, Ranking prescribed pharmaceuticals in terms of environmental risk: inclusion of hospital data and the importance of regular review, *Environ. Toxicol. Chem.*, 2016, **35**, 1043–1050.

[96] ECWFD, *Priority Substances and Certain Other Pollutants according to Annex II of Directive 2008/105/EC*, http://ec.europa.eu/environment/water/water-framework/priority_substances.htm, Accessed: 2020-04-20.

[97] G. Odling, Z. Y. Pong, G. Gilfillan, C. R. Pulham and N. Robertson, Bismuth titanate modified and immobilized TiO 2 photocatalysts for water purification:

broad pollutant scope, ease of re-use and mechanistic studies, *Environmental Science: Water Research & Technology*, 2018, **4**, 2170–2178.

[98] EU, *Establishing a watch list of substances for Union-wide monitoring in the field of water policy pursuant to Directive 2008/105/EC of the European Parliament and of the Council*, https://eur-lex.europa.eu/eli/dec_impl/2015/495/oj, Accessed: 2020-05-12.

[99] EU, *Establishing a watch list of substances for Union-wide monitoring in the field of water policy pursuant to Directive 2008/105/EC of the European Parliament and of the Council and repealing Commission Implementing Decision (EU) 2015/495*, https://eur-lex.europa.eu/eli/dec_impl/2018/840/oj, Accessed: 2020-05-12.

[100] W. F. Von Oettingen, The toxicity and potential dangers of aliphatic and aromatic hydrocarbons, *The Yale Journal of Biology and Medicine*, 1942, **15**, 167.

[101] C. for Disease Control and Prevention", *Organic Solvents*, https://www.cdc.gov/niosh/topics/organsolv/default.html, Accessed 2020-07-02.

[102] D. R. Joshi and N. Adhikari, An overview on common organic solvents and their toxicity, *Journal of Pharmaceutical Research International*, 2019, 1–18.

[103] WHO, *Ten threats to global health in 2019*, https://www.who.int/news-room/feature-stories/ten-threats-to-global-health-in-2019, Accessed: 2020-04-16.

[104] WHO, *Guidelines for drinking-water quality, Second Edition, Volume 3 - Surveillance and control of community supplies*, https://apps.who.int/iris/bitstream/handle/10665/39989/9241540249_eng.pdf?sequence=1, Accessed: 2020-04-20.

[105] T. J. Silhavy, D. Kahne and S. Walker, The bacterial cell envelope, *Cold Spring Harbor perspectives in biology*, 2010, **2**, a000414.

[106] W. Vollmer, D. Blanot and M. A. De Pedro, Peptidoglycan structure and architecture, *FEMS microbiology reviews*, 2008, **32**, 149–167.

[107] D. Mengin-Lecreulx and B. Lemaitre, Structure and metabolism of peptidoglycan and molecular requirements allowing its detection by the Drosophila innate immune system, *Journal of endotoxin research*, 2005, **11**, 105–111.

[108] J. Mir, J. Morato and F. Ribas, Resistance to chlorine of freshwater bacterial strains, *Journal of applied microbiology*, 1997, **82**, 7–18.

[109] R. Virto, P. Manas, I. Alvarez, S. Condon and J. Raso, Membrane damage and microbial inactivation by chlorine in the absence and presence of a chlorine-demanding substrate, *Appl. Environ. Microbiol.*, 2005, **71**, 5022–5028.

[110] N. Birben, C. Uyguner-Demirel and M. Bekbolet, Photocatalytic removal of microbiological consortium and organic matter in greywater, *Catalysts*, 2016, **6**, 91.

[111] J. Bogdan, J. Zarzyńska and J. Pławińska-Czarnak, Comparison of infectious agents susceptibility to photocatalytic effects of nanosized titanium and zinc oxides: a practical approach, *Nanoscale Res. Lett.*, 2015, **10**, 309.

[112] A. Pal, S. O. Pehkonen, E. Y. Liya and M. B. Ray, Photocatalytic inactivation of Gram-positive and Gram-negative bacteria using fluorescent light, *J. Photoch. Photobio A*, 2007, **186**, 335–341.

[113] WHO, *International Standard for Drinking Water, Third Edition*, https://www.who.int/water_sanitation_health/dwq/2edvol3a.pdf, Accessed: 2020-04-20.

[114] D. Wetzel and R.-J. Fischer, Small acid-soluble spore proteins of Clostridium acetobutylicum are able to protect DNA in vitro and are specifically cleaved by germination protease GPR and spore protease YyaC, *Microbiology*, 2015, **161**, 2098–2109.

[115] M. Berney, H.-U. Weilenmann, A. Simonetti and T. Egli, Efficacy of solar disinfection of Escherichia coli, Shigella flexneri, Salmonella Typhimurium and Vibrio cholerae, *Journal of applied microbiology*, 2006, **101**, 828–836.

[116] J. M. Robertson, P. K. Robertson and L. A. Lawton, A comparison of the effectiveness of TiO2 photocatalysis and UVA photolysis for the destruction of three pathogenic micro-organisms, *Journal of Photochemistry and Photobiology A: Chemistry*, 2005, **175**, 51–56.

[117] S. Kehoe, M. Barer, L. Devlin and K. McGuigan, Batch process solar disinfection is an efficient means of disinfecting drinking water contaminated with Shigella dysenteriae type I, *Letters in applied microbiology*, 2004, **38**, 410–414.

[118] WHO, *Microbial Fact Sheets*, https://www.who.int/water_sanitation_health/dwq/GDW11rev1and2.pdf, Accessed 2020-05-26.

[119] S. Dejung, I. Fuentes, G. Almanza, R. Jarro, L. Navarro, G. Arias, E. Urquieta, A. Torrico, W. Fenandez, M. Iriarte *et al.*, Effect of solar water disinfection (SODIS) on model microorganisms under improved and field SODIS conditions, *Journal of Water Supply: Research and Technology—AQUA*, 2007, **56**, 245–256.

[120] A. G. Cobián Güemes, M. Youle, V. A. Cantú, B. Felts, J. Nulton and F. Rohwer, Viruses as winners in the game of life, *Annual Review of Virology*, 2016, **3**, 197–214.

[121] M. Woolhouse, F. Scott, Z. Hudson, R. Howey and M. Chase-Topping, Human viruses: discovery and emergence, *Philosophical Transactions of the Royal Society B: Biological Sciences*, 2012, **367**, 2864–2871.

[122] A. M. Gall, B. J. Mariñas, Y. Lu and J. L. Shisler, Waterborne viruses: a barrier to safe drinking water, *PLoS pathogens*, 2015, **11**, e1004867.

[123] A. M. Kahler, T. L. Cromeans, J. M. Roberts and V. R. Hill, Effects of source water quality on chlorine inactivation of adenovirus, coxsackievirus, echovirus, and murine norovirus, *Appl. Environ. Microbiol.*, 2010, **76**, 5159–5164.

[124] A. C. Eischeid, J. A. Thurston and K. G. Linden, UV disinfection of adenovirus: present state of the research and future directions, *Critical reviews in environmental science and technology*, 2011, **41**, 1375–1396.

[125] K. D. Mena and C. P. Gerba, in *Reviews of environmental contamination and toxicology*, Springer, 2008, pp. 133–167.

[126] S. C. Jiang, Human adenoviruses in water: occurrence and health implications: a critical review, *Environmental science & technology*, 2006, **40**, 7132–7140.

[127] M. Divizia, R. Gabrieli, D. Donia, A. Macaluso, A. Bosch, S. Guix, G. Sanchez, C. Villena, R. Pinto, L. Palombi *et al.*, Waterborne gastroenteritis outbreak in Albania, *Water Science and Technology*, 2004, **50**, 57–61.

[128] M. Kukkula, P. Arstila, M.-L. Klossner, L. Maunula, C.-H. V. Bonsdorff and P. Jaatinen, Waterborne outbreak of viral gastroenteritis, *Scandinavian journal of infectious diseases*, 1997, **29**, 415–418.

[129] C. Villena, R. Gabrieli, R. Pinto, S. Guix, D. Donia, E. Buonomo, L. Palombi, F. Cenko, S. Bino, A. Bosch *et al.*, A large infantile gastroenteritis outbreak in Albania caused by multiple emerging rotavirus genotypes, *Epidemiology & Infection*, 2003, **131**, 1105–1110.

[130] J. Van Heerden, M. M. Ehlers, W. B. Van Zyl and W. O. Grabow, Incidence of adenoviruses in raw and treated water, *Water Research*, 2003, **37**, 3704–3708.

[131] H. K. Lee and Y. S. Jeong, Comparison of total culturable virus assay and multiplex integrated cell culture-PCR for reliability of waterborne virus detection, *Appl. Environ. Microbiol.*, 2004, **70**, 3632–3636.

[132] C. E. Enriquez, C. J. Hurst and C. P. Gerba, Survival of the enteric adenoviruses 40 and 41 in tap, sea, and waste water, *Water Research*, 1995, **29**, 2548–2553.

[133] J. Lee, K. Zoh and G. Ko, Inactivation and UV disinfection of murine norovirus with TiO2 under various environmental conditions, *Appl. Environ. Microbiol.*, 2008, **74**, 2111–2117.

[134] J. K. Sponseller, J. K. Griffiths and S. Tzipori, The evolution of respiratory Cryptosporidiosis: evidence for transmission by inhalation, *Clinical microbiology reviews*, 2014, **27**, 575–586.

[135] B. Wells, H. Shaw, E. Hotchkiss, J. Gilray, R. Ayton, J. Green, F. Katzer, A. Wells and E. Innes, Prevalence, species identification and genotyping Cryptosporidium from livestock and deer in a catchment in the Cairngorms with a history of a contaminated public water supply, *Parasites & vectors*, 2015, **8**, 66.

[136] J. Samuelson, G. G. Bushkin, A. Chatterjee and P. W. Robbins, Strategies to discover the structural components of cyst and oocyst walls, *Eukaryotic cell*, 2013, **12**, 1578–1587.

[137] Z. Bukhari, T. M. Hargy, J. R. Bolton, B. Dussert and J. L. Clancy, Medium-

pressure UV for oocyst inactivation, *Journal-American Water Works Association*, 1999, **91**, 86–94.

[138] J. Shen, R. Steinbach, J. M. Tobin, M. M. Nakata, M. Bower, M. R. McCoustra, H. Bridle, V. Arrighi and F. Vilela, Photoactive and metal-free polyamide-based polymers for water and wastewater treatment under visible light irradiation, *Applied Catalysis B: Environmental*, 2016, **193**, 226–233.

[139] K. McGuigan, F. Méndez-Hermida, J. Castro-Hermida, E. Ares-Mazás, S. Kehoe, M. Boyle, C. Sichel, P. Fernández-Ibáñez, B. Meyer, S. Ramalingham *et al.*, Batch solar disinfection inactivates oocysts of Cryptosporidium parvum and cysts of Giardia muris in drinking water, *Journal of Applied Microbiology*, 2006, **101**, 453–463.

[140] F. Méndez-Hermida, J. A. Castro-Hermida, E. Ares-Mazás, S. C. Kehoe and K. G. McGuigan, Effect of Batch-Process Solar Disinfection on Survival of Cryptosporidium parvum Oocysts in Drinking Water, *Applied and Environmental Microbiology*, 2005, **71**, 1653–1654.

[141] F. Méndez-Hermida, E. Ares-Mazás, K. G. McGuigan, M. Boyle, C. Sichel and P. Fernández-Ibáñez, Disinfection of drinking water contaminated with Cryptosporidium parvum oocysts under natural sunlight and using the photocatalyst TiO2, *Journal of Photochemistry and Photobiology B: Biology*, 2007, **88**, 105–111.

[142] J. Lonnen, S. Kilvington, S. Kehoe, F. Al-Touati and K. McGuigan, Solar and photocatalytic disinfection of protozoan, fungal and bacterial microbes in drinking water, *Water research*, 2005, **39**, 877–883.

[143] M. N. Babič, N. Gunde-Cimerman, M. Vargha, Z. Tischner, D. Magyar, C. Veríssimo, R. Sabino, C. Viegas, W. Meyer and J. Brandão, Fungal contaminants in drinking water regulation? A tale of ecology, exposure, purification and clinical relevance, *International journal of environmental research and public health*, 2017, **14**, 636.

[144] M. Novak Babič, J. Zupančič, J. Brandão and N. Gunde-Cimerman, Opportunistic Water-Borne Human Pathogenic Filamentous Fungi Unreported from Food, *Microorganisms*, 2018, **6**, 79.

[145] EEC, *COUNCIL DIRECTIVE 98/83/EC of 3 November 1998 on the quality of water intended for human consumption*, http://www.dwi.gov.uk/stakeholders/legislation/eudir98_83_EC.pdf, Accessed: 2020-04-20.

[146] DEFRA, *A Review of Fungi in Drinking Water and the Implications for Human Health*, http://dwi.defra.gov.uk/research/completed-research/reports/DWI70-2-255.pdf, Accessed: 2020-04-20.

[147] V. Pereira, M. Basílio, D. Fernandes, M. Domingues, J. Paiva, M. Benoliel, M. Crespo and M. San Romão, Occurrence of filamentous fungi and yeasts in three different drinking water sources, *Water Research*, 2009, **43**, 3813–3819.

[148] G. Hageskal, A. K. Knutsen, P. Gaustad, G. S. de Hoog and I. Skaar, Diversity and significance of mold species in Norwegian drinking water, *Appl. Environ. Microbiol.*, 2006, **72**, 7586–7593.

[149] V. Patil and B. Borse, Checklist of freshwater mitosporic fungi of India, *International Journal of Bioassays*, 2015, **4**, 4090–4099.

[150] M. N. Babič, P. Zalar, B. Ženko, S. Džeroski and N. Gunde-Cimerman, Yeasts and yeast-like fungi in tap water and groundwater, and their transmission to household appliances, *Fungal Ecology*, 2016, **20**, 30–39.

[151] J. Zupančič, M. N. Babič, P. Zalar and N. Gunde-Cimerman, The black yeast Exophiala dermatitidis and other selected opportunistic human fungal pathogens spread from dishwashers to kitchens, *PLoS One*, 2016, **11**, e0148166.

[152] M. N. Babič, J. Zupančič, N. Gunde-Cimerman, S. De Hoog and P. Zalar, Ecology of the human opportunistic black yeast Exophiala dermatitidis indicates preference for human-made habitats, *Mycopathologia*, 2018, **183**, 201–212.

[153] G. Heinrichs, I. Hübner, C. K. Schmidt, G. S. de Hoog and G. Haase, Analysis of black fungal biofilms occurring at domestic water taps (II): Potential routes of entry, *Mycopathologia*, 2013, **175**, 399–412.

[154] M. Najafzadeh, S. Dolatabadi, M. S. Keisari, A. Naseri, P. Feng and G. De Hoog, Detection and identification of opportunistic Exophiala species using the rolling

circle amplification of ribosomal internal transcribed spacers, *Journal of microbiological methods*, 2013, **94**, 338–342.

[155] H. Madrid, M. Hernandez-Restrepo, J. Gené, J. Cano, J. Guarro and V. Silva, New and interesting chaetothyrialean fungi from Spain, *Mycological progress*, 2016, **15**, 1179–1201.

[156] G. Tripathy and P. Chowdhry, Study of filamentous fungal flora from polluted river Yamuna water from Delhi catchment areas as a basis to determine water pollution, *World Journal of Pharmacy and Pharmacutical Sciences*, 2017, **6**, 534–541.

[157] H. Oliveira, C. Santos, R. R. M. Paterson, N. B. Gusmão and N. Lima, Fungi from a groundwater-fed drinking water supply system in Brazil, *International journal of environmental research and public health*, 2016, **13**, 304.

[158] H. M. Al-Gabr, T. Zheng and X. Yu, in *Reviews of Environmental Contamination and Toxicology Volume 228*, Springer, 2014, pp. 121–139.

[159] M. A. Hossain, M. S. Ahmed and M. A. Ghannoum, Attributes of Stachybotrys chartarum and its association with human disease, *Journal of Allergy and Clinical Immunology*, 2004, **113**, 200–208.

[160] G. F. Schiavano, L. Parlani, M. Sisti, G. Sebastianelli and G. Brandi, Occurrence of fungi in dialysis water and dialysate from eight haemodialysis units in central Italy, *Journal of Hospital Infection*, 2014, **86**, 194–200.

[161] W. G. Abdalla *et al.*, Isolation and Identification of Water-borne Fungi from Poultry Farms in Khartoum State, Sudan, *Sudan J. Vet. Res*, 2017, **32**, 35–38.

[162] V. Pereira, R. Marques, M. Marques, M. Benoliel and M. B. Crespo, Free chlorine inactivation of fungi in drinking water sources, *Water research*, 2013, **47**, 517–523.

[163] S. Ifuku, Chitin and chitosan nanofibers: Preparation and chemical modifications, *Molecules*, 2014, **19**, 18367–18380.

[164] T. P. d. Mello, A. C. Aor, D. d. S. Gonçalves, S. H. Seabra, M. H. Branquinha and A. L. S. d. Santos, Scedosporium apiospermum, Scedosporium aurantiacum, Scedosporium minutisporum and Lomentospora prolificans: a comparative study

of surface molecules produced by conidial and germinated conidial cells, *Memórias do Instituto Oswaldo Cruz*, 2018, **113**, e180102.

[165] D. Rynga, M. R. Capoor, S. Varshney, M. Naik, V. Gupta *et al.*, Scedosporium apiospermum, an emerging pathogen in India: Case series and review of literature, *Indian Journal of Pathology and Microbiology*, 2017, **60**, 550.

[166] G. San-Blas, O. Guanipa, B. Moreno, S. Pekerar and F. San-Blas, Cladosporium carrionii and Hormoconis resinae (C. resinae): cell wall and melanin studies, *Current microbiology*, 1996, **32**, 11–16.

[167] L. Durrell, The composition and structure of walls of dark fungus spores, *Mycopathologia et mycologia applicata*, 1964, **23**, 339–345.

[168] W. Heaselgrave and S. Kilvington, Antimicrobial activity of simulated solar disinfection against bacterial, fungal, and protozoan pathogens and its enhancement by riboflavin, *Appl. Environ. Microbiol.*, 2010, **76**, 6010–6012.

[169] T. Z. Mitakakis, T. J. O'Meara and E. R. Tovey, The effect of sunlight on allergen release from spores of the fungus Alternaria, *Grana*, 2003, **42**, 43–46.

[170] C. Sichel, M. De Cara, J. Tello, J. Blanco and P. Fernández-Ibáñez, Solar photocatalytic disinfection of agricultural pathogenic fungi: Fusarium species, *Applied Catalysis B: Environmental*, 2007, **74**, 152–160.

[171] L. Kirchhoff, M. Olsowski, P.-M. Rath and J. Steinmann, Exophiala dermatitidis: Key issues of an opportunistic fungal pathogen, *Virulence*, 2019, **10**, 984–998.

[172] W. Bank, *Waterlife: Improving Access to Safe Drinking Water in India*, https://documents1.worldbank.org/curated/en/586371495104964514/pdf/115133-WP-P152203-PUBLIC-17-5-2017-12-28-1-WaterlifeCaseApril.pdf, Accessed 2022-06-06.

[173] C. P. C. Board, *Status of Water Treatment Plants in India*, https://cpcb.nic.in/openpdffile.php?id=UmVwb3J0RmlsZXMvTmV3SXRlbV8xMDNfc3RhdHVzb2Z3YXRlcnF1YWxpdHlwYWNrYWdlLnBkZg==, Accessed 2022-24-06.

[174] M. Jain, R. Fishman, P. Mondal, G. L. Galford, N. Bhattarai, S. Naeem, U. Lall, Balwinder-Singh and R. S. DeFries, Groundwater depletion will reduce cropping intensity in India, *Science Advances*, 2021, **7**, 1–9.

[175] U. W. Bengaluru, *Wastewater Treatment and Reuse*, http://bengaluru.urbanwaters.in/wastewater-treatment-and-reuse-49/, Accessed 2022-06-06.

[176] D. Malghan, M. Sekhar, K. Balakrishnan, S. Thiyaku, M. Gautam and V. K. Mehta, A model-based estimate of the groundwater budget and associated uncertainties in Bengaluru, India, *urban water Journal*, 2021, **18**, 1–11.

[177] R. Subbaraman and S. L. Murthy, The right to water in the slums of Mumbai, India, *Bulletin of the World Health Organization*, 2015, **93**, 815–816.

[178] A. D. R. Institute, *India Water Facts*, https://www.adriindia.org/adri/india_water_facts, Accessed 2022-06-06.

[179] WHO, *The Global health Observatory - SDG 3.9.6 WASH Deaths*, https://www.who.int/data/gho/data/indicators/indicator-details/GHO/sdg-3-9-2-wash-deaths, Accessed 2022-06-06.

[180] C. P. C. Board", *Water Quality Data Year 2016*, https://cpcb.nic.in/nwmp-data-2016/, Accessed 2020-06-19.

[181] C. P. C. Board, *Evaluation Of Operation And Maintenance Of Sewage Treatment Plants In India-2007*, http://www.indiaenvironmentportal.org.in/files/sewage.pdf, Accessed 2020-06-19.

[182] C. Mukhopadhyay, S. Vishwanath, V. K. Eshwara, S. A. Shankaranarayana and A. Sagir, Microbial quality of well water from rural and urban households in Karnataka, India: A cross-sectional study, *Journal of infection and Public Health*, 2012, **5**, 257–262.

[183] A. Schriewer, M. Odagiri, S. Wuertz, P. R. Misra, P. Panigrahi, T. Clasen and M. W. Jenkins, Human and animal fecal contamination of community water sources, stored drinking water and hands in rural India measured with validated microbial source tracking assays, *The American journal of tropical medicine and hygiene*, 2015, **93**, 509.

[184] I. W. Portal, *Water contamination and pollution - A growing challenge for health and biodiversity*, https://www.indiawaterportal.org/faqs/water-contamination-and-pollution-growing-challenge-health-and-biodiversity#:~:text=Groundwater%20resources%20in%20India%20are,harmful%20pesticide%20and%20fertiliser%20residues, Accessed 2022-06-06.

[185] I. Khurana and R. Sen, Drinking water quality in rural India: Issues and approaches, *WaterAid India*, 2008, **89**, 1–23.

[186] S. Sharma and A. Bhattacharya, Drinking water contamination and treatment techniques, *Applied water science*, 2017, **7**, 1043–1067.

[187] A. Verma, B. K. Shetty, V. Guddattu, M. K. Chourasia and P. Pundir, High prevalence of dental fluorosis among adolescents is a growing concern: a school based cross-sectional study from Southern India, *Environmental health and preventive medicine*, 2017, **22**, 1–7.

[188] F. W. Pontius, K. G. Brown and C.-J. Chen, Health implications of arsenic in drinking water, *Journal-American Water Works Association*, 1994, **86**, 52–63.

[189] B. C. Crone, T. F. Speth, D. G. Wahman, S. J. Smith, G. Abulikemu, E. J. Kleiner and J. G. Pressman, Occurrence of per-and polyfluoroalkyl substances (PFAS) in source water and their treatment in drinking water, *Critical reviews in environmental science and technology*, 2019, **49**, 2359–2396.

[190] A. for Toxic Substances and D. Registry, *Toxicological Profile for Perfluoroalkyls*, https://www.atsdr.cdc.gov/toxprofiles/tp200.pdf, Accessed 2022-06-06.

[191] P. Sharma, H. M. Iqbal and R. Chandra, Evaluation of pollution parameters and toxic elements in wastewater of pulp and paper industries in India: A case study, *Case Studies in Chemical and Environmental Engineering*, 2022, **5**, 100163.

[192] S. Saha, N. Narayanan, N. Singh and S. Gupta, Occurrence of endocrine disrupting chemicals (EDCs) in river water, ground water and agricultural soils of India, *International Journal of Environmental Science and Technology*, 2022, 1–16.

[193] K. G. Nayar, P. Sundararaman, C. L. O'Connor, J. D. Schacherl, M. L. Heath, M. O. Gabriel, S. R. Shah, N. C. Wright, A. G. Winter *et al.*, Feasibility study of an

electrodialysis system for in-home water desalination in urban India, *Development Engineering*, 2017, **2**, 38–46.

[194] G. Rosa and T. Clasen, Consistency of use and effectiveness of household water treatment among Indian households claiming to treat their water, *The American journal of tropical medicine and hygiene*, 2017, **97**, 259.

[195] M. C. Freeman, V. Trinies, S. Boisson, G. Mak and T. Clasen, Promoting household water treatment through women's self help groups in rural India: assessing impact on drinking water quality and equity, *PLOS One*, 2012, **7**, 1–9.

[196] G. Balasubramanian, D. Dionysiou, M. Suidan, V. Subramanian, I. Baudin and J.-M. Laîné, Titania powder modified sol-gel process for photocatalytic applications, *Journal of materials science*, 2003, **38**, 823–831.

[197] L. Vesce, R. Riccitelli, G. Soscia, T. M. Brown, A. Di Carlo and A. Reale, Optimization of nanostructured titania photoanodes for dye-sensitized solar cells: Study and experimentation of TiCl4 treatment, *Journal of Non-crystalline solids*, 2010, **356**, 1958–1961.

[198] B. A. Zaitoon, R. I. Yousef and S. M. Musleh, Modification of jordanian diatomite and its use for the removal of some organic pollutants from Water, *Oriental Journal of Chemistry*, 2011, **27**, 1357.

[199] C. Ferreiro, J. Sanz, N. Villota, A. de Luis and J. I. Lombraña, Kinetic modelling for concentration and toxicity changes during the oxidation of 4-chlorophenol by UV/H2O2, *Scientific reports*, 2021, **11**, 1–15.

[200] G. Odling and N. Robertson, SILAR BiOI-Sensitized TiO2 Films for Visible-Light Photocatalytic Degradation of Rhodamine B and 4-Chlorophenol, *ChemPhysChem*, 2017, **18**, 728–735.

[201] A. A. Kokhanovsky, Physical interpretation and accuracy of the Kubelka–Munk theory, *journal of physics d: applied physics*, 2007, **40**, 2210.

[202] R. López and R. Gómez, Band-gap energy estimation from diffuse reflectance measurements on sol–gel and commercial TiO2: a comparative study, *Journal of sol-gel science and technology*, 2012, **61**, 1–7.

[203] P. Makuła, M. Pacia and W. Macyk, *How to correctly determine the band gap energy of modified semiconductor photocatalysts based on UV–Vis spectra*, 2018.

[204] S. G. enez, *Photoelectrochemical solar fuel production*, Springer International Publishing, 2016.

[205] G. E. Lloyd, Atomic number and crystallographic contrast images with the SEM: a review of backscattered electron techniques, *Mineralogical Magazine*, 1987, **51**, 3–19.

[206] G. Odling, A. Ivaturi, E. Chatzisymeon and N. Robertson, Improving Carbon-Coated TiO2 Films with a TiCl4 Treatment for Photocatalytic Water Purification, *ChemCatChem*, 2018, **10**, 234–243.

[207] G. Odling and N. Robertson, BiVO4-TiO2 Composite Photocatalysts for Dye Degradation Formed Using the SILAR Method, *ChemPhysChem*, 2016, **17**, 2872–2880.

[208] G. Odling, E. Chatzisymeon and N. Robertson, Sequential ionic layer adsorption and reaction (SILAR) deposition of Bi 4 Ti 3 O 12 on TiO 2: an enhanced and stable photocatalytic system for water purification, *Catalysis Science & Technology*, 2018, **8**, 829–839.

[209] G. S. Kumar, S. S. Kar and A. Jain, Health and environmental sanitation in India: Issues for prioritizing control strategies, *Indian journal of occupational and environmental medicine*, 2011, **15**, 93.

[210] K. Nath, Home hygiene and environmental sanitation: a country situation analysis for India, *International Journal of Environmental Health Research*, 2003, **13**, S19–S28.

[211] Bureau of Indian Standards, *Indian standard: Drinking Water - Specification (Second Revision)*, http://cgwb.gov.in/Documents/WQ-standards.pdf, Accessed: 2020-05-18.

[212] E. M. Wurtzler and D. Wendell, Selective Photocatalytic Disinfection by Coupling StrepMiniSog to the Antibody Catalyzed Water Oxidation Pathway, *PloS one*, 2016, **11**, e0162577.

[213] CDC, *Environmental Infection Control Guidelines - Appendix C. Water*, https://www.cdc.gov/infectioncontrol/guidelines/environmental/appendix/water.html, Accessed 2022-11-09.

[214] V. Porley and N. Robertson, in *Nanostructured photocatalysts*, Elsevier, 2020, ch. Substrate and support materials for photocatalysis, pp. 129–171.

[215] A. Kafizas, S. Kellici, J. A. Darr and I. P. Parkin, Titanium dioxide and composite metal/metal oxide titania thin films on glass: a comparative study of photocatalytic activity, *Journal of Photochemistry and Photobiology A: Chemistry*, 2009, **204**, 183–190.

[216] N. Serpone, E. Borgarello, R. Harris, P. Cahill, M. Borgarello and E. Pelizzetti, Photocatalysis over TiO2 supported on a glass substrate, *Solar Energy Materials*, 1986, **14**, 121–127.

[217] D. L. Cunha, A. Kuznetsov, C. A. Achete, A. E. da Hora Machado and M. Marques, Immobilized TiO2 on glass spheres applied to heterogeneous photocatalysis: Photoactivity, leaching and regeneration process, *PeerJ*, 2018, **6**, e4464.

[218] A. Haenel, P. Moreń, A. Zaleska and J. Hupka, Photocatalytic activity of TiO2 immobilized on glass beads, *Physicochem. Probl. Miner. Process*, 2010, **45**, 49–56.

[219] C. J. Pestana, C. Edwards, R. Prabhu, P. K. Robertson and L. A. Lawton, Photocatalytic degradation of eleven microcystin variants and nodularin by TiO2 coated glass microspheres, *Journal of hazardous materials*, 2015, **300**, 347–353.

[220] S.-C. Kim and D.-K. Lee, Preparation of TiO2-coated hollow glass beads and their application to the control of algal growth in eutrophic water, *Microchemical Journal*, 2005, **80**, 227–232.

[221] M. Coto, S. Troughton, J. Duan, R. Kumar and T. Clyne, Development and assessment of photo-catalytic membranes for water purification using solar radiation, *Applied Surface Science*, 2018, **433**, 101–107.

[222] A. Fernandez, G. Lassaletta, V. Jimenez, A. Justo, A. Gonzalez-Elipe, J.-M. Herrmann, H. Tahiri and Y. Ait-Ichou, Preparation and characterization of TiO2 photocatalysts supported on various rigid supports (glass, quartz and stainless steel).

Comparative studies of photocatalytic activity in water purification, *Applied Catalysis B: Environmental*, 1995, **7**, 49–63.

[223] C.-G. Wu, L.-F. Tzeng, Y.-T. Kuo and C. H. Shu, Enhancement of the photocatalytic activity of TiO2 film via surface modification of the substrate, *Applied Catalysis A: General*, 2002, **226**, 199–211.

[224] N. Samsudin, Y. Z. H.-Y. Hashim, M. A. Arifin, M. Mel, H. M. Salleh, I. Sopyan and D. N. Jimat, Optimization of ultraviolet ozone treatment process for improvement of polycaprolactone (PCL) microcarrier performance, *Cytotechnology*, 2017, **69**, 601–616.

[225] T. Yamamoto, M. Okubo, N. Imai and Y. Mori, Improvement on hydrophilic and hydrophobic properties of glass surface treated by nonthermal plasma induced by silent corona discharge, *Plasma Chemistry and Plasma Processing*, 2004, **24**, 1–12.

[226] S. Sakka, T. Yoko, R. Reisfeld and C. Jorgensen, *Chemistry, Spectroscopy and Applications of Sol-Gel Glasses*, Spring-Verlag, 1992.

[227] W. Que, Z. Sun, Y. Zhou, Y. Lam, S. Cheng, Y. Chan and C. Kam, Preparation of hard optical coatings based on an organic/inorganic composite by sol–gel method, *Materials Letters*, 2000, **42**, 326–330.

[228] J. L. Yang, S. J. An, W. I. Park, G.-C. Yi and W. Choi, Photocatalysis using ZnO thin films and nanoneedles grown by metal–organic chemical vapor deposition, *Advanced materials*, 2004, **16**, 1661–1664.

[229] M. Karches, M. Morstein, P. R. Von Rohr, R. L. Pozzo, J. L. Giombi and M. A. Baltanás, Plasma-CVD-coated glass beads as photocatalyst for water decontamination, *Catalysis Today*, 2002, **72**, 267–279.

[230] C. Casado, S. Mesones, C. Adán and J. Marugán, Comparing potentiostatic and galvanostatic anodization of titanium membranes for hybrid photocatalytic/microfiltration processes, *Applied Catalysis A: General*, 2019, **578**, 40–52.

[231] Q. Zheng, H.-J. Lee, J. Lee, W. Choi, N.-B. Park and C. Lee, Electrochromic titania nanotube arrays for the enhanced photocatalytic degradation of phenol and pharmaceutical compounds, *Chemical Engineering Journal*, 2014, **249**, 285–292.

[232] M. K. Arfanis, P. Adamou, N. G. Moustakas, T. M. Triantis, A. G. Kontos and P. Falaras, Photocatalytic degradation of salicylic acid and caffeine emerging contaminants using titania nanotubes, *Chemical Engineering Journal*, 2017, **310**, 525–536.

[233] J. M. Macak, H. Tsuchiya, A. Ghicov, K. Yasuda, R. Hahn, S. Bauer and P. Schmuki, TiO2 nanotubes: Self-organized electrochemical formation, properties and applications, *Current Opinion in Solid State and Materials Science*, 2007, **11**, 3–18.

[234] M. Ge, C. Cao, J. Huang, S. Li, Z. Chen, K.-Q. Zhang, S. Al-Deyab and Y. Lai, A review of one-dimensional TiO 2 nanostructured materials for environmental and energy applications, *Journal of Materials Chemistry A*, 2016, **4**, 6772–6801.

[235] A. Steels, *Stainless Steel Grade Datasheets*, http://www.worldstainless.org/Files/issf/nonimage-files/PDF/Atlas_Grade_datasheet_-_all_datasheets_rev_Aug_2013.pdf, Accessed 2019-04-23.

[236] F. Kurtuldu and E. Altuncu, 4th International Symposium on Innovative Technologies in Engineering and Science (ISITES2016) 3-5 Nov 2016 Alanya/Antalya-Turkey, 2016.

[237] Y. Chen and D. D. Dionysiou, TiO2 photocatalytic films on stainless steel: the role of Degussa P-25 in modified sol–gel methods, *Applied Catalysis B: Environmental*, 2006, **62**, 255–264.

[238] L. Besra and M. Liu, A review on fundamentals and applications of electrophoretic deposition (EPD), *Progress in materials science*, 2007, **52**, 1–61.

[239] M. Yarazavi, E. Noroozian and M. Mousavi, Headspace solid-phase microextraction of menthol using a sol–gel titania-based coating along with multiwalled carbon nanotubes on the surface of stainless steel fiber, *Journal of the Iranian Chemical Society*, 2018, **15**, 2593–2603.

[240] X. Du, S. You, X. Wang, Q. Wang and J. Lu, Switchable and simultaneous oil/water separation induced by prewetting with a superamphiphilic self-cleaning mesh, *Chemical Engineering Journal*, 2017, **313**, 398–403.

[241] Y. Cai, J. Song, X. Liu, X. Yin, X. Li, J. Yu and B. Ding, Soft BiOBr@ TiO 2 nanofibrous membranes with hierarchical heterostructures as efficient and recyclable visible-light photocatalysts, *Environmental Science: Nano*, 2018, **5**, 2631–2640.

[242] J. O. Tijani, O. O. Fatoba, T. Totito, W. Roos and L. Petrik, Synthesis and characterization of carbon doped TiO2 photocatalysts supported on stainless steel mesh by sol-gel method, 2017, **22**, 48–59.

[243] M. Foruzanmehr, S. M. Hosainalipour, S. Mirdamadi Tehrani and M. Aghaeipour, Nano-structure TiO2 film coating on 316L stainless steel via sol-gel technique for blood compatibility improvement, *Nanomedicine Journal*, 2014, **1**, 128–136.

[244] E. Nurhayati, H. Yang, C. Chen, C. Liu, Y. Juang, C. Huang and C.-c. Hu, Electrophotocatalytic fenton decolorization of orange G using mesoporous TiO2/stainless steel mesh photo-electrode prepared by the sol-gel dip-coating method, *Int. J. Electrochem. Sci*, 2016, **11**, 3615–3632.

[245] A. Acra, M. Jurdi, H. Mu'allem, Y. Karahagopian and Z. Raffoul, *Water disinfection by solar radiation: assessment and application*, IDRC, Ottawa, ON, CA, 1990.

[246] J. M. Meichtry, H. J. Lin, L. de la Fuente, I. K. Levy, E. A. Gautier, M. A. Blesa and M. I. Litter, Low-cost TiO 2 photocatalytic technology for water potabilization in plastic bottles for isolated regions. Photocatalyst Fixation, *Journal of Solar Energy Engineering*, 2007, 119.

[247] A. L. de Barros, A. A. Q. Domingos, P. B. A. Fechine, D. de Keukeleire and R. F. do Nascimento, PET as a support material for TiO2 in advanced oxidation processes, *Journal of applied polymer science*, 2014, **131**, 40175.

[248] M. M. d. M. Santos, M. M. M. B. Duarte, G. E. d. Nascimento, N. B. G. d. Souza and O. R. S. d. Rocha, Use of TiO2 photocatalyst supported on residues of polystyrene packaging and its applicability on the removal of food dyes, *Environmental Technology*, 2019, **40**, 1494–1507.

[249] İ. Altın and M. Sökmen, Preparation of TiO2-polystyrene photocatalyst from waste material and its usability for removal of various pollutants, *Applied Catalysis B: Environmental*, 2014, **144**, 694–701.

[250] R. Díaz, S. Macías and E. Cázares, Fourier Transform Infrared Spectroscopy and Atomic Force Microscopy Studies of a SiO2-TiO2-Zeolite Matrix for a CuO-CoO Catalyst Prepared by a Sol–Gel Method, *Journal of Sol-Gel Science and Technology*, 2005, **35**, 13–20.

[251] S. Landi Jr, J. Carneiro, S. Ferdov, A. M. Fonseca, I. C. Neves, M. Ferreira, P. Parpot, O. S. Soares and M. F. Pereira, Photocatalytic degradation of Rhodamine B dye by cotton textile coated with SiO2-TiO2 and SiO2-TiO2-HY composites, *Journal of Photochemistry and Photobiology A: Chemistry*, 2017, **346**, 60–69.

[252] S. Landi Jr, J. Carneiro, O. S. Soares, M. F. Pereira, A. C. Gomes, A. Ribeiro, A. M. Fonseca, P. Parpot and I. C. Neves, Photocatalytic performance of N-doped TiO2nano-SiO2-HY nanocomposites immobilized over cotton fabrics, *Journal of Materials Research and Technology*, 2019, **8**, 1933–1943.

[253] J. Zhang, M. Zhang, L. Lin and X. Wang, Sol processing of conjugated carbon nitride powders for thin-film fabrication, *Angewandte Chemie*, 2015, **127**, 6395–6399.

[254] D. C. Look, Recent advances in ZnO materials and devices, *Materials science and engineering: B*, 2001, **80**, 383–387.

[255] Ş. S. Ugur, M. Sariişik and A. H. Aktaş, The fabrication of nanocomposite thin films with TiO2 nanoparticles by the layer-by-layer deposition method for multifunctional cotton fabrics, *Nanotechnology*, 2010, **21**, 325603.

[256] S. Afzal, W. A. Daoud and S. J. Langford, Self-cleaning cotton by porphyrin-sensitized visible-light photocatalysis, *Journal of Materials Chemistry*, 2012, **22**, 4083–4088.

[257] J. Kiwi and C. Pulgarin, Innovative self-cleaning and bactericide textiles, *Catalysis Today*, 2010, **151**, 2–7.

[258] A. Bozzi, T. Yuranova and J. Kiwi, Self-cleaning of wool-polyamide and polyester textiles by TiO2-rutile modification under daylight irradiation at ambient temperature, *Journal of Photochemistry and Photobiology A: Chemistry*, 2005, **172**, 27–34.

[259] R. Dastjerdi and M. Montazer, A review on the application of inorganic nano-structured materials in the modification of textiles: focus on anti-microbial properties, *Colloids and surfaces B: Biointerfaces*, 2010, **79**, 5–18.

[260] C. Colleoni, M. R. Massafra and G. Rosace, Photocatalytic properties and optical characterization of cotton fabric coated via sol–gel with non-crystalline TiO2 modified with poly (ethylene glycol), *Surface and Coatings Technology*, 2012, **207**, 79–88.

[261] Y. Wang, X. Ding, P. Zhang, Q. Wang, K. Zheng, L. Chen, J. Ding, X. Tian and X. Zhang, Convenient and recyclable TiO2/g-C3N4 photocatalytic coating: layer-by-layer self-assembly construction on cotton fabrics leading to improved catalytic activity under visible light, *Industrial & Engineering Chemistry Research*, 2019, **58**, 3978–3987.

[262] Y. Fan, J. Zhou, J. Zhang, Y. Lou, Z. Huang, Y. Ye, L. Jia and B. Tang, Photocatalysis and self-cleaning from g-C3N4 coated cotton fabrics under sunlight irradiation, *Chemical Physics Letters*, 2018, **699**, 146–154.

[263] M. Kete, O. Pliekhova, L. Matoh and U. L. Štangar, Design and evaluation of a compact photocatalytic reactor for water treatment, *Environmental Science and Pollution Research*, 2018, **25**, 20453–20465.

[264] S. Lakshmi, R. Renganathan and S. Fujita, Study on TiO2-mediated photocatalytic degradation of methylene blue, *Journal of Photochemistry and Photobiology A: Chemistry*, 1995, **88**, 163–167.

[265] G. Sivalingam, K. Nagaveni, M. Hegde and G. Madras, Photocatalytic degradation of various dyes by combustion synthesized nano anatase TiO2, *Applied Catalysis B: Environmental*, 2003, **45**, 23–38.

[266] C. McCullagh, P. K. Robertson, M. Adams, P. M. Pollard and A. Mohammed, Development of a slurry continuous flow reactor for photocatalytic treatment of industrial waste water, *Journal of Photochemistry and Photobiology A: Chemistry*, 2010, **211**, 42–46.

[267] M. Melchionna and P. Fornasiero, Updates on the Roadmap for Photocatalysis, *ACS Catalysis*, 2020, **10**, 5493–5501.

[268] J. A. Rengifo-Herrera, P. Osorio-Vargas and C. Pulgarin, A critical review on N-modified TiO2 limits to treat chemical and biological contaminants in water. Evidence that enhanced visible light absorption does not lead to higher degradation rates under whole solar light, *Journal of Hazardous Materials*, 2022, **425**, 127979.

[269] I. Justicia, P. Ordejón, G. Canto, J. L. Mozos, J. Fraxedas, G. A. Battiston, R. Gerbasi and A. Figueras, Designed self-doped titanium oxide thin films for efficient visible-light photocatalysis, *Advanced materials*, 2002, **14**, 1399–1402.

[270] J. Wang, Z. Wang, B. Huang, Y. Ma, Y. Liu, X. Qin, X. Zhang and Y. Dai, Oxygen vacancy induced band-gap narrowing and enhanced visible light photocatalytic activity of ZnO, *ACS applied materials & interfaces*, 2012, **4**, 4024–4030.

[271] Y. Nosaka and A. Y. Nosaka, Generation and detection of reactive oxygen species in photocatalysis, *Chemical reviews*, 2017, **117**, 11302–11336.

[272] T. B. Nguyen and R.-a. Doong, Heterostructured ZnFe 2 O 4/TiO 2 nanocomposites with a highly recyclable visible-light-response for bisphenol A degradation, *RSC Advances*, 2017, **7**, 50006–50016.

[273] S. Zhao, M. Fu, Y. Li, X. Hu, C. Yuan and R. Pan, Facile hydrothermal preparation of a ZnFe2O4/TiO2 heterojunction for NOx removal, *Molecular Catalysis*, 2021, **507**, 111570.

[274] M. Dhiman, R. Sharma, V. Kumar and S. Singhal, Morphology controlled hydrothermal synthesis and photocatalytic properties of ZnFe2O4 nanostructures, *Ceramics International*, 2016, **42**, 12594–12605.

[275] T. T. ThanhThuy, H. Feng and Q. Cai, Photocatalytic degradation of pen-

tachlorophenol on ZnSe/TiO2 supported by photo-Fenton system, *Chemical Engineering Journal*, 2013, **223**, 379–387.

[276] Y. Wang, F. Pan, W. Dong, L. Xu, K. Wu, G. Xu and W. Chen, Recyclable silver-decorated magnetic titania nanocomposite with enhanced visible-light photocatalytic activity, *Applied Catalysis B: Environmental*, 2016, **189**, 192–198.

[277] M. Janczarek and E. Kowalska, On the origin of enhanced photocatalytic activity of copper-modified titania in the oxidative reaction systems, *Catalysts*, 2017, **7**, 317.

[278] V. Porley, E. Chatzisymeon, B. C. Meikap, S. Ghosal and N. Robertson, Field testing of low-cost titania-based photocatalysts for enhanced solar disinfection (SODIS) in rural India, *Environmental Science: Water Research & Technology*, 2020, **6**, 809–816.

[279] X. Meng and Z. Zhang, Bismuth-based photocatalytic semiconductors: introduction, challenges and possible approaches, *Journal of Molecular Catalysis A: Chemical*, 2016, **423**, 533–549.

[280] X. Meng and Z. Zhang, Facile synthesis of BiOBr/Bi2WO6 heterojunction semiconductors with high visible-light-driven photocatalytic activity, *Journal of Photochemistry and Photobiology A: Chemistry*, 2015, **310**, 33–44.

[281] A. Huizhong, D. Yi, W. Tianmin, W. Cong, H. Weichang and J. ZHANG, Photocatalytic properties of biox (X= Cl, Br, and I), *Rare Metals*, 2008, **27**, 243–250.

[282] L. Denardo, G. Raffaini, F. Ganazzoli and R. Chiesa, in *Surface modification of biomaterials*, Elsevier, 2011, pp. 102–142.

[283] D. Solís-Casados, L. Escobar-Alarcón, A. Arrieta-Castañeda and E. Haro-Poniatowski, Bismuth–titanium oxide nanopowders prepared by sol–gel method for photocatalytic applications, *Materials Chemistry and Physics*, 2016, **172**, 11–19.

[284] D. A. Solís-Casados, L. Escobar-Alarcón, V. Alvarado-Pérez and E. Haro-Poniatowski, Photocatalytic activity under simulated sunlight of Bi-modified TiO2 thin films obtained by sol gel, *International Journal of Photoenergy*, 2018, **2018**, 1–9.

[285] S. Madeswaran, N. Giridharan and R. Jayavel, Sol–gel synthesis and property studies of layered perovskite bismuth titanate thin films, *Materials chemistry and physics*, 2003, **80**, 23–28.

[286] W. Yi, C. Yan, M. S. Hamdy, J. Baltrusaitis and G. Mul, Effects of bismuth addition and photo-deposition of platinum on (surface) composition, morphology and visible light photocatalytic activity of sol–gel derived TiO2, *Applied catalysis B: environmental*, 2014, **154**, 153–160.

[287] M. H. Nateq and R. Ceccato, Sol-gel synthesis of TiO2 nanocrystalline particles with enhanced surface area through the reverse micelle approach, *Advances in Materials Science and Engineering*, 2019, **2019**, 1–14.

[288] T. Watanabe, S. Furukawa, J. Hirata, T. Koyama, H. Ogihara and M. Yamasaki, Inactivation of Geobacillus stearothermophilus spores by high-pressure carbon dioxide treatment, *Applied and Environmental Microbiology*, 2003, **69**, 7124–7129.

[289] Z.-h. Yuan *et al.*, Synthesis, characterization and photocatalyticactivity of ZnFe2O4/TiO2 nanocomposite, *Journal of Materials Chemistry*, 2001, **11**, 1265–1268.

[290] G. Song, F. Xin and X. Yin, Photocatalytic reduction of carbon dioxide over ZnFe2O4/TiO2 nanobelts heterostructure in cyclohexanol, *Journal of colloid and interface science*, 2015, **442**, 60–66.

[291] N. Ahmadpour, M. H. Sayadi, S. Sobhani and M. Hajiani, Photocatalytic degradation of model pharmaceutical pollutant by novel magnetic TiO2@ ZnFe2O4/Pd nanocomposite with enhanced photocatalytic activity and stability under solar light irradiation, *Journal of Environmental Management*, 2020, **271**, 110964.